SAPIENZA
UNIVERSITÀ DI ROMA

A thesis submitted for the degree of Doctor of Philosophy

Department of Structural and Geotechnical Engineering

XXXI Cycle

Elastic anisotropy and elastoplastic coupling of soils: a thermodynamic approach

Candidate:
Fabio Rollo

Supervisor:
Prof. Eng. Angelo Amorosi

Academic year 2017/2018

Contents

Acknowledgements

I would like to express my thanks to my supervisor Prof. Angelo Amorosi, who is a great teacher and an enthusiastic supporter. His continuous presence has been fundamental and inspired me throughout the research project.

I am grateful to Prof. Yannis F. Dafalias for sharing with me some of his knowledge and experience of constitutive modelling. The period of September-October 2017 in occasion of his visit to the Department of Structural and Geotechnical Engineering of the Sapienza University of Rome has been for me a fantastic experience. Working under his supervision has been fundamental for the achievement of part of this work and brought me fresh energy and motivation.

I express my gratitude to Prof. Guy T. Houlsby for his valuable comments and suggestions concerning the hyperelastic formulation. His rigorous analytical approach and his experience of constitutive modelling inspired and motivated me to do even better.

I also thank Prof. Alexander M. Puzrin for the fruitful discussions about some aspects of the thermodynamic constitutive modelling of geomaterials.

I would also like to thank all the members and researchers of the Department of Structural and Geotechnical Engineering of the Sapienza University of Rome. In particular, special thanks are devoted to Prof. Stefano Vidoli for his precious advises and suggestions on the theory of invariants and the representation theorems and Prof. Davide Bernardini for the lessons and discussions on continuum thermomechanics that inspired me at the beginning of the research activity.

Last, but not least, I would like to extend my thanks to my family and many friends who supported and encouraged me during these years.

Introduction

In the last few decades several efforts have been made in the field of geotechnical engineering to develop constitutive models able to reproduce the mechanical behaviour of soils. It is well recognised that the behaviour of geomaterials is highly nonlinear, with both strength and stiffness depending on stress and strain levels. Taking into account in constitutive models the dependence of the small strain stiffness on the current stress is crucial to accurately predict the response of many geotechnical systems for both static and dynamic loading. Furthermore, soils can be characterised by a significant degree of anisotropy due to an oriented internal microstructure. Neglecting the anisotropy of soil behaviour may lead to inaccurate prediction of the response, as pointed out by Zdravkovic *et al.* (2002) while Lee & Rowe (1989), Simpson *et al.* (1996), Ng *et al.* (2004), Franzius *et al.* (2005) and Puzrin *et al.* (2012) showed that the small strain stiffness anisotropy can play a non-negligible role in the prediction of settlements induced by tunnelling and deep excavations. Finally, an other important feature often ignored in the engineering practice is the role of the previous stress history experienced by the material, and the related development of irreversible strains, on the small strain behaviour of soils.

This research concerns the constitutive modelling of soils to capture the features of soil behaviour mentioned above. Firstly, the elastic constitutive modelling of soils is considered to describe the anisotropy of the small strain stiffness in a thermodynamically consistent way. Subsequently, within the framework of classical elastoplasticity a reference model, the single surface hardening model for clays proposed by Dafalias & Taiebat (2013), is adopted and a form of elastoplastic coupling is introduced by a dependence of the small strain stiffness anisotropy on the plastic strain. This permits to reproduce the evolution of the directional properties observed in clayey soils at small strain levels. Finally, the Dafalias & Taiebat (2013) model is reformulated in a thermodynamically consistent way to develop more sophisticated forms of elastoplastic coupling.

In chapter 1 the small strain mechanical behaviour of geomaterials is discussed from an experimental perspective. The elastic stiffness dependency on the mean

effective pressure and, more generally, on the current state of stress is supported by experimental results and by some empirical relationships valid for both sandy and clayey soils. Subsequently, the anisotropic character of the elastic stiffness is explored and distinction is made between the inherent anisotropy due to the material microstructure and that induced by the current stress/strain state based on experimental data available in the literature and clarified by micromechanical considerations. In addition, the influence of the previous stress loading history on the elastic stiffness of clays via the preconsolidation pressure and the evolution of the small strain stiffness anisotropy with plastic strain are critically analysed based on experimental evidences.

In chapter 2 a critical review of some significant existing elastic models is proposed. Firstly, linear and nonlinear isotropic formulations are illustrated and later the elastic anisotropic model are discussed. Particular emphasis is given to the hyperelastic formulations.

In chapter 3 a nonlinear anisotropic hyperelastic model is proposed. The formulation is based on the definition of a free energy potential that ensures the thermodynamic consistency. The model is able to reproduce the nonlinear dependence of the elastic stiffness on the current stress state, the stress/strain induced anisotropy and the permanent anisotropic characteristics through the introduction of a symmetric second order fabric tensor. The proposed formulation is compared to the existing ones reported in chapter 2 highlighting similarities and differences. Finally, the performance of the model is investigated with reference to a series of experimental results observed on both sands and clays.

In chapter 4 the single surface elastoplastic rotational hardening model for clays formulated by Dafalias & Taiebat (2013) is first illustrated. The aim is to improve the performance of this latter accounting for the evolution of the elastic stiffness anisotropy with plastic strains. Therefore, the model is enriched with the nonlinear anisotropic hyperelastic formulation described in chapter 3 and a relationship between the internal variables controlling the anisotropy in the plastic regime and the fabric tensor pertaining to the reversible response of the model is established. This leads to a form of elastoplastic coupling whose effects on the elastic response are illustrated with reference to the experimental results shown in chapter 1.

Chapter 5 is devoted to the reformulation of the Dafalias & Taiebat (2013) model in a thermodynamically consistent way. The approach followed here is based on the thermodynamics with internal variables, denoted as hyperplasticity by Houlsby & Puzrin (2000, 2006), which is critically discussed in the first part of the chapter. The new formulation is developed for both associated and non-associated flow rule

and the analogies and differences with a family of existing hyperplastic anisotropic models are illustrated. The performance of the model is presented through the results of numerical simulations.

Finally, in chapter 6 two thermodynamically consistent forms of elastoplastic coupling are proposed. After a general introduction of the hyperplastic approach for coupled materials, the isotropic and anisotropic elastoplastic coupling via the preconsolidation pressure and the fabric tensor, respectively, are introduced in the associated version of the hyper-elastoplastic Dafalias & Taiebat (2013) model. In particular, the second form of coupling represents a new achievement never attempted before. The implications of elastoplastic coupling on the overall response of the model are analysed with reference to a series of numerical simulations.

Chapter 1

Small strain mechanical behaviour of geomaterials

In this chapter some relevant properties characterising the mechanical behaviour of geomaterials at small strain levels are discussed from an experimental perspective. First, the dependence of the elastic stiffness on the mean effective pressure and more generally on the current state of stress are investigated. Some empirical relationships useful to determine the shear modulus of both sandy and clayey soils at small strain levels are reported and few considerations on the variables affecting the Poisson's ratio are developed. Secondly, the anisotropic character of the elastic stiffnesses is explored, separately highlighting the effect of the inherent or structure anisotropy and that induced by the current stress/strain state. To support the discussion, experimental data available in the literature for sands and clays are illustrated and commented based on micromechanical considerations. Finally, the influence of the plastic strains on the small strain behaviour of geomaterials is described, with particular care to the evolution of the elastic stiffness anisotropy typically observed in clays.

1.1 Small strain stiffness

In the past three decades the small strain stiffness of soils has received particular attention because of the crucial role that plays in many geotechnical applications, such as the prediction of the settlements induced around an engineering structure and in any dynamic problem. The elastic behaviour of soils is characterised by a nonlinear dependence of the stiffness on the level of stress, not to be confused with the dependence of the secant stiffness on the strain amplitude. This latter, although is very important in both static and dynamic problems, is beyond the scope of this

chapter because the attention is herein limited to the very small strain levels. The improvement of laboratory testing systems equipped with local strain measurements, the use of high precision sensors and more recently the wide spread of non-destructive wave propagation measurements permit to perform reliable experiments in the small-strain domain. The initial shear modulus G_0, for which the response is usually assumed to be reversible, has been investigated by many researchers for both sandy and clayey soils. The majority of these studies were based on dynamic laboratory tests carried out on samples of natural or reconstituted soils, under isotropic or more general triaxial conditions. The experimental data are principally derived from measurements of the velocity of propagation of the shear waves in the specimen using bender elements incorporated in a triaxial apparatus, as discussed in detail by Viggiani (1992) and Jovičić (1995). The small strain shear modulus is related to the velocity of the shear waves through the well known relationship $G_0 = \rho V_s^2$, where ρ is the density of soil and V_s the velocity of propagation of the shear waves. Lateral benders measure the velocities V_{hv} and V_{hh} of vertically and horizontally polarised shear waves, propagating in the horizontal direction, whereas benders installed in the end platens measured the velocity V_{vh} of horizontally polarised shear waves propagating along the vertical direction, as depicted in figure (1.1).

In few cases this technique is combined with resonant column tests and with the measurements of small strain stiffness in the hollow cylinder apparatus. Throughout this section, the directional character of the shear modulus will not be specifically taken into account, thus the small strain shear modulus will be simply indicated by G.

In the literature two main approaches are possible to describe the small strain stiffness of soils. The first one is based on the micromechanical theory, in which the contact between the particles of the idealised soil are modelled. In this theoretical framework, Chang *et al.* (1989, 1991) presented numerical results of the small-strain shear modulus using the classic Hertz-Mindlin contact model for the case of an isotropic fabric assembly. Subsequently, Yimsiri & Soga (2000) simulated the interaction between rough particles, similarly to what discussed by Goddard (1990) but incorporating a fabric tensor into the micromechanics model to take into account the particles rearrangements occurring when the stress conditions change. Clearly, this method can be more efficiently employed for sandy and gravelly soils rather than for clays, in which the electro-magnetic forces and the particles shape are more complex to model. The second approach for studying the small-strain modulus of soils consists in deriving empirical expressions from experimental results. In particular, the small strain shear modulus was found to be a power function of

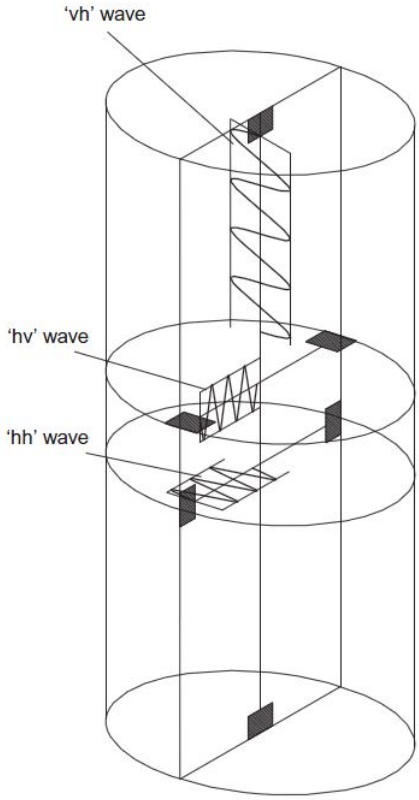

Figure 1.1: *Measurement of waves velocity through bender elements (from Callisto & Rampello (2002))*

the mean effective stress. If the soil is idealised as an assembly of elastic spheres in contact, following the micromechanical framework, the shear modulus should depend on the mean stress raised to the power of $\frac{1}{3}$. These relationships include many factors that influence the elastic shear modulus, as will be shown in the following. This empirical approach will be discussed in the following and the factors influencing the elastic shear modulus will be shown. However, it is worth noting that the physical origin of these expressions is not always very clear; in this sense the micromechanics framework offers a way to understand the origin of these empirical equations.

Hardin (1978) observed that the elastic shear modulus of sands depends on the current stress state, on the current void ratio e, and on the previous stress history experienced by the soil, simply represented by the overconsolidation ratio. He proposed the following empirical relationship in which G varies as power function of the mean pressure p:

$$\frac{G}{p_r} = Sf\left(e\right)\left(\frac{p}{p_r}\right)^n \mathrm{OCR}^k \tag{1.1}$$

where $f\left(e\right)$ is a decreasing function of the void ratio, p_r is a reference pressure

usually assumed as the atmospheric pressure and S, n and k are additional parameters. The elastic shear modulus increases as the mean effective pressure increases and the void ratio decreases and, at the same mean effective stress, it increases as the overconsolidation ratio increases. Note that because of the introduction of a reference pressure, these parameters of above are dimensionless and depend on the nature of the soil. In the past years many efforts heve been directed to study the influence of the void ratio on the shear modulus. For instance, alternative expressions for the function $f(e)$ originally proposed by Hardin & Richart (1963) have been introduced by Hardin & Black (1969) and more recently by Ishihara (1982) and Jamiolkowski *et al.* (1994) for soils of various composition and index properties. The parameter S in eq. (1.1) depends on the choice of the void ratio function and of the reference pressure. Then other researchers investigated the influence of the grain size and uniformity of sands on their stiffness. For instance, Iwasaki & Tatsuoka (1977) explored from an experimental perspective the influence of the uniformity and the shape of the particles and the fines content on the elastic shear modulus and Hardin & Kalinski (2005) the effect of the grains diameter specifically for gravelly soils.

Eq. (1.1) can be modified for clays. In fact, the experiments conducted by Weiler (1988) and Houlsby & Wroth (1991) demonstrate that under isotropic stress conditions, the current values of mean effective stress and overconsolidation ratio are sufficient to describe the small strain stiffness of clays, and that only two of the three variables e, p and OCR in eq. (1.1) are necessary. In particular, Viggiani (1992) and then Rampello *et al.* (1994) proposed the following expression for G:

$$\frac{G}{p_r} = S^* \left(\frac{p}{p_r}\right)^{n^*} R^{k^*} \tag{1.2}$$

where R is the overconsolidation ratio in terms of mean effective pressure $R = \frac{p_c}{p}$, with p_c being the mean preconsolidation pressure. The parameters S^*, n^* and k^* have similar meaning to those in eq. (1.1) but the asterisks are added to remember that the values are different. Their values depend on the clay type, particularly on the plastic index, with n^* typically varying in the range $0.5 \div 0.9$ and k^* in the range $0.2 \div 0.3$. The influence of the overconsolidation ratio on the small strain shear modulus through the parameter k^* is relatively small if compared to the effect of the mean pressure and the parameter S^*. About that, Viggiani & Atkinson (1995) measured the elastic shear modulus through bender element tests on undisturbed and reconstitued samples of the London clay, highlighting that the experimental data are well reproduced by a linear law in the bilogarithmic scale $\left(\frac{G}{G_{nc}}, R\right)$, with G_{nc} denoting the shear modulus for the normal consolidated clay, as reported in figure (1.2).

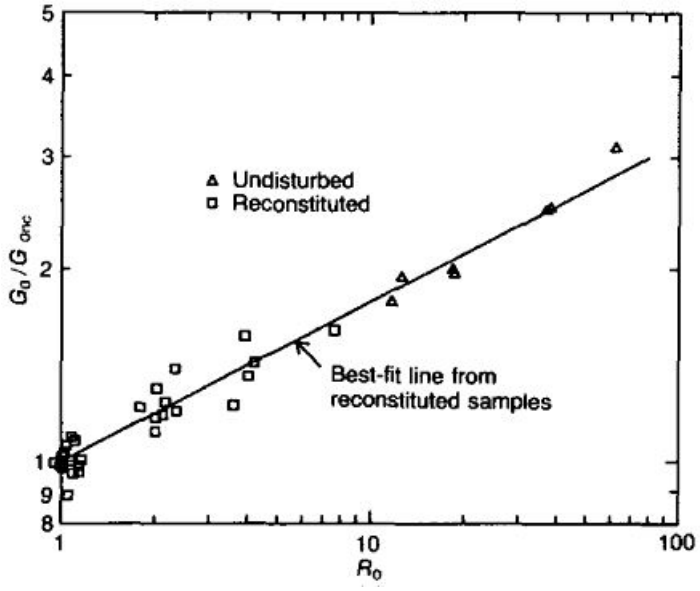

Figure 1.2: *Variation of G with overconsolidation ratio for the London clay (from Viggiani & Atkinson (1995))*

In addition, from figure (1.2) it can be seen that the effect of the overconsolidation ratio on the stiffness of soil at very small strain is basically unaffected by whether the sample is undisturbed or reconstituted.

Fewer observations are available concerning the small strain stiffness of soil under anisotropic stress conditions. For sandy soils Ni (1987) and Hardin & Blandford (1989) proposed the following empirical expression:

$$\frac{G}{p_r} = S_{ij} f(e) \frac{(\sigma_i \sigma_j)^{\frac{n}{2}}}{p_r^n} \mathrm{OCR}^k \tag{1.3}$$

where σ_i and σ_j are the principal stresses in the plane in which G is measured. Note that the factor S_{ij} could be in principle a function of the stress ratio, thus introducing more uncertainty in its evaluation, motivating eq. (1.3) more complex.

For fine grained soils Viggiani & Atkinson (1995) studied the dependence of G on the deviatoric stress q in triaxial test for both triaxial compression and extension. Subsequently, Jovičić & Coop (1996) carried out triaxial tests on reconstituted samples of kaolin following a series of constant p paths starting from different mean effective pressures. Then for clays, Rampello *et al.* (1997) experimentally investigated the effect of anisotropic stress states on the small strain shear stiffness of the reconstituted Vallericca clay: they compressed the material along radial stress paths in a triaxial apparatus for different values of the stress ratio $\eta = \frac{q}{p}$ while measuring the shear modulus using bender elements. These latter were embedded in the top and base of the triaxial cell, thus the direction of propagation of the shear

waves is vertical and the particle motion is horizontal, so that the component G_{vh} is measured. The values of the small strain shear modulus are higher than those obtained under isotropic stress conditions and, as depicted in figure (1.3), for fixed mean pressure, they increase as the stress ratio increases.

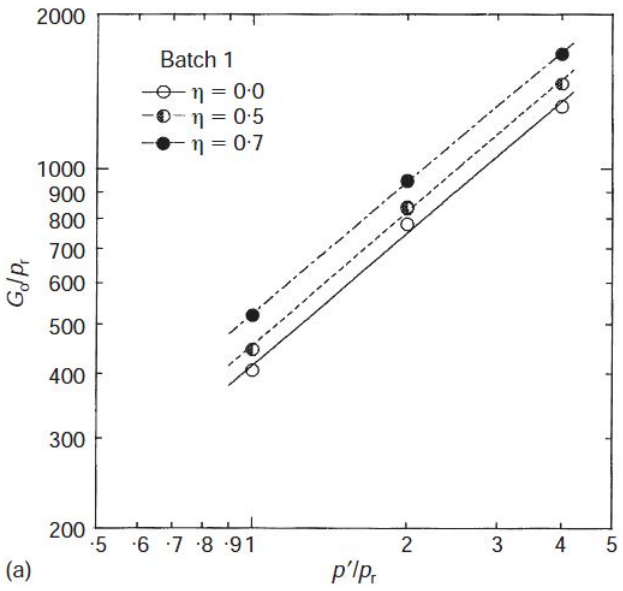

Figure 1.3: *Elastic shear modulus with the mean effective pressure for different stress ratios (from Rampello et al. (1997))*

This could be explained only in part by the fact that for anisotropically compressed samples the void ratio is smaller in comparison with the isotropic condition. In addition, the data points in the bilogarithmic plane $\left(\frac{p}{p_r}, \frac{G}{p_r}\right)$ fall along parallel lines irrespective of the current stress ratio. Therefore, a modification of eq. (1.2) was proposed to take into account the influence of the current anisotropic stress state. Rampello *et al.* (1997) referred to the following expression:

$$\frac{G}{p_r} = S^*_\eta \left(\frac{p}{p_r}\right)^{n^*} R^{k^*}_\eta \tag{1.4}$$

where $R^{k^*}_\eta$ is the overconsolidation ratio defined with respect to the anisotropic compression line and S^*_η can be empirically related to the corresponding value under isotropic stress conditions. The experimental results obtained by Rampello *et al.* (1997) and synthetised in the empirical expression (1.4) indicate that the small strain shear modulus is characterised by a nonlinear dependence on the mean effective pressure and in general on the current stress state and, at least for clays, another key ingredient is the previous stress history experienced by the material. The samples were loaded and unloaded along radial stress paths in order to highlight the effect

of the overconsolidation ratio on the small strain shear modulus. In figure (1.4), for a stess ratio $\eta = 0.3$, for the same mean effective pressure the shear modulus varies with the overconsolidation ratio and in particular, according to the results obtained by Viggiani & Atkinson (1995), G increases as the overconsolidation ratio increases. The dashed lines represent lines at constant overconsolidation ratio.

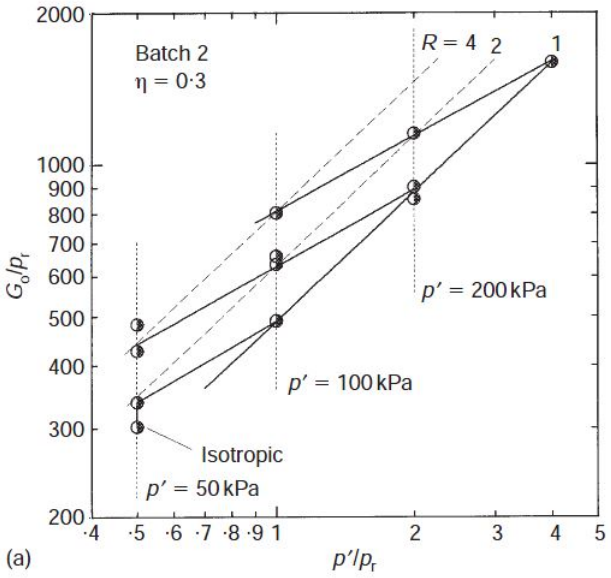

Figure 1.4: *Elastic shear modulus for different overconsolidation ratios (from Rampello et al. (1997))*

1.1.1 Poisson's ratio

Many studies have been carried out in last few years to experimentally determine through laboratory tests the value of the Poisson's ratio and its evolution with the stress level for different stress paths. The evaluation of the Poisson's ratios is very challenging and from the literature two main experimental procedures for their determination emerge. A first strategy consists in employing well established empirical correlations, once the velocity of propagation of the body and shear waves in the specimen are measured. For instance Kumar & Madhusudhan (2010), and Gu *et al.* (2013) employed bender elements and extender elements to measure the velocities of both the shear (S) and primary (P) waves in the same apparatus for different sand specimens and then computed the magnitude of the Poisson's ratio through the expression:

$$\nu = \frac{0.5V_p^2 - V_s^2}{V_p^2 - V_s^2} \tag{1.5}$$

They observed that the Poisson's ratio increases as the void ratio decreases and as the mean effective pressure decreases. However, a drawback of this approach is that for saturated soils the V_p coincides with the velocity of propagation of P-waves in water so the resulting Poisson's ratio is systematically overestimated. This is why a more diffused approach in the literature consists in determining the Poisson's ratios ν_{hh} and ν_{vh}, assuming the soil as transverse isotropic, by directly monitoring the displacements of the sample. In detail, the previous procedure consists in the execution of static and dynamic tests in triaxial cell or through the hollow cylinder apparatus, equipped with very high resolution local displacement transducers (LDT or LVDT) and bender elements for the measurement of velocity of propagation of shear waves in the solid. The key assumption is that these transducers resolve strains as small as those measured in waves propagation. This procedure permits to obtain results much more reliable than those obtained by the use of empirical correlations, thus in the following solely the experimental studies included in this category will be considered. The available experimental results mainly involve granular materials like sands (e.g. Hoque & Tatsuoka (1998), Kuwano & Jardine (2002), Chaudhary *et al.* (2004), De Silva (2004), HongNam & Koseki (2005), Ezaoui & Di Benedetto (2009), Ibraim *et al.* (2011), Suwal & Kuwano (2013)).

A first attempt to investigate the role of the current state of stress on the Poisson's ratio was made by Hoque & Tatsuoka (1998). They performed triaxial tests on different sands and determined the parameter ν_{vh} through the measurements of axial and radial displacements in the specimens and found that the ν_{vh} values are not sensitive to the magnitude of the normal stresses at fixed stress ratio but gradually increases as the stress ratio increases. HongNam & Koseki (2005) performed triaxial and torsional tests in hollow cylinder apparatus on Toyoura sand and demonstrated that the Poisson's ratio $\nu_{z\theta}$, being z the axial (vertical) direction and θ the radial (horizontal) one, is almost constant under isotropic loading, as depicted in figure (1.5) and increases with the stress ratio as shown in figure (1.6).

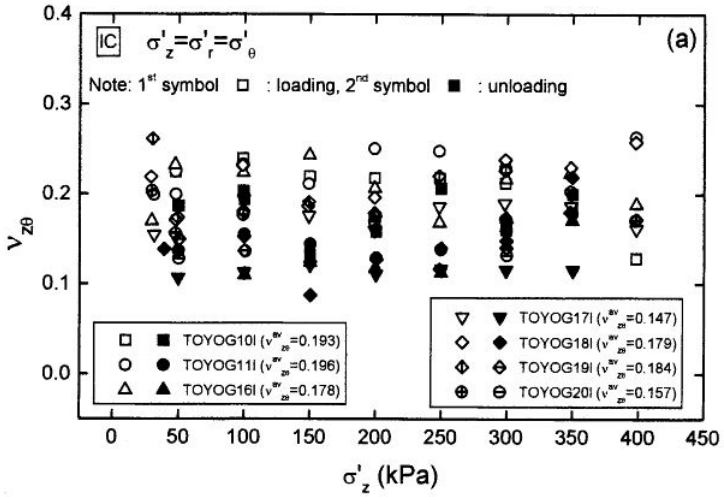

Figure 1.5: *Evolution of Poisson's ratio during isotropic consolidation (from HongNam & Koseki (2005))*

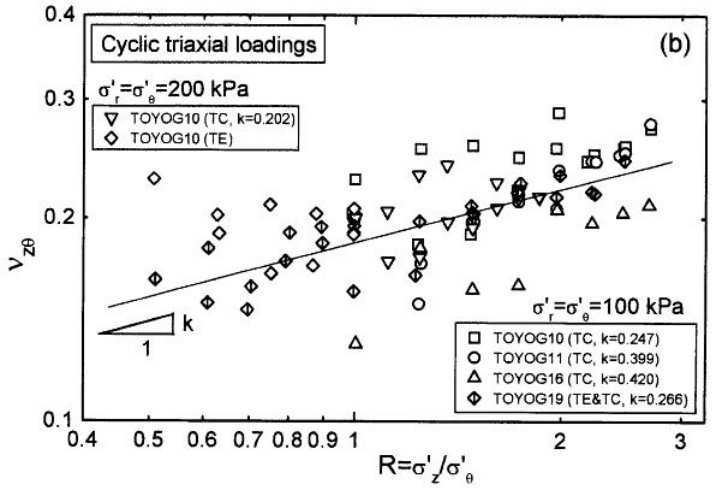

Figure 1.6: *Evolution of Poisson's ratio with the stress ratio (from HongNam & Koseki (2005))*

Furthermore, Ezaoui & Di Benedetto (2009) carried out static and dynamic tests on dry specimens of Hostun sand in a triaxial apparatus equipped with high resolution local displacements transducers and determined the Poisson's ratios in the vertical and horizontal plane. Again, despite the dispersion of the experimental data, the ratios results to be independent of the mean effective pressure during isotropic loading, as reported in figure (1.7). Nevertheless, their values seem to depend on the sample preparation methods, with the average values resulting higher for the case of pluviation and vibration than those obtained for tamping.

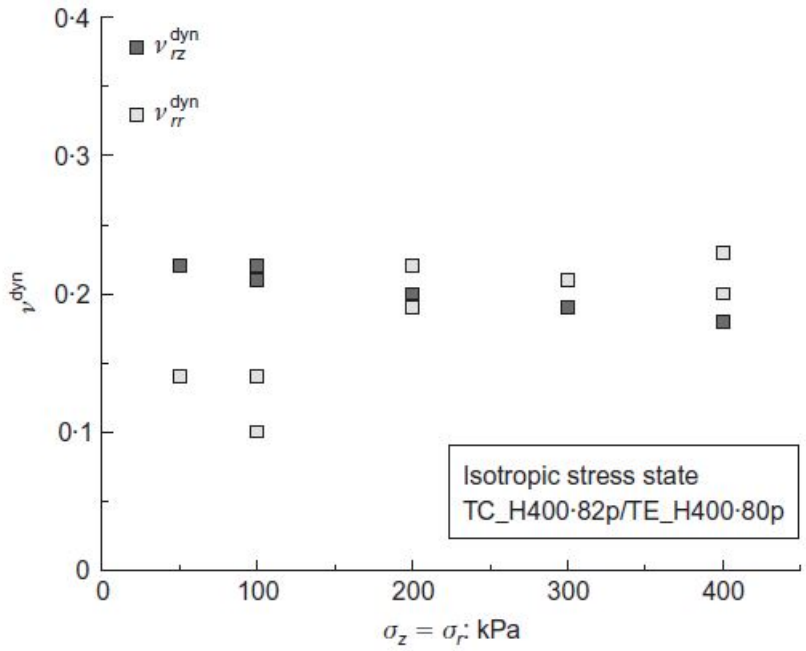

Figure 1.7: *Evolution of Poisson's ratio during isotropic consolidation (from Ezaoui & Di Benedetto (2009))*

Apart of the results reported by Suwal & Kuwano (2013), where a very slight reduction of the Poisson's ratio with the mean effective pressure is encountered for the Toyoura sand and the Hime gravel, the general trend emerging from the literature is that the Poisson's ratio is almost constant along sufficiently large isotropic stress paths.

1.2 Anisotropy

The internal structure of natural soils is rarely isotropic, thus leads to a different mechanical behaviour depending on the considered direction. Anisotropy of soils can be recognised at different scales, depending on the strain level involved. At very small strains, soils stiffness is often characterised by directional properties but, depending on the origin of these latter, anisotropy is usually distinguished in inherent and induced. Casagrande & Carillo (1944) described the inherent (or structural) anisotropy as a physical characteristic inherent in the material and entirely independent of the applied stresses and strains. Oda *et al.* (1985) detected three main sources of structural anisotropy in soils: the distribution of contact normals, the shape of the particles and the shape of the voids. In fact, the grain characteristics, the arrangement of particles and the presence of void, fissures and cracks constituting the microscopic structure of soils, are the reasons of the manifestation of

directional properties of the material at the macroscopic level. The specific arrangement and orientation of the particles is mainly due to the processes of formation of the soil deposits in situ and to the samples preparation technique in laboratory. Very often, reference has been made to a transverse isotropic description of the small-strain stiffness, with the plane of isotropy corresponding to the horizontal or the depositional plane. This is a very good and common assumption, confirmed by several experimental data, as will be shown in the following. In fact, the sedimentation of particles in situ often occurs along the vertical direction, leading to the formation of horizontal layers, suggesting that in the horizontal plane the material is isotropic, with the vertical direction representing the axis of anisotropy. For instance, under these conditions clays, for which the particles are oriented along the horizontal plane, present higher stiffness in the horizontal direction than in the vertical one. A transverse isotropic elastic solid is characterised by two shear moduli, in the horizontal plane G_{hh} and in the vertical one $G_{hv} = G_{vh}$ (see figure (1.1)) and the Young's moduli E_v and E_h along the vertical and horizontal directions, respectively. Based on experimental evidences, several Authors have deduced that the small strain behaviour of soils is anisotropic and quantified the stiffness through parameters of a cross-anisotropic elastic model.

There are different ways in which the very small strain stiffnesses can be determined. The elastic anisotropic behaviour of soils can be investigated experimentally by in situ and/or laboratory tests. The measurement of the shear waves velocity propagated along different directions and polarised in three orthogonal planes allows the determination of the corresponding small strain shear moduli. The field seismic tests (e.g. cross-hole, down-hole) are generally employed to measure the shear modulus in the vertical plane G_{vh} but, as indicated by Hight *et al.* (2007) and illustrated in figure (1.8) by Clayton (2011), performing a cross hole test equipped with an horizontally polarised hammer, one can determine the shear modulus G_{hh}, too.

In addition to the field tests, a series of laboratory tests permit to estimate the stiffness anisotropy. In particular, as already described, bender element tests can be successfully used to determine the shear moduli propagated and polarised along different directions. Nevertheless, it is worth noting that advanced laboratory devices, such as the hollow cylinder apparatus are needed to characterise a cross-anisotropic material. In this sense true triaxial tests equipped with high resolution displacement sensors are useful to measure the Young's moduli under both drained and undrained conditions and the Poisson's ratios, whereas torsional shear tests on hollow cylinder apparatus provide the shear modulus $G_{z\theta}$ and the Poisson's ratio

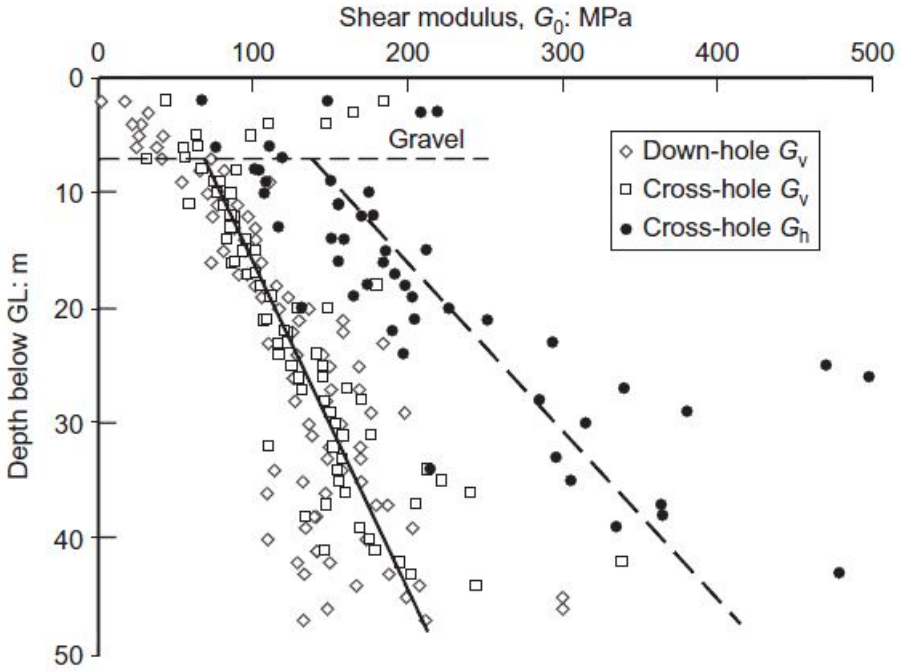

Figure 1.8: *Cross-hole data for the London clay (from Clayton (2011))*

$\nu_{z\theta}$, being z the axial (vertical) direction and θ the radial one. Therefore, laboratory testing, although complex, time consuming, and affected by sampling disturbance, can provide data from a range of stiffnesses greater than that obtained through field testing.

1.2.1 Inherent and stress/strain induced anisotropy

The structural anisotropy, depending on the microstructural characteristics and the history of formation of the deposit, represents an intrinsic property of the soil. As long as no external perturbations able to modify the internal structure of the material occur, the inherent anisotropy character is preserved, independently of the current state of stress/strain the soil is subjected to. As will be more clear in the following, unless irrecoverable (plastic) deformations are experienced by the material or, in other terms, if the overall soil response involves very small strain levels, no modification of the internal structure is observed. Nonetheless, in addition to the inherent anisotropy, the current stress (or strain) state causes the material to behave anisotropically under anisotropic loading. Therefore, this second form of anisotropy is commonly called stress/strain induced anisotropy. Several evidences demonstrate that the dependence of elastic stiffness on the current state of stress determines a difference in the elastic moduli along different directions due to the application of an anisotropic state of stress. Even a soil characterised by an isotropic

internal structure becomes anisotropic if an anisotropic stress state is applied. However, it is worth noting that switching back to the isotropic stress state, isotropy is recovered, demonstrating that the induced anisotropy is not an intrinsic property of the material. Stemming from the latter consideration, the inherent anisotropy can be directly detected for isotropic stress states whereas for anisotropic stress states it is more complex to separate the contribution to anisotropy due to the internal structure and to the current state of stress.

Properties due to structural anisotropy are often encountered in the field. For the case of clays, from the literature it clearly emerges that the elastic stiffnesses are usually higher in the horizontal direction than in the vertical one due to the typical sedimentation process and the particles shape. For sands the evidence is less straightforward because anisotropy is strongly affected not only by the shape of the particles but also, as hightlighted by Ezaoui & Di Benedetto (2009), by the significant differences in the orientation of interparticle contact planes caused by different sample preparation techniques. They obtained, in agreement with Mulilis *et al.* (1977) and Ibrahim & Kagawa (1991), a higher stiffness in directions close to the horizontal than the vertical for samples prepared by pluviation and vibration and an opposite trend in the case of moist tamping. Analogously, Stokoe *et al.* (1991) and Bellotti *et al.* (1996) found that for isotropic stress states, in samples prepared by pluviation, of Mortar sand and Ticino sand, respectively, the longitudinal and shear moduli are greater in the horizontal direction than in the vertical one, while Hoque & Tatsuoka (1998), adopting the same sample preparation procedure on various sands, obtained higher Young's moduli in the vertical direction than in the horizontal one.

The stress-induced anisotropy has been experimentally confirmed by many researchers, focusing on granular materials. Hoque & Tatsuoka (1998) realised that sands become more anisotropic as the stress state becomes more anisotropic. In particular, according to Hardin & Blandford (1989) and Yamashita & Suzuki (1999), the Young's modulus in a generic direction is primary controlled by the normal stress acting in the same direction. On the other side, Roesler (1979), Yu & Richart (1984), Stokoe *et al.* (1991, 1995) and Bellotti *et al.* (1996) showed that the shear modulus is controlled by the effective stresses acting in the plane of distortion and is slightly influenced by the stress component normal to the same plane. This means that in a transversely isotropic material, the horizontal shear modulus G_{hh} is a function of horizontal effective stress alone, whereas the vertical shear modulus G_{vh} is a function of both vertical and horizontal effective stress.

Some Authors investigated this feature from a micromechanical perspective in

order to clarify the role of the current stress on the elastic stiffness anisotropy. A first attempt to clarify the difference between the stress-induced anisotropy due to anisotropic stress states and fabric-induced or inherent anisotropy caused by the geometry of the soil particles and soil packing was made by Oda *et al.* (1985) and Rothenburg & Bathurst (1989, 1992). They proposed analytical descriptions of the normal forces acting on the particles through an associated probability density distribution in different directions. In particular, it is opinion of Oda *et al.* (1985) that along the direction of maximum principal compression the particles contact forces increase and column-like load paths appear. As a consequence, from a macroscopical point of view, the material becomes stiffer in that direction. More recently numerical studies based on micromechanical theory (e.g., Chang *et al.* (1991), Yimsiri and Soga (2000, 2002)) and numerical simulations using the discrete element method (DEM) have been carried out to model the stiffness anisotropy of soils. Guided by these studies, Wang & Mok (2008) first performed a series of measurements of shear waves propagation velocities with bender elements on Toyoura sand and rice grains assembly for both isotropic and anisotropic stress paths to isolate the effect of the stress induced anisotropy. Then they verified the experiments through DEM simulations of shear tests, adopting random packing of multisized spheres and incorporating the Hertz-Mindlin contact law. Note that the use of spheres in DEM simulation limits the anisotropic character to that induced by the current state of stress. The shear modulus was found to be relatively independent of the out-of-plane stress component, which can be revealed by the change in the contact normal distribution and the normal contact forces on that plane in the DEM simulations. These observations, again, suggest that an increase of the contact normal forces on the shearing planes can lead to a higher associated shear modulus, whereas an increase of normal contact forces in the orthogonal direction does not change the shear stiffness in the shear plane. In addition, the fact that G_{vh} and G_{hv} increase at the same rate not only indicates that the out-of-plane stress component contributes equally to the shear modulus, but it also implies that the horizontal plane of the sample is the plane of isotropy. Only small inherent stiffness anisotropy for Toyoura sand has been observed whereas they measured very pronounced stiffness anisotropy in rice. Rice grains, having relatively more anisotropic geometric shapes than Toyoura sand, exhibit greater inherent stiffness anisotropy, with $G_{hh} > G_{hv} = G_{vh}$, which is comparable to the typical case of clays. Similar results have been subsequently obtained by Gao & Wang (2013) by bender elements measurements on the Leighton Buzzard sand. They proposed a micromechanical insight by performing DEM simulations applying anisotropic loading paths. Accordingly to Wang & Mok (2008),

the increase normal contact forces in the vertical direction due to an increase of the vertical normal stress induced an increase of the shear modulus in the vertical plane rather than in the horizontal one.

In the following some typical experimental results obtained for both sandy and clayey soils are reported, with special enphasis on the few sets of data in which both measurements of the shear moduli in the horizontal and vertical planes and the Young's moduli along the horizontal and vertical directions have been carried out.

1.2.2 Clays

Several Authors have measured the velocity of propagation of shear waves along different directions in natural and reconstituted clay samples, by bender elements with different position and orientation (Jamiolkowski *et al.* (1994), Hight *et al.* (1997), Pennington *et al.* (1997), Jovičić & Coop (1998), Ling *et al.* (2000), Callisto & Rampello (2002), Gasparre (2005), Gasparre *et al.* (2007), Ng & Yung (2008), Teachavorasinskun & Lukkanaprasit (2008), Cho & Finno (2009), Yimsiri & Soga (2011), Kim & Finno (2014)). For instance, Jovičić & Coop (1998) obtained the elastic shear moduli G_{hh}, G_{hv} and G_{vh} for undisturbed samples of London clay for different mean effective pressures, under isotropic stress conditions. As reported in figure (1.9), the material is transverse isotropic, with $G_{hv} = G_{vh}$ and higher values of the shear modulus were measured in the horizontal plane.

This is a typical result for clays; in fact, due to the formation processes, the clay particles tend to acquire an horizontal orientation during deposition, therefore the material is stiffer in the horizontal plane than in the vertical one. The effect of the soil internal structure on the elastic stiffness anisotropy was pointed out by Teachavorasinskun & Lukkanaprasit (2008). They performed bender elements tests on undisturbed samples of the Bangkok clay in a square oedometer apparatus (thus, under K_0 conditions) while measuring the shear moduli G_{hh} and G_{vh}. For samples trimmed parallel to the bedding direction, as conventionally done, the horizontal shear modulus is larger than the vertical one; then, for the same stress conditions, samples were trimmed 90 degrees apart and an opposite trend was observed. In the first case the anisotropy ratio is greater than unity while in the second case is less than unity, as reported in figure (1.10). This clearly indicates the influence of the particles orientation on the inherent anisotropy.

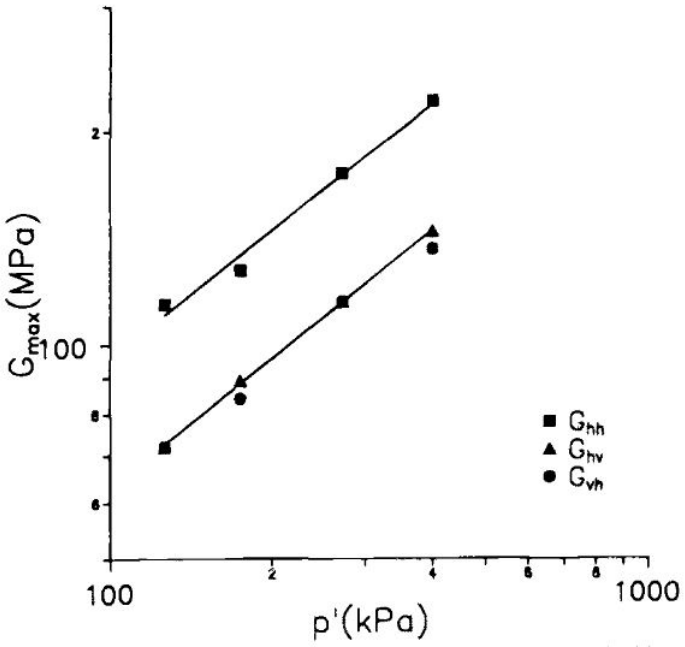

Figure 1.9: *Shear moduli for samples of industurbed London clay under isotropic stress state (from Jovičić & Coop (1998))*

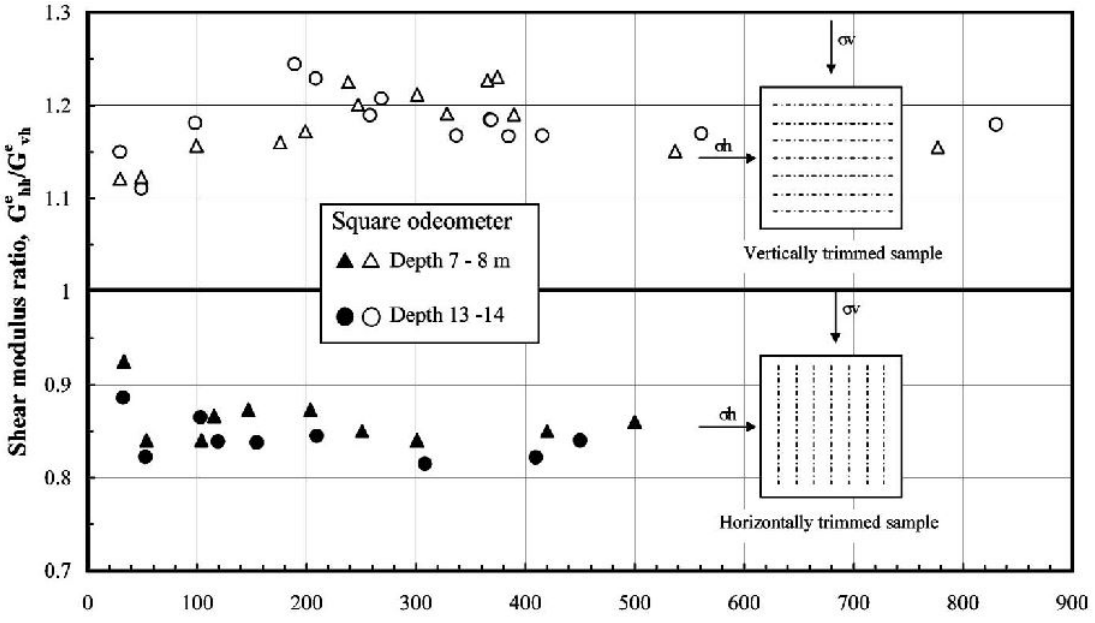

Figure 1.10: *Effect of inherent anisotropy in Bangkok clay samples (from Teachavorasinskun & Lukkanaprasit (2008))*

Additional interesting results have been obtained by Callisto & Rampello (2002) on the natural Pietrafitta clay. They compressed the material along radial stress paths for different stress ratios under drained conditions in true triaxial apparatus and measured the elastic shear moduli for different mean effective pressures. In

agreement with Jovičić & Coop (1998) they found that $G_{hh} > G_{hv} = G_{vh}$ and that the anisotropy ratio $\frac{G_{hh}}{G_{hv}}$ is not significantly affected by the mean effective pressure; specifically it is almost constant for overconsolidated states. However, as depicted in figure (1.11), a dependency of the anisotropy ratio on the current stress ratio was found, clearly indicating the effect of the stress induced anisotropy.

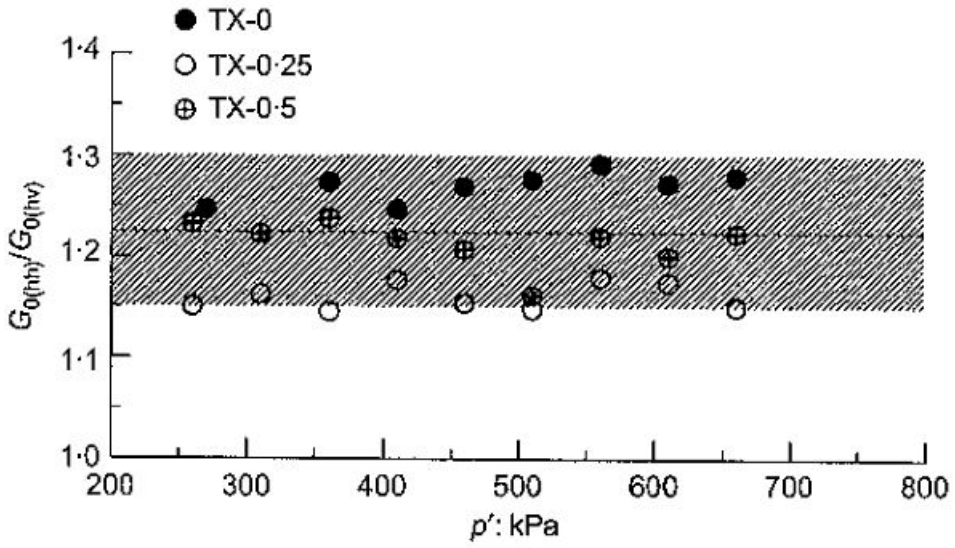

Figure 1.11: *Anisotropy ratio against mean effective pressure for Pietrafitta clay (from Callisto & Rampello (2002))*

Despite the number of Authors cited above, only few studies have been carried out in sufficient depth to determine the full set of anisotropic stiffness parameters. Few studies of anisotropy in heavily overconsolidated clays are noteworthy: the works by Ling *et al.* (2000) and Yimsiri & Soga (2011) for the Gault clay and by Gasparre (2005) and Gasparre *et al.* (2007) for the London clay. Both these sources showed that the shear stiffness on horizontal planes was about two times greater than the shear stiffness on vertical planes. Limiting the attention to the latter two works, the elastic anisotropic behaviour of intact London clay has been investigated performing triaxial and hollow cylinder tests with high resolution axial and radial LVDT transducers and bender elements, under static and dynamic test conditions. Gasparre (2005) and Gasparre *et al.* (2007) detected the terms of the instantaneous elastic stiffness matrix assuming the hypothesis of cross anisotropy. They obtained the Young's moduli E_v and E_h along the vertical and horizontal directions through static and hybrid dynamic triaxial tests and the shear moduli G_{hh} and G_{hv} by bender element probing. In addition, a hollow cylinder apparatus (HCA) was used to perform measurements of the shear stiffness component G_{vh} and the Young's moduli. They conclude that the results obtained using the two different experimental setups

generally exhibit good agreement in terms of stiffness parameters. The samples of London clay, retrieved at different depths, were reconsolidated at the three different in situ stress states, illustrated in figure (1.12) by black dots, based on the geological history of London clay as reported by Hight *et al.* (2003).

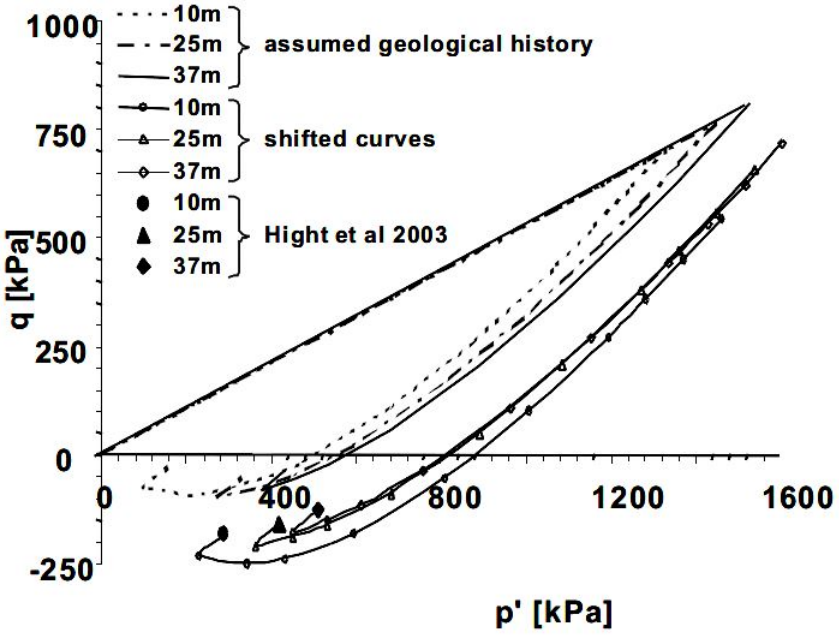

Figure 1.12: *Stress states reconsolidation of London clay samples (from Hight et al. (2003))*

London Clay is a heavily overconsolidated soil, characterised in situ by high horizontal effective stresses ($K_0 > 1$) and a stiffer response in the plane of deposition (horizontal) than in the vertical direction. This is not only due to the anisotropic in situ stress state but also to the typical planar shape of the grains and the depositional processes, which lead to a preferred particles orientation along the horizontal plane.

In the laboratory, the consolidation process consisted of an initial isotropic stress path, followed by a constant mean effective pressure increment until the presumed in situ stress state was reached, as depicted in figure (1.13). With B2(c), B2(a) and A3 are indicated the main London clay stratigraphic units.

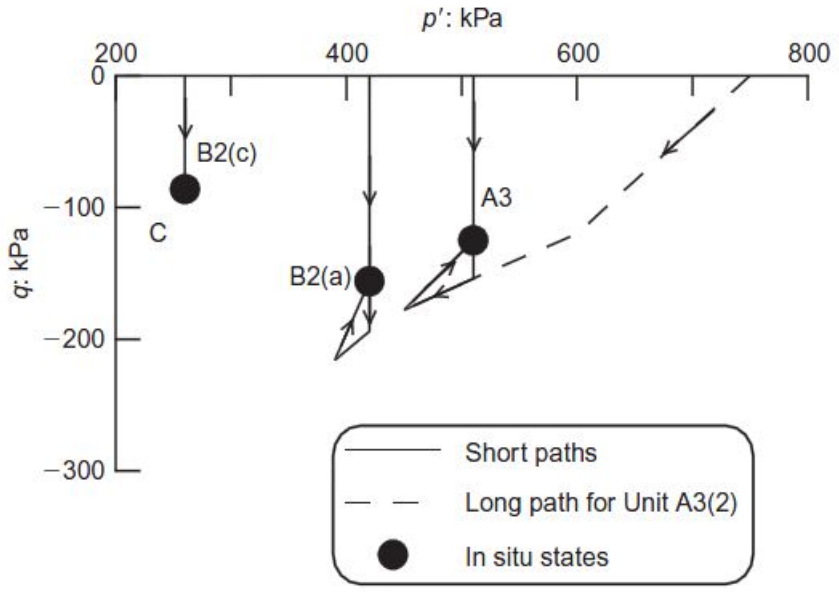

Figure 1.13: *Consolidation paths of London clay samples (from Gasparre et al. 2007)*

To match the estimated in situ stresses, determined from in situ suction measurements from extruded samples, a single final representative average stress point was adopted for each stratigraphic unit. Common in situ stresses were applied to units B2(c) and C. The specimens were then subjected to the static and dynamic probing to detect their stiffness characteristics and the bulk moduli were directly measured by constant q triaxial probing tests. The Young's, shear and bulk moduli profiles are reported in figure (1.14) together with the main stratigraphic units.

The obtained elastic moduli show a general good agreement, irrespectively of the different testing techniques adopted, and this confirms the strong anisotropic character of the London clay, with $E_h > E_v$ and $G_{hh} > G_{vh}$ and anisotropy ratio $\frac{G_{hh}}{G_{hv}}$ around 2. Note that despite samples from different depths were tested at the same stress state, a scatter in the experimental results was found, probably due to the slightly different initial void ratios of the samples. In addition, Gasparre (2005) carried out tests on the same intact material compressed along the isotropic axis, determining the shear moduli at different mean effective pressures by bender elements polarised along perpendicular planes. In this sense, she obtained qualitatively analogous results to those reported by Jovičić & Coop (1998).

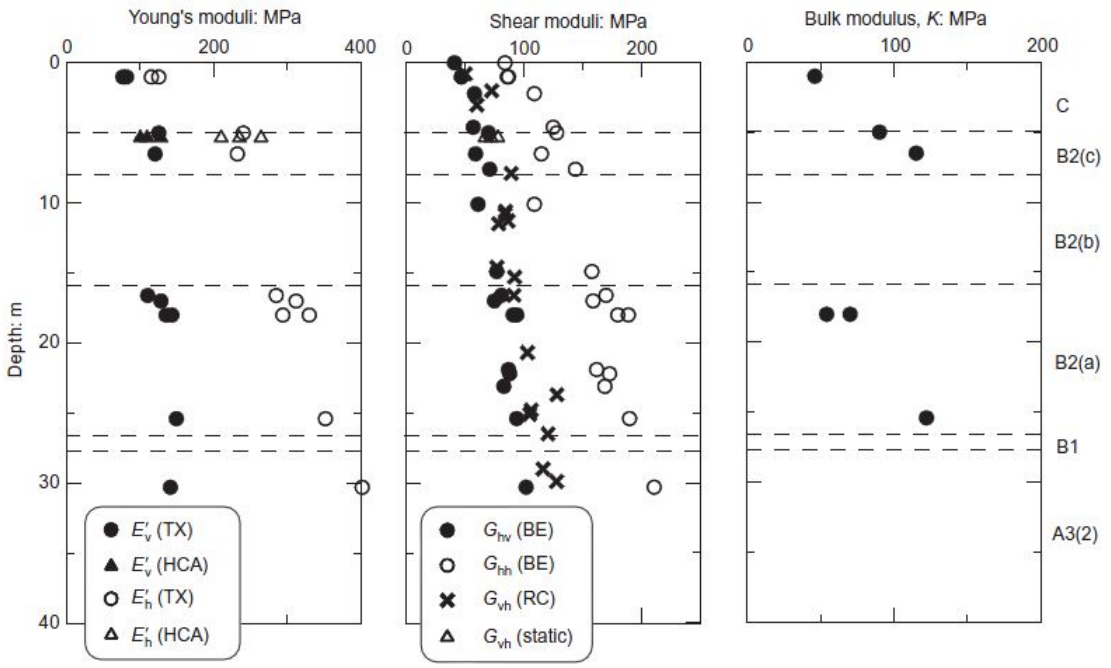

Figure 1.14: *Profiles of elastic moduli with depth for London clay (from Gasparre et al. 2007)*

1.2.3 Sands

Similarly to what shown for clays, most of the experimental results available for sands consist in the evaluation of the elastic shear moduli based on the measurement of the shear waves velocity by bender element tests (Lo Presti and O'Neill (1991), Stokoe *et al.* (1991), Bellotti *et al.* (1996), Zeng & Ni (1999), Kuwano & Jardine (2002), Wang & Mok (2008), Gao & Wang (2013), Gu *et al.* (2013)). In other cases the Young's moduli E_v and E_h along the vertical and horizontal directions were determined by local transducers fitted in triaxial testing device under isotropic stress states (Hoque & Tatsuoka (1998)) while the vertical Young's modulus E_z, the shear modulus $G_{z\theta}$ and the Poisson's ratio $\nu_{z\theta}$ by both static and dynamic triaxial and torsional shear tests on hollow cylinder apparatus (HongNam & Koseki (2005), Chaudhary *et al.* (2003), Ezaoui & Di Benedetto (2009)). A more complete set of elastic parameters was proposed by Bellotti *et al.* (1996) and Kuwano & Jardine (2002).

Bellotti *et al.* (1996) performed laboratory seismic tests to investigate the anisotropic nature of the small strain stiffness of the Ticino river sand for different effective stresses and relative densities. The uniform, coarse to medium-sized Ticino sand was deposited by pluviation in large specimens at medium density ($D_r = 41\%$) and then subjected to radial triaxial stress paths characterised by different K_0. A series

of geophones were employed to generate P and S waves in three orthogonal planes (the horizontal and the two vertical). During the loading process they measured the shear wave velocities propagating along the vertical and horizontal directions and polarised in the vertical and horizontal planes; they also carried out measurements of the compression wave velocities along the same directions. As a consequence, in addition to the shear moduli G_{hh}, G_{hv} and G_{vh} they obtained, under the hypothesis of transverse isotropy, the Young's moduli E_v and E_h. In fact, because of the absence of the liquid phase in the samples, the velocity of the compression waves provides data on the normal elastic stiffness components. Furthermore, they found that the velocity of waves propagated and polarised in the horizontal plane were independent of the direction of propagation, thus indicating that the horizontal plane is characterised by an isotropic behaviour (i.e. cross anisotropy holds for those experiments). The elastic parameters are syntethised in table (1.1).

K	ρ: Mg/m^3	σ'_v: kPa	σ'_h: kPa	C_{13}: kPa	C_{12}: kPa	M_h: kPa	M_v: kPa	G_{hh}: kPa	G_{vh}: kPa	E_v: kPa	E_h: kPa	υ_{hh}	υ_{vh}	υ_{hv}
0·5	1·503	50	25	25 500	30 493	142 766	167 819	56 136	56 958	160 313	133 790	0·192	0·147	0·123
	1·505	100	50	35 000	42 266	196 481	235 258	77 108	79 545	224 996	184 094	0·194	0·147	0·120
	1·507	150	75	42 000	51 190	236 967	286 803	92 888	96 767	274 560	222 028	0·195	0·146	0·118
	1·509	200	100	48 000	58 659	270 758	330 225	106 050	111 240	316 236	253 655	0·196	0·146	0·117
	1·511	250	125	53 000	65 212	300 346	368 440	117 567	123 983	353 072	281 393	0·197	0·145	0·116
	1·512	300	150	57 000	71 093	326 763	402 891	127 835	135 409	386 559	306 234	0·198	0·143	0·113
1.0	1·502	50	50	44 500	40 659	194 173	163 913	76 757	63 165	146 148	177 559	0·157	0·189	0·230
	1·504	100	100	61 000	58 194	272 005	227 224	106 906	88 883	204 686	248 788	0·164	0·185	0·225
	1·506	150	150	72 500	71 801	331 473	276 094	129 836	108 595	250 026	303 525	0·169	0·180	0·218
	1·508	200	200	82 500	83 357	381 538	317 153	149 090	125 227	287 873	349 437	0·172	0·177	0·215
	1·510	250	250	91 000	93 630	425 665	353 244	166 017	139 906	321 351	389 975	0·174	0·175	0·213
	1·512	300	300	99 000	102 975	465 583	385 873	181 304	153 207	351 396	426 512	0·176	0·174	0·211
1.5	1·504	50	75	32 000	41 995	227 283	145 356	92 644	73 138	137 751	214 692	0·159	0·119	0·185
	1·505	67	100	35 000	50 214	262 469	168 063	106 128	87 901	160 227	247 790	0·168	0·112	0·173
	1·508	100	150	39 000	64 513	321 846	206 691	128 666	101 972	198 817	304 100	0·182	0·101	0·154
	1·511	150	225	44 000	82 659	394 631	254 061	155 986	123 905	245 949	372 461	0·194	0·092	0·140
	1·513	200	300	48 000	98 351	456 020	204 090	178 834	142 264	285 778	429 904	0·202	0·087	0·130
	1·515	250	375	50 000	112 619	510 296	329 528	198 839	158 401	321 501	480 765	0·209	0·080	0·120
	1·517	300	450	53 000	125 714	559 545	361 724	216 916	172 970	353 525	526 567	0·214	0·077	0·115
2.0	1·507	50	100	46 000	57 067	274 628	145 646	108 781	74 432	132 887	253 143	0·164	0·139	0·264
	1·507	60	120	51 000	63 089	300 062	159 667	118 487	81 309	145 342	276 054	0·165	0·140	0·267
	1·511	100	200	66 000	83 688	385 587	207 102	150 949	104 435	188 537	353 785	0·172	0·141	0·264
	1·514	150	300	81 000	104 658	470 476	254 565	182 909	127 371	231 750	430 710	0·177	0·141	0·262
	1·516	200	400	94 000	122 568	541 765	294 673	209 598	146 629	268 072	495 031	0·181	0·141	0·261
	1·519	250	500	104 000	138 624	604 979	330 398	233 177	163 709	301 307	552 649	0·185	0·140	0·257
	1·521	300	600	115 000	153 245	661 865	362 677	254 310	179 090	330 228	603 594	0·187	0·141	0·258

Table 1.1: *Elastic parameters of medium dense dry Ticino sand (from Bellotti et al. (1996))*

These results show that the Ticino sand is characterised by a non-negligible degree of anisotropy. It is worth analysing the results obtained in terms of elastic moduli for different K_0 radial stress paths. Under isotropic stress conditions the inherent anisotropy is measured, with the shear and Young's moduli higher in the horizontal plane than in the vertical one. The structural anisotropy is then modified by a subsequent application of an anisotropic loading. For stress states characterised by $K_0 \geq 1$ the anisotropic ratio $\frac{G_{hh}}{G_{hv}}$, as well as the ratio $\frac{E_h}{E_v}$, are greater than unity whereas for $K_0 = 0.5$ the elastic stiffnesses in the vertical direction become greater than those in the horizontal one. These results are in full agreement with other experimental results and with the numerical DEM simulations previously illus-

trated and clearly show the influence of the stress ratio on the small strain stiffness anisotropy.

Another interesting investigation was conducted by Kuwano & Jardine (2002) on the elastic anisotropic behaviour of the Ham River sand, a uniform, medium-sized and sub-angular-shaped quartz sand. They employed large specimens, of 100mm in diameter and 200mm height, obtained by air pluviation and then water saturated. They performed triaxial tests equipped with high-resolution axial and radial LVDT transducers for the measurement of radial and vertical displacements and bender elements for the measurement of velocity of propagation of shear waves. Figure (1.15) illustrates the stress path imposed to each specimen, consisting of an initial triaxial compression from $p = 30\,\text{kPa}$ until the state of stress related to $K_0 = 0.45$, this followed by an anisotropic consolidation path characterised by constant stress ratio.

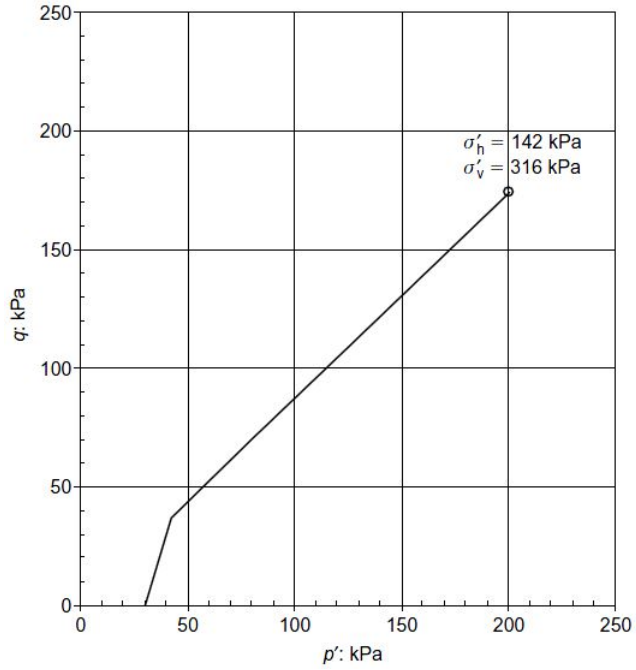

Figure 1.15: *Effective anisotropic stress path (from Kuwano & Jardine, 2002)*

Under the hypothesis of cross anisotropy, they illustrate the evolution of the instantaneous elastic stiffness matrix components with the mean effective pressure. In detail, they obtained the Young's moduli E_v and E_h along the vertical and horizontal directions through static tests and, for the same states, the shear moduli G_{hh}, G_{hv} and G_{vh} by bender elements probing, as illustrated in figure (1.16). The material appears to be characterised by a non-negligible degree of anisotropy, as indicated by the different Young's and shear stiffness moduli observed along different directions

by the very beginning of the probing, carried out once the required anisotropic stress state had first been achieved. The results also highlight a well-defined non-linear dependency of the stiffness terms on the current stress state.

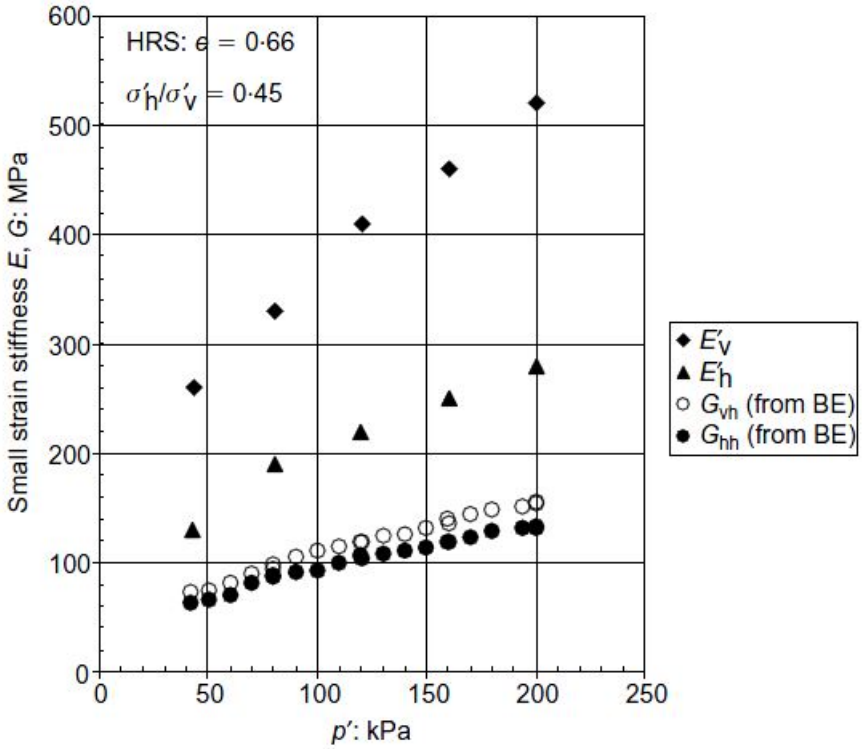

Figure 1.16: *Young's and shear moduli against the mean effective pressure (from Kuwano & Jardine, 2002)*

1.3 Effect of plastic strains on the elastic behaviour

Several experimental data show that plastic deformations may strongly affect the current elastic modulus of many solids like soils, rocks and concrete: this phenomenon is commonly referred to as elastoplastic coupling. For instance in clays the elastic stiffness depends, as illustrated above, on the past history of the material through the preconsolidation pressure, which plays the role of hardening variable in many constitutive models and usually depends on the volumetric plastic strains. The elastoplastic coupling can occur in many other forms and for different materials. The rocks and concrete behaviour can be idealised as elastoplastic and the elastic stiffness may drastically change as plastic strains develop. For such materials the raise of plastic deformations typically leads to a reduction of the elastic stiffness, as depicted in figure (1.17), where the stress-strain experimental response of a

sandstone specimen subjected to cyclic uniaxial compression is reported (Bieniawski (1969)).

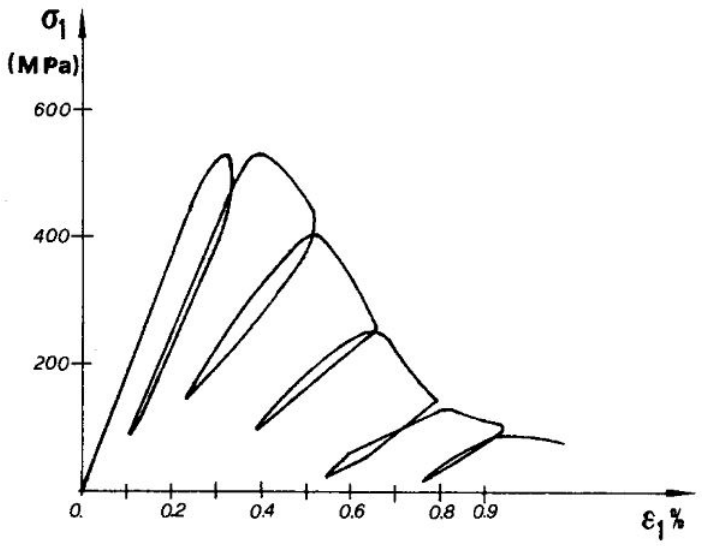

Figure 1.17: *Stress-strain response of rock specimen under uniaxial compression (from Bieniawski (1969))*

When the material undergoes large strains, the elastic moduli reduce due to the reopening, the creation and the propagation of new fissures and cracks and the breakage of cemented bonds. In other terms, the occurrence of plastic strains within the specimen induces a degradation of the elastic stiffness of the material.

Another interesting form of elastoplastic coupling involves the effect induced by the plastic strains on the elastic stiffness anisotropy of clays.

The small strain anisotropy of soils can be altered by the application of loads that produce large distortion in the material. In fact, the development of plastic strains is often characterised by a change in the orientation of the particles and the arrangement of the internal microstructure. Very few experimental studies have been conducted in order to investigate the influence of irreversible deformations on the small strain stiffness anisotropy. In particular, for clays two works are worth noting.

Jovičić & Coop (1998) measured the elastic shear moduli G_{hh}, G_{hv} and G_{vh} in a triaxial apparatus equipped with bender elements for reconstituted samples of the London clay. The material was reconsolidated in consolidometer at the estimated in situ preconsolidation pressure of 1500 kPa and then unloaded to $p = 400$ kPa, then the samples were subjected to large isotropic stresses in order to observe how the anisotropy would be affected by the increased isotropic straining of the clay. The material was loaded beyond the preconsolidation pressure experienced in the

consolidometer and at the same time the shear moduli were measured. As depicted in figure (1.18), the material is characterised by an initial degree of anisotropy that remains constant up to the preconsolidation pressure. As the isotropic loading increases, the clay tends to become isotropic, even though it is clear that very large strains would be necessary to obtain the anisotropy ratio $\frac{G_{hh}}{G_{hv}} = 1$. Therefore, these processes of change are very slow, requiring the development of very large plastic strains. The elastic anisotropy due to the previous history experienced by the material persists as long as the strain increments reach a level appropriate to the new state.

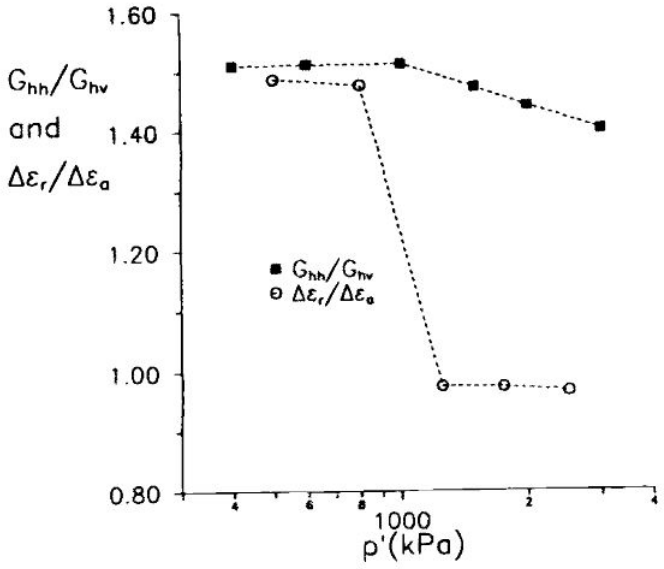

Figure 1.18: *Anisotropy ratio for reconstituted London clay (from Jovičić & Coop (1998))*

Mitaritonna *et al.* (2014) experimentally investigated the small strain behaviour of the reconstituted Lucera clay to observe the evolution of the stiffness anisotropy with the state of stress along isotropic and anisotropic stress paths. They employed a stress path controlled triaxial apparatus equipped with local strain transducers (LVDT) and bender elements for the measurements of velocity of the shear waves. In detail, from the horizontally propagated and polarised in the horizontal plane velocity, V_{hh} and that propagated in the horizontal direction and polarised in the vertical plane, V_{hv}, they determined the elastic shear moduli G_{hh} and G_{hv} respectively. The Authors employed a reconstituted clay to directly relate the stiffness anisotropy observed during the test to the imposed stress path. Differently from Jovičić & Coop (1998), the reconstituted clay was first compressed in a consolidometer up to a nominal vertical effective stress of 100 kPa, low enough to allow the material to experience a wide modification of its initial state during the following

radial compression paths imposed in the triaxial apparatus. In fact, after the one-dimensional consolidation the specimens were subjected to a first isotropic stress increment and then either further compressed isotropically or, after a constant p path, compressed along radial, stress ratio η constant, stress paths, reaching mean effective pressures much higher (up to $p = 1350$ kPa) than those previously imposed in the consolidometer, as depicted in figure (1.19).

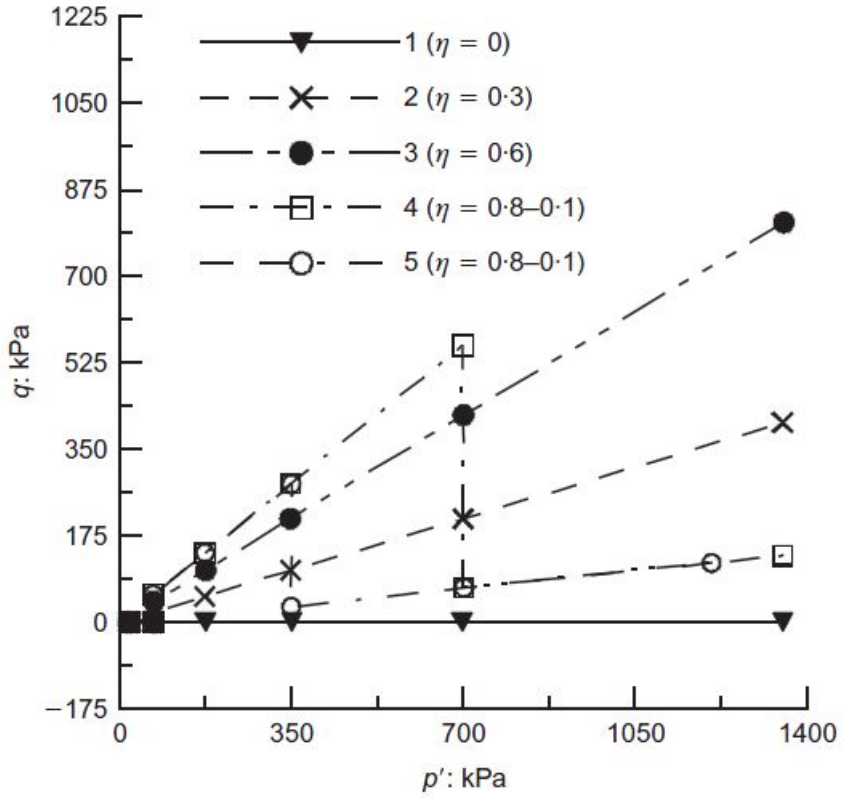

Figure 1.19: *Stress paths for the reconstituted Lucera clay (from Mitaritonna et al. (2014))*

The results show that the small strain anisotropy stiffness ratio $\frac{G_{hh}}{G_{hv}}$, which denotes the anisotropic character, smoothly adapts to the imposed stress history, evolving during the imposed radial loading histories until achieving different constant values for different stress ratios. As shown in figure (1.20), during the test corresponding to $\eta = 0.6$, the anisotropy ratio is always constant at the value 1.12, corresponding to the initial anisotropy of the clay. This result is consistent with the hypothesis that the soil in the consolidometer was subjected to the same stress ratio, corresponding to the value of $K_0 = 0.56$ computed through the Jaky's formula. Compression paths characterised by stress ratio $\eta = 0$ and $\eta = 0.3$, lower than the initial $\eta = 0.6$, induce a permanent reduction in the degree of anisotropy whereas

the anisotropy ratio increases up to 1.22 where the soil was compressed along the highest ratio $\eta = 0.8$.

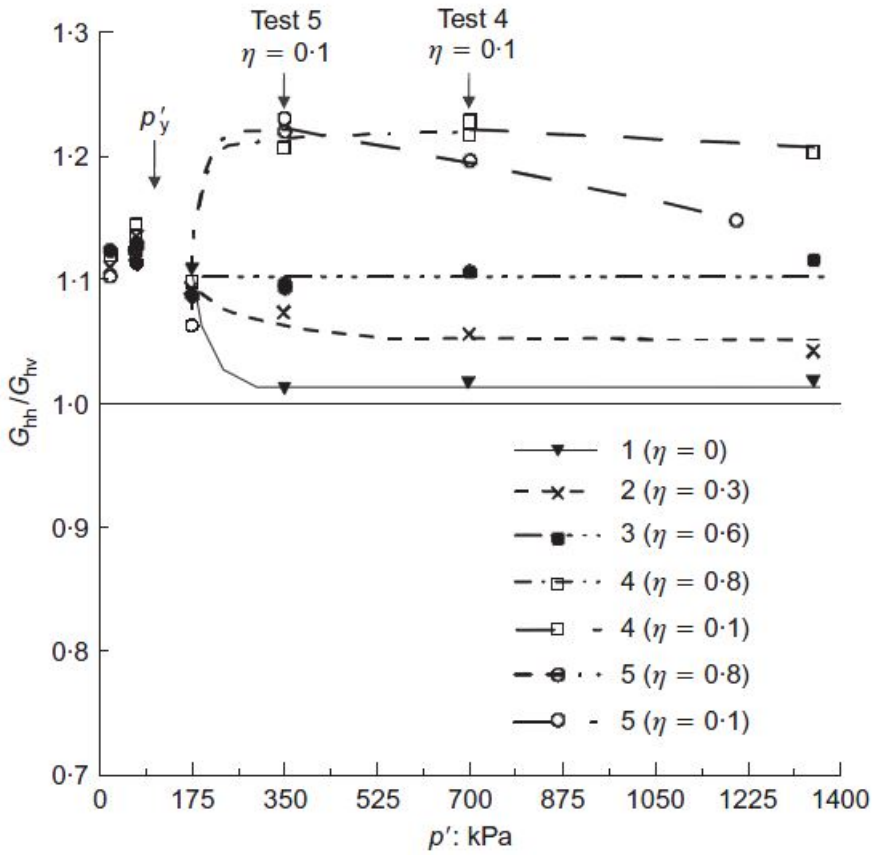

Figure 1.20: *Evolution of the anisotropy ratio with the mean effective pressure for the Lucera clay (from Mitaritonna et al. (2014))*

The large values of effective stresses reached during the tests, as compared to the initial preconsolidation pressure of the clay as induced in the consolidometer, trigger large plastic deformations along the virgin radial paths, thus modifying the internal structure of the soil, which controls the elastic anisotropic response at the macroscopic level. It is worth noting that constant values of the anisotropy ratio are reached for mean effective pressures $p > 350$ kPa, which corresponds approximately to four times the preconsolidation pressure imposed in the consolidometer. This latter result indicates that the clay has to be compressed well beyond the preconsolidation pressure in order to observe a significant modification of its directional properties. In other words, a change in the degree of stiffness anisotropy is possible in clays when the stress ratio varies only if large plastic strains occur, as a small amount of irreversible deformation is not sufficient to modify the previous directional character of the soil (see Jovičić & Coop (1998)).

In order to corroborate the above results, the changes in clay fabric have been

investigated by means of scanning electron microscopy (SEM). At the end of the tests samples have been fracturated along horizontal and vertical surfaces, then high resolution pictures have been taken and the fabric orientation has been detected through a digital image processing. The fabric orientation is described by a series of vectors determined by a line algorithm and a rose histogram is used to represent their orientation distribution. Then a statistical analysis of the vector lengths permits to synthetically describe the degree of orientation with the scalar L. The higher is the value of L, the more iso-oriented is the internal structure. In figure (1.21) the SEM picture and the corresponding direction histogram at the end of consolidation in consolidometer are reported.

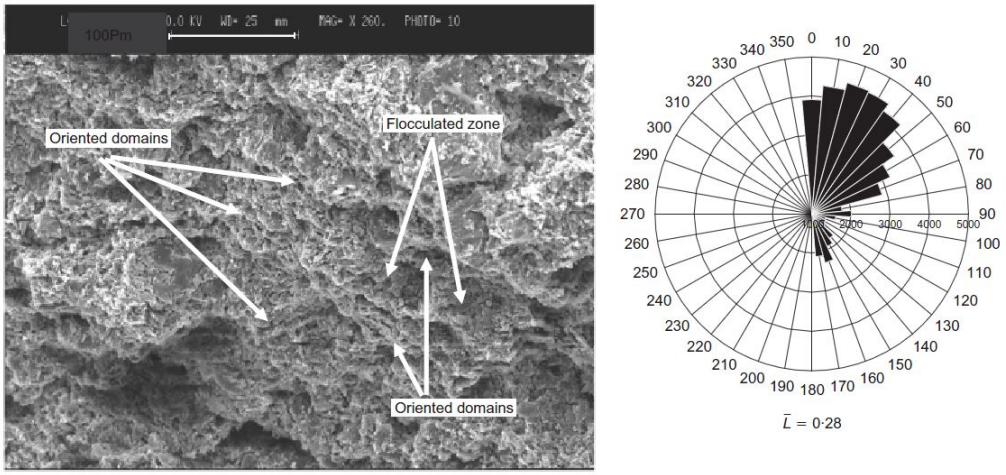

Figure 1.21: *SEM picture and direction histogram at the end of consolidation in consolidometer (from Mitaritonna et al. (2014))*

The micro characteristics of the different clay specimens are then compared to those observed after the application of the triaxial radial stress paths. Figures (1.22) and (1.23) refer to the final stage for $\eta = 0.6$ and $\eta = 0.3$, respectively. In both cases the fabric is more densely packed as compared to that prior to the loading stages. However, in the case $\eta = 0.6$ the scalar L varies from 0.28 to 0.27, indicating that the internal microstructure is almost the same, whereas in the case $\eta = 0.3$ the value 0.13 is attained, demonstrating a rearrangement of the fabric, characterised by a lower degree of orientation.

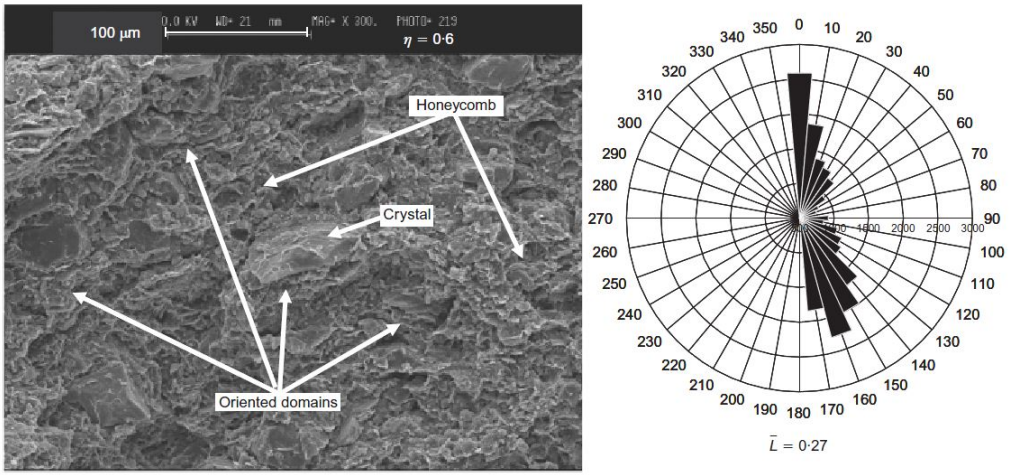

Figure 1.22: *SEM picture and direction histogram at the end of the radial stress path* ($\eta = 0.6$)*(from Mitaritonna et al. (2014))*

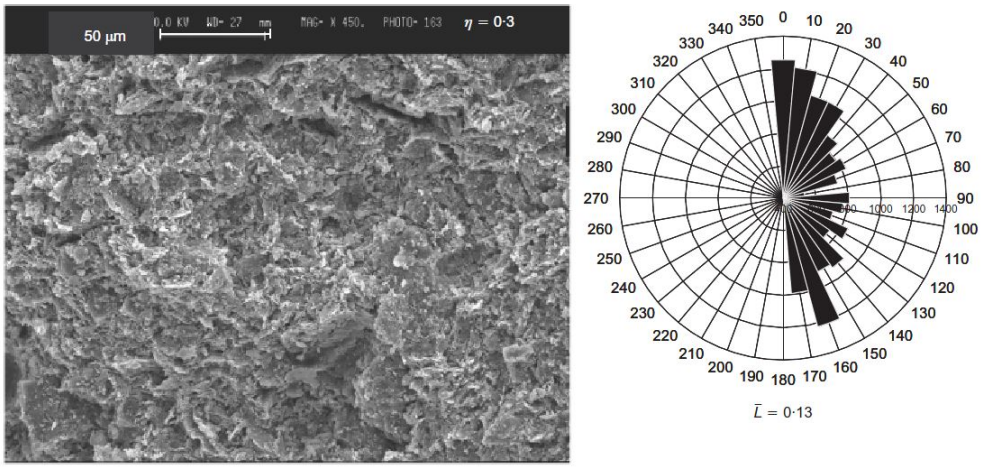

Figure 1.23: *SEM picture and direction histogram at the end of the radial stress path* ($\eta = 0.3$)*(from Mitaritonna et al. (2014))*

The works of Jovičić & Coop (1998) and Mitaritonna *et al.* (2014) show that the inherent anisotropy in clays is a variable factor controlled by the microstructural modification induced by plastic straining only if large continuous strains along the same radial path are applied to achieve the corresponding permanent modification of the soil fabric and, related to this, of the elastic anisotropy.

Chapter 2

Isotropic and anisotropic elasticity: state of the art

In the present chapter the reversible mechanical behaviour of soils is discussed from a constitutive modelling point of view. It is universally accepted that for very small strain levels the soil exhibites a recoverable and conservative response, which can be modelled as elastic. However, as supported by the experimental evidences, the elastic behaviour of most soils does not conform to the linear isotropic elasticity and two additional important features need to be taken into account: anisotropy and nonlinearity. Particularly, in the following some significant existing models are illustrated, first with reference to the linear and nonlinear isotropic formulations and subsequently to the anisotropic ones.

In the present work the soil mechanics sign convention is assumed and all stresses are effective stresses. The notation employed here is mainly that of Chaves (2013), Holzapfel (2000) and Bigoni (2012). All tensor and vector quantities are written in boldface form, italic letters are used for the vectors. The fourth order tensors are represented by the character $\mathbb{A}$. Considering the Cartesian basis $\boldsymbol{e}_i$, $\boldsymbol{e}_j$, $\boldsymbol{e}_k$, $\boldsymbol{e}_l$ and two second order tensors $\mathbf{a}$ and $\mathbf{b}$ the products are defined as $\mathbf{a} : \mathbf{b} = a_{ij}b_{ij}$, $\mathbf{ab} = a_{ij}b_{jk}\boldsymbol{e}_i\boldsymbol{e}_k$, $\mathbf{a} \otimes \mathbf{b} = a_{ij}b_{kl}\boldsymbol{e}_i\boldsymbol{e}_j\boldsymbol{e}_k\boldsymbol{e}_l$, $\mathbf{a} \bar{\otimes} \mathbf{b} = \frac{1}{2}\left(a_{ik}b_{jl} + a_{il}b_{jk}\right)\boldsymbol{e}_i\boldsymbol{e}_j\boldsymbol{e}_k\boldsymbol{e}_l$, $\mathbf{a} \underline{\otimes} \mathbf{b} = a_{ik}b_{jl}\boldsymbol{e}_i\boldsymbol{e}_j\boldsymbol{e}_k\boldsymbol{e}_l$ and $\mathbf{a} \underline{\otimes} \mathbf{b} = a_{il}b_{jk}\boldsymbol{e}_i\boldsymbol{e}_j\boldsymbol{e}_k\boldsymbol{e}_l$, where repeated indeces indicate a summation, according to the Einstein convention. The trace of a second order tensor is $\mathrm{tr}\left(\mathbf{a}\right) = a_{ij}\delta_{ji} = a_{ii}$ with δ_{ji} denoting the Kronecker delta and $\mathbf{I} = \delta_{ij}\boldsymbol{e}_i\boldsymbol{e}_j$ is the second order identity tensor. The strain tensor $\boldsymbol{\varepsilon} = \frac{1}{3}\mathrm{tr}\left(\boldsymbol{\varepsilon}\right)\mathbf{I} + \mathbf{e}$ and the stress one $\boldsymbol{\sigma} = \mathrm{tr}\left(\boldsymbol{\sigma}\right)\mathbf{I} + \mathbf{s}$ are symmetric, with $\mathbf{e}$ and $\mathbf{s}$ denoting their deviatoric parts. The stress invariants are the mean pressure $p = \frac{1}{3}\mathrm{tr}\left(\boldsymbol{\sigma}\right) = \frac{1}{3}\sigma_{ij}\delta_{ji}$ and the deviatoric stress $q = \sqrt{\frac{3}{2}\mathbf{s} : \mathbf{s}} = \sqrt{\frac{3}{2}s_{ij}s_{ij}}$ while their conjugate strain invariants are the volu-

metric strain $\varepsilon_v = \mathrm{tr}\,(\boldsymbol{\varepsilon}) = \varepsilon_{ij}\delta_{ji}$ and the deviatoric strain $\varepsilon_s = \sqrt{\frac{2}{3}\mathbf{e} : \mathbf{e}} = \sqrt{\frac{2}{3}e_{ij}e_{ij}}$. In the present chapter the strains have to be intended as elastic. Further details about tensor notation and derivatives can be found in appendix A.

2.1 Generality

The mechanical behaviour of soils at very small strain levels can be successfully reproduced in the framework of elasticity, which guarantees a reversible (i.e. fully recoverable) response. From a constitutive point of view, the material is considered elastic if a one-to-one relationship between the stress $\boldsymbol{\sigma}$ and the strain $\boldsymbol{\varepsilon}$ tensors exists. In particular the stress tensor can be expressed as a single valued function of the strain in the form:

$$\boldsymbol{\sigma} = f\,(\boldsymbol{\varepsilon}) \tag{2.1}$$

where $f\,(\boldsymbol{\varepsilon})$ is a second order tensor valued function of the strain. If this function is linear in $\boldsymbol{\varepsilon}$ eq. (2.1) can be specialised as:

$$\boldsymbol{\sigma} = \mathbb{D}\boldsymbol{\varepsilon} \tag{2.2}$$

where $\mathbb{D}$ is the well-known constant fourth order stiffness tensor. Eq. (2.1) can be also expressed in the incremental form. However, if the stress-strain relationship is originally expressed in incremental form, the model is called hypoelastic (Fung (1965)):

$$\dot{\boldsymbol{\sigma}} = \mathbb{D}\,(\boldsymbol{\varepsilon}, \boldsymbol{\sigma})\,\dot{\boldsymbol{\varepsilon}} \tag{2.3}$$

with the stiffness tensor generally function of the stress and/or the strain tensors. It is worth mentioning that the elasticity represents a particular form of hypoelasticity. In fact, all the elastic materials are also hypoelastic but the converse is not true unless the tensor $\mathbb{D}\,(\boldsymbol{\varepsilon}, \boldsymbol{\sigma})$ can be expressed as an integrable function of the strain only. Conversely, as a special case of the elasticity, if the stress is derived from a strain energy potential, as reported in eq. (2.4), the material is called hyperelastic.

$$\boldsymbol{\sigma}\,(\boldsymbol{\varepsilon}) = \frac{\partial \varphi\,(\boldsymbol{\varepsilon})}{\partial \boldsymbol{\varepsilon}} \tag{2.4}$$

where φ is a scalar-valued function, also known as the Helmholtz free energy. By further differentiation of eq. (2.4) one obtains the fourth order elastic stiffness tensor:

$$\mathbb{D}(\boldsymbol{\varepsilon}) = \frac{\partial^2 \varphi(\boldsymbol{\varepsilon})}{\partial \boldsymbol{\varepsilon} \otimes \partial \boldsymbol{\varepsilon}} \tag{2.5}$$

If $\mathbb{D}$ does not depend on the stress, the material is linear. In the framework of hyperelasticity, an equivalent statement is that the strains are the differential of the complementary energy ψ, or the Gibbs free energy for isothermal processes, function of the stress, related to the strain energy through the Legendre transform:

$$\varphi(\boldsymbol{\varepsilon}) + \psi(\boldsymbol{\sigma}) = \boldsymbol{\sigma} : \boldsymbol{\varepsilon} \tag{2.6}$$

Differentiating once and twice the complementary energy with respect to the stresses one obtains the strain and the compliance $\mathbb{C}$ tensors, respectively:

$$\boldsymbol{\varepsilon}(\boldsymbol{\sigma}) = \frac{\partial \psi(\boldsymbol{\sigma})}{\partial \boldsymbol{\sigma}} \qquad \mathbb{C}(\boldsymbol{\sigma}) = \frac{\partial^2 \psi(\boldsymbol{\sigma})}{\partial \boldsymbol{\sigma} \otimes \partial \boldsymbol{\sigma}} \tag{2.7}$$

The hyperelasticity is a particular form of elasticity and an elastic model is also hyperelastic if the function $f(\boldsymbol{\varepsilon})$ in eq. (2.1) is an integrable function of the strains. Thus, a hierarchical structure can be identified, where the hypoelasticity is the most general form, followed by elasticity and hyperelasticity. Elasticity theories should be consistent with the laws of thermodynamics, and it is widely accepted that this can only be guaranteed if the material can be described as hyperelastic. Another advantage of the hyperelastic approach is that it solely requires the definition of a scalar-valued function from which one can derive the whole stress-strain relationship. Contrary, in general in elasticity and hypoelasticity a second order and a fourth order tensors need to be defined, respectively.

2.2 Linear isotropic elasticity

Within the hyperelastic framework, linear isotropic elasticity is described by the classical quadratic free energy:

$$\varphi(\boldsymbol{\varepsilon}) = \frac{\lambda}{2}\left[\mathrm{tr}(\boldsymbol{\varepsilon})\right]^2 + \mu \mathrm{tr}(\boldsymbol{\varepsilon})^2 = \frac{1}{2}\left[\left(K - \frac{2}{3}G\right)\left[\mathrm{tr}(\boldsymbol{\varepsilon})\right]^2 + 2G\mathrm{tr}\left(\boldsymbol{\varepsilon}^2\right)\right] \tag{2.8}$$

where K and G are the bulk and the shear moduli, $\lambda = K - \frac{2}{3}G$ and $\mu = G$ the two Lamé constants and $\boldsymbol{\varepsilon}^2 = \varepsilon_{ik}\varepsilon_{kj}$. K and G are related to the Poisson's ratio ν through the ratio $\frac{G}{K} = \frac{3(1-2\nu)}{2(1+\nu)}$. Differentiating eq. (2.8) with respect to the strains, one obtains the stress tensor

$$\boldsymbol{\sigma} = \lambda \mathrm{tr}\left(\boldsymbol{\varepsilon}\right)\mathbf{I} + 2\mu\boldsymbol{\varepsilon} = \left(K - \frac{2}{3}G\right)\mathrm{tr}\left(\boldsymbol{\varepsilon}\right)\mathbf{I} + 2G\boldsymbol{\varepsilon} \tag{2.9}$$

and the constant fourth order stiffness tensor:

$$\mathbb{D} = \lambda \mathbf{I}\otimes\mathbf{I} + 2\mu\mathbf{I}\underset{-}{\otimes}\mathbf{I} = \left(K - \frac{2}{3}G\right)\mathbf{I}\otimes\mathbf{I} + 2G\mathbf{I}\underset{-}{\otimes}\mathbf{I} \tag{2.10}$$

In a dual way, the complementary energy can be defined:

$$\begin{aligned}\psi &= -\frac{\lambda}{4\mu\left(3\lambda+2\mu\right)}\left[\mathrm{tr}\left(\boldsymbol{\sigma}\right)\right]^2 + \frac{1}{4\mu}\mathrm{tr}\left(\boldsymbol{\sigma}^2\right) = \\ &= \frac{1}{2K}\left[\left(\frac{1}{9} - \frac{K}{6G}\right)\left[\mathrm{tr}\left(\boldsymbol{\sigma}\right)\right]^2 + \frac{K}{2G}\mathrm{tr}\left(\boldsymbol{\sigma}^2\right)\right]\end{aligned} \tag{2.11}$$

Because of the rather complex form of eq. (2.11) in terms of the Lamé constants, it is more convenient to express the strain and the compliance tensors in terms of the bulk and shear moduli:

$$\boldsymbol{\varepsilon} = \left(\frac{1}{9} - \frac{K}{6G}\right)\mathrm{tr}\left(\boldsymbol{\sigma}\right)\mathbf{I} + \frac{1}{2G}\boldsymbol{\sigma} \tag{2.12}$$

$$\mathbb{C} = \left(\frac{1}{9} - \frac{K}{6G}\right)\mathbf{I}\otimes\mathbf{I} + \frac{1}{2G}\mathbf{I}\underset{-}{\otimes}\mathbf{I} \tag{2.13}$$

2.3 Nonlinear isotropic elasticity

Nonlinearity of geomaterials at small strains usually arises from the dependence of both the bulk and shear moduli on the mean effective pressure and on the current stress state, as widely confirmed by experimental evidences. This feature is most usually modelled by expressing the moduli as power functions of the pressure according to many well-known empirical relationships, like those recalled in chapter 1. In this section the nonlinear hyperelastic model proposed by Houlsby *et al.* (2005) is briefly summarised, referring where necessary to the recent work by Houlsby, Amorosi and Rollo (2019) for further details.

2.3.1 The Houlsby *et al.* model (2005)

The strain energy can be written as:

$$\varphi\left(\boldsymbol{\varepsilon}\right) = \frac{p_r}{k\left(2-n\right)}\left[r_0^{(2-n)/(1-n)} - N\right] \tag{2.14}$$

with

$$r_0^2 = k\left(1-n\right)\left\{\left[k\left(1-n\right)-\frac{2}{3}g\right]\left(\mathrm{tr}\boldsymbol{\varepsilon}\right)^2+2g\mathrm{tr}\left(\boldsymbol{\varepsilon}^2\right)\right\}+N\left[N-2k\left(1-n\right)\mathrm{tr}\boldsymbol{\varepsilon}\right] \tag{2.15}$$

where k, g and n are dimensionless parameters and p_r is a reference stress, typically corresponding to the atmospheric pressure, while the switch parameter N allows to shift the reference point for zero elastic strain on the isotropic axis from 0 ($N = 0$) to the mean effective stress equal to p_r ($N = 1$). From hereinafter, for the sake of simplicity the discussion will be limited to the case $N = 0$, thus assuming the reference point for zero strain at zero stress, as conventionally done in most elastic models. The parameter n controls the nonlinearity of the model producing a non-quadratic free energy. Eq. (2.14) holds for $0 \leq n < 1$, thus encompasses all the possible cases except for the one characterised by the stiffness being linearly dependent on stress ($n = 1$). For the limiting case $n = 1$ eq. (2.14) assumes a different expression, as discussed in more detail in Houlsby, Amorosi and Rollo (2019). The existence of a strain energy potential and a complementary one allows to derive the whole elastic response in a thermodynamically acceptable way. Differentiating eq. (2.14) with respect to the strains one obtains the stress tensor:

$$\boldsymbol{\sigma} = p_r r_0^{\frac{n}{1-n}}\left\{\left[k\left(1-n\right)-\frac{2}{3}g\right]\left(\mathrm{tr}\boldsymbol{\varepsilon}\right)\mathbf{I}+2g\boldsymbol{\varepsilon}\right\} \tag{2.16}$$

and by further differentiation the stiffness tensor:

$$\begin{aligned}\mathbb{D} = {} & p_r\left[k\left(1-n\right)-\frac{2}{3}g\right]\left\{kr_0^{\frac{3n-2}{1-n}}n\left[k\left(1-n\right)-\frac{2}{3}g\right]\left(\mathrm{tr}\boldsymbol{\varepsilon}\right)^2+r_0^{\frac{n}{1-n}}\right\}\mathbf{I}\otimes\mathbf{I}+\\ & +4p_r kr_0^{\frac{3n-2}{1-n}}ng^2\left(\boldsymbol{\varepsilon}\otimes\boldsymbol{\varepsilon}\right)+2p_r kr_0^{\frac{3n-2}{1-n}}ng\left[k\left(1-n\right)-\frac{2}{3}g\right]\mathrm{tr}\boldsymbol{\varepsilon}\left(\boldsymbol{\varepsilon}\otimes\mathbf{I}+\mathbf{I}\otimes\boldsymbol{\varepsilon}\right)+\\ & +2p_r r_0^{\frac{n}{1-n}}g\left(\mathbf{I}\underset{-}{\otimes}\mathbf{I}\right)\end{aligned} \tag{2.17}$$

This latter under triaxial (i.e. axisymmetric) conditions simplifies into:

$$\left\{\begin{array}{c}\delta p\\ \delta q\end{array}\right\} = \left[\begin{array}{cc}\frac{\partial^2\varphi}{\partial\varepsilon_v^2} & \frac{\partial^2\varphi}{\partial\varepsilon_s\partial\varepsilon_v}\\ \frac{\partial^2\varphi}{\partial\varepsilon_s\partial\varepsilon_v} & \frac{\partial^2\varphi}{\partial\varepsilon_s^2}\end{array}\right]\left\{\begin{array}{c}\delta\varepsilon_v\\ \delta\varepsilon_s\end{array}\right\} = \left[\begin{array}{cc}D_{11} & D_{12}\\ D_{21} & D_{22}\end{array}\right]\left\{\begin{array}{c}\delta\varepsilon_v\\ \delta\varepsilon_s\end{array}\right\} \tag{2.18}$$

with

$$
\begin{aligned}
D_{11} &= p_r k^{\frac{2-n}{2-2n}} \left(k\varepsilon_v^2 + \frac{3g}{1-n}\varepsilon_s^2 \right)^{\frac{3n-2}{2-2n}} (1-n)^{\frac{1}{1-n}} \left(\frac{k}{1-n}\varepsilon_v^2 + \frac{3g}{1-n}\varepsilon_s^2 \right) \\
D_{12} = D_{21} &= p_r k^{\frac{2-n}{2-2n}} \left(k\varepsilon_v^2 + \frac{3g}{1-n}\varepsilon_s^2 \right)^{\frac{3n-2}{2-2n}} 3gn\varepsilon_v\varepsilon_s (1-n)^{\frac{2n-1}{1-n}} \\
D_{22} &= p_r k^{\frac{2-n}{2-2n}} \left(k\varepsilon_v^2 + \frac{3g}{1-n}\varepsilon_s^2 \right)^{\frac{3n-2}{2-2n}} 3\frac{g}{k} (1-n)^{\frac{n}{1-n}} \left(k\varepsilon_v^2 + \frac{3g}{(1-n)^2}\varepsilon_s^2 \right)
\end{aligned}
\tag{2.19}
$$

Once calibrated, usually under triaxial states, the model can be used to explore the reversible response for general loading conditions (non-isotropic, non-triaxial states). For $n = 0$ the classical linear isotropic model is recovered and the two parameters k e g are directly related to the bulk and shear moduli K and G and the two Lamé constants:

$$
\lambda = \left(K - \frac{2}{3}G \right) = p_r \left(k - \frac{2}{3}g \right) \quad ; \quad \mu = G = p_r g \tag{2.20}
$$

The complementary energy assumes the form:

$$
\psi(\boldsymbol{\sigma}) = \frac{1}{p_r^{1-n} k (1-n)(2-n)} p_0^{2-n} \tag{2.21}
$$

where the scalar term p_0 is the dual expression of r_0 and takes the form:

$$
p_0^2 = \left[\left(\frac{1}{9} - \frac{k(1-n)}{6g} \right) [\mathrm{tr}(\boldsymbol{\sigma})]^2 + \frac{k(1-n)}{2g} \mathrm{tr}\left(\boldsymbol{\sigma}^2\right) \right] \tag{2.22}
$$

As a consequence the strain tensor reads:

$$
\boldsymbol{\varepsilon} = \frac{1}{2p_r^{1-n} k (1-n)} p_0^n \left[2 \left(\frac{1}{9} - \frac{k(1-n)}{6g} \right) \mathrm{tr}(\boldsymbol{\sigma}) \mathbf{I} + \frac{k(1-n)}{g} \boldsymbol{\sigma} \right] \tag{2.23}
$$

and the compliance fourth order tensor is:

$$
\begin{aligned}
\mathbb{C} = \frac{1}{p_r^{1-n} k (1-n)} \Bigg\{ & \left(-\frac{n}{2} \right) p_0^{-(n+2)} 2 \left(\frac{1}{9} - \frac{k(1-n)}{6g} \right) [\mathrm{tr}(\boldsymbol{\sigma})]^2 + \\
& + p_0^{-n} \left(\frac{1}{9} - \frac{k(1-n)}{6g} \right) \Bigg\} \mathbf{I} \otimes \mathbf{I} - \frac{n}{4p_r^{1-n}} p_0^{-(n+2)} \frac{k(1-n)}{g^2} (\boldsymbol{\sigma} \otimes \boldsymbol{\sigma}) + \\
& - \frac{n}{2p_r^{1-n} g} p_0^{-(n+2)} \left(\frac{1}{9} - \frac{k(1-n)}{6g} \right) \mathrm{tr}(\boldsymbol{\sigma}) (\boldsymbol{\sigma} \otimes \mathbf{I} + \mathbf{I} \otimes \boldsymbol{\sigma}) + \\
& + \frac{1}{2p_r^{1-n} g} p_0^{-n} \left(\mathbf{I} \underset{-}{\otimes} \mathbf{I} \right)
\end{aligned}
\tag{2.24}
$$

Under the hypothesis of isotropic stress/strain state, the elastic bulk and shear moduli K and G depend on the mean effective pressure following the expressions:

$$\begin{aligned} K &= p_r k \left(\frac{p}{p_r}\right)^n \\ G &= p_r g \left(\frac{p}{p_r}\right)^n \end{aligned} \tag{2.25}$$

Therefore, the model can reproduce the typical nonlinear dependence of the elastic stiffness with the mean pressure, as suggested by many empirical relationships for both sandy and clayey soils (Hardin (1978), Rampello *et al.* (1994)).

2.3.1.1 Stress/strain induced anisotropy

The key feature of eq. (2.14) is that of reproducing the experimentally observed dependence of soil stiffness on the current stress state by a nonlinear hyperelastic formulation. An interesting side effect is the resulting volumetric-deviatoric coupling, which naturally stems from the energy-based formulation when the material is subjected to non-isotropic stress/strain states. This can be easily verified, under simplified triaxial conditions, by the activation of the off-diagonal terms $D_{12} = D_{21}$ in eq. (2.19) for $\varepsilon_s > 0$. To highlight this feature, Houlsby *et al.* (2005) performed ideal tests under either constant volumetric (i.e. undrained) or constant deviatoric strain conditions. Figure (2.1) illustrates the results in terms of volumetric and deviatoric strain contours plotted on a p-q space for different values of n. It confirms that when the nonlinearity is taken into account, a purely volumetric strain path does not correspond to a constant deviatoric stress path and, vice versa, a purely distortional strain path does not lead to a constant p stress path. In particular, the greater is the exponent n (i.e. the model becomes more nonlinear), the more pronounced is the the volumetric-deviatoric coupling and for $n = 0$ the classical uncoupled response of the linear model is recovered . In granular materials different possible sources of volumetric-deviatoric coupling exist, the most obvious one being related to irreversible behaviour (i.e. plasticity): it is thus worth remarking that in this kind of coupling, by definition, no plastic deformations occur. The volumetric-deviatoric coupling has often been related in the literature to the so called "stress induced anisotropy". This latter should not be confused with the inherent anisotropy. In fact, the first essentially accounts for the directional properties induced by the current anisotropic stress/strain state, while the second is independent of it, as being related to pre-existing features of the soil possibly stemming from its internal structure, as those due to the prevailing orientation of the particles. The model by Houlsby *et al.* (2005) is formulated in terms of invariants of the strain tensor,

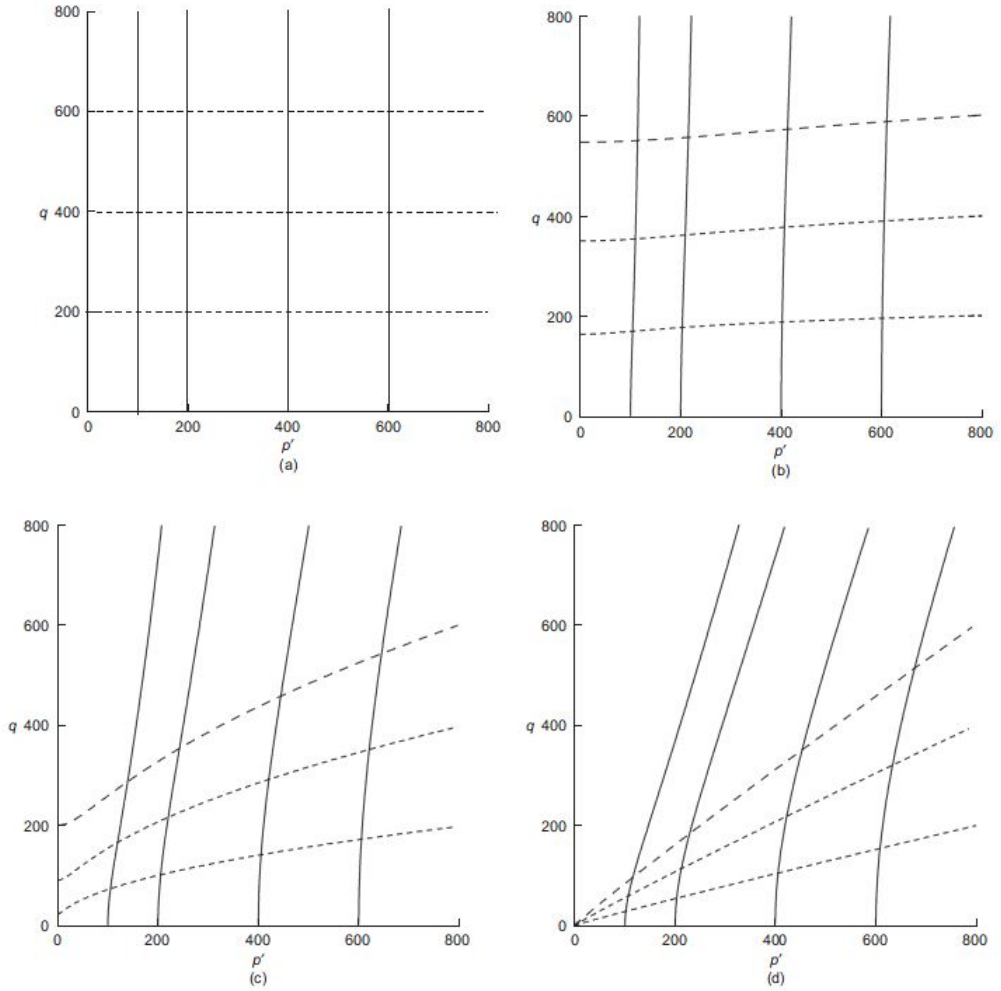

Figure 2.1: *Constant volumetric (countinous lines) and constant deviatoric (dashed lines) strain contours for different n* - (a) *n=0,* (b) *n=0.1,* (c) *n=0.5,* (d) *n=0.95 (from Houlsby et al. (2005))*

i.e. no fabric-related directional information is included: as such, the stress-induced anisotropy reproduced by the model is not related to a proper anisotropic structural character, but rather to the current orientation of the principal directions and the relative intensity of the corresponding stress/strain tensor components. This can easily be detected by unloading the material from any initial anisotropic state back to an isotropic stress/strain condition: the hyperelastic formulation will obviously return an isotropic response.

Remark In order to clarify the effect of stress induced anisotropy, ideal tests under more general stress/strain conditions were performed in the present work, based on eq. (2.17), illustrating the modification of the matrix associated to the stiffness tensor for different states of strain. Here the parameters of the model are those

reported in table (2.1).

Parameter	Value
p_r	100
n	0.47
k	1250
g	1050

Table 2.1: *Model parameters for ideal tests*

Under isotropic strain state, the terms D_{1111}, D_{2222} and D_{3333} are equal each other's and could be expressed by a combination of the current unique Young modulus and Poisson's ratio (stress and stiffness are in expressed kPa):

ε_{11}	0.001	σ_{11}	365	487284	101134	101134	0	0	0
ε_{22}	0.001	σ_{22}	365	101134	487284	101134	0	0	0
ε_{33}	0.001	σ_{33}	365	101134	101134	487284	0	0	0
ε_{12}	0	σ_{12}	0	0	0	0	193075	0	0
ε_{13}	0	σ_{13}	0	0	0	0	0	193075	0
ε_{23}	0	σ_{23}	0	0	0	0	0	0	193075

Table 2.2: *Stiffness matrix for isotropic strain/stress state*

Increasing the strain component ε_{11} leads to both an overall modification of the stiffness matrix, because of non-linearity, and to a stiffer component D_{1111}, as compared to D_{2222} and D_{3333}:

ε_{11}	0.0015	σ_{11}	648	648072	101134	125671	0	0	0
ε_{22}	0.001	σ_{22}	423	125671	530238	125671	0	0	0
ε_{33}	0.001	σ_{33}	423	125671	125671	530238	0	0	0
ε_{12}	0	σ_{12}	0	0	0	0	225540	0	0
ε_{13}	0	σ_{13}	0	0	0	0	0	225540	0
ε_{23}	0	σ_{23}	0	0	0	0	0	0	225540

Table 2.3: *Stiffness matrix for anisotropic strain/stress state*

When a shear strain component ε_{12} is added to a isotropic state, the off-diagonal terms $D_{1112} = D_{1211}$ are activated and the corresponding shear stiffness term D_{1212} is larger than those on the other planes ($D_{1313} = D_{2323}$).

ε_{11}	0.001	σ_{11}	463	560694	71553	71553	84832	0	0
ε_{22}	0.001	σ_{22}	463	71553	560694	71553	84832	0	0
ε_{33}	0.001	σ_{33}	463	71553	71553	560694	84832	0	0
ε_{12}	0.001	σ_{12}	489	84832	84832	848320	334205	0	0
ε_{13}	0	σ_{13}	0	0	0	0	0	244570	0
ε_{23}	0	σ_{23}	0	0	0	0	0	0	244570

Table 2.4: *Stiffness matrix in presence of shear strain*

2.4 Linear anisotropic elasticity

In this section some significant existing linear anisotropic models are briefly described. From a mathematical point of view, a possible strategy to take into account the anisotropic character of soils is to introduce a symmetric second order fabric tensor that can condense all scalar and directional information pertaining to the anisotropy of the material. This tensorial entity permits to link the microstructural characteristics to the macroscopic mechanical behaviour of soils. The use of a second order tensor restricts the material symmetry to orthotropy if its three eigenvalues are distinct and, as special cases, transverse isotropy if two of them are identical and isotropy if the tensor is proportional to the identity one. The description of other material symmetries would require the introduction of higher order fabric tensors, but this is beyond the scope of this work. In spite of these limitations, however, this approach is probably sufficient to describe the anisotropy of most soils and geomaterials. There are different ways to introduce anisotropy in the reversible behaviour of soils and the majority of the models proposed in the following are developed within the hyperelastic framework. In particular, the approach is based on the formulation of a free energy potential which does no longer solely depend on the strain tensor, as in the previous section, but is enriched by the fabric tensor. The two tensors are combined consistently with the representation theorems for scalar valued isotropic functions (Truesdell & Noll (1965), Wang (1970), Boehler (1987)). This approach leads to the most general form for the strain energy potential, in terms of a set of irreducible invariants of the strain and fabric tensors. It is worth mentioning that the fabric tensor adopted here and in the following chapter is constant, i.e. no evolution of the elastic stiffness anisotropy with plastic strains is considered here. Therefore, within the hyperelastic framework, denoting with $\mathbf{A}$ a generic fabric tensor and defining with φ and ψ the two free energy forms, the stress and the stiffness tensors read:

$$\boldsymbol{\sigma}(\boldsymbol{\varepsilon}, \mathbf{A}) = \frac{\partial \varphi(\boldsymbol{\varepsilon}, \mathbf{A})}{\partial \boldsymbol{\varepsilon}} \qquad \mathbb{D}(\boldsymbol{\varepsilon}, \mathbf{A}) = \frac{\partial^2 \varphi(\boldsymbol{\varepsilon}, \mathbf{A})}{\partial \boldsymbol{\varepsilon} \otimes \partial \boldsymbol{\varepsilon}} \tag{2.26}$$

and the strain and the compliance tensors as:

$$\boldsymbol{\varepsilon}(\boldsymbol{\sigma}, \mathbf{A}) = \frac{\partial \psi(\boldsymbol{\sigma}, \mathbf{A})}{\partial \boldsymbol{\sigma}} \qquad \mathbb{C}(\boldsymbol{\sigma}, \mathbf{A}) = \frac{\partial^2 \psi(\boldsymbol{\sigma}, \mathbf{A})}{\partial \boldsymbol{\sigma} \otimes \partial \boldsymbol{\sigma}} \tag{2.27}$$

2.4.1 The Lodge model (1955)

In 1955 Lodge suggested a pioneering procedure to take into account the elastic anisotropy of solids in the framework of hyperelasticity. In particular he suggested that a linear transformation exists, such that an equivalent strain tensor $\bar{\boldsymbol{\varepsilon}} = \mathbf{a}\boldsymbol{\varepsilon}\mathbf{a}$ can be defined, where $\mathbf{a}$ is a symmetric second order fabric tensor. In such a way the free energy potential is formally identical to the well-known simple quadratic form for the isotropic case but is able to describe the anisotropic behaviour of an elastic material:

$$\varphi(\bar{\boldsymbol{\varepsilon}}) = \frac{\lambda}{2}\left[\mathrm{tr}(\bar{\boldsymbol{\varepsilon}})\right]^2 + \mu \mathrm{tr}(\bar{\boldsymbol{\varepsilon}})^2 = \frac{\lambda}{2}\left[\mathrm{tr}(\mathbf{a}\boldsymbol{\varepsilon}\mathbf{a})\right]^2 + \mu \mathrm{tr}\left[(\mathbf{a}\boldsymbol{\varepsilon}\mathbf{a})^2\right] \tag{2.28}$$

For $\mathbf{a} = \mathbf{I}$ the isotropic model is recovered.

2.4.2 The Graham & Houlsby model (1983)

The Graham & Houlsby (1983) model represents a pioneering attempt to take into account the elastic anisotropy of soils from a constitutive modelling point of view. They proposed a linear anisotropic elastic model formulated in the triaxial space to describe transverse isotropy. They introduced the anisotropic character in the elastic stiffness tensor multiplying the stiffness coefficients in the horizontal direction (supposing the horizontal plane as that of isotropy) by a scalar factor α, often indicated as anisotropy coefficient. Expressing the elastic stiffness tensor in terms of the bulk modulus K and the shear modulus G, choosing the vertical direction as 1 it results:

$$\begin{Bmatrix} \sigma_1 \\ \sigma_2 \\ \sigma_3 \end{Bmatrix} = \begin{bmatrix} \alpha^{-\frac{4}{3}}\left(K + \frac{4}{3}G\right) & \alpha^{-\frac{1}{3}}\left(K - \frac{2}{3}G\right) & \alpha^{-\frac{1}{3}}\left(K - \frac{2}{3}G\right) \\ \alpha^{-\frac{1}{3}}\left(K - \frac{2}{3}G\right) & \alpha^{\frac{2}{3}}\left(K + \frac{4}{3}G\right) & \alpha^{\frac{2}{3}}\left(K - \frac{2}{3}G\right) \\ \alpha^{-\frac{1}{3}}\left(K - \frac{2}{3}G\right) & \alpha^{\frac{2}{3}}\left(K - \frac{2}{3}G\right) & \alpha^{\frac{2}{3}}\left(K + \frac{4}{3}G\right) \end{bmatrix} \begin{Bmatrix} \varepsilon_1 \\ \varepsilon_2 \\ \varepsilon_3 \end{Bmatrix} \tag{2.29}$$

For $\alpha > 1$ the material is stiffer horizontally than vertically and the ratio of the stiffnesses in the horizontal and vertical directions is α^2, namely the ratio of the

second and the first diagonal terms of the matrix in eq. (2.29). α is a direct measure of the anisotropy of the material and for $\alpha = 1$ isotropic elasticity is recovered.

2.4.3 The Zysset & Curnier model (1995)

The first attempt to model the anisotropic character of porous media following the representation theorems for scalar valued isotropic functions was made by Cowin (1985), introducing a traceless second order symmetric fabric tensor in the elastic stiffness tensor. In the most general case of orthotropy nine independent constants have to be defined, which reduce to five and two for transverse isotropy and isotropy, respectively.

Inspired by the results obtained by Cowin, Zysset & Curnier (1995) derived a general expression for the elastic strain energy potential. They considered the directional properties of materials as characterised by an orientation distribution function:

$$f(\boldsymbol{n}) = f + \boldsymbol{n}\mathbf{F}\boldsymbol{n} \tag{2.30}$$

where f is a scalar value, the vector $\boldsymbol{n}$ specifies the internal structural orientation and $f(\boldsymbol{n})$ denotes a distribution function characterising the directional properties of the material. The microstructural properties of the material are described by a scalar f, which is the average of the function, thus representing intensity of the anisotropy, and a traceless second order tensor $\mathbf{F}$, pertaining specifically to the directional anisotropic character. Eq. (2.30) can be thought as an expansion of the function $f(\boldsymbol{n})$ where the terms higher than second order are neglected. For $\mathbf{F} = \mathbf{0}$ isotropy is recovered.

Representation theorems provide the most general form of isotropic scalar function; particularly, stemming from the work by Boehler (1987), for the scalar f and the strain tensor $\boldsymbol{\varepsilon}$ and the fabric tensor $\mathbf{F}$ the Authors specify a list of corresponding irreducible invariants:

$$\begin{aligned} &\mathrm{tr}\boldsymbol{\varepsilon}, \quad \mathrm{tr}\left(\boldsymbol{\varepsilon}^2\right), \quad \mathrm{tr}\left(\boldsymbol{\varepsilon}^3\right), \\ &f, \quad \mathrm{tr}\left(\mathbf{F}^2\right), \quad \mathrm{tr}\left(\mathbf{F}^3\right), \\ &\mathrm{tr}\left(\boldsymbol{\varepsilon}\mathbf{F}\right), \quad \mathrm{tr}\left(\boldsymbol{\varepsilon}^2\mathbf{F}\right), \quad \mathrm{tr}\left(\boldsymbol{\varepsilon}\mathbf{F}^2\right), \quad \mathrm{tr}\left(\left(\boldsymbol{\varepsilon}\mathbf{F}\right)^2\right) \end{aligned} \tag{2.31}$$

Retaining only the quadratic terms in the strain tensor $\boldsymbol{\varepsilon}$ to come up with linear elasticity, the Authors defined the following free energy function:

$$\begin{aligned}\varphi(\boldsymbol{\varepsilon},\, f, \mathbf{F}) = &\frac{c_1}{2}\left(\mathrm{tr}\boldsymbol{\varepsilon}\right)^2 + \frac{c_2}{2}\mathrm{tr}\left(\boldsymbol{\varepsilon}^2\right) + \frac{c_3}{2}\left(\mathrm{tr}\left(\boldsymbol{\varepsilon}\mathbf{F}\right)\right)^2 + \\ &+ c_4\mathrm{tr}\left(\boldsymbol{\varepsilon}^2\mathbf{F}\right) + \frac{c_5}{2}\left(\mathrm{tr}\left(\boldsymbol{\varepsilon}\mathbf{F}^2\right)\right)^2 + \frac{c_6}{2}\mathrm{tr}\left(\boldsymbol{\varepsilon}\mathbf{F}\right)^2 + \\ &+ c_7\left(\mathrm{tr}\boldsymbol{\varepsilon}\right)\mathrm{tr}\left(\boldsymbol{\varepsilon}\mathbf{F}\right) + c_8\mathrm{tr}\left(\boldsymbol{\varepsilon}\mathbf{F}\right)\mathrm{tr}\left(\boldsymbol{\varepsilon}\mathbf{F}^2\right) + c_9\left(\mathrm{tr}\boldsymbol{\varepsilon}\right)\mathrm{tr}\left(\boldsymbol{\varepsilon}\mathbf{F}^2\right)\end{aligned} \tag{2.32}$$

where the nine constants c_i are function of f and the two invariants of $\mathbf{F}$. The corresponding fourth order elastic stiffness tensor is obtained differentiating twice the free energy with respect to the strain tensor $\boldsymbol{\varepsilon}$.

$$\begin{aligned}\mathbb{D} = &c_1\mathbf{I}\otimes\mathbf{I} + c_2\mathbf{I}\underset{-}{\otimes}\mathbf{I} + c_3\mathbf{F}\otimes\mathbf{F} + c_4\left(\mathbf{F}\underset{-}{\otimes}\mathbf{I} + \mathbf{I}\underset{-}{\otimes}\mathbf{F}\right) + c_5\mathbf{F}^2\otimes\mathbf{F}^2 + \\ &+ c_6\mathbf{F}\underset{-}{\otimes}\mathbf{F} + c_7\left(\mathbf{I}\otimes\mathbf{F} + \mathbf{F}\otimes\mathbf{I}\right) + c_8\left(\mathbf{F}\otimes\mathbf{F}^2 + \mathbf{F}^2\otimes\mathbf{F}\right) + c_9\left(\mathbf{I}\otimes\mathbf{F}^2 + \mathbf{F}^2\otimes\mathbf{I}\right)\end{aligned} \tag{2.33}$$

that is the same expression reported by Cowin. Eq. (2.33) represents the most general form of the elastic stiffness tensor for the linear anisotropic case.

Zysset & Curnier (1995) also proposed a more heuristic way to characterise linear anisotropic elasticity, starting from the classical linear isotropic elastic stiffness tensor:

$$\mathbb{D} = \lambda\mathbf{I}\otimes\mathbf{I} + 2\mu\mathbf{I}\underset{-}{\otimes}\mathbf{I} \tag{2.34}$$

where λ and μ are the two Lamé constants, and substituting the identity tensor with the tensor $f\mathbf{I} + \mathbf{F}$ they obtained a new expression for the anisotropic elastic stiffness:

$$\mathbb{D} = \lambda\left(f\mathbf{I} + \mathbf{F}\right)\otimes\left(f\mathbf{I} + \mathbf{F}\right) + 2\mu\left(f\mathbf{I} + \mathbf{F}\right)\underset{-}{\otimes}\left(f\mathbf{I} + \mathbf{F}\right) \tag{2.35}$$

In fact, this simplification corresponds to assume a particular case of the nine constants of eq. (2.32), here dependent on f and the Lamé-like constants:

$$\begin{aligned}&c_1 = \lambda f^2,\ c_2 = 2\mu f^2,\ c_3 = \lambda, \\ &c_4 = 2\mu f,\ c_5 = 0,\ c_6 = 2\mu, \\ &c_7 = \lambda f,\ c_8 = 0,\ c_9 = 0\end{aligned} \tag{2.36}$$

Specialising eq. (2.32) with the coefficients in eq. (2.36) one can write the free energy in the form: (2.37).

$$\begin{aligned}\varphi\left(\boldsymbol{\varepsilon},\, f, \mathbf{F}\right) = \frac{\lambda f^2}{2}\left(\mathrm{tr}\boldsymbol{\varepsilon}\right)^2 + \mu f^2 \mathrm{tr}\left(\boldsymbol{\varepsilon}^2\right) + \frac{\lambda}{2}\left(\mathrm{tr}\left(\boldsymbol{\varepsilon}\mathbf{F}\right)\right)^2 + \\ + 2\mu f \mathrm{tr}\left(\boldsymbol{\varepsilon}^2\mathbf{F}\right) + \mu \mathrm{tr}\left(\boldsymbol{\varepsilon}\mathbf{F}\right)^2 + \lambda f\left(\mathrm{tr}\boldsymbol{\varepsilon}\right)\mathrm{tr}\left(\boldsymbol{\varepsilon}\mathbf{F}\right)\end{aligned} \tag{2.37}$$

It is worth noting that despite the fact that eq. (2.37) represents a special case of the more general eq. (2.32), with the constants reduced by three, it is still able to reproduce at most an orthotropic material. Clearly, for $\mathbf{F} = \mathbf{0}$ isotropic elasticity is recovered. For further details, see appendix A for the spectral decomposition of a second order tensor.

2.4.4 The Bigoni & Loret model (1999)

Bigoni & Loret (1999), following a similar approach of that adopted by Zysset & Curnier (1995), replaced the identity tensor in the isotropic elastic stiffness tensor of eq. (2.34) with the symmetric second order fabric tensor $\mathbf{B}$, to be positive definite. The fabric tensor $\mathbf{B}$ can be decomposed in the isotropic and deviatoric parts as follow:

$$\mathbf{B} = f\mathbf{I} + \mathbf{F} \tag{2.38}$$

where f and $\mathbf{F}$ assume the same scalar and fabric tensor introduced by Zysset & Curnier. The substitution leads to the free energy potential:

$$\varphi\left(\boldsymbol{\varepsilon}, \mathbf{B}\right) = \frac{\lambda}{2}\left[\mathrm{tr}\left(\mathbf{B}\boldsymbol{\varepsilon}\right)\right]^2 + \mu \mathrm{tr}\left(\mathbf{B}\boldsymbol{\varepsilon}\right)^2 \tag{2.39}$$

and, by differentiating with respect to strain, the stress and stiffness tensors take the form:

$$\boldsymbol{\sigma} = \lambda \mathrm{tr}\left(\mathbf{B}\boldsymbol{\varepsilon}\right)\mathbf{B} + 2\mu \mathbf{B}\boldsymbol{\varepsilon}\mathbf{B} \tag{2.40}$$

and

$$\mathbb{D} = \lambda \mathbf{B} \otimes \mathbf{B} + 2\mu \mathbf{B} \underline{\bar{\otimes}} \mathbf{B} \tag{2.41}$$

Isotropic elasticity is recovered when $\mathbf{B} = \mathbf{I}$. In particular, in order to facilitate the comparison with the isotropic case, Bigoni & Loret proposed that the fabric tensor should be normalised imposing the constraint $\mathrm{tr}(\mathbf{B}^2)=3$. A detailed discussion about the possible constraints on the fabric tensor can be found in chapter 3.

Furthermore, Bigoni & Loret rewrite the free energy in eq. (2.39) adopting the

spectral decomposition of the fabric tensor:

$$\mathbf{B} = \sum_{i=1}^{3} b_i \boldsymbol{b}_i \otimes \boldsymbol{b}_i = \sum_{i=1}^{3} b_i \mathbf{M}_i \tag{2.42}$$

where b_i are the eigenvalues of $\mathbf{B}$, being positive because of the positive definiteness of the tensor, $\boldsymbol{b}_i$ are unit normal vectors representing the eigenvectors of the fabric tensor and $\mathbf{M}_i$ represents the eigenprojections of $\mathbf{B}$. The alternative representation in eq. (2.42) is very useful because permits to demonstrate that despite the number of invariants appearing in the free energy function, introducing in the formulation a second order fabric tensor, the most general case of orthotropy can be described. In fact, being the eigenvalues of $\mathbf{B}$ distinct, the strain energy depends on nine coefficients, as reported in eq. (2.43).

$$\begin{aligned}\varphi\left(\boldsymbol{\varepsilon}, \mathbf{M}_i\right) = & \frac{c_1}{2}\left[\mathrm{tr}\left(\mathbf{M}_1\boldsymbol{\varepsilon}\right)\right]^2 + \frac{c_2}{2}\left[\mathrm{tr}\left(\mathbf{M}_2\boldsymbol{\varepsilon}\right)\right]^2 + \frac{c_3}{2}\left[\mathrm{tr}\left(\mathbf{M}_3\boldsymbol{\varepsilon}\right)\right]^2 + \\ & + c_4 \mathrm{tr}\left(\mathbf{M}_1\boldsymbol{\varepsilon}\right)\mathrm{tr}\left(\mathbf{M}_2\boldsymbol{\varepsilon}\right) + c_5 \mathrm{tr}\left(\mathbf{M}_1\boldsymbol{\varepsilon}\right)\mathrm{tr}\left(\mathbf{M}_3\boldsymbol{\varepsilon}\right) + c_6 \mathrm{tr}\left(\mathbf{M}_2\boldsymbol{\varepsilon}\right)\mathrm{tr}\left(\mathbf{M}_3\boldsymbol{\varepsilon}\right) + \\ & + c_7 \mathrm{tr}\left(\mathbf{M}_1\boldsymbol{\varepsilon}^2\right) + c_8 \mathrm{tr}\left(\mathbf{M}_2\boldsymbol{\varepsilon}^2\right) + c_9 \mathrm{tr}\left(\mathbf{M}_3\boldsymbol{\varepsilon}^2\right)\end{aligned} \tag{2.43}$$

Under the hypothesis of transverse isotropy $\boldsymbol{b}$ is the axis of material symmetry and only one of the three eigenvalues is retained. Therefore, the free energy can be expressed as a function of a single eigenprojection $\mathbf{M}$ and involves five coefficients:

$$\varphi\left(\boldsymbol{\varepsilon}, \mathbf{M}\right) = \frac{c_1}{2}\left[\mathrm{tr}\left(\boldsymbol{\varepsilon}\right)\right]^2 + \frac{c_2}{2}\mathrm{tr}\left(\boldsymbol{\varepsilon}^2\right) + c_3 \mathrm{tr}\left(\boldsymbol{\varepsilon}\right)\mathrm{tr}\left(\mathbf{M}\boldsymbol{\varepsilon}\right) + \frac{c_4}{2}\left[\mathrm{tr}\left(\mathbf{M}\boldsymbol{\varepsilon}\right)\right]^2 + c_5 \mathrm{tr}\left(\mathbf{M}\boldsymbol{\varepsilon}^2\right) \tag{2.44}$$

For further analytical details on the spectral decomposition see appendix A.

2.4.5 The Lashkari model (2010)

In 2010 Lashkari proposed an extension of a bounding surface plasticity model (Dafalias & Manzari (2004)) to account for the anisotropic elastic behaviour of sands. This feature was added by introducing a deviatoric, symmetric second order fabric tensor $\mathbf{F}$, which has the same character described above. Following the expression of the elastic stiffness tensor developed by Cowin (1985), and incorporating only the first order terms in $\mathbf{F}$, Lashkari obtained:

$$\begin{aligned}\mathbb{D} = \left(K - \frac{2}{3}G\right)\left[\mathbf{I}\otimes\mathbf{I} + \omega_1\left(\mathbf{I}\otimes\mathbf{F} + \mathbf{F}\otimes\mathbf{I}\right)\right] + 2G\mathbf{I}\underset{-}{\otimes}\mathbf{I} + \\ + 2G\omega_2\left(\mathbf{I}\underset{-}{\otimes}\mathbf{F} + \mathbf{F}\underset{-}{\otimes}\mathbf{I}\right)\end{aligned} \tag{2.45}$$

where ω_1 and ω_2 are scalar material constants and K and G are the elastic bulk modulus and the elastic shear modulus. Since these moduli are assumed as non-linearly dependent on stress, the elastic formulation is hypoelastic.

Remark Although the formulation is strictly speaking hypoelastic, for its linear case it is possible to demonstrate that the free energy function leading to eq. (2.45) would take the form:

$$\begin{aligned}\varphi\left(\boldsymbol{\varepsilon},\mathbf{F}\right) = \frac{1}{2}\left(K - \frac{2}{3}G\right)\left\{\left(\mathrm{tr}\boldsymbol{\varepsilon}\right)^2 + 2\omega_1\mathrm{tr}\boldsymbol{\varepsilon}\mathrm{tr}\left(\mathbf{F}\boldsymbol{\varepsilon}\right)\right\} + \\ + G\mathrm{tr}\left(\boldsymbol{\varepsilon}^2\right) + 2G\omega_2\mathrm{tr}\left(\mathbf{F}\boldsymbol{\varepsilon}^2\right)\end{aligned} \tag{2.46}$$

In such a way it will be possible to compare the Laskari model with other formulations not only in terms of stiffness tensor but also in terms of free energy, identifying the mixed invariants.

2.4.6 The Mašín & Rott model (2014)

Mašín & Rott (2014) formulated a linear anisotropic elastic model using the representation theorems for transversely isotropic tensor functions. Defining the second order fabric tensor as $\mathbf{p} = \boldsymbol{n}\otimes\boldsymbol{n}$, where $\boldsymbol{n}$ is a unit normal vector to the plane of symmetry, their fourth order elastic stiffness assumes the form:

$$\begin{aligned}\mathbb{D} = a_1\mathbf{I}\underset{-}{\otimes}\mathbf{I} + a_2\mathbf{I}\otimes\mathbf{I} + a_3\left(\mathbf{I}\otimes\mathbf{p} + \mathbf{p}\otimes\mathbf{I}\right) + \\ + a_4\left(\mathbf{I}\underset{-}{\otimes}\mathbf{p} + \mathbf{p}\underset{-}{\otimes}\mathbf{I}\right) + a_5\mathbf{p}\otimes\mathbf{p}\end{aligned} \tag{2.47}$$

where $a_i,\ i = 1,5$ are material constants, possibly expressed in terms of the Young and shear moduli and the Poisson ratios in the plane of symmetry and along the orthogonal direction. The elastic moduli along the plane of symmetry and the orthogonal direction can be related each other employing anisotropic coefficients, following an approach similar to that adopted by Graham & Houlsby (1983).

Remark Mašín & Rott did not express the model in terms of a free energy potential. However, the strain energy function leading to the elastic stiffness tensor in

eq. (2.47) can be evaluated and takes the form:

$$\begin{aligned}\varphi\left(\boldsymbol{\varepsilon},\mathbf{p}\right)=\frac{a_1}{2}\mathrm{tr}\left(\boldsymbol{\varepsilon}^2\right)+\frac{a_2}{2}\left(\mathrm{tr}\boldsymbol{\varepsilon}\right)^2+a_3\left(\mathrm{tr}\boldsymbol{\varepsilon}\right)\mathrm{tr}\left(\boldsymbol{\varepsilon}\mathbf{p}\right)+\\+a_4\mathrm{tr}\left(\boldsymbol{\varepsilon}^2\mathbf{p}\right)+\frac{a_5}{2}\left(\mathrm{tr}\left(\boldsymbol{\varepsilon}\mathbf{p}\right)\right)^2\end{aligned}\tag{2.48}$$

2.4.7 The Zhao & Gao model (2015)

Zhao & Gao (2015) proposed, in the framework of hypoelasticity, an anisotropic elastic stiffness tensor expressed in terms of a deviatoric, symmetric second order fabric tensor $\mathbf{F}$. This latter is employed to describe the fabric anisotropy in sand and characterises the isotropic, transverse isotropic and orthotropic reversible response of the model. Starting from the work by Cowin (1985), and neglecting the second and higher order terms of $\mathbf{F}$, Zhao & Gao (2015) obtained an expression similar to eq. (2.45) proposed by Lashkari (2010):

$$\begin{aligned}\mathbb{D}=\left(K-\frac{2}{3}G\right)\left[\mathbf{I}\otimes\mathbf{I}+\frac{1}{2}\left(\mathbf{I}\otimes\mathbf{F}+\mathbf{F}\otimes\mathbf{I}\right)\right]+\\+2G\mathbf{I}\underset{-}{\otimes}\mathbf{I}+G\left(\mathbf{I}\underset{-}{\otimes}\mathbf{F}+\mathbf{F}\underset{-}{\otimes}\mathbf{I}\right)\end{aligned}\tag{2.49}$$

where K and G denote the elastic bulk modulus and the elastic shear modulus.

Remark Similarly to what done for the model by Lashkari, the free energy potential leading to the elastic stiffness tensor in eq. (2.49) for the linear case is easily defined as:

$$\begin{aligned}\varphi\left(\boldsymbol{\varepsilon},\mathbf{F}\right)=\frac{1}{2}\left(K-\frac{2}{3}G\right)\left\{\left(\mathrm{tr}\boldsymbol{\varepsilon}\right)^2+\mathrm{tr}\boldsymbol{\varepsilon}\mathrm{tr}\left(\mathbf{F}\boldsymbol{\varepsilon}\right)\right\}+\\+G\mathrm{tr}\left(\boldsymbol{\varepsilon}^2\right)+G\mathrm{tr}\left(\mathbf{F}\boldsymbol{\varepsilon}^2\right)\end{aligned}\tag{2.50}$$

2.5 Nonlinear hyperelastic anisotropic models

2.5.1 The Gajo & Bigoni model (2008)

Gajo & Bigoni (2008) proposed a nonlinear anisotropic hyperelastic model developed in the framework of elastoplasticity. The model can describe the nonlinear stress dependency of the elastic stiffness and, at the same time, includes a tensor-based description of the structural anisotropy (by the second order symmetric tensor $\mathbf{B}$), which in their formulation evolves with the plastic strains. Limiting the attention to

the pure reversible behaviour (namely, in absence of plastic deformation), the fabric tensor is constant and their free energy potential assumes the form:

$$\varphi\left(\boldsymbol{\varepsilon}, \mathbf{B}\right) = \alpha\left[\mathrm{tr}\left(\mathbf{B}\boldsymbol{\varepsilon}\right)\right]^{n} + \beta\left[\mathrm{tr}\left(\mathbf{B}\boldsymbol{\varepsilon}\right)^{2}\right]^{l} \tag{2.51}$$

where α, β, n and l are model parameters. The nonlinear response is governed by the two independent exponents n and l, acting through a nonlinearisation of the mixed invariants $\mathrm{tr}\left(\mathbf{B}\boldsymbol{\varepsilon}\right)$ and $\mathrm{tr}\left(\mathbf{B}\boldsymbol{\varepsilon}\right)^{2}$, respectively. For $n = 2$ and $l = 1$ the linear anisotropic behaviour obtained by the Bigoni & Loret (1999) model is recovered and when $\mathbf{B} = \mathbf{I}$ the elastic behaviour becomes isotropic. Following the hyperelastic framework, differentiating with respect to the strains, Gajo & Bigoni obtain the stress tensor:

$$\boldsymbol{\sigma} = \alpha n\left[\mathrm{tr}\left(\mathbf{B}\boldsymbol{\varepsilon}\right)\right]^{n-1}\mathbf{B} + 2l\beta\left[\mathrm{tr}\left(\mathbf{B}\boldsymbol{\varepsilon}\right)^{2}\right]^{l-1}\mathbf{B}\boldsymbol{\varepsilon}\mathbf{B} \tag{2.52}$$

and, by further differentiation, the elastic stiffness tensor:

$$\begin{aligned}\mathbb{D} = {} & \alpha n\left(n-1\right)\left[\mathrm{tr}\left(\mathbf{B}\boldsymbol{\varepsilon}\right)\right]^{n-2}\mathbf{B}\otimes\mathbf{B} + 4l\beta\left(l-1\right)\left[\mathrm{tr}\left(\mathbf{B}\boldsymbol{\varepsilon}\right)^{2}\right]^{l-2} \\ & \mathbf{B}\boldsymbol{\varepsilon}\mathbf{B}\otimes\mathbf{B}\boldsymbol{\varepsilon}\mathbf{B} + 2l\beta\left[\mathrm{tr}\left(\mathbf{B}\boldsymbol{\varepsilon}\right)^{2}\right]^{l-1}\mathbf{B}\underline{\otimes}\mathbf{B}\end{aligned} \tag{2.53}$$

2.5.2 The Cudny & Partyka model (2017)

Cudny & Partyka (2017) proposed an extension of the nonlinear isotropic hyperelastic model developed by Vermeer (1982) to describe the transverse isotropic behaviour of soils. Following an approach similar to that of Mašín & Rott (2014), they introduced in the original isotropic formulation a second order fabric tensor $\mathbf{N}$, defined as the dyadic product of a unit vector $\boldsymbol{v}$ ($\mathbf{N} = \boldsymbol{v}\otimes\boldsymbol{v}$). In detail, they modify the original complementary energy function by Vermeer introducing the mixed invariant $\mathrm{tr}\left(\mathbf{N}\boldsymbol{\sigma}^{2}\right)$ as follows:

$$\psi\left(\boldsymbol{\sigma}\right) = \frac{3p_{ref}^{1-\beta}}{2G_{0}^{ref}\left(1+\beta\right)}\left[\frac{c_1}{3}\mathrm{tr}\left(\boldsymbol{\sigma}^{2}\right) + \frac{c_2}{3}\mathrm{tr}\left(\mathbf{N}\boldsymbol{\sigma}^{2}\right)\right]^{\frac{1+\beta}{2}} \tag{2.54}$$

where G_{0}^{ref} is the reference shear modulus at the reference mean pressure p_{ref} and β is the material constant controlling the nonlinear dependence of the elastic stiffness with the state of stress. If $c_1 = 1$ and $c_2 = 0$ or $c_1 = 1$ and $\mathbf{N} = \mathbf{0}$ the structural anisotropy is deactivated and the Vermeer isotropic formulation is recovered.

Chapter 3

The proposed hyperelastic anisotropic model

In this chapter a nonlinear anisotropic hyperelastic model is proposed. After the formulation is introduced and discussed, the model is compared to the existing ones reported in the previous chapter for the cases of nonlinear isotropic, linear anisotropic and the nonlinear anisotropic one, highlighting similarities and differences. Finally, the model is critically analysed and validated against experimental data proposed in the literature. It results that the proposed formulation encompasses most of the existing anisotropic hyperelastic models and nicely back-predicts laboratory experimental data observed on both sands and clays.

3.1 Formulation of the model

Stemming from the work by Lodge (1955), the equivalent strain tensor $\bar{\boldsymbol{\varepsilon}}$ is defined as $\bar{\boldsymbol{\varepsilon}} = \mathbf{a}\boldsymbol{\varepsilon}\mathbf{a}$ where $\mathbf{a}$ is the symmetric second order fabric tensor. Employing this linear transformation, an extension of the isotropic nonlinear hyperelastic model by Houlsby *et al.* (2005) is proposed, in order to take into account the inherent elastic anisotropy of soils. In particular the strain energy in eq. (2.14), for the case $N = 0$, can be generalised as:

$$\begin{aligned}\varphi\left(\boldsymbol{\varepsilon}, \mathbf{a}\right) = \frac{p_r}{k\left(2-n\right)} r_0^{\frac{2-n}{1-n}} = \frac{p_r}{k\left(2-n\right)} k^{\frac{2-n}{2-2n}} \left(1-n\right)^{\frac{2-n}{2-2n}} \\ \left\{ \left[k\left(1-n\right) - \frac{2}{3} g \right] \left[\mathrm{tr}\left(\mathbf{a}\boldsymbol{\varepsilon}\mathbf{a}\right)\right]^2 + 2g\mathrm{tr}\left[\left(\mathbf{a}\boldsymbol{\varepsilon}\mathbf{a}\right)^2\right] \right\}^{\frac{2-n}{2-2n}}\end{aligned} \tag{3.1}$$

In the framework of hyperelasticity, differentiating eq. (3.1) with respect to the strains one obtains the stress tensor:

$$\boldsymbol{\sigma} = p_r r_0^{\frac{n}{1-n}} \left\{ \left[k\left(1-n\right) - \frac{2}{3}g \right] \mathrm{tr}\left(\mathbf{a}\boldsymbol{\varepsilon}\mathbf{a}\right) \mathbf{a}^2 + 2g\mathbf{a}^2\boldsymbol{\varepsilon}\mathbf{a}^2 \right\} \tag{3.2}$$

and by further differentiating, the fourth order stiffness tensor:

$$\begin{aligned}\mathbb{D} = {} & p_r \left[k\left(1-n\right) - \frac{2}{3}g \right] \left\{ k r_0^{\frac{3n-2}{1-n}} n \left[k\left(1-n\right) - \frac{2}{3}g \right] \left[\mathrm{tr}\left(\mathbf{a}\boldsymbol{\varepsilon}\mathbf{a}\right)\right]^2 + r_0^{\frac{n}{1-n}} \right\} \mathbf{a}^2 \otimes \mathbf{a}^2 + \\ & + 2p_r k r_0^{\frac{3n-2}{1-n}} n g \left[k\left(1-n\right) - \frac{2}{3}g \right] \mathrm{tr}\left(\mathbf{a}\boldsymbol{\varepsilon}\mathbf{a}\right) \left(\mathbf{a}^2\boldsymbol{\varepsilon}\mathbf{a}^2 \otimes \mathbf{a}^2 + \mathbf{a}^2 \otimes \mathbf{a}^2\boldsymbol{\varepsilon}\mathbf{a}^2 \right) + \\ & + 4p_r k r_0^{\frac{3n-2}{1-n}} n g^2 \left(\mathbf{a}^2\boldsymbol{\varepsilon}\mathbf{a}^2 \otimes \mathbf{a}^2\boldsymbol{\varepsilon}\mathbf{a}^2 \right) + 2p_r r_0^{\frac{n}{1-n}} g \left(\mathbf{a}^2 \underset{-}{\otimes} \mathbf{a}^2 \right)\end{aligned} \tag{3.3}$$

Following the same philosophy as above, an equivalent stress tensor $\bar{\boldsymbol{\sigma}} = \mathbf{a}^{-1}\boldsymbol{\sigma}\mathbf{a}^{-1}$ can be defined, in order to express the formulation in the stress form, too. Taking into account the symmetry of the fabric tensor $\mathbf{a}$, it is worth noting that the tensors $\bar{\boldsymbol{\varepsilon}}$ and $\bar{\boldsymbol{\sigma}}$ are work-conjugate in the same way as $\boldsymbol{\sigma}$ and $\boldsymbol{\varepsilon}$:

$$\bar{\boldsymbol{\sigma}} : \bar{\boldsymbol{\varepsilon}} = \mathrm{tr}\left(\bar{\boldsymbol{\sigma}}\bar{\boldsymbol{\varepsilon}}\right) = \mathrm{tr}\left(\mathbf{a}^{-1}\boldsymbol{\sigma}\mathbf{a}^{-1}\mathbf{a}\boldsymbol{\varepsilon}\mathbf{a}\right) = \mathrm{tr}\left(\mathbf{a}\mathbf{a}^{-1}\boldsymbol{\sigma}\boldsymbol{\varepsilon}\right) = \boldsymbol{\sigma} : \boldsymbol{\varepsilon} \tag{3.4}$$

The result in eq. (3.4) proves that the strain and complementary energies are Legendre transforms of each other not only for the isotropic case but also for the anisotropic one. As a consequence, the complementary energy in eq. (2.21) can be generalised to the anisotropic case in the form:

$$\begin{aligned}\psi\left(\boldsymbol{\sigma}, \mathbf{a}\right) = {} & \frac{1}{p_r^{1-n} k\left(1-n\right)\left(2-n\right)} p_0^{2-n} = \frac{1}{p_r^{1-n} k\left(1-n\right)\left(2-n\right)} \\ & \left\{ \left(\frac{1}{9} - \frac{k\left(1-n\right)}{6g} \right) \left[\mathrm{tr}\left(\mathbf{a}^{-1}\boldsymbol{\sigma}\mathbf{a}^{-1}\right)\right]^2 + \frac{k\left(1-n\right)}{2g} \mathrm{tr}\left[\left(\mathbf{a}^{-1}\boldsymbol{\sigma}\mathbf{a}^{-1}\right)^2 \right] \right\}^{\frac{2-n}{2}}\end{aligned} \tag{3.5}$$

In fact, it is possible to verify that the previous equation, combined with the strain energy in eq. (3.1), satisfies the Legendre transform (eq. (2.6)). Differentiation of eq. (3.5) with respect to the stresses leads to the strain tensor:

$$\boldsymbol{\varepsilon} = \frac{1}{2p_r^{1-n} k\left(1-n\right)} p_0^n \left[2\left(\frac{1}{9} - \frac{k\left(1-n\right)}{6g} \right) \mathrm{tr}\left(\mathbf{a}^{-1}\boldsymbol{\sigma}\mathbf{a}^{-1}\right) \mathbf{a}^{-2} + \frac{k\left(1-n\right)}{g} \mathbf{a}^{-2}\boldsymbol{\sigma}\mathbf{a}^{-2} \right] \tag{3.6}$$

and further differentiating, the compliance tensor:

$$
\begin{aligned}
\mathbb{C} = & \frac{1}{p_r^{1-n} k\,(1-n)} \left\{ \left(-\frac{n}{2}\right) p_0^{-(n+2)} 2 \left(\frac{1}{9} - \frac{k\,(1-n)}{6g}\right) \left[\mathrm{tr}\left(\mathbf{a}^{-1}\boldsymbol{\sigma}\mathbf{a}^{-1}\right)\right]^2 + \right. \\
& \left. + p_0^{-n} \left(\frac{1}{9} - \frac{k\,(1-n)}{6g}\right) \right\} \mathbf{a}^{-2} \otimes \mathbf{a}^{-2} + \\
& - \frac{n}{4p_r^{1-n}} p_0^{-(n+2)} \frac{k\,(1-n)}{g^2} \left(\mathbf{a}^{-2}\boldsymbol{\sigma}\mathbf{a}^{-2} \otimes \mathbf{a}^{-2}\boldsymbol{\sigma}\mathbf{a}^{-2}\right) + \\
& - \frac{n}{2p_r^{1-n} g} p_0^{-(n+2)} \left(\frac{1}{9} - \frac{k\,(1-n)}{6g}\right) \mathrm{tr}\left(\mathbf{a}^{-1}\boldsymbol{\sigma}\mathbf{a}^{-1}\right) \\
& \left(\mathbf{a}^{-2}\boldsymbol{\sigma}\mathbf{a}^{-2} \otimes \mathbf{a}^{-2} + \mathbf{a}^{-2} \otimes \mathbf{a}^{-2}\boldsymbol{\sigma}\mathbf{a}^{-2}\right) + \frac{1}{2p_r^{1-n} g} p_0^{-n} \left(\mathbf{a}^{-2} \underset{-}{\overset{-}{\otimes}} \mathbf{a}^{-2}\right)
\end{aligned}
\tag{3.7}
$$

Again, it is worth remarking that these latter equations imply that $\mathbf{a}$ = constant, such that inherent anisotropy (i.e. not evolving) is only accounted for. Nonetheless, it is worth mentioning that in such a circumstance, following Maier & Hueckel (1979) and Collins & Houlsby (1997), eq. (3.3) would describe the instantaneous reversible stiffness of the soil. The proposed formulation accounts for both inherent and stress-induced anisotropy. In fact, it not only reproduces the non-linearly stress-dependent stiffness and the related evolving directional elastic properties with the current stress/strain state, but also allows to model the permanent anisotropic characteristics via the $\mathbf{a}$ tensor. All the above features are enriched by the energy-based derivation of the formulation, which ensures its thermodynamic consistency. Clearly, for $\mathbf{a} = \mathbf{I}$ the nonlinear isotropic formulation is recovered.

An alternative representation of the model, useful for the comparison with many existing formulations, can be achieved using $\mathbf{B} = \mathbf{a}^2$ in the expression of the fabric tensor. As a consequence, the equivalent strain and stress tensors are defined as $\tilde{\boldsymbol{\varepsilon}} = \mathbf{B}\boldsymbol{\varepsilon}$ and $\tilde{\boldsymbol{\sigma}} = \mathbf{B}^{-1}\boldsymbol{\sigma}$, respectively. These are still work-conjugate terms, in fact:

$$
\tilde{\boldsymbol{\sigma}} : \tilde{\boldsymbol{\varepsilon}} = \mathrm{tr}\left(\mathbf{B}^{-1}\boldsymbol{\sigma}\mathbf{B}\boldsymbol{\varepsilon}\right) = \boldsymbol{\sigma} : \boldsymbol{\varepsilon} \tag{3.8}
$$

Eqs. (3.1) – (3.7) are clearly inspired by the concept that the strain $\boldsymbol{\varepsilon}$ and the stress $\boldsymbol{\sigma}$ in the strain and stress energy expressions for an isotropic material can simply be replaced by an equivalent strain and stress in order to define the energy functions for an anisotropic material. However, this analogy should be approached with caution. It is worth noting that $\tilde{\boldsymbol{\varepsilon}}$ and $\tilde{\boldsymbol{\sigma}}$ are different from $\bar{\boldsymbol{\varepsilon}}$ and $\bar{\boldsymbol{\sigma}}$ and in particular, whilst the first two are in general not symmetric, the second ones are. To treat the unsymmetric tensor $\mathbf{B}\boldsymbol{\varepsilon}$ (or $\mathbf{B}^{-1}\boldsymbol{\sigma}$) as if it were directly analogous to the symmetric tensor $\boldsymbol{\varepsilon}$ (or $\boldsymbol{\sigma}$) is open to question. Here the concern relates solely to the implicit interpretation that the symmetric $\boldsymbol{\varepsilon}$ (or $\boldsymbol{\sigma}$) can be generalised to a

non-symmetric one. In this sense, the choice of the fabric tensor $\mathbf{a}$ appears more consistent with the requirement of the symmetries of the strain and stress tensors. Nevertheless, this concern does not invalidate the use of the tensor $\mathbf{B}$. In fact, the mixed invariants $\mathrm{tr}\,(\mathbf{B}\boldsymbol{\varepsilon})$ and $\mathrm{tr}\left[(\mathbf{B}\boldsymbol{\varepsilon})^2\right]$ are equal to $\mathrm{tr}\,(\mathbf{a}\boldsymbol{\varepsilon}\mathbf{a})$ and $\mathrm{tr}\left[(\mathbf{a}\boldsymbol{\varepsilon}\mathbf{a})^2\right]$, as can be demonstrated:

$$\mathrm{tr}\,(\bar{\boldsymbol{\varepsilon}}) = \mathrm{tr}\,(\mathbf{a}\boldsymbol{\varepsilon}\mathbf{a}) = \mathrm{tr}\left(\mathbf{a}^2\boldsymbol{\varepsilon}\right) = \mathrm{tr}\,(\mathbf{B}\boldsymbol{\varepsilon}) = \mathrm{tr}\,(\tilde{\boldsymbol{\varepsilon}}) \tag{3.9}$$

and

$$\mathrm{tr}\left(\bar{\boldsymbol{\varepsilon}}^2\right) = \mathrm{tr}\left[(\mathbf{a}\boldsymbol{\varepsilon}\mathbf{a})^2\right] = \mathrm{tr}\,(\mathbf{aa}\boldsymbol{\varepsilon}\mathbf{aa}\boldsymbol{\varepsilon}) = \mathrm{tr}\left[(\mathbf{B}\boldsymbol{\varepsilon})^2\right] = \mathrm{tr}\left(\tilde{\boldsymbol{\varepsilon}}^2\right) \tag{3.10}$$

Therefore, eqs. (3.1) – (3.7) can be equivalently expressed in terms of the $\mathbf{B}$ tensor. For the sake of conciseness, the resulting equations are reported in appendix A. Furthermore, considering the spectral decomposition of the two fabric tensors, it follows that $\mathbf{a}$ and $\mathbf{B}$ have the same eigenvectors, which give the direction of the orthotropic axes, and the eigenvalues of $\mathbf{a}$ are simply the squares of those of $\mathbf{B}$ (see appendix A for details).

3.2 The role of the constraint on the fabric tensor

The fabric tensor is aimed at condensate the relative directional characteristics of the soil, as such it is worth normalising it. In the literature different normalisation rules are proposed, however no clear indication emerges on which of them is more appropriate: in this section all the proposed constraints are adopted and examined, aiming at highlighting their effects on the fabric tensor, thus providing further information to guide the user in the choice. From a historical perspective, the first attempt of introducing a normalising constraint was that of Lodge (1955), who proposed to assign a fixed value to the determinant of the fabric tensor $\mathbf{a}$. A convenient choice is $\det(\mathbf{a}) = 1$, such that for the isotropic case ($\mathbf{a} = \mathbf{I}$) one recovers $\det(\mathbf{I}) = 1$. Bigoni & Loret (1999) perform a more systematic discussion on the character and constraints of their fabric tensor $\mathbf{B}$. Firstly, for the elastic tensor to be positive definite, $\mathbf{B}$ should as well be positive definite, such that the necessary and sufficient conditions for the positive definiteness of the elastic stiffness tensor are the Lamé constants λ and μ being strictly positive. In addition, they impose for the fabric tensor the constraint $\mathrm{tr}\,(\mathbf{B}^2) = 3$. By virtue of the decomposition of eq. (2.38), the tensor $\mathbf{B}$ is the sum of an isotropic part, that controls the intensity of anisotropy through the scalar f , and a deviatoric one, governing the

directional character of anisotropy. The normalisation should only affect the scalar value, such that $0 < f \leq 1$. It results that the constraint $\mathrm{tr}\,(\mathbf{B}^2) = 3$ corresponds to $\mathbf{F} : \mathbf{F} = 3 - 3f^2$. Here the alternative normalisation rule $\mathrm{tr}\,(\mathbf{B}) = 3$ is proposed that, by the decomposition of $\mathbf{B}$, leads to $f = 1$. The above constraints on $\mathbf{B}$ can be straightforwardly rewritten in terms of the anisotropy tensor $\mathbf{a}$. In fact, recalling the relation $\mathbf{B} = \mathbf{a}^2$, the rules $\mathrm{tr}\,(\mathbf{B}^2) = 3$ and $\mathrm{tr}\,(\mathbf{B}) = 3$ take the form $\mathrm{tr}\,(\mathbf{a}^4) = 3$ and $\mathrm{tr}\,(\mathbf{a}^2) = 3$, respectively. There is no reason to prefer a priori one or another of the above mentioned constraints, hence the user can indistinctly choose the most convenient among them.

3.3 Comparison with existing formulations

The proposed model is characterised by a hierarchical form: nonlinearity and anisotropy can be activated separately or in combination. Simpler cases are incorporated in the formulation and are recovered simply by appropriate parameter settings. For instance, for $n = 0$ the nonlinearity is deactivared and for the fabric tensor coinciding with the identity tensor the model reproduces the isotropic elastic behaviour of soils. Therefore, in this section both the linear and the nonlinear anisotropic model reported in the previous chapter are critically discussed and compared with the proposed one.

3.3.1 Linear models

Specialising eqs. (3.1) - (3.3) to the linear anisotropic case ($n = 0$ and $\mathbf{a} \neq \mathbf{I}$) one obtains:

$$\varphi\left(\boldsymbol{\varepsilon}, \mathbf{a}\right) = \frac{p_r}{2}\left\{\left[k - \frac{2}{3}g\right]\left[\mathrm{tr}\left(\mathbf{a}\boldsymbol{\varepsilon}\mathbf{a}\right)\right]^2 + 2g\mathrm{tr}\left[\left(\mathbf{a}\boldsymbol{\varepsilon}\mathbf{a}\right)^2\right]\right\} \tag{3.11}$$

$$\boldsymbol{\sigma} = p_r\left[\left(k - \frac{2}{3}g\right)\mathrm{tr}\left(\mathbf{a}\boldsymbol{\varepsilon}\mathbf{a}\right)\mathbf{a}^2 + 2g\mathbf{a}^2\boldsymbol{\varepsilon}\mathbf{a}^2\right] \tag{3.12}$$

$$\mathbb{D} = p_r\left(k - \frac{2}{3}g\right)\mathbf{a}^2 \otimes \mathbf{a}^2 + 2p_r g\left(\mathbf{a}^2 \underset{-}{\otimes} \mathbf{a}^2\right) \tag{3.13}$$

In order to compare the Graham & Houlsby (1983) model to the proposed one for the linear anisotropic case, eq. (3.12) can be specialised for triaxial conditions. Furthermore, in the principal direction reference system, the tensor $\mathbf{a}$ is assumed diagonal and coaxial with the principal stresses and strains and characterised by its eigenvalues a_1, a_2 and a_3. It results:

$$\left\{ \begin{array}{c} \sigma_1 \\ \sigma_2 \\ \sigma_3 \end{array} \right\} = p_r \left[\begin{array}{ccc} \left(k + \frac{4}{3}g\right) a_1^4 & \left(k - \frac{2}{3}g\right) a_2^2 a_1^2 & \left(k - \frac{2}{3}g\right) a_3^2 a_1^2 \\ \left(k - \frac{2}{3}g\right) a_1^2 a_2^2 & \left(k + \frac{4}{3}g\right) a_2^4 & \left(k - \frac{2}{3}g\right) a_3^2 a_2^2 \\ \left(k - \frac{2}{3}g\right) a_1^2 a_3^2 & \left(k - \frac{2}{3}g\right) a_2^2 a_3^2 & \left(k + \frac{4}{3}g\right) a_3^4 \end{array} \right] \left\{ \begin{array}{c} \varepsilon_1 \\ \varepsilon_2 \\ \varepsilon_3 \end{array} \right\} \tag{3.14}$$

Assuming for the matrix associated to the anisotropy tensor the following form ($a_1 \neq a_2 = a_3$ because of the transverse isotropy), defining $a_1 = a$ and selecting for the matrix representing $\mathbf{a}$ the so called multiplicative form, one obtains:

$$\left[\begin{array}{ccc} a & 0 & 0 \\ 0 & ya & 0 \\ 0 & 0 & ya \end{array} \right] \tag{3.15}$$

where the parameter y is the ratio of the stiffness along the two relevant principal directions. Depending on the choice, this parameter assumes different forms for the following three different normalisations:

$$\begin{cases} y = a^{-\frac{3}{2}} & for \quad \det(\mathbf{a}) = 1 \\ y = \sqrt{\frac{3-a^2}{2a^2}} & for \quad \mathrm{tr}(\mathbf{a}^2) = 3 \\ y = \left(\frac{3-a^4}{2a^4}\right)^{\frac{1}{4}} & for \quad \mathrm{tr}(\mathbf{a}^4) = 3 \end{cases} \tag{3.16}$$

Specialising eq. (3.14) to the case of transverse isotropy and comparing with eq. (2.29), it results $y = \alpha^2$, irrespectively of the adopted normalisation for $\mathbf{a}$, indicating that the proposed formulation encompasses that of Graham & Houlsby.

Comparing the strain energy in eq. (3.11) to that by Bigoni & Loret (1999) in eq. (2.39) it emerges that the two expressions are equivalent: in fact $\mathbf{B} = \mathbf{a}^2$, $\mathrm{tr}(\mathbf{B}\boldsymbol{\varepsilon}) = \mathrm{tr}(\mathbf{a}\boldsymbol{\varepsilon}\mathbf{a})$ and $\mathrm{tr}\left[(\mathbf{B}\boldsymbol{\varepsilon})^2\right] = \mathrm{tr}\left[(\mathbf{a}\boldsymbol{\varepsilon}\mathbf{a})^2\right]$ with λ and μ related to k and g as reported in eq. (2.20). Alternatively, recalling that the fabric tensor $\mathbf{B}$ can be expressed as the sum of its isotropic and deviatoric parts, as in eq. (2.38), eqs. (3.11) - (3.13) now specialise as follow:

$$\begin{aligned} \varphi(\boldsymbol{\varepsilon},\, f, \mathbf{F}) = \frac{p_r}{2}\left(k - \frac{2}{3}g\right)\left\{f^2\,(\mathrm{tr}\boldsymbol{\varepsilon}) + 2f\,(\mathrm{tr}\boldsymbol{\varepsilon})\,\mathrm{tr}\,(\boldsymbol{\varepsilon}\mathbf{F}) + [\mathrm{tr}\,(\boldsymbol{\varepsilon}\mathbf{F})]^2\right\} + \\ + p_r g f^2 \mathrm{tr}\left(\boldsymbol{\varepsilon}^2\right) + 2p_r g f\,\mathrm{tr}\left(\boldsymbol{\varepsilon}^2\mathbf{F}\right) + p_r g \mathrm{tr}\left[(\boldsymbol{\varepsilon}\mathbf{F})^2\right] \end{aligned} \tag{3.17}$$

$$\boldsymbol{\sigma} = p_r\left[\left(k - \frac{2}{3}g\right)\mathrm{tr}\,(f\mathbf{I}\boldsymbol{\varepsilon} + \mathbf{F}\boldsymbol{\varepsilon})\,(f\mathbf{I} + \mathbf{F}) + 2gf^2\boldsymbol{\varepsilon} + 2gf\boldsymbol{\varepsilon}\mathbf{F} + 2gf\mathbf{F}\boldsymbol{\varepsilon} + 2g\mathbf{F}\boldsymbol{\varepsilon}\mathbf{F}\right] \tag{3.18}$$

$$\begin{aligned}\mathbb{D} = p_r\left(k-\frac{2}{3}g\right)\left[f^2\mathbf{I}\otimes\mathbf{I}+f\left(\mathbf{I}\otimes\mathbf{F}+\mathbf{F}\otimes\mathbf{I}\right)+\mathbf{F}\otimes\mathbf{F}\right]+\\ +2p_r g f^2\mathbf{I}\underset{-}{\otimes}\mathbf{I}+2p_r g f\left(\mathbf{F}\underset{-}{\otimes}\mathbf{I}+\mathbf{I}\underset{-}{\otimes}\mathbf{F}\right)+2p_r g\mathbf{F}\underset{-}{\otimes}\mathbf{F}\end{aligned} \tag{3.19}$$

that correspond to the simplified version of the model proposed by Zysset & Curnier (1995) (eq. (2.37)), in which the coefficients $c_5 = c_8 = c_9 = 0$ in the more general free energy in eq. (2.32).

Comparing the structure of the free energy pertaining to the Lashkari (2010) model in eq. (2.46) to eq. (3.17) it results that the latter represents a more general formulation, as that by Lashkari neglects the two invariants $\left[\mathrm{tr}\left(\boldsymbol{\varepsilon}\mathbf{F}\right)\right]^2$ and $\mathrm{tr}\left[\left(\boldsymbol{\varepsilon}\mathbf{F}\right)^2\right]$. In fact, referring to the general free energy expression of eq. (2.32) proposed by Cowin (1985), this corresponds to consider the constants c_3 and c_6 equal to zero, too. As a consequence, contrary to the stiffness tensor in eq. (3.19), that obtained by Lashkari in eq. (2.45) does not include the terms $\mathbf{F}\otimes\mathbf{F}$ and $\mathbf{F}\underset{-}{\otimes}\mathbf{F}$.

Analogous considerations can be done for the Zhao & Gao (2015) model, which results as a simplified version of the proposed formulation in the same way of the Lashkari one.

Finally, to compare the proposed linear anisotropic formulation to that of Mašín & Rott (2014), the fabric tensor $\mathbf{a}$ can be expressed by its spectral decomposition, as reported in appendix A. In particular, for the case of transverse isotropy, the free energy of eq. (3.11) reads:

$$\begin{aligned}\varphi\left(\boldsymbol{\varepsilon},\mathbf{M}\right) = \frac{c_1}{2}\mathrm{tr}\left(\boldsymbol{\varepsilon}^2\right)+\frac{c_2}{2}\left(\mathrm{tr}\boldsymbol{\varepsilon}\right)^2+c_3\left(\mathrm{tr}\boldsymbol{\varepsilon}\right)\mathrm{tr}\left(\mathbf{M}\boldsymbol{\varepsilon}\right)+\\ +c_4\mathrm{tr}\left(\mathbf{M}\boldsymbol{\varepsilon}^2\right)+\frac{c_5}{2}\left[\mathrm{tr}\left(\mathbf{M}\boldsymbol{\varepsilon}\right)\right]^2\end{aligned} \tag{3.20}$$

For the transverse isotropy, the strain energy involves five coefficients c_i, which can be expressed as a function of the material constants k and g and the eigenvalues a_1 and a_2 of the fabric tensor $\mathbf{a}$ as follows:

$$\begin{aligned}&c_1 = 2p_r g a_2^4,\ c_2 = p_r\left(k-\frac{2}{3}g\right)a_2^4,\ c_3 = p_r\left(k-\frac{2}{3}g\right)a_2^2\left(a_1^2-a_2^2\right)\\ &c_4 = 2p_r g a_2^2\left(a_1^2-a_2^2\right),\ c_5 = \left(k+\frac{4}{3}g\right)\left(a_1^2-a_2^2\right)^2\end{aligned} \tag{3.21}$$

Comparing eq. (3.20) and (2.48) it follows that the formulations are equivalent since both $\mathbf{M}$ and $\mathbf{p}$ are defined as a dyadic product of a unit normal vector and the strain energy functions are expressed in terms of the same invariants of the fabric and

strain tensors. Nonetheless, it is worth recalling that the Mašín & Rott formulation is only valid for linear transverse isotropy, therefore it represents a particular case of the proposed one in its linear version. For $\mathbf{M} = \mathbf{0}$ (or equivalently $\mathbf{p} = \mathbf{0}$) the linear isotropic formulation is recovered.

3.3.2 Nonlinear models

The proposed nonlinear formulation employes for the strain energy the same mixed invariants $\mathrm{tr}\,(\mathbf{B}\boldsymbol{\varepsilon})$ and $\mathrm{tr}\left[(\mathbf{B}\boldsymbol{\varepsilon})^2\right]$ adopted by Gajo & Bigoni (2008). The main difference between the free energy potential of eq. (2.51) and that proposed in this work (eq. (3.1)) is in the adopted non-linearisation procedure: in the Gajo & Bigoni case it is characterised by the adoption of two different exponents, n and l, acting separately on the two mixed invariants, thus making the free energy a non-homogeneous function of $\boldsymbol{\varepsilon}$, while in the proposed case it is introduced as an overall modification of the linear quadratic expression. Therefore, apart from the trivial linear case, there is no way to handle the model parameters in order to attain the same constitutive response. Performing a comparison between the two formulations is not straightforward in the general anisotropic case. Nonetheless, as the main differences are in the nonlinear features, without loss of generality in the following the comparison is illustrated in the simplified isotropic case ($\mathbf{B} = \mathbf{I}$) under triaxial conditions. Eq. (2.51) can thus be rewritten as:

$$\varphi\left(\varepsilon_v, \varepsilon_s\right) = \alpha\varepsilon_v^n + \beta\left(\frac{3}{2}\varepsilon_s^2 + \frac{1}{3}\varepsilon_v^2\right)^l \tag{3.22}$$

and the components of the stiffness matrix are:

$$\begin{aligned}
D_{11} &= \beta l\left(l-1\right)\left(\frac{3}{2}\varepsilon_s^2 + \frac{1}{3}\varepsilon_v^2\right)^{l-2}\left[\frac{4}{9}\varepsilon_v^2 + \frac{2}{3}\frac{1}{l-1}\left(\frac{3}{2}\varepsilon_s^2 + \frac{1}{3}\varepsilon_v^2\right)\right] + \alpha n\left(n-1\right)\varepsilon_v^{n-2} \\
D_{12} &= D_{21} = \beta l\left(l-1\right)\left(\frac{3}{2}\varepsilon_s^2 + \frac{1}{3}\varepsilon_v^2\right)^{l-2} 2\varepsilon_v\varepsilon_s \\
D_{22} &= \beta l\left(l-1\right)\left(\frac{3}{2}\varepsilon_s^2 + \frac{1}{3}\varepsilon_v^2\right)^{l-2}\left[9\varepsilon_s^2 + \frac{3}{l-1}\left(\frac{3}{2}\varepsilon_s^2 + \frac{1}{3}\varepsilon_v^2\right)\right]
\end{aligned} \tag{3.23}$$

Comparing the isotropic elastic stiffness obtained using the proposed model (eq. (2.19)) and the Gajo & Bigoni one, it can easily be noted that the major difference lies in the term D_{11}. It is then worth evaluating the ratio between the two diagonal terms of the stiffness matrix under isotropic state of strain/stress ($\varepsilon_s = 0$), which in the case of the Gajo & Bigoni model is:

$$\frac{D_{11}}{D_{22}} = \frac{\alpha n\left(n-1\right)\varepsilon_v^{n-2}}{3\beta l\left(\frac{1}{3}\varepsilon_v^2\right)^{l-1}} + \left(l-1\right)\frac{4}{27}\left(\frac{1}{3}\right)^{l-2} + \frac{2}{9} \tag{3.24}$$

while for the proposed model it assumes the expression:

$$\frac{D_{11}}{D_{22}} = \frac{k}{3g} = \frac{2\left(1+\nu\right)}{9\left(1-2\nu\right)} \tag{3.25}$$

Under the above hypotheses, this ratio can be interpreted as the ratio between the bulk modulus K and the shear one G, thus it can be thought as a function of the Poisson's ratio. The difference between the formulations is substantial, as in the new proposed model the above ratio is constant, while in the model by Gajo & Bigoni it depends on the volumetric strain (except for the special case of $l = n/2$, in which the free energy becomes a homogeneous function of degree proporsional to n). This would obviously imply a constant Poisson's ratio for the proposed formulation under isotropic compression, while in that of Gajo & Bigoni it should evolve during the same stress path. In order to assess which response is more realistic, it is convenient to refer to some experimental evidences collected in the literature.

In recent years the improvement of the laboratory testing devices allowed to investigate the small strain behaviour of soils with relatively high accuracy. In particular, the set up of triaxial or hollow cylinder apparatus fitted with high resolution local transducers and bender elements has provided a wide and consistent set of experimental data on the reversible response of different materials as observed in the small strain range (i.e. in the reversible regime). As discussed with more detail in chapter 1, many attempts have been made to evaluate the Poisson's ratio under different loading conditions. Specifically, the experimental data indicate that the Poisson's ratio attains an approximately constant value along an isotropic stress path, as for example illustrated in figure (1.7) for the Hostun sand (Ezaoui & Di Benedetto (2009)). This result is consistent with what predicted by the elastic formulation discussed in this work.

Another possible drawback of the model formulated by Gajo & Bigoni (2008) is in the absence of a rigorous definition of the complementary energy function: in fact they propose an approximated expression, whose consistency with their free energy function is only verified for a specific set of material parameters. Conversely, in the proposed model the complementary energy function is always valid as it stems from a Legendre transform. The definition of a complementary energy function is very appealing as it allows to define the constitutive equations in both stiffness and compliance form. This aspect can be very attractive in the context of the implicit numerical integration of elasto-plastic constitutive models, as discussed by many

Authors (e.g.: Borja *et al.* (1997); Tamagnini *et al.*, (2002); Amorosi *et al.* (2008)).

Finally, in order to compare the Cudny & Partyka (2017) model to the proposed one, the complementary energy of eq. (3.5) has to be rewritten adopting the spectral decomposition, as explained in detail in appendix A. In particular, denoting as $\mathbf{N}$ the eigenprojection of the fabric tensor $\mathbf{a}^{-1}$ under the hypothesis of transverse isotropy, the energy reads:

$$\begin{aligned}\psi(\boldsymbol{\sigma},\mathbf{N}) = \frac{1}{p_r^{1-n}k(1-n)(2-n)}\left[c_1(\mathrm{tr}\boldsymbol{\sigma})^2 + c_2\mathrm{tr}\left(\boldsymbol{\sigma}^2\right) + c_3\mathrm{tr}\boldsymbol{\sigma}\mathrm{tr}(\mathbf{N}\boldsymbol{\sigma}) + \right.\\ \left. + c_4\left[\mathrm{tr}(\mathbf{N}\boldsymbol{\sigma})\right]^2 + c_5\mathrm{tr}\left(\mathbf{N}\boldsymbol{\sigma}^2\right)\right]^{\frac{2-n}{2}}\end{aligned} \tag{3.26}$$

with the five coefficients c_i function of material constants k, g and n and the eigenvalues a_1^{-1} and a_2^{-1} of the tensor $\mathbf{a}^{-1}$.

$$\begin{aligned}c_1 &= \left(\frac{1}{9} - \frac{k(1-n)}{6g}\right)a_2^{-4},\ c_2 = \frac{k(1-n)}{2g}a_2^{-4}\\ c_3 &= 2\left(\frac{1}{9} - \frac{k(1-n)}{6g}\right)a_2^{-2}\left(a_1^{-2} - a_2^{-2}\right),\ c_4 = \left(\frac{1}{9} + \frac{k(1-n)}{3g}\right)\left(a_1^{-2} - a_2^{-2}\right)^2\\ c_5 &= \frac{k(1-n)}{g}a_2^{-2}\left(a_1^{-2} - a_2^{-2}\right)\end{aligned} \tag{3.27}$$

Comparing the complementary energy functions of eqs. (2.54) and (3.26) it results that the way in which the non-linearisation is introduced is similar, though the model by Cudny & Partyka is simpler than the one proposed here. In fact, in the former the three additional invariants $\mathrm{tr}\boldsymbol{\sigma}$, $\mathrm{tr}\boldsymbol{\sigma}\mathrm{tr}(\mathbf{N}\boldsymbol{\sigma})$ and $\mathrm{tr}(\mathbf{N}\boldsymbol{\sigma})$ appear. It is also worth recalling that the Cudny & Partyka model only holds for the transverse isotropy case.

3.4 Calibration and model performance

In this section, the parameters calibration strategy and the predictive capability of the model are discussed with reference to both clays and sands. The isotropic model parameters consist in three scalar quantities g, k, and n directly affecting the magnitude of the components of the elastic stiffness tensor and their dependence on the current state of stress, while the fabric tensor $\mathbf{a}$ controls the structural character of anisotropy. The first three constants can be calibrated with reference to the evolution of the elastic modulus G and the volumetric modulus K (or equivalently

the Young's modulus E) with the state of stress for an isotropic material or along a specific direction for an anisotropic one. The inherent anisotropic behaviour is controlled by the tensor $\mathbf{a}$, which leads, in the most general case, to six extra parameters to be calibrated. Nevertheless, it is often the case that the principal directions of anisotropy are coaxial with those of the stress (or strain) thus leading to only three extra parameters. Under the further restrictive hypothesis of transverse isotropy, only two terms of the fabric tensor have to be defined. In the following the constraint $\mathrm{tr}\,(\mathbf{a}^2) = 3$ is adopted for the fabric tensor but any of the three possible normalisation of $\mathbf{a}$ discussed in section 3.2 is in principle applicable. All the constraints allow to further reduce the independent anisotropy-related parameters by one (they then become five in the general orthotropic case, two in the coaxial and only one in the coaxial transverse isotropic formulation). It is worth remembering that for a transverse isotropic material, the matrix associated to the compliance tensor takes the general form:

$$\mathbb{C} = \begin{bmatrix} \frac{1}{E_v} & -\frac{\nu_{hv}}{E_h} & -\frac{\nu_{hv}}{E_h} & 0 & 0 & 0 \\ -\frac{\nu_{vh}}{E_v} & \frac{1}{E_h} & -\frac{\nu_{hh}}{E_h} & 0 & 0 & 0 \\ -\frac{\nu_{vh}}{E_v} & -\frac{\nu_{hh}}{E_h} & \frac{1}{E_h} & 0 & 0 & 0 \\ 0 & 0 & 0 & \frac{1}{G_{vh}} & 0 & 0 \\ 0 & 0 & 0 & 0 & \frac{1}{G_{hv}} & 0 \\ 0 & 0 & 0 & 0 & 0 & \frac{1}{G_{hh}} \end{bmatrix} \tag{3.28}$$

where, considering the direction 1 vertical coinciding with the axis of anisotropy, E_v and E_h are the Young's moduli along the vertical and horizontal directions, G_{hh}, G_{hv} and G_{vh} the shear moduli and ν_{hh}, ν_{hv} and ν_{vh} the Poisson's ratios.

The elastic anisotropic behaviour of soils can be experimentally investigated by in situ and/or laboratory tests. The measurement of the shear wave velocities propagated along different directions and polarised in three orthogonal planes allows to determine the corresponding small strain shear moduli. This can be achieved through dynamic field techniques like cross-hole tests (Hight *et al.* 2007, Clayton 2011) and laboratory bender elements probing. Combining these latter with small strain triaxial static and dynamic tests and assuming the soil as being an elastic transverse isotropic material, it is possible to detect all the terms of the elastic stiffness tensor. More sophisticated laboratory devices, such as the hollow cylinder apparatus, allow to directly estimate the five independent parameters of a cross-anisotropic material.

Sands In the context of sands, Kuwano & Jardine (2002) investigated the elastic anisotropic behaviour of the Ham River sand. As described with more detail in chapter 1, they performed triaxial tests with high-resolution axial and radial LVDT transducers and bender elements on samples prepared by pluviation and then saturated. As reported in figure (1.15) they compressed the material following an anisotropic stress path characterised by constant shear ratio corresponding to to $K_0 = 0.45$.

Under the hypothesis of cross anisotropy, they obtained the Young's moduli E_v and E_h along the vertical and horizontal directions through static tests and, for the same states, the shear moduli G_{hh}, G_{hv} and G_{vh} by bender elements probing. In figure (3.1) the experimental data are shown with dots together with the simulations of the model. The material appears to be characterised by a non-negligible degree of structural anisotropy, as indicated by the different Young's and shear stiffness moduli observed along different directions by the very beginning of the probing, carried out once the required anisotropic stress state had been first achieved. The results also highlight a well-defined nonlinear dependency of the stiffness terms on the current stress state. The parameters of the proposed hyperelastic model have been calibrated with reference to the above experimental data under the hypothesis of cross anisotropy. Namely, in a principal direction system assumed as coaxial with the triaxial principal stress and strain reference, the tensor $\mathbf{a}$ is diagonal with $a_{11} \neq a_{22} = a_{33}$, with the principal direction 1 corresponding to the vertical one. Furthermore, stemming from the ratio D_{2323}/D_{1212} between the terms of the elastic stiffness matrix one can straightforwardly demonstrate that the ratio $(a_{22}/a_{11})^2$ is equal to the shear moduli ratio G_{hh}/G_{vh}. The parameters are reported in table (3.1).

Parameter	Ham River sand	Ticino sand	London clay
p_r (kPa)	100	100	100
n	0.47	0.5	0.8
k	1250	1300	350
g	1050	940	340
a_{22}/a_{11}	0.922	0.98÷1.118	1.378

Table 3.1: *Parameters for various soils*

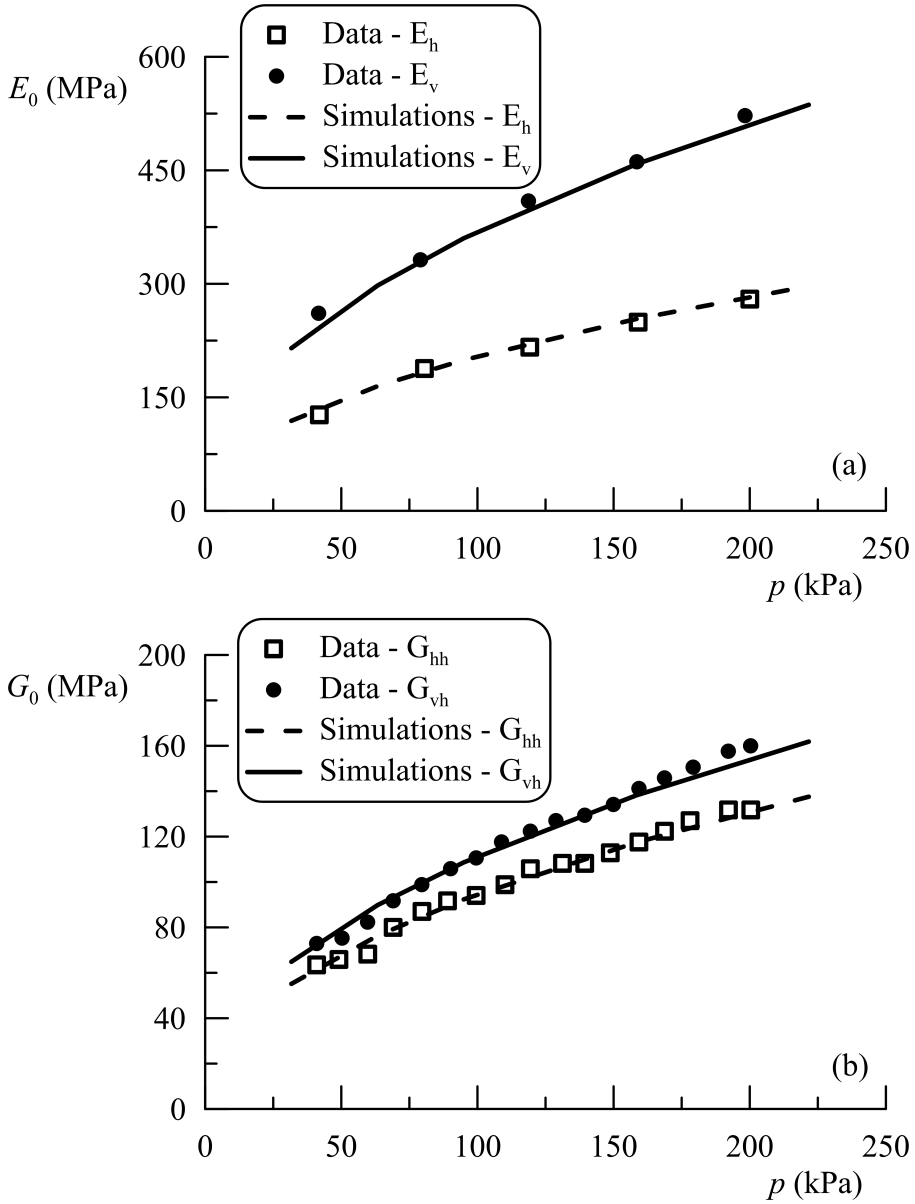

Figure 3.1: *Ham River sand: evolution of Young's moduli* (a) *and shear moduli* (b) *during anisotropic stress path*

Bellotti *et al.* (1996) performed laboratory dynamic tests on the Italian Ticino River sand to investigate the anisotropic nature of the small strain stiffness response for different effective stresses and void ratios. As illustrated in table (1.1), they evaluated the shear moduli G_{hh}, G_{hv} and G_{vh} and the Young's moduli E_v and E_h for different mean effective pressures following radial triaxial stress paths characterised by different K_0.

Figures (3.2) - (3.4) show the experimental results in terms of shear and Young's moduli against the mean effective pressure for a medium dense sand ($D_r = 41\%$) compressed along three different radial paths, characterised by K_0 equal to 0.5, 1

and 1.5 respectively. The figures also show the simulations of the model carried out for the set of parameters reported in table (3.1) and ratios a_{22}/a_{11} equal to 0.98, 1.086 and 1.118 for the corresponding increasing values of K_0.

The results obtained under isotropic stress conditions (figure (3.3)) reveal the presence of an inherent anisotropy reflecting the internal structure of the material, possibly stemming from the grain shape and sample preparation technique.

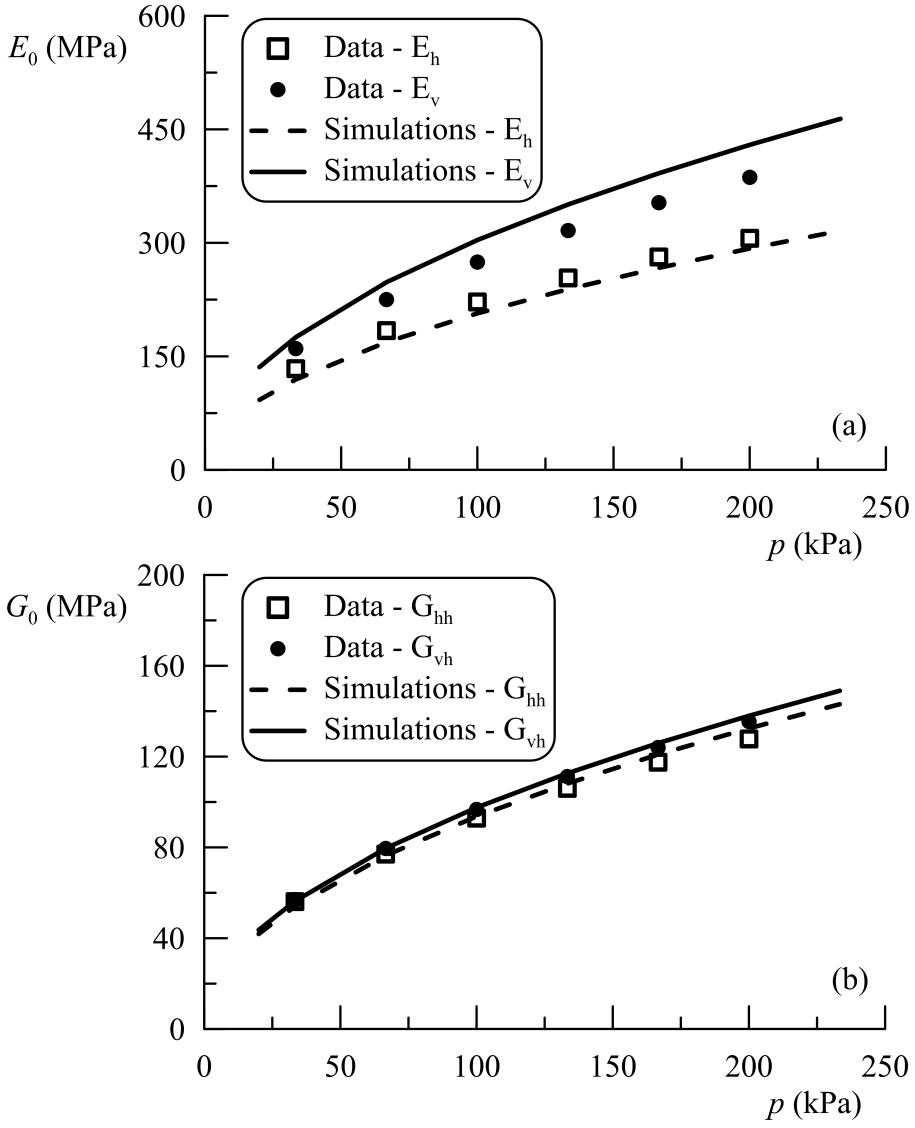

Figure 3.2: *Ticino River sand: evolution of Young's moduli* (a) *and shear moduli* (b) *during anisotropic consolidation* ($K_0 = 0.5$)

It is worth noting that different K_0 anisotropic compression lead to different ways in which anisotropy shows up leading, for example, to $E_v > E_h$ for $K_0 < 1$ and $E_v < E_h$ for $K_0 > 1$. The model simulations nicely reproduce the observed response for a unique set of parameters g, k, and n and an ad hoc selection of the ratio

a_{22}/a_{11} for each investigated K_0 value to account for the corresponding structural modification of the internal microstructure.

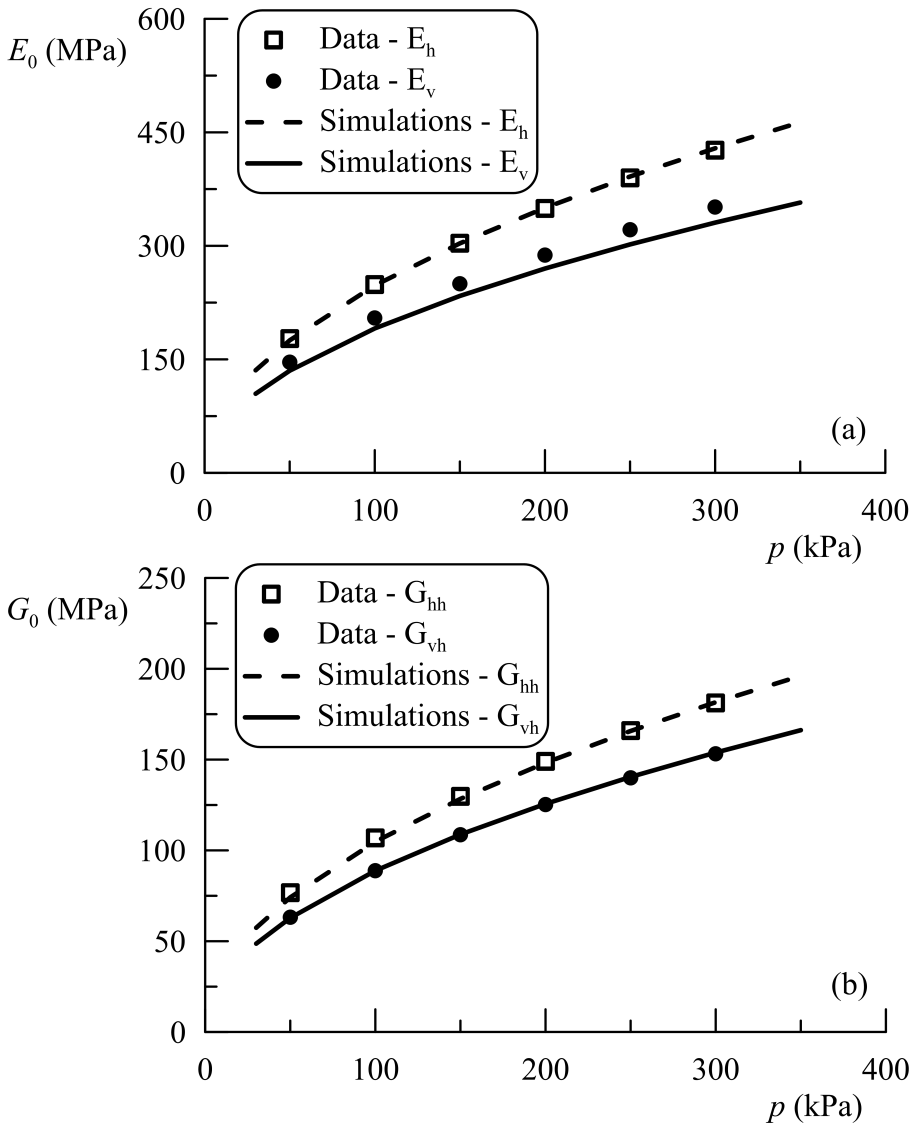

Figure 3.3: *Ticino River sand: evolution of Young's moduli* (a) *and shear moduli* (b) *during isotropic consolidation* ($K_0 = 1$)

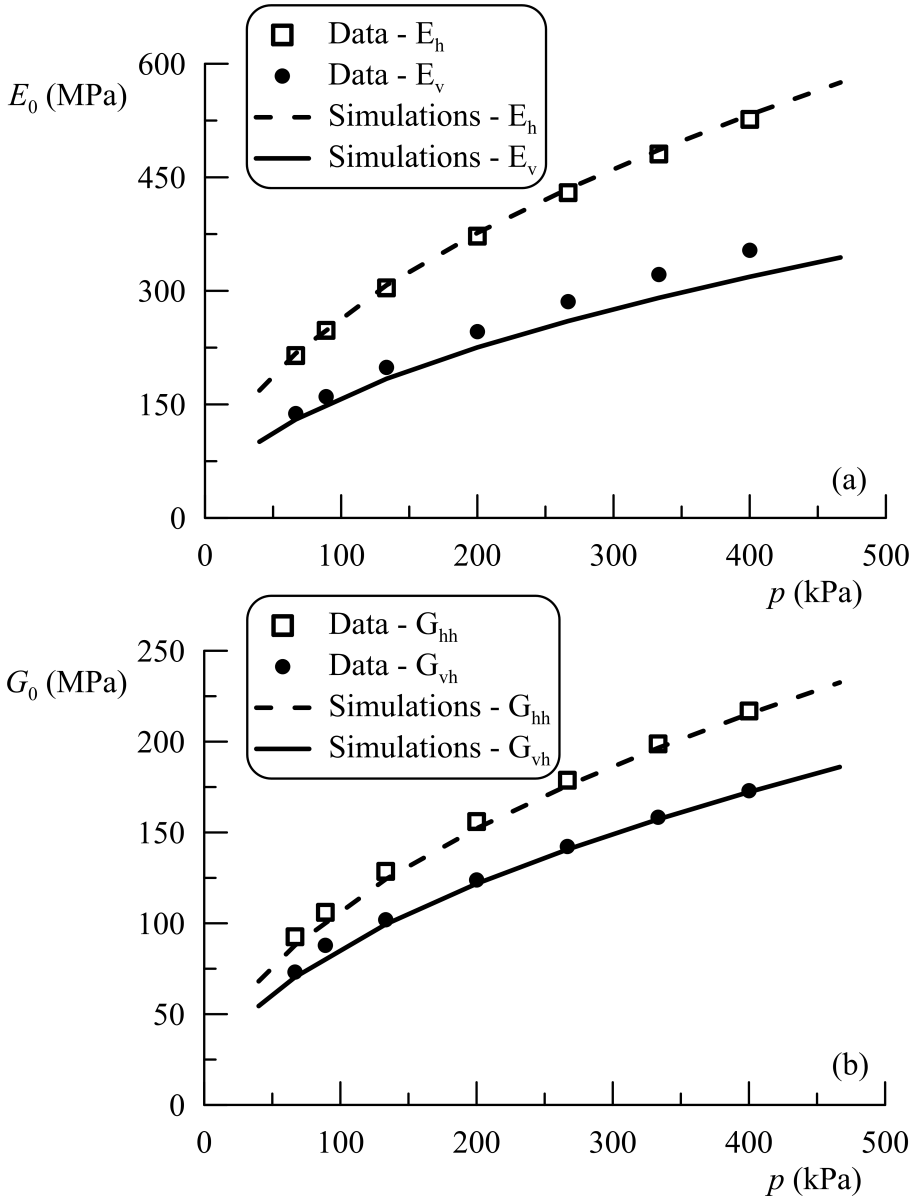

Figure 3.4: *Ticino River sand: evolution of Young's moduli* (a) *and shear moduli* (b) *during anisotropic consolidation* ($K_0 = 1.5$)

It is worth recalling that the sets of data obtained by Bellotti *et al.* (1996) are characterised by three degrees of anisotropy because different radial stress paths are applied during the tests. In fact, as discussed in chapter 1, the elastic shear moduli essentially depend on the normal stress components acting in the plane of shearing. In other words, the differences in the measured anisotropy ratios are uniquely produced by the current state of stress. This kind of stress induced anisotropy cannot be reproduced by the model because only a change in the shear stress components can induce a modification of the corresponding shear moduli. In other words, under different test conditions the material undergoes modifications of its internal

microstructure that cannot be considered with the present formulation. This is why the only way to nicely reproduce the experimental results of above is to assume three different ratios a_{22}/a_{11}. Conversely, in this case the model is able to take into account the effect of the stress-induced anisotropy on the Young's moduli.

Clays The elastic anisotropic behaviour of intact London clay has been experimentally investigated by Gasparre (2005) and Gasparre *et al.* (2007), who performed triaxial and hollow cylinder tests with high-resolution axial and radial LVDT transducers and bender elements, under static and dynamic test conditions. They detected the terms of the instantaneous elastic stiffness matrix assuming the hypothesis of cross anisotropy. In a similar way to Kuwano & Jardine (2002), they obtained the Young's moduli E_v and E_h along the vertical and horizontal directions through static and hybrid dynamic triaxial tests and the shear moduli G_{hh} and G_{hv} by bender element probing. In addition, a hollow cylinder apparatus (HCA) was used to perform measurements of the shear stiffness component G_{vh} and the Young's moduli. As discussed in chapter 1, the samples of the London clay were reconsolidated at the three different in situ stress states following the history of the material (figure (1.12)).

The model parameters are reported in table (3.1) for an experimentally observed constant shear stiffness ratio $G_{hh}/G_{vh} = 1.9$, which corresponds to the anisotropy ratio $a_{22}/a_{11} = 1.378$.

The results are illustrated in figure (3.5) in terms of the evolution of Young's and shear moduli with the mean effective pressure. While the experimental data only refer to the three stress states of figure (1.13), the model simulations are extended to higher p values following the shifted curve reported in figure (1.12). The scatter in the experimental results is probably due to the slightly different initial void ratios of the samples. It is worth recalling that the proposed model does not take into account the dependence of the stiffness on voids ratio or preconsolidation pressure, thus a single back-prediction is available for each stress state. The overall performance of the model reproduces the laboratory results in a satisfactory way.

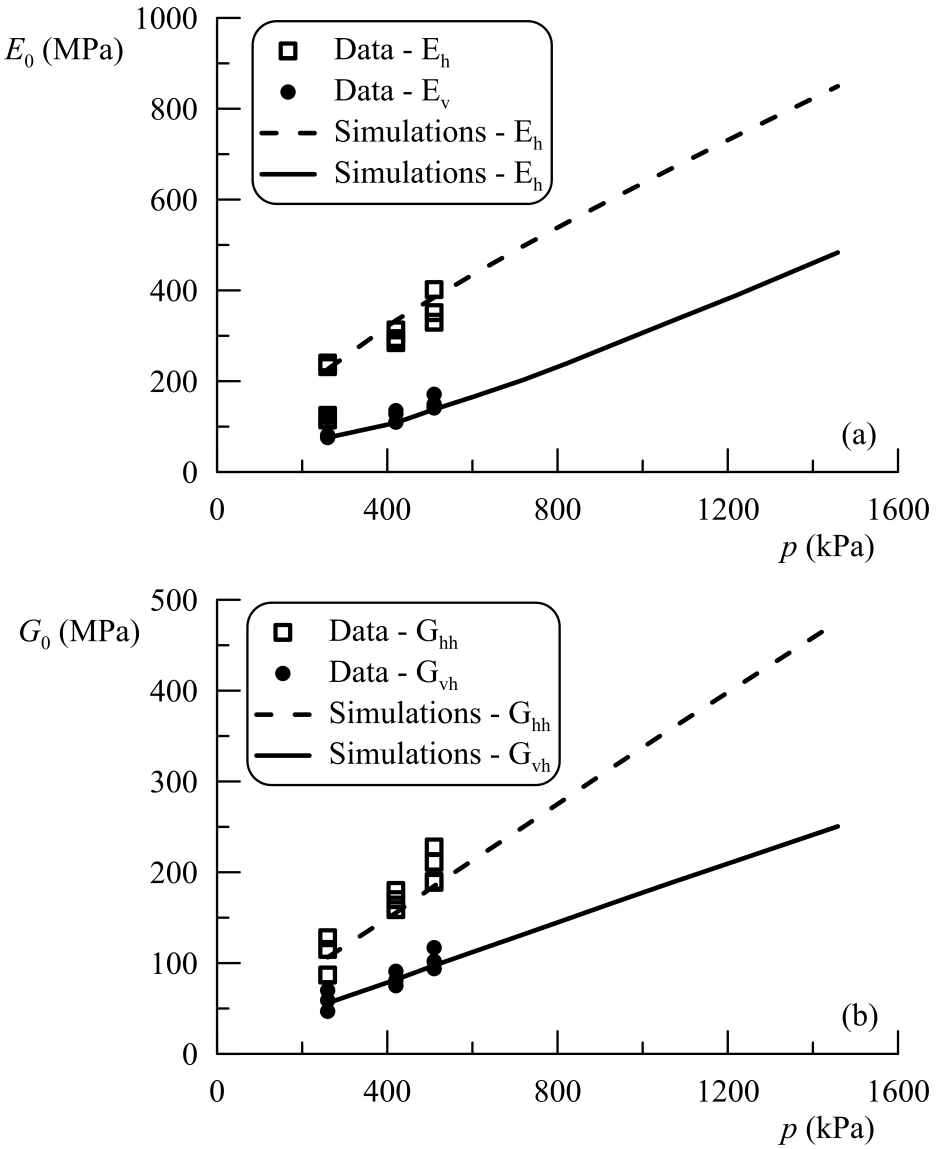

Figure 3.5: *London Clay: evolution of Young's moduli* (a) *and shear moduli* (b) *with mean effective pressure*

In addition, Gasparre (2005) carried out tests on the same intact material compressed along the isotropic axis and determined the shear moduli at different mean effective pressures by bender elements polarised along the vertical and horizontal planes. In this case a larger number of experimental data are available and illustrated in figure (3.6), together with the corresponding model fitting. These show that the model is capable of capturing the observed trend in the evolution of the two components of the stiffness investigated in the experiments.

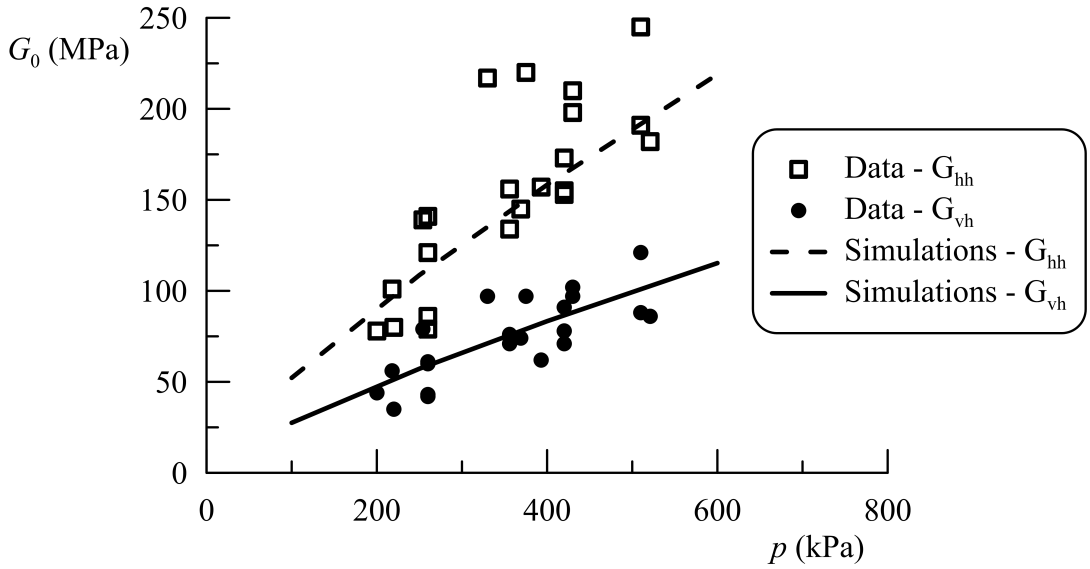

Figure 3.6: *London Clay: evolution of shear moduli during isotropic consolidation*

Chapter 4

Weak form of coupling in the framework of elastoplasticity

The work illustrated in the present chapter is the result of a research activity carried out under the supervision of prof. Yannis F. Dafalias in occasion of his visit to the Department of Structural and Geotechnical Engineering of the Sapienza University of Rome in the period of September-October 2017.

The experimental evidences described in chapter 1 show that the elastic properties of soils are affected by their plastic response. In particular, many solids like soils, rocks and concrete show a strong dependence of the elastic stiffness on the plastic deformations; a well-known result is the typical degradation of the elastic modulus observed in rocks under cyclic loading (figure (1.17)). These phenomena are what Hueckel (1976), Hueckel & Maier (1977) and Maier & Hueckel (1979) denote as elastoplastic coupling. Within the framework of classical elastoplasticity, Hueckel & Maier investigated these aspects in their pioneering works, highlighting the effect of the elastoplastic coupling on the elastic response and its implications on the flow rule. Considering a hyperelastic formulation, in which the free energy potential $\varphi = \varphi(\boldsymbol{\sigma}, \boldsymbol{\varepsilon}^p)$ is a function of the stress and the plastic strains $\boldsymbol{\varepsilon}^p$, the total strain rate results:

$$\dot{\boldsymbol{\varepsilon}} = \frac{\partial^2 \varphi}{\partial \boldsymbol{\sigma} \otimes \partial \boldsymbol{\sigma}} \dot{\boldsymbol{\sigma}} + \frac{\partial^2 \varphi}{\partial \boldsymbol{\sigma} \otimes \partial \boldsymbol{\varepsilon}^p} \dot{\boldsymbol{\varepsilon}}^p + \dot{\boldsymbol{\varepsilon}}^p = \dot{\boldsymbol{\varepsilon}}^r + \dot{\boldsymbol{\varepsilon}}^c + \dot{\boldsymbol{\varepsilon}}^p = \dot{\boldsymbol{\varepsilon}}^r + \dot{\boldsymbol{\varepsilon}}^i \tag{4.1}$$

where $\dot{\boldsymbol{\varepsilon}}^c$ is the coupling strain increment, $\dot{\boldsymbol{\varepsilon}}^r$ is the reversible component such that the elastic strain rate is $\dot{\boldsymbol{\varepsilon}}^e = \dot{\boldsymbol{\varepsilon}}^r + \dot{\boldsymbol{\varepsilon}}^c$ and $\dot{\boldsymbol{\varepsilon}}^i$ is the irreversible one, sum of the coupled and the plastic strain rates. Because of the elastoplastic coupling, whenever plastic deformations occur during the loading process, the elastic response changes and, considering an associated flow rule with respect to the plastic strain rate, the

irreversible strain increment will not result normal to the yield surface in the stress space. By now, the above features will be defined as a "weak" form of coupling or "one way coupling", in which plasticity affects elasticity, while the formulation of the first is not influenced by the coupling. As will be clear in chapter 6, this form of coupling is incomplete and the consequent formulation is not thermodynamically consistent. Nevertheless, in the framework of classical elastoplasticity, it represents a useful tool to take into account phenomena which otherwise would be impossible to characterise.

In this chapter a form of weak coupling is proposed, in order to reproduce the evolution of the elastic stiffness anisotropy with the plastic strains experimentally observed by Mitaritonna *et al.* (2014) on the Lucera clay. In fact, they proved that the change of the internal structure of the soil related to the development of irreversible deformation leads to a different anisotropic elastic response as compared to the initial configuration of the material. An attempt to model the elastoplastic coupling of the small strain stiffness anisotropy was made by Gajo & Bigoni (2008), who introduced in their anisotropic hyperelastic formulation a dependence of the fabric tensor on the plastic strains. Here a different approach is proposed, as discussed in the following.

In the framework of elastoplasticity, a possible strategy to take into account the anisotropy of soils within the plastic regime is to adopt an asymmetric yield surface in the stress space. In particular, the inherent and induced anisotropy can be efficiently described by the introduction of a distorted yield surface, able to rotate around the origin of the stress space according to a specific rotational hardening rule, as originally proposed by Hashiguchi (1977) and Sekiguchi & Ohta (1977). As a matter of fact, the yield surface is distorted and the result is an apparent rotation. This is why in the following to the terms rotation and distorsion will be simplistically attributed the same meaning. The initial anisotropy of soils, reflecting the internal microstructure due to the formation processes of the material, can be modelled by a rotated yield surface and the induced anisotropy due to plastic deformation is described by its further rotation. This represents a way to reproduce the change of the internal structure as induced by plastic strains in terms of rearrangement of the particles orientation.

The identification of the initial (in situ) rotation of the yield surface is very challenging from an experimental perspective. In fact, limiting the attention to the triaxial space, several probes in the p-q plane at different stress ratios are necessary to identify the initial shape and the size of the yield surface. It is worth mentioning that such an experimental activity can only be carried on clayey soils, for which

undisturbed samples can be retrieved from the ground. Furthermore, the detection of the yield surface is based on the assumption that the probing itself is not inducing any evolution of the anisotropy of the material. One of the most comprehensive databases on the shapes of the yield surfaces of natural clays was presented by Diaz-Rodriguez *et al.* (1992), who collected data on yield surfaces for 17 different natural clays characterised by different angles of internal friction. Later, Wheeler *et al.* (2003) performed a series of drained triaxial tests on the Finnish Otaniemi clay to investigate the validity of their model. In particular the objective was not only that of finding the yield point defining the initial size and orientation of the yield surface, but also to identify the rotation and the expansion of the yield surface after a second loading stage was applied. In figure (4.1) the initial yield curves predicted by the model by Wheeler *et al.* (2003) are depicted for four soft clays, demonstrating that the experimental evidences support the introduction of a rotated yield surface within elastoplastic constitutive models for clays.

Note that plastic strains induce a permanent modification of the internal structure that should not to be confused with the stress/strain induced anisotropy arising within nonlinear hyperelastic formulations, which by definition is lost whenever an isotropic stress/strain state is recovered.

Within this class of elastoplastic rotational hardening models, the one formulated by Dafalias & Taiebat (2013) is adopted herein. They describe the plastic anisotropic character of clays introducing a rotational hardening rule that allows both the yield and plastic potential surfaces to rotate. The advantages of this model with respect to others available in the literature are the following: its relative simple formulation and the attention devoted by the Authors to the control of the excessive rotation of the surfaces and to the proper attainment of the critical state conditions.

The aim of the present work is to improve the performance of the model to account for the evolution of the elastic stiffness anisotropy of soils with plastic strains along the line tracked by the pioneering work of Hueckel & Tutumluer (1994) on clays. From a mathematical point of view, this feature can be achieved linking the rotational hardening internal variables pertaining to the plastic response with the second order fabric tensor controlling the anisotropic response in the elastic domain. The original isotropic hypoelastic formulation of the model is substituted by the proposed nonlinear anisotropic hyperelastic one, in which the former constant fabric tensor, controlling the elastic directional properties of the clay, is allowed to evolve as linked to the rotational hardening variables of the model. The following developments refer to the hyperelastic formulation expressed in the fabric tensor $\mathbf{B}$-form, preferred to that in $\mathbf{a}$-form, as it leads to a more elegant and analytically

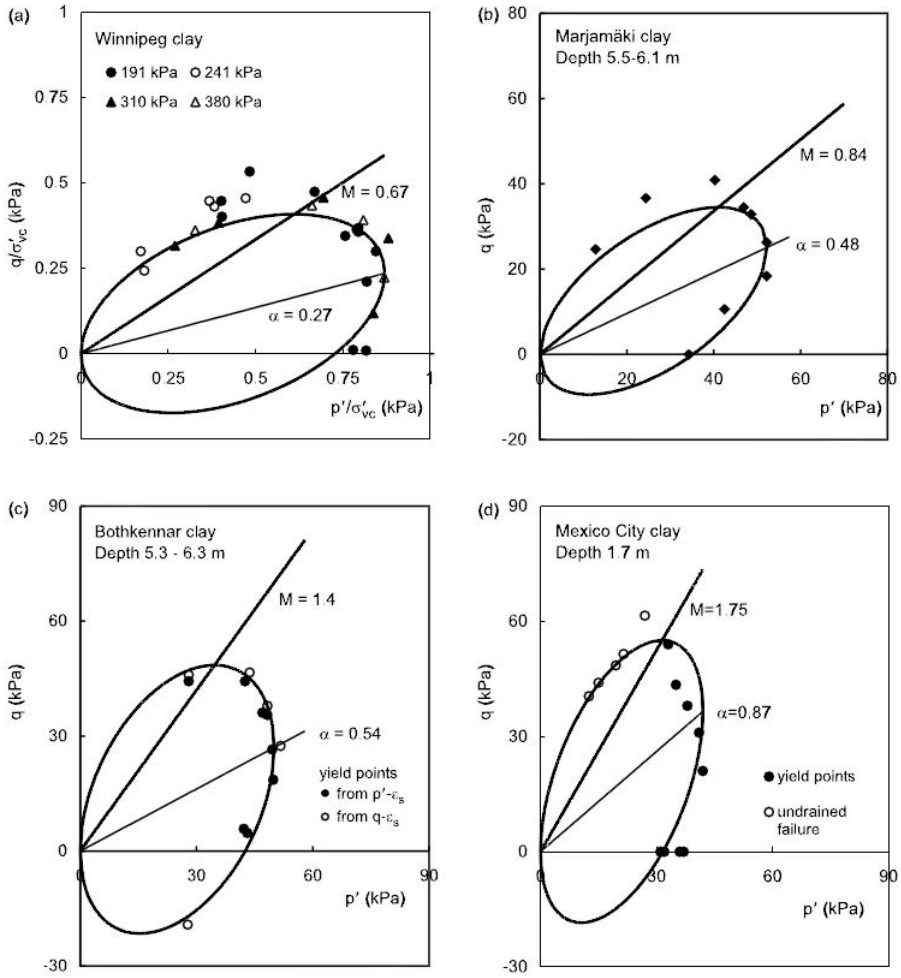

Figure 4.1: *Initial yield surfaces for different natural clays (from Wheeler et al. (2003))*

convenient formulation. The rotation of the yield and plastic potential surfaces are governed by a rotational hardening rule through an internal variable represented in the multiaxial formulation by a stress ratio-type second order deviatoric tensor. Dafalias & Taiebat (2013) proposed different alternatives for the hardening rule and particular attention is addressed to the evolution of the rotational internal variable in order to guarantee the uniqueness of the critical state condition and to avoid excessive and unrealistic rotations of the surfaces. The model is mainly presented in the triaxial formulation, though it can be easily extended to the most general multiaxial one. The performance of the model is finally illustrated with reference to the experimental results carried out by Mitaritonna *et al.* (2014) described in chapter 1.

4.1 The Dafalias & Taiebat (2013) model

The constitutive law by Dafalias & Taiebat (2013) is a single surface plasticity model, in which both the yield surface $f = 0$ and the plastic potential surface $g = 0$ are represented in the p-q plane by two distorted ellipses with equations:

$$g = f = (q - p\beta)^2 - \left(M^2 - \beta^2\right) p\,(p_0 - p) = 0 \tag{4.2}$$

where the parameter M denotes the slope of the critical state line in the p-q plane, assuming the value of M_c and M_e in compression and extension, for $\eta \geq \beta$ and $\eta \leq \beta$, respectively. p_0, defining the size of the surfaces, is the value of the mean effective pressure where the line characterised by the slope β intersects the yield surface, as reported in figure (4.2). This internal variable assumes the meaning of a preconsolidation pressure and identifies the normal consolidation line (NCL) in the e-ln$p$ plane. The slope α is a nondimensional scalar value internal variable expressed by a stress ratio, controlling the rotation of the surfaces (note that the symbol β is adopted herein instead of α in order to avoid confusion with the notation used in the following chapters). The use of the factor $(M^2 - \beta^2)$ in eq. (4.2) means that the yield curve has horizontal tangents at the points of intersection with the critical state lines in triaxial compression and extension. For $p = 0$ and $p = p_0$ the curve has vertical tangents.

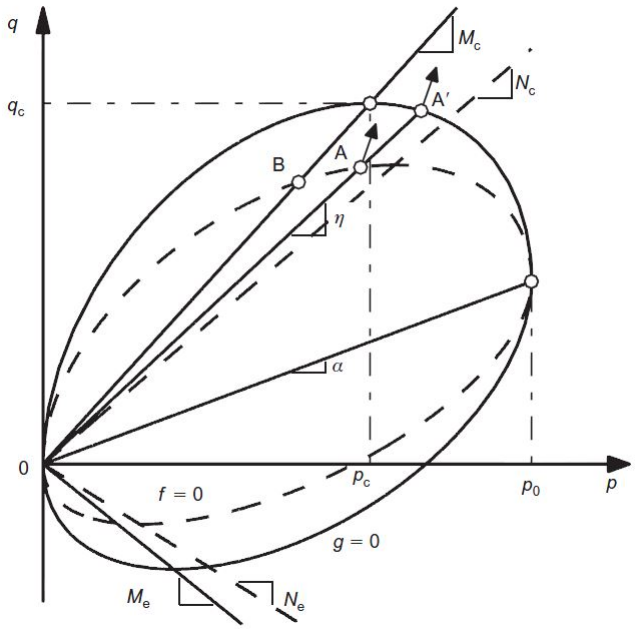

Figure 4.2: *Yield and plastic potential surfaces in the p-q plane*

For non-associative flow rule the additional parameter N is introduced, typically

lower than M and assuming the values N_c and N_e in compression and extension, respectively. In this case the direction of the plastic strain increment at a generic point A on the yield surface is specified by the normal to the plastic potential surface at a point A' defined by the same stress ratio. Although they are characterised by the same equation, in the most general case the two surfaces are two ellipses characterised by different eccentricity. It is worth noting that in order to guarantee that eq. (4.2) has real roots for q, the external constraint $|\beta| < M$ is required. For the special case of $\beta = 0$ the modified Cam Clay model is recovered.

The response of the model within the yield surface is characterised by hypoelastic isotropic strain-rate relations. In detail, the elastic volumetric and deviatoric strain increments are given by:

$$\begin{aligned} \dot{\varepsilon}_v^e &= \frac{\dot{p}}{K} \\ \dot{\varepsilon}_s^e &= \frac{\dot{q}}{3G} \end{aligned} \tag{4.3}$$

where K and G are the elastic bulk and shear moduli, related each other through the Poisson ratio ν. The elastic muduli depend linearly on the mean effective pressure, in particular for the bulk modulus is:

$$K = \frac{p}{\kappa}\left(1 + e_{in}\right) \tag{4.4}$$

where κ is a material constant representing the slope of the swelling line in the e-ln$p$ plane and e_{in} is the initial void ratio. The flow rule, in conjunction with the plastic potential surface in eq. (4.2) yields to the volumetric and deviatoric plastic strain increments reported below:

$$\begin{aligned} \dot{\varepsilon}_v^p &= \langle L \rangle \, p \left(M^2 - \eta^2\right) \\ \dot{\varepsilon}_s^p &= \langle L \rangle \, 2p \left(\eta - \beta\right) \end{aligned} \tag{4.5}$$

where L inside the Macauley brackets denotes the plastic multiplier, obtained by imposing the consistency condition $\dot{f} = 0$.

The model is characterised by a volumetric isotropic hardening governing the contraction and the expansion of the yield and the plastic potential surfaces and is expressed through the rate of the internal variable p_0, controlled by the volumetric plastic strain increment following the typical and well known relation:

$$\dot{p}_0 = \frac{1 + e_{in}}{\lambda - \kappa} p_0 \dot{\varepsilon}_v^p \tag{4.6}$$

where λ is the slope of the normal consolidation line in the e-ln$p$ plane and the

plastic volumetric strain increment $\dot{\varepsilon}_v^p = \langle L \rangle \frac{\partial g}{\partial p}$ is reported in eq. (4.5).

4.1.1 Rotational hardening

The yield and the plastic potential surfaces can rotate by virtue of a rotational hardening law controlling the rate of the internal variable β: once plastic loading occurs, the two surfaces start rotating according to:

$$\dot{\beta} = \langle L \rangle \, c p_{at} \frac{p}{p_0} \left(\beta_b - \beta \right) \tag{4.7}$$

where p_{at} is the atmospheric pressure and c is a model parameter controlling the pace of the evolution. The fundamental aspect characterising this law is that the evolution of β depends on the distance between a bounding value β_b, or equilibrium value, representing the constant value attained by β for a given stress ratio and function of the current η, and the current rotational internal variable. For a constant η stress path the surface will rotate from the initial configuration until reaching and then maintaining the equilibrium position. In this configuration the yield and the plastic potential surfaces continue to harden isotropically, homothetically evolving at fixed orientation. This means that if one projects the current values of p and p_0 in the e-ln$p$ plane, a line parallel to the normal consolidation line and the line itself are followed, respectively, similarly to what happens for the Cam Clay model. In comparison with other existing rotational hardening rules, that reported herein guarantees the uniqueness of the critical state line whatever are the initial state and the followed loading path, as demonstrated and widely discussed in the original paper. Another important aspect concerns the control of excessive rotations of the yield and the plastic potential surfaces. In fact, without introducing some constraints on the possible values assumed by the internal variable β, the model would lead to unrealistic rotations, not consistent with the typical experimental evidence on clays. As will be shown in the following, these conditions limit the range of the possible values of the model parameters related to the rotational hardening rules. Three possible expressions for the equilibrium value of the internal variable are reported in this section, the latter introduced in a subsequent work by the same Authors (Dafalias & Taiebat (2014)).

4.1.1.1 Linear rule

The first law reported here was proposed by Dafalias (1986) and represents the simplest expression to evaluate the equilibrium value for the rotational hardening internal variable β. It evolves linearly with the stress ratio η according to the

following expression:

$$\beta_b(\eta) = \frac{\eta}{x} \tag{4.8}$$

where x denotes an additional positive parameter of the model defining the bounding value of β for constant η stress paths.

4.1.1.2 Exponential rule

Dafalias & Taiebat (2013) propose an exponential dependence of the bounding value β_b with the stress ratio η according to the law:

$$\beta_b(\eta) = \pm\frac{M}{z}\left[1 - \exp\left(-s\frac{|\eta|}{M}\right)\right] \tag{4.9}$$

where z and s are two positive model parameters and for $\eta \geq 0$ and $\eta \leq 0$, M assumes the values M_c and M_e with the sign $\pm$, respectively.

The reason for the increasing analytical complexity of eq. (4.9) with respect to eq. (4.8) and the presence of an additional parameter can be justified by a more satisfactory capability of the model to reproduce the experimental results considered by the Authors. The equilibrium value in terms of ratio β_b/M monotonically increases with the ratio η/M and reaches asymptotically the value M/z. This feature guarantees the rotation not to exceed this latter value, irrespectively of the current stress ratio. Conversely, employing the linear equation, the value of the internal variable indefinitely increases with η, causing excessive rotations of the surfaces, thus leading to an unrealistic response of the model, this being more evident for increasing values of the current stress ratio η.

4.1.1.3 Dafalias & Taiebat (2014) rule

An additional evolution law for the bounding value β_b was proposed by Dafalias & Taiebat (2014) to improve the predictive capability of the model for high values of η and in correspondence of the critical state conditions. In particular, a still debatable issue is whether the inherent anisotropy should persist or not in the soil once the critical state conditions are reached, namely whether the fabric anisotropy should be zero or non-zero. From an experimental point of view reaching and maintaining the critical state condition in clays for a sufficient long time to monitor and measure the evolution of the fabric anisotropy represents a very challenging issue and, at the present time, no experimental evidences are available to fully clarify the problem. The geotechnical community is divided between those who argue that for critical state failure conditions there must be no anisotropic fabric due to the looseness of

the original internal structure, and those who suggest that the classical critical state theory is incomplete and should be revisited to include the effects of fabric. This is why Dafalias & Taiebat (2014) proposed a new law able to take into account both the zero and non-zero fabric anisotropy at critical state. Therefore, from an analytical perspective, the question is whether for $\eta = M$ the internal variable β should attain a constant value or should be zero.

The proposed law is characterised by two independent equations, the first one valid for$|\eta| \leq M$ and the second one for$|\eta| \geq M$, as follow:

$$\begin{aligned} \beta_b(\eta) &= \eta\left(\frac{\beta_c}{M} + m\left[1 - \left(\frac{|\eta|}{M}\right)^n\right]\right) \;\; for \;\; |\eta| \leq M \\ \beta_b(\eta) &= \eta\frac{\beta_c}{M}\exp\left(-\mu\left[\frac{|\eta|}{M} - 1\right]\right) \;\; for \;\; |\eta| \geq M \end{aligned} \tag{4.10}$$

where m, n and μ are positive model constants and β_c is the value of β in correspondence of the critical state condition. The first expression in eq. (4.10) leads to $\beta_b(0) = 0$ and $\beta_b(M) = \beta_c$ and the second one $\beta_b(M) = \beta_c$ and $\beta_b(\infty) = 0$, thus the continuity of the function for $\eta = M$ is guaranteed. According to eq. (4.10), the value of β increases as the stress ratio increases until reaching the maximun value and then decreases till attaining asymptotically the zero value following an exponential rule. The critical state value β_c becomes and additional parameter to be calibrated by the user and will be always less than the maximum one; in particular, according to eq. (4.10), $\beta_b(\eta) = 0$ for $|\eta| \geq 0$ when $\beta_c = 0$.

4.1.2 Multiaxial generalisation

The extension of the previous formulation to the general strain/stress space is straightforward. The crucial aspect is that the scalar-valued rotational internal variable β generalises into a stress ratio-type second order symmetric deviatoric tensor $\boldsymbol{\beta}$, with $\beta = \sqrt{(3/2)\,\boldsymbol{\beta} : \boldsymbol{\beta}}$. The structure of the rotational hardening rules is analogous to that presented above, with the bounding value β_b replaced with its tensor-valued counterpart $\boldsymbol{\beta}_b$, the stress ratio η is substituted by the second order deviatoric stress ratio tensor $\mathbf{r} = \mathbf{s}/p$, with $\mathbf{s}$ denoting the deviatoric stress tensor and $|\eta| = \sqrt{(3/2)\,\mathbf{r} : \mathbf{r}}$.

4.2 A modified rotational hardening rule

In this section a different rotational hardening rule is proposed instead of the original one in eq. (4.7) proposed by Dafalias & Taiebat (2013). In fact, the original equation

does not automatically guarantees that the current rotational variable β attains the equilibrium value β_b for a specific stress ratio η. In other words, for constant stress ratio paths, a bounding value for β different from β_b is reached. In order to demonstrate this assessment, consider the response of eq. (4.7) for a fixed η stress path.

Recalling the expression for the volumetric plastic strain rate of Dafalias & Taiebat (2013) in eq. (4.5), the plastic multiplier takes the form:

$$L = \frac{1}{p\left(M^2 - \eta^2\right)} \dot{\varepsilon}_v^p \tag{4.11}$$

Then, knowing the relation between the plastic void ratio change and the plastic volumetric strain change and introducing the isotropic hardening variable p_0 one obtains:

$$\dot{e}^p = -\left(\lambda - \kappa\right) \frac{\dot{p}_0}{p_0} = -\left(1 + e_{in}\right) \dot{\varepsilon}_v^p \tag{4.12}$$

Substituting the volumetric plastic strain rate of eq. (4.12) in eq. (4.11), the plastic multiplier becomes:

$$L = \frac{\lambda - \kappa}{1 + e_{in}} \frac{1}{p\left(M^2 - \eta^2\right)} \frac{\dot{p}_0}{p_0} \tag{4.13}$$

Then substituting eq. (4.13) in eq. (4.7), the evolution equation for β reads:

$$\dot{\beta} = \frac{\lambda - \kappa}{1 + e_{in}} \frac{1}{M^2 - \eta^2} c p_{at} \left(\beta_b\left(\eta\right) - \beta\right) \frac{\dot{p}_0}{p_0^2} \tag{4.14}$$

that, defining $C = c \frac{\lambda - \kappa}{1 + e_{in}} \frac{1}{M^2 - \eta^2}$, can be more efficiently rewritten as:

$$\frac{\dot{\beta}}{\beta_b\left(\eta\right) - \beta} = C p_{at} \frac{\dot{p}_0}{p_0^2} \tag{4.15}$$

Generally, eq. (4.15) cannot be solved analytically for β but, in the very special case of a radial stress path, being the stress ratio fixed throughout the loading process, it can be integrated in a closed form by separation of variables with respect to β and p_0. Denoting with β_{in} and $p_{0,in}$ the initial values, one obtains:

$$\beta = \beta_b - \left(\beta_b - \beta_{in}\right) \exp\left[p_{at} C \left(\frac{1}{p_0} - \frac{1}{p_{0,in}}\right)\right] \tag{4.16}$$

It is worth noting that according to eq. (4.16) $\beta = \beta_{in}$ for $p_0 = p_{0,in}$ and $\beta = \beta_b - \left(\beta_b - \beta_{in}\right) \exp\left[-p_{at} \frac{C}{p_{0,in}}\right]$ for $p_0 \to \infty$, thus never attaining the limit value β_b. This result is due to the square of p_0 in eq. (4.15). Consider now a more

generalised form of the same equation, with n a real number:

$$\dot{\beta} = \langle L \rangle \, c p_{at}^{n} \frac{p}{p_0^{n}} \left(\beta_b - \beta \right) \tag{4.17}$$

that, similarly as above, can be rewritten as:

$$\frac{\dot{\beta}}{\beta_b \left(\eta \right) - \beta} = C p_{at}^{n} \frac{\dot{p}_0}{p_0^{n+1}} \tag{4.18}$$

The former, integrated following the same technique as above, leads to:

$$\beta = \beta_b - \left(\beta_b - \beta_{in} \right) \exp \left[-p_{at}^{n} \frac{C}{n} \left(p_{0,in}^{-n} - p_0^{-n} \right) \right] \tag{4.19}$$

Eq. (4.19) automatically satisfies the initial condition $\beta = \beta_{in}$ at $p_0 = p_{0,in}$, but the condition $\beta = \beta_b$ for $p_0 \to \infty$ is verified only if $n \leq 0$. Stemming from this latter result, a proposed modification of the rotational hardening law consists in choosing $n = 0$, leading to:

$$\dot{\beta} = \langle L \rangle \, c p \left(\beta_b - \beta \right) \tag{4.20}$$

Remark Notice that during the transition of β when loading changes from one value of η to another, the analogy $\frac{\dot{p}_0}{p_0} = \frac{\dot{p}}{p}$ does not hold, because the corresponding consolidation lines in the e-ln$p$ plane are not parallel till the rotational internal variable reaches its equilibrium value β_b. Recalling the expression proposed by Dafalias (1986), the value of the mean effective pressure p corresponding to p_0 can be determined as follow:

$$\frac{p}{p_0} = \frac{M^2 - \beta^2}{\eta^2 - 2\beta\eta + M^2} \tag{4.21}$$

It is worth remembering that eq. (4.21) is valid for associative flow rule; in case of yield surface different from plastic potential, N substitutes for M.

Differentiating eq. (4.21) under constant η loading, after some algebra one can write:

$$\frac{\dot{p}}{p} - \frac{\dot{p}_0}{p_0} = 2 \left(\frac{\eta}{\eta^2 - 2\beta\eta + M^2} - \frac{\beta}{M^2 - \beta^2} \right) \dot{\beta} \tag{4.22}$$

Hence, this proves that $\frac{\dot{p}_0}{p_0} \neq \frac{\dot{p}}{p}$ unless the rotational variable saturates its evolution, i.e. the projection of p and p_0 in the e-ln$p$ plane are identified by parallel lines.

4.3 Constraints on β and parameters calibration

The internal variable β must satisfy certain conditions in order to avoid excessive rotation of the yield and the plastic potential surfaces. Although the equation of the yield surface requires the analytical restriction $|\beta| < M$, from an experimental point of view it appears that a further control of the entity of the rotation is necessary. In particular, since M and N are smaller in extension than in compression, the condition on the maximum value of the rotational variable is $\beta_{max} < min\,(M_e, N_e)$. However, this condition still might not be sufficient to limit the excessive rotations for high values of η. In fact, under this condition, for the linear case the ratio η/x can exceed the value of M. For the exponential law, the requirement $\beta_{max} = \frac{M_c}{z}$ combined with the former constraint on β_{max} leads to the restriction $z > \frac{M_c}{min(M_e,N_e)}$, but N_e can be much smaller than M_c, then the condition on z can be violated. A remedy to limit the excessive rotation of β is to introduce an upper bound of this latter for stress ratios greater than ξM, where ξ is a positive constant. A detailed analytical discussion of this issue is beyond the scope of this work, but again it is worth remembering that a check of the values adopted by the rotational variable is always necessary to avoid unrealistic responses of the model. Conversely, it is useful to analyse with attention the parameters calibration procedure. The list of the constitutive parameters is reported in table (4.1).

Parameter	Meaning
M_c, M_e	slope of the critical state line in the p-q plane
N_c, N_e	yield surface parameters
λ	slope of the NCL in the e-ln$p$ plane
κ	slope of the rebound line in the e-ln$p$ plane
ν	Poisson's ratio
c	rate of evolution of rotational variable
x	parameter for the linear rule
z, s	parameters for the exponential rule
m, n, μ	parameters for the Dafalias & Taiebat (2014) rule

Table 4.1: *Model parameters*

Parameters M, N, λ, κ and the Poisson's ratio can be calibrated following the standard procedures. The calibration of the parameters related to the rotational hardening is less trivial because of the uncertainty and the difficulties of determining the initial position of the yield surface in the stress space and, as a consequence,

the initial value of the rotational variable β. From an experimental perspective, the position of the yield surface for a given stress state can be determined probing the material along different stress paths in the p-q plane until plastic strains occur. Although through this probing one can desume the initial value of the rotational variable, the procedure requires great experimental efforts and can only provide information for one specific state of the material. Whenever the initial stress ratio changes, a new probing should be carried out. Therefore this procedure is barely adopted in standard geotechnical applications. In order to overcome this problem, Dafalias & Taiebat (2013) proposed a procedure to determine the rotational internal variable β under K_0 conditions.

Considering the unloading-reloading line in the e-ln$p$ plane the rate of volumetric strain leads to an infinitesimal variation of the void ratio according to:

$$\dot{e}^e = -\kappa \frac{\dot{p}}{p} = -\left(1 + e_{in}\right) \dot{\varepsilon}_v^e \tag{4.23}$$

and analogously, considering the NCL one can write:

$$\dot{e}^p = \dot{e} - \dot{e}^e = -\left(\lambda - \kappa\right) \frac{\dot{p}}{p} = -\left(1 + e_{in}\right) \dot{\varepsilon}_v^p \tag{4.24}$$

Combining eqs. (4.23) and (4.24) one obtains the well-known relation:

$$\dot{\varepsilon}_v = \frac{\lambda}{\lambda - \kappa} \dot{\varepsilon}_v^p \tag{4.25}$$

Defining $\epsilon = \dot{\varepsilon}_v / \dot{\varepsilon}_s$ and adopting the approximation of neglecting the elastic shear strain rate and recalling the eq. (4.5), the dilatancy Ψ takes the form:

$$\Psi = \frac{\dot{\varepsilon}_v^p}{\dot{\varepsilon}_s^p} = \left(1 - \frac{\kappa}{\lambda}\right) \epsilon = \frac{M^2 - \eta^2}{2\left(\eta - \beta\right)} \tag{4.26}$$

Solving eq. (4.26) for β, under K_0 consolidation $\left(\epsilon = \frac{2}{3}\right)$ it follows $\beta = \beta_{K_0}$ and $\eta = \eta_{K_0} = \frac{3(1-K_0)}{1+2K_0}$:

$$\beta_{K_0} = \frac{\eta_{K_0}^2 + 3\left[1 - (\kappa/\lambda)\right] \eta_{K_0} - M^2}{3\left[1 - (\kappa/\lambda)\right]} \tag{4.27}$$

Given the values of parameters M, κ and λ and knowing the stress ratio from the K_0 condition, one can determine the corresponding rotational internal variable. This condition often represents the in situ initial state of the soil, thus eq. (4.27) can be employed to determine the initial rotation of the yield and the plastic potential surfaces. In such a way the rotational variable can be easily initialised and the value obtained can be used within any of the rotational hardening rules described above,

since the process leading to eq. (4.27) does not depend on any of them. The basic idea is that the parameters of the different rules described above can be determined imposing that the K_0 loading represents the equilibrium value of β, such that $\dot{\beta} = 0$. In other words, the bounding value of β is known, being $\beta_b = \beta_{K_0}$ and $\eta = \eta_{K_0}$. In particular, for the first law in eq. (4.8), it follows that

$$x = \frac{\eta_{K_0}}{\beta_{K_0}} \tag{4.28}$$

Along the same philosophy, zeroing the rate of the internal variable in eq. (4.9), one obtains:

$$\beta_b = \beta_{K_0} = \pm \frac{M}{z} \left[1 - \exp\left(-s \frac{|\eta_{K_0}|}{M} \right) \right] \tag{4.29}$$

This latter equation is in principle not sufficient to determine both the parameters z and s. However, as shown in detail in the original paper by Dafalias & Taiebat (2013), one must have $s \leq z$ and a good assumption, in absence of additional information, is to assume $s = z$. An alternative approach would be that of calculating the equilibrium value β_b for various constant stress ratios and, if experimental results are available in this sense, calibrating the parameters z and s in order to properly fit the data.

For what concernes the rule proposed Dafalias & Taiebat (2014), imposing the K_0 condition on the first of eq. (4.10), one can express the parameter m as a function of n and β_c:

$$m = \left(\frac{\beta_{K_0}}{\eta_{K_0}} - \frac{\beta_c}{M} \right) \left[1 - \left(\frac{|\eta_{K_0}|}{M} \right)^n \right]^{-1} \tag{4.30}$$

There is no way to calibrate the critical state value of the rotational variable by direct measurements, thus it can be chosen as a percentage of $\frac{\beta_{K_0}}{M}$. The parameter m can be calculated for different n, with $n > 1$. Then the condition imposed by the continuity of the first derivative of both the expressions in eq. (4.10) yields

$$\frac{\beta_c}{M} = \frac{mn}{\mu} \tag{4.31}$$

that can be employed to calculate μ as a function of n, which is the remaining parameter to be calibrated. In addition, the requirements $\beta_b(\eta) < \eta$, for preventing the excessive rotation, and $\beta_c < \beta_{b,max}$, as discussed with more detail in Dafalias & Taiebat (2014), represent three constraints for the independent parameter n. The calibration procedure of the previous law is more complex and would require a set of experimental data showing the initial rotation of the yield surface for different

stress ratios.

Finally, the parameter c, controlling the pace of the rotation, is calibrated by a trial and error procedure.

4.4 Relationship between B and $\boldsymbol{\beta}$

In order to reproduce the evolution of the elastic stiffness anisotropy experimentally observed in clays, in this section a link between the fabric tensor $\mathbf{B}$ and the rotational hardening internal variable $\boldsymbol{\beta}$ is proposed. In doing that, the original isotropic hypoelastic formulation of the Dafalias & Taiebat (2013) model is substituted by the proposed nonlinear anisotropic hyperelastic one. The tensor $\mathbf{B}$ can be conveniently decomposed in its isotropic and deviatoric parts, as reported in eq. (2.38), as the tensor $\boldsymbol{\beta}$ is traceless. Furthermore, recalling the constraint $\mathrm{tr}\mathbf{B} = 3$, it results the scalar $f = 1$. The basic idea is that $\boldsymbol{\beta}$ can be included in the deviatoric part of the tensor $\mathbf{B}$. The starting point to develop this relationship are the experimental data carried out by Mitaritonna *et al.* (2014) on the Lucera clay illustrated in chapter 1. In fact, inspired by the elastic stiffness anisotropy evolution observed in laboratory along radial stress paths, the following empirical relationship between $\mathbf{B}$ and $\boldsymbol{\beta}$ was found:

$$\mathbf{B} = \mathbf{I} - \omega\beta\boldsymbol{\beta} \tag{4.32}$$

where ω is a new model parameter. Note that eq. (4.32) automatically respect the constraint $\mathrm{tr}\mathbf{B} = 3$ by virtue of the tracelessness character of $\boldsymbol{\beta}$. For $\beta = 0$, namely when no rotation of the yield surface is considered, isotropic elasticity is recovered. For the specific case of a transverse isotropic material characterised by the principal directions of $\mathbf{B}$ coinciding with those of the strain/stress tensors, recalling that $\beta = \sqrt{(3/2)\,\boldsymbol{\beta} : \boldsymbol{\beta}}$, eq. (4.32) reads in matrix form:

$$\begin{bmatrix} B_{11} & 0 & 0 \\ 0 & B_{22} & 0 \\ 0 & 0 & B_{33} \end{bmatrix} = \begin{bmatrix} 1 & 0 & 0 \\ 0 & 1 & 0 \\ 0 & 0 & 1 \end{bmatrix} - \omega\beta^2 \begin{bmatrix} \frac{2}{3} & 0 & 0 \\ 0 & -\frac{1}{3} & 0 \\ 0 & 0 & -\frac{1}{3} \end{bmatrix} \tag{4.33}$$

In particular, assuming the maximum principal direction 1 to be vertical and coinciding with the axis of anisotropy and $B_{22} = B_{33}$, the anisotropy ratio can be written as:

$$\frac{B_{22}}{B_{11}} = \frac{G_{hh}}{G_{hv}} = \frac{1 + \frac{1}{3}\omega\beta^2}{1 - \frac{2}{3}\omega\beta^2} \tag{4.34}$$

Eq. (4.34) clarifies the choice of the negative sign in eq. (4.32): taking into account that typically $G_{hh} > G_{hv}$ for clays, to obtain $\omega > 0$ the minus sign is necessary. Nonetheless, in order to guarantee the fabric tensor to be positive definite, namely the eigenvalues of $\mathbf{B}$ being positive, the condition $1 - \frac{2}{3}\omega\beta^2 > 0$ must also be respected. At the equilibrium values of β along constant stress ratio paths, eq. (4.34) takes the form:

$$\left(\frac{B_{22}}{B_{11}}\right)_b = \left(\frac{G_{hh}}{G_{hv}}\right)_b = \frac{1 + \frac{1}{3}\omega\beta_b^2}{1 - \frac{2}{3}\omega\beta_b^2} \tag{4.35}$$

Eq. (4.35) proves to be very useful for the calibration of the parameter ω.

Before discussing the implication of this form of elastoplastic coupling on the response of the model and the suggested calibration procedure with reference to the experimental data carried out by Mitaritonna *et al.* (2014) on Lucera clay, further considerations about the introduction of the nonlinear anisotropic hyperelastic model are necessary.

4.4.1 Some considerations on the use of the hyperelastic formulation

When the standard hypoelasticity is taken into account, the Poisson's ratio and the parameter κ, identifying the slope of the unloading-reloading line in the e-ln$p$ plane, control the elastic bulk and shear moduli of clays (eq. (4.4)); conversely, when the proposed hyperelastic formulation is adopted, the parameters g, k, n are considered. Nonetheless, the parameter κ still enters in eq. (4.27), affecting the initial value of β under K_0 conditions. Therefore, an investigation on the relation between the hyperelastic constitutive parameters and the slope κ is necessary. In particular, the introduction of the nonlinear hyperelastic formulation leads to an equivalent constant κ variable with the stress.

In the following the equivalent κ is first obtained based on the proposed hyperelastic formulation and then examined to quantitatively evaluate the role of the stress dependency mentioned above. In order to express this latter parameter as a result of the hyperelastic formulation, the following procedure is presented. Consider, under triaxial conditions, the general relation between the increments of the volumetric and deviatoric elastic strains $\dot{\varepsilon}_v^e$ and $\dot{\varepsilon}_s^e$ and the increments of mean pressure $\dot{p}$ and deviatoric stress $\dot{q}$:

$$\begin{Bmatrix} \dot{\varepsilon}_v^e \\ \dot{\varepsilon}_s^e \end{Bmatrix} = \begin{bmatrix} C_{11} & C_{12} \\ C_{21} & C_{22} \end{bmatrix} \begin{Bmatrix} \dot{p} \\ \dot{q} \end{Bmatrix} \tag{4.36}$$

where C_{ij} are the terms of the matrix associated to the compliance tensor. Noting that for constant stress ratio loading $\eta = \frac{\dot{q}}{\dot{p}} = \frac{q}{p}$, the elastic volumetric strain increment rewrites into:

$$\dot{\varepsilon}_v^e = C_{11}\dot{p} + C_{12}\dot{q} = (C_{11} + C_{12}\eta)\,\dot{p} \tag{4.37}$$

Then substituting eq. (4.37) in eq. (4.23) one obtains the slope κ of the unloading-reloading line expressed as a function of the elastic formulation:

$$\kappa = (1 + e_{in})\,(C_{11} + C_{12}\eta)\,p \tag{4.38}$$

Considering now the new hyperelastic formulation for the isotropic case, i.e. the fabric tensor coinciding with the identity tensor, eq. (4.38) can be specialised as:

$$\kappa = (1 + e_{in})\left(1 + \frac{k\,(1-n)}{3g}\eta^2\right)^{-\frac{n}{2}} \frac{1}{k}\left(\frac{p}{p_r}\right)^{1-n} \tag{4.39}$$

From eq. (4.39) it follows that κ is not constant as it depends on the mean effective pressure. Note that for the linear case ($n = 0$), κ evolves linearly with p, whereas for $n = 1$, namely the case in which the elastic stiffness depends linearly on the state of stress, κ is constant and the formulation by Dafalias & Taiebat (2013) is recovered. It is worth noting that when the hyperelastic parameters g, k, n are calibrated with reference to the very small strain response, the resulting values of κ are lower than those typically adopted in the Dafalias & Taiebat (2013) model. This is consistent with the fact that in the latter model κ is evaluated as the slope of a swelling line, in a range of mean effective pressure characterised by higher levels of strain. In fact, strictly speaking κ is not an elastic constant, as opposed to the parameters of the hyperelastic model that are calibrated on the very small strain soil response but represents the slope of the swelling line in the e-ln$p$ plane, varying with the current stress state.

In the following eq. (4.39) will be generalised to the anisotropic case. For the most general anisotropic hyperelastic formulation (see chapter 3), an expression for κ similar to that of eq. (4.39) cannot be straightforwardly obtained because the model is formulated in the general stress/strain space in terms of mixed invariants of the stress/strain tensors and the fabric one. It is more convenient to employ the definitions of the stress and strain invariants in order to express the compliance matrix in eq. (4.36) in terms of the components of the 6x6 one. In particular, specialising the general constitutive relationship $\dot{\boldsymbol{\varepsilon}} = \mathbb{C}\dot{\boldsymbol{\sigma}}$ to the triaxial formulation, being $\varepsilon_{11} \neq \varepsilon_{22} = \varepsilon_{33}$ and $\sigma_{11} \neq \sigma_{22} = \sigma_{33}$, one can write:

$$\begin{aligned}\dot{\varepsilon}_{11} &= C_{1111}\dot{\sigma}_{11} + 2C_{1122}\dot{\sigma}_{22} \\ \dot{\varepsilon}_{22} &= C_{2211}\dot{\sigma}_{11} + (C_{2222} + C_{2233})\,\dot{\sigma}_{22}\end{aligned} \tag{4.40}$$

Then, by definition of the strain invariants ε_v and ε_s, the constitutive relationship becomes:

$$\begin{aligned}\dot{\varepsilon}_v &= (C_{1111} + 2C_{2211})\,\dot{\sigma}_{11} + 2\,(C_{1122} + C_{2222} + C_{2233})\,\dot{\sigma}_{22} \\ \dot{\varepsilon}_s &= \frac{2}{3}\left[(C_{1111} - C_{2211})\,\dot{\sigma}_{11} + (2C_{1122} - C_{2222} - C_{2233})\,\dot{\sigma}_{22}\right]\end{aligned} \tag{4.41}$$

Furthermore, the stress components are expressed in terms of the stress invariants p and q:

$$\begin{aligned}\dot{\varepsilon}_v &= (C_{1111} + 4C_{2211} + C_{2222} + C_{2233})\,\dot{p} + \frac{2}{3}\,(C_{1111} + C_{2211} - C_{2222} - C_{2233})\,\dot{q} \\ \dot{\varepsilon}_s &= \frac{2}{3}\,(C_{1111} + C_{2211} - C_{2222} - C_{2233})\,\dot{p} + \frac{2}{9}\,(2C_{1111} - 4C_{2211} + C_{2222} + C_{2233})\,\dot{q}\end{aligned} \tag{4.42}$$

Once the terms of the compliance matrix in the general stress-strain space are known stemming from the anisotropic nonlinear hyperelastic formulation, the terms of the compliance matrix of the triaxial formulation in eq. (4.36) can be determined:

$$\begin{aligned}C_{11} &= C_{1111} + 4C_{2211} + C_{2222} + C_{2233} \\ C_{12} = C_{21} &= \frac{2}{3}\,(C_{1111} + C_{2211} - C_{2222} - C_{2233}) \\ C_{22} &= \frac{2}{9}\,(2C_{1111} - 4C_{2211} + C_{2222} + C_{2233})\end{aligned} \tag{4.43}$$

Of course, even for the anisotropic case, the equivalent value of κ is not constant but depends on the current state of stress. As a consequence, in order to evaluate the rotational internal variable under K_0 condition, one should determine the value of κ for the range of mean effective pressure of interests for the specific problem and then assume a representative value to be used in eq. (4.27). For the set of parameters reported in table (4.2) for Lucera clay, figure (4.3) depicts the evolution of κ with the mean effective pressure for the proposed nonlinear anisotropic hyperelastic model along a constant $\eta = 0.6$ loading path corresponding to the K_0 condition, combining eqs. (4.38) and (4.43). Under the hypothesis of transverse isotropy, with the tensor $\mathbf{B}$ coaxial with the stress and strain tensors and the direction 1 coinciding with the axis of anisotropy, for the initial state $\eta_{in} = \eta_{K_0} = 0.6$ it results $B_{11} = 0.937$ and $B_{22} = B_{33} = 1.031$, corresponding to the anisotropic ratio $G_{hh}/G_{vh} = B_{22}/B_{11} = 1.1$.

Parameter	Value
p_r	100
n	0.78
k	888.3
g	533
M	1.08
λ	0.143
η_{K_0}	0.6
e_{in}	0.8

Table 4.2: *Model parameters for Lucera clay*

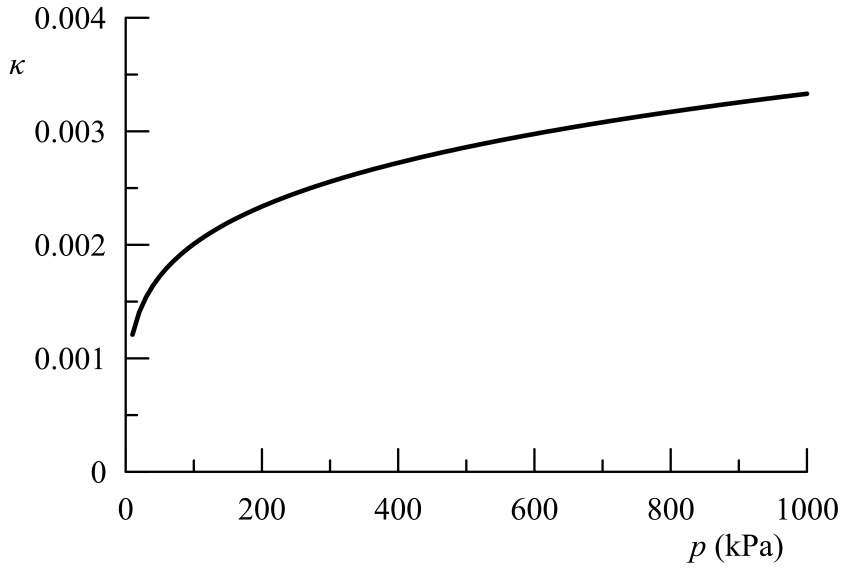

Figure 4.3: *Evolution of κ with the mean effective pressure*

Figure (4.3) shows that, despite the unquestionable evolution of κ, the range of values attained in a wide range of mean pressure (10÷1000 kPa) is not large. Even more, when using eq. (4.27) it emerges that β_{K_0} does not show any relevant sensitivity to κ (figure (4.4)), when this latter is varied in its range. This should be related to its relatively small value as compared to that of λ. As a consequence, instead of specifying the rotational variable for different mean effective pressures, for practical purposes a good assumption is to consider a constant value for β_{K_0}. For the specific problem, correspondingly to the initial mean effective pressure $p = 175\,\text{kPa}$, it results $\beta_{K_0} = 0.327$.

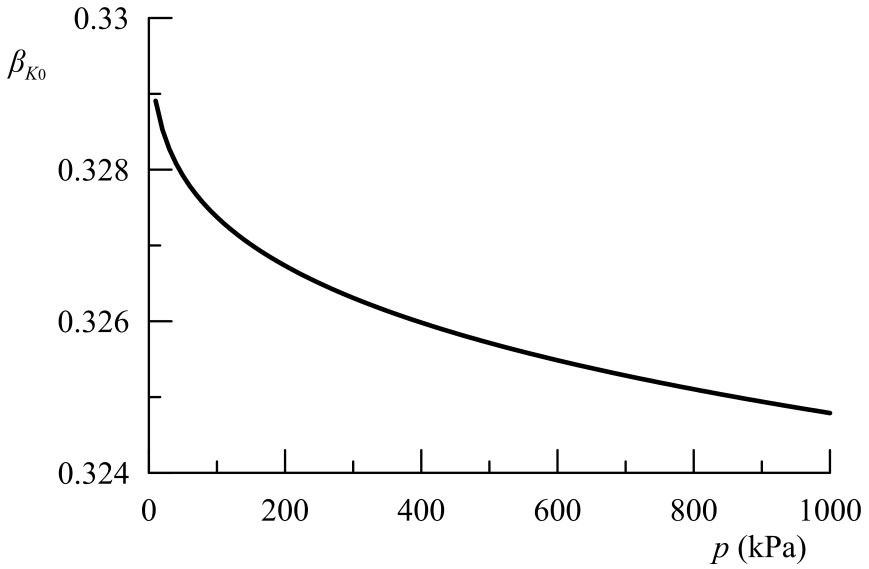

Figure 4.4: *Evolution of β_{K_0} with the mean effective pressure*

4.5 Model performance and calibration

As discussed above, eq. (4.32) represents a weak form of elastoplastic coupling, in which the plasticity, through the rotation of the yield and the plastic potential surfaces, affects the elastic response of the model. The first advantage of this relationship is in its analytical simplicity, requiring solely the parameter ω to be calibrated and, more important, in the fact that it introduces an evolution character to the fabric tensor as a consequence of the evolution of the tensor-valued rotational variable $\boldsymbol{\beta}$. In other words, a rotation of the surfaces from an initial configuration produces an evolution of the elastic stiffness anisotropy. In addition, note that whenever β reaches its bounding value β_b for fixed η, the anisotropy ratio attains a constant value.

The parameter ω can be easily calibrated with reference to the K_0 condition, which often represents the in situ stress state of the soil. In correspondence of η_{K_0}, the equilibrium value of the rotational variable β is $\beta_b = \beta_{K_0}$, calculated through eq. (4.27). For the case of transverse isotropy, which represents a reasonable hypothesis in many geotechnical applications due to the typical geological processes leading to the formation of the soil deposit, if the anisotropy ratio is known from the measurements of the elastic shear moduli corresponding to the K_0 condition, eq. (4.35) can be employed to determine ω. In other words, once the equilibrium value β_b is calibrated for a fixed stress ratio η according to the specific rotational hardening rule, one can select the constant ω in order to obtain the desired ratio G_{hh}/G_{vh} experimentally observed in laboratory or in situ tests. Note that because

of eq. (4.32), a single measurement of the elastic shear moduli for a specific stress ratio is required to calibrate the new parameter. In case more than one experimental results are available for different stress ratios, like for the data by Mitaritonna *et al.*, one can select the value of ω that better fits the data. Once this latter is determined, the evolution of the elastic stiffness anisotropy can be monitored by virtue of the value attained by the rotational variable for the current stress state. In particular, following the same philosophy described above, eq. (4.20) can be more conveniently rewritten as:

$$\frac{\dot{\beta}}{\beta_b(\eta) - \beta} = C\frac{\dot{p}_0}{p_0} \tag{4.44}$$

with $C = c\frac{\lambda-\kappa}{1+e_{in}}\frac{1}{M^2-\eta^2}$. For constant stress ratios loading paths, eq. (4.44) can be analytically integrated, leading to:

$$\beta = \beta_b - (\beta_b - \beta_{in})\left(\frac{p_{0,in}}{p_0}\right)^C \tag{4.45}$$

In addition, considering an associative flow rule, one can determine the evolution of the rotational variable with the mean pressure p recalling eq. (4.21) originally proposed by Dafalias (1986). Combining this latter with the relationship between $\boldsymbol{\beta}$ and $\mathbf{B}$ of eq. (4.32), eq. (4.45) provides the evolution of the fabric tensor and the elastic stiffness anisotropy with the mean effective pressure for constant η stress paths. Finally, parameter c, controlling the evolution of β, can be calibrated in order to mimic the variation of the anisotropic ratio with the mean effective pressure experimentally observed for the Lucera clay. Similarly to what happens for ω, as the assumed law for β_b changes, different c are necessary to better reproduce the laboratory results.

In the following the evolution of the elastic anisotropy ratio for the values of η experimentally obtained by Mitaritonna *et al.* (2014) and discussed in chapter 1 are reproduced through the proposed coupled formulation. In particular, the response of the model is explored for the three possible laws of the equilibrium value of the rotational internal variable. The basic parameters of the model are reported in table (4.2), with $\kappa = 0.002$ and $\beta_{K_0} = 0.327$, evaluated for $\eta_{K_0} = 0.6$ in correspondence of the initial mean effective pressure for the test on the Lucera clay ($p = 175\,\text{kPa}$) and maintained constant throughout the simulation. Then the parameters concerning the laws for β_b and ω and c will be introduced for the specific case.

4.5.1 Linear law

As introduced above, in case of measurements of the elastic moduli along different directions are available for different stress ratios, the parameter ω should be determined aiming at better catching the whole experimental database. Here, a calibration procedure is proposed. As a first step, adopting the linear law for β_b, the parameter x is determined on the K_0 condition, using eq. (4.27). Then the equilibrium values of β are calculated for different stress ratios and, since the anisotropy ratios G_{hh}/G_{vh} are known for the corresponding η, different ω would result from eq. (4.35). These results can be represented in the plane $\beta_b - \omega\beta_b$, as shown in figure (4.5). The value of ω can be obtained by a linear least squares regression of the data. Note that from the latter results $\omega \simeq 1$. In such a way one can determine the anisotropy ratio for any η. Figure (4.6) compares the steady values of G_{hh}/G_{vh} experimentally measured for different stress ratio to the back predictions of the model.

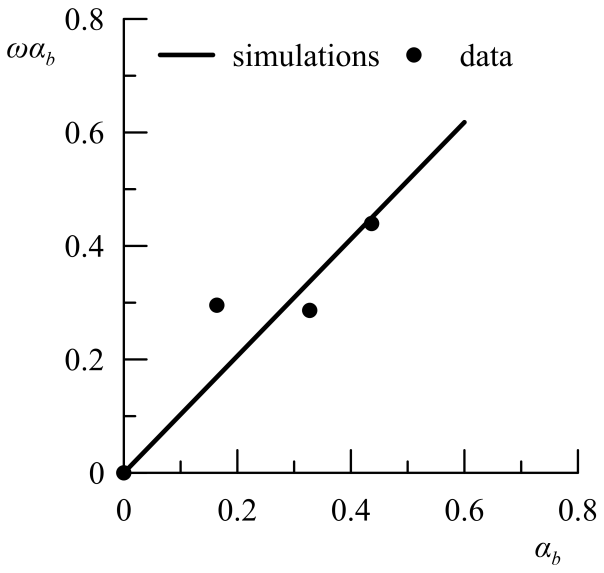

Figure 4.5: *Calibration of* ω

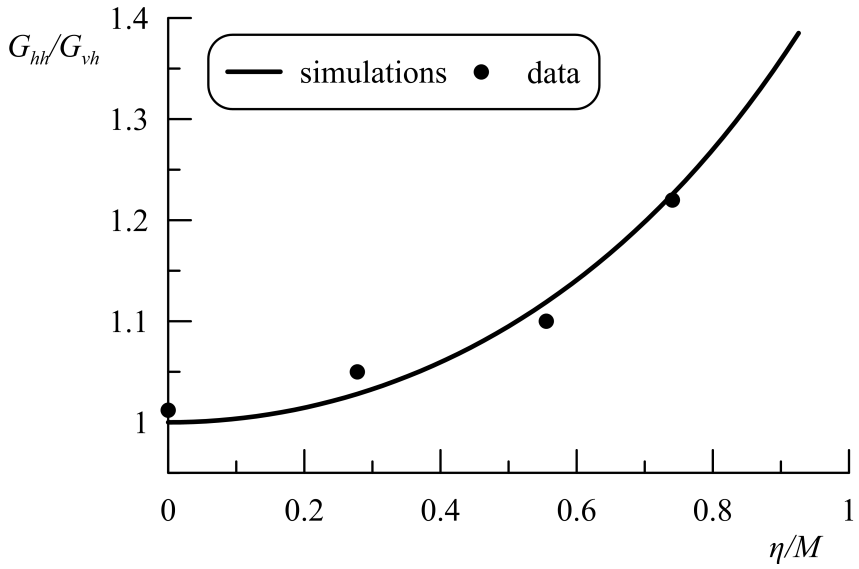

Figure 4.6: *Anisotropy ratio for different stress ratios*

Parameter	Value
x	1.833
ω	1.03
c	13

Table 4.3: *Model parameters*

Once the values of the rotational internal variable, or analogously, the elastic shear moduli are determined for the initial state ($p = 175\,\text{kPa}$, $\eta_{in} = \eta_{K_0} = 0.6$) and in correspondence of the bounding values for $\eta = 0$, 0.3, 0.8, as described above the evolution equation for β provides the evolution of G_{hh}/G_{vh} with the mean effective pressure when the stress ratio changes from an initial value to another. The parameter c, governing the rate of this evolution, is calibrated in order to fit the experimental results. The evolution of the anisotropy ratio measured in laboratory tests on the reconstituted Lucera clay with the mean effective pressure is depicted in figure (4.7) with dots and the lines are the results of the model simulation. The model parameters are reported in table (4.3).

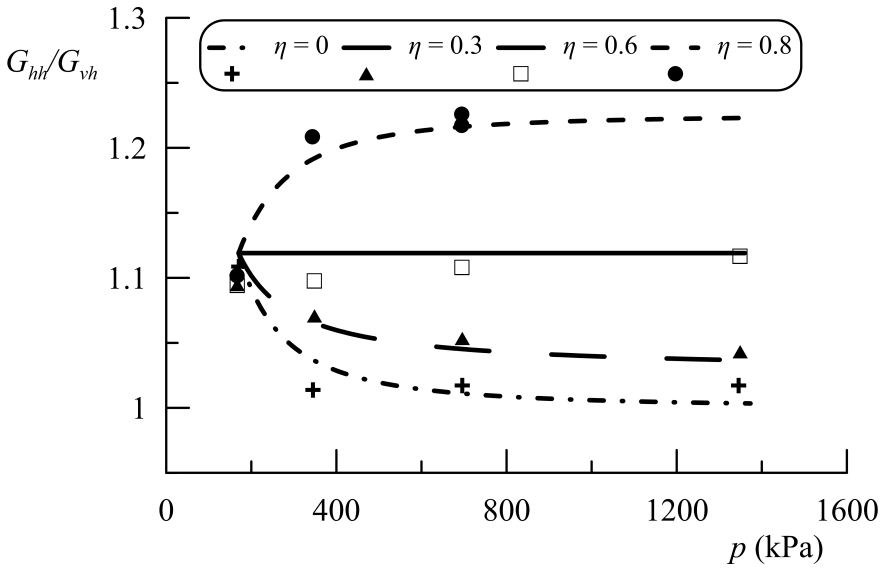

Figure 4.7: *Evolution of anisotropy ratio with the mean effective pressure*

4.5.2 Exponential law

A similar procedure to calibrate the parameter ω is followed in the case of an exponential dependence of the bounding value of β (eq. (4.9)). In this case two parameters, s and z have to be determined in order to evaluate the limit value β_b for a specific stress ratio η. In case of only one experimental result, for instance related to the K_0 condition, a reasonable assumption is $s = z$, but whenever a reacher set of data is available one can choose different values, respecting the constraint $s \leq z$.

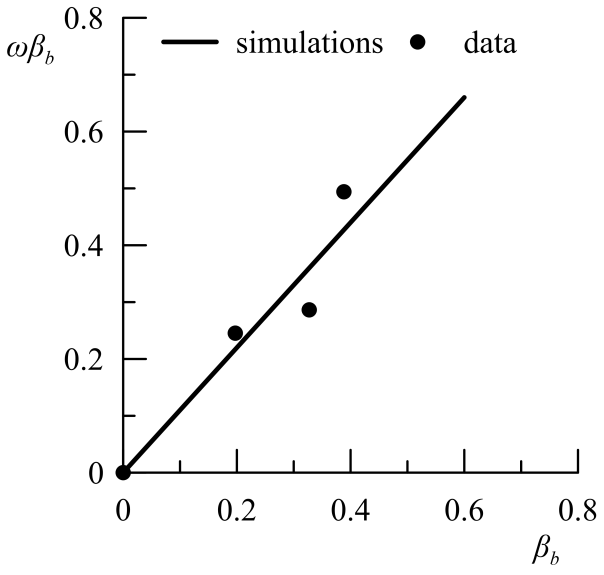

Figure 4.8: *Calibration of* ω

In particular, since the choice of ω depends on β_b, s and z can be calibrated taking into account eq. (4.27) and minimising the standard deviation of the linear regression in figure (4.8). In detail, one can first assume $s = z$ and calculate the value for the K_0 condition and then, keeping fixed one of them and changing the other so that the dots in figure (4.8) accomodate, as far as possible, on a linear trend. In other words, the parameter ω controls the slope of the linear regression, while s and z adjust the deviation of the values of β_b corresponding to different η of the experimental results from the linear law. The resulting parameters for the case of exponential law are reported in table (4.4).

Parameter	Value
s	1.500
z	1.866
ω	1.100
c	20

Table 4.4: *Model parameters*

Then, similarly to what done for the linear law, the resulting anisotropy ratio G_{hh}/G_{vh} for the equilibrium condition along different stress ratios is shown in figure (4.9), the dots indicating the experimental data and the line denoting the prediction of the model.

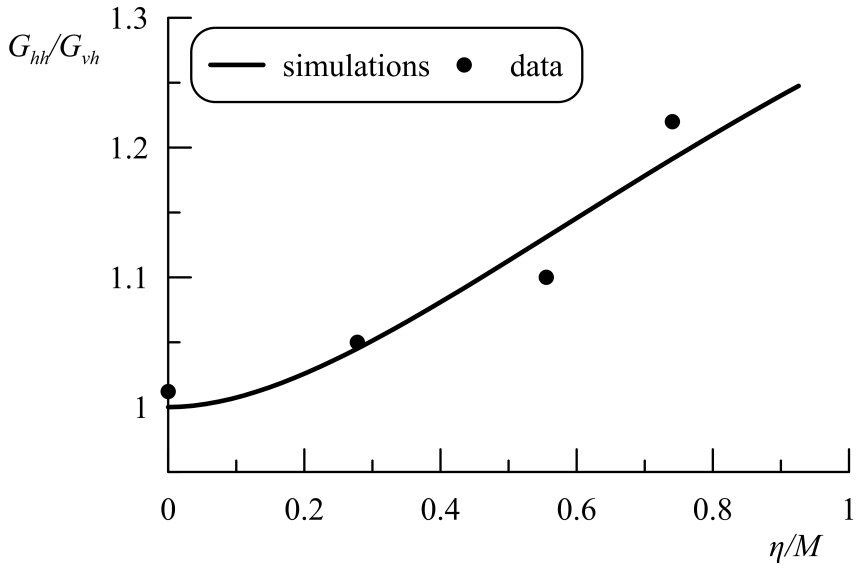

Figure 4.9: *Anisotropy ratio for different stress ratios*

Finally, the evolution of the elastic anisotropy with the mean effective pressure from the initial K_0 condition is reported in figure (4.10).

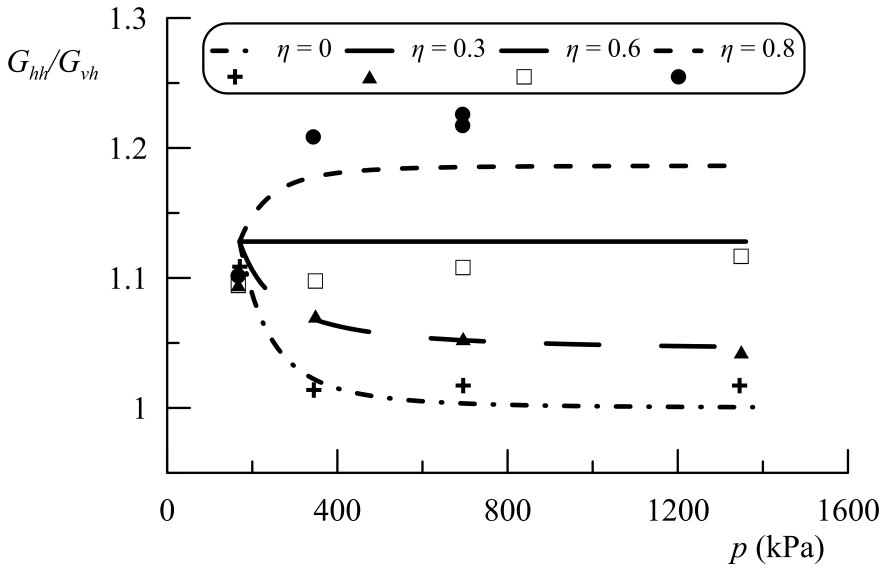

Figure 4.10: *Evolution of anisotropy ratio with the mean effective pressure*

4.5.3 Dafalias & Taiebat (2014) law

Finally, for the sake of completeness, an analogous procedure is carried out for the law reported in eq. (4.10) for the bounding value of the rotational internal variable. In this case the value of β of the critical state condition is assumed as $\beta_c = 0.5\beta_{K_0}$and the calibration of m, n and μ follows a procedure similar to the previous one.

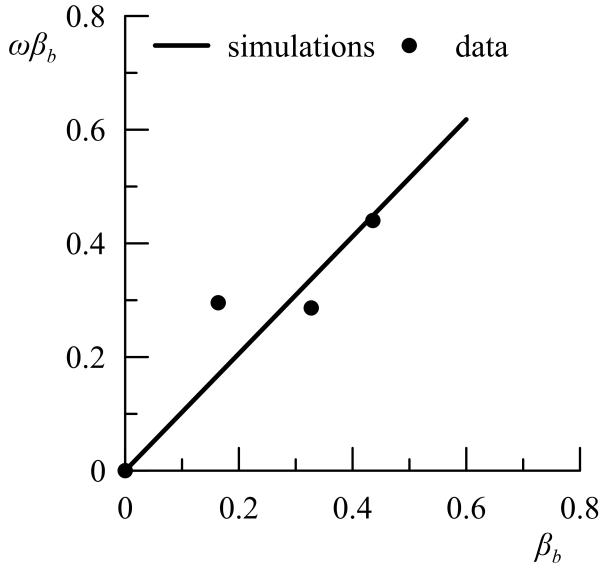

Figure 4.11: *Calibration of* ω

Adopting the same philosophy described for the case of the exponential law, the parameter n can be chosen to minimise the standar deviation of the dots in figure

(4.11) with respect to the linear regression. Clearly, the requirements of limiting the excessive rotation of the surfaces and the value of β at critical state act as additional constraints on the parameter n. The model parameters resulting for this law are reported in table (4.5).

Parameter	Value
α_c	0.164
n	20
m	0.394
μ	52
ω	1.03
c	16

Table 4.5: *Model parameters*

Figure (4.12) shows the asymptotic anisotropy ratio G_{hh}/G_{vh} in correspondence of different stress ratios, while figure (4.13) plots its evolution with the mean effective pressure when the stress ratio changes from an initial value to another.

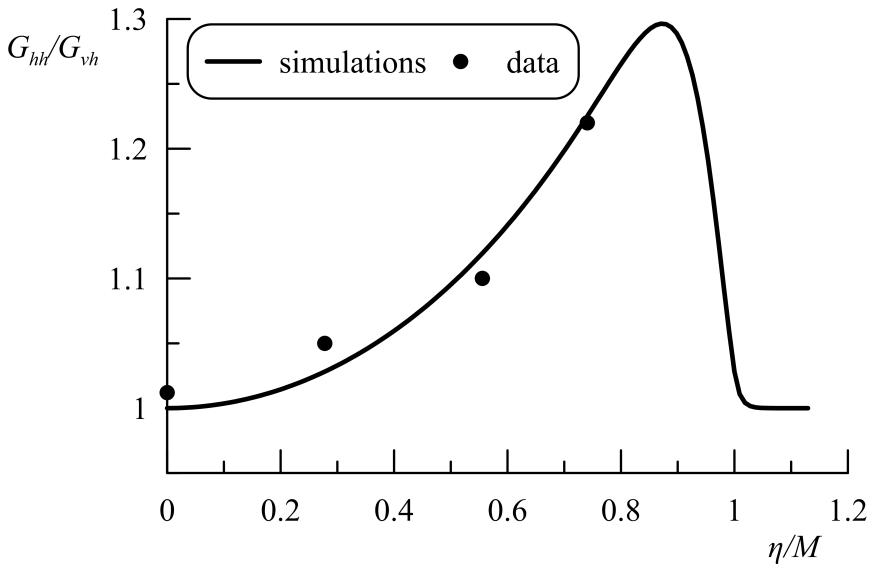

Figure 4.12: *Anisotropy ratio for different stress ratios*

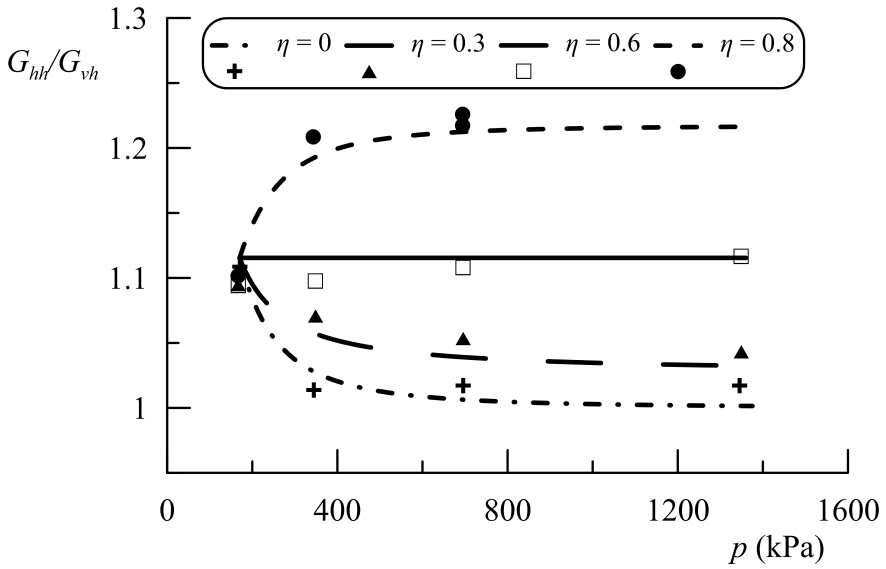

Figure 4.13: *Evolution of anisotropy ratio with the mean effective pressure*

The relationship between the internal variable $\boldsymbol{\beta}$ and the fabric tensor $\mathbf{B}$ proposed herein enables the model to satisfactorily reproduce the evolution of the elastic stiffness anisotropy along η constant stress paths, otherwise impossible to mimic without the introduction of a form of elastoplastic coupling. In particular, with reference to the specific set of experimental data employed above, the linear law for the evaluation of the equilibrium value β_b represents the best compromise between a good performance of the model and the number of parameters to be calibrated. In this sense, it is worth noting that solely the extra parameter ω has to be defined in order to reproduce the observed elastoplastic coupling: the remaining parameters are the standard ones of the Dafalias & Taiebat (2013) model and those related to the anisotropic hyperelastic formulation. Furthermore, a relevant consequence of the proposed elastoplastic coupling is that the initial value of β and the parameters necessary to calculate the equilibrium value β_b can be inferred by the elastic properties of clays, measured in laboratory or in situ tests.

Clearly, a possible limitation of the proposed formulation is that it was empirically determined on the base of just one set of data because of the lack of other similar experimental investigations in the literature. Finally, despite the specific analytical expression, the main result achieved in this section is the introduction of a weak elastoplastic coupling affecting the elastic anisotropy of clays, in a form never pursued before.

Chapter 5

Thermodynamic constitutive modelling of geomaterials

In this chapter a theoretical framework is described to model the behaviour of geomaterials in a thermodynamically consistent way. Many thermodynamic approaches for elastoplastic materials have been developed in the past few decades. A possible classification of the thermodynamic-based approaches can be done depending on how the history of the material is taken into account. Within the approach commonly termed "rational thermodynamics", the behaviour of the material is expressed through general functionals of the history of the state and the thermodynamics principles are applied to ensure that the evolution of the state during a generic process is thermodynamically consistent. This approach is mainly due to Coleman (1964), Green and Naghdi (1965), Coleman and Gurtin (1967), who generalised the formulations based on classical elastoplasticity within a thermodynamic framework. The second approach, adopted in this work, is based on what is often termed "generalised thermodynamics" and it makes large use of internal variables to describe the past history of the material; thus it is also called thermodynamics with internal variables. The origins of this approach can be found in the work by Moreau (1970), Halphen & Nguyen (1975) and Ziegler (1983). More recently, relevant contributions in the same field have been achieved by Lemaitre & Chaboche (1990), Maugin (1992, 1999), Coussy (1995) and in the works by Houlsby (1981) and Collins & Houlsby (1997). In particular, this theory was termed "hyperplasticity" by Houlsby & Puzrin (2000) and has much in common with the work of Lubliner (1972), Halphen and Nguyen (1975), Ziegler (1977), and Maugin (1992). Initially, the term was coined for elastoplastic models derivable from potentials, or pseudo-potentials (Wu and Kolymbas (1990)). Later, Houlsby & Puzrin (2006) adopted the use of this term for elastoplastic models that satisfy the laws of thermodynamics and identified a

group of standard procedures for obtaining any constitutive model starting from the definition of these potentials. The first and second laws of thermodynamics are enforced directly in this approach, so that any constitutive model formulated following this procedure automatically satisfies the laws of thermodynamics. In the following, the constitutive relationships formulated within this theoretical framework will be denoted as hyper-elastoplastic models. When modelling the whole aspects of soil behaviour, for instance including cyclic response, an infinite number of internal variables would be needed. This is achieved in continuous hyperplasticity (Houlsby & Puzrin (2006)), where functionals are accounted for but is beyond the scope of this work. In the following, however, a fairly small number of internal variables can be used to construct close approximations of the more general models.

In this theoretical framework, one can describe in a thermodynamically consistent way a wide range of engineering materials including geotechnical materials, even those exhibiting non-associated plastic flow rules. The principal advantage of formulating such models in a thermodynamic framework is that they cannot produce thermodynamically unreasonable results. This is not automatically verified using different approaches in constitutive modelling, such as classical elastoplasticity. Models that violate the thermodynamics principles might lead to unrealistic phenomena, one of which is the absence of dissipation or, even worse, the creation of energy under cyclic loading. A second advantage is that the framework makes considerable use of potential functions, from which it is possible to derive the entire constitutive response. In such a way, a large number of elastoplastic models can be formulated within a single rigorous framework. In addition, the hyperplastic approach can be adopted to derive continuum damage models, as demonstrated by Einav *et al.* (2007) and enables to take into account forms of elastoplastic coupling more complex than those obtained within the framework of classical elastoplasticity. This latter aspect will be treated in detail in chapter 6.

In this study the procedure proposed by Collins & Houlsby (1997), Houlsby & Puzrin (2000) and Houlsby & Puzrin (2006) are followed and the hypotheses of rate independent materials and isothermal processes will be assumed. Then the Ziegler orthogonality principle will be considered valid and its implications will be briefly discussed. Special emphasis will be given to the fact that the entire constitutive response of a material can be derived from the definition of only two scalar functions. The use of the Legendre transform allows to switch from one to another form of these functions to formulate the constitutive model in the most suitable way for the specific application.

After an introduction on the general principles of hyperplasticity, some consid-

erations about the role of the key ingredients of this approach and the relationship with classical elastoplasticity will be discussed in detail. Then the rotational hardening model by Dafalias & Taiebat (2013) described in chapter 4 will be reformulated within the framework of hyperplasticity, highlighting analogies and differences with a general family of hyperplastic anisotropic models proposed by Collins & Hilder (2002). Finally some numerical results will be presented to show the performance of the model and to clarify the differences with the original elastoplastic version.

5.1 Laws of thermodynamics. Free energy

In thermodynamics a closed system is a body separated from its surrounding and characterised by a state described by a certain number of internal variables, which is believed to be in thermodynamic equilibrium with the surrounding during any process. In classical thermodynamics only infinitesimally slow processes are considered but in practice the concepts of classical thermodynamics can be successfully adopted also for non-quasi-static processes. Given the above, the fundamental starting points for the development of a thermodynamically consistent constitutive model are the first and second laws of thermodynamics. The first law of thermodynamics is essentially the principle of conservation of energy, which in the local rate form can be expressed as:

$$\dot{u} = \dot{W} + \dot{Q} = \sigma_{ij}\dot{\varepsilon}_{ij} - q_{k,k} \tag{5.1}$$

where u is the internal energy, W is the mechanical work per unit volume, Q is the heat flux vector per unit volume and the term $q_{k,k}$ denotes the divergence of the heat flux vector. Eq. (5.1) expresses a power balance, in which the sum of the sources of power to the system is equal to the rate of the internal energy of the body. Note that this equation represents a particular form of the first law, in which the local heat source is assumed to be zero and other input powers, due for instance to a gravitational field, are neglected.

The second law of thermodynamics controls the form of a transformation introducing some restrictions to the processes that can occur. There are different ways in which the second law can be expressed and here the Clausius-Duhem inequality form is adopted. Particularly, in the local form it reads:

$$\theta\dot{s} \geq -q_{k,k} + \frac{q_k\theta_{,k}}{\theta} \tag{5.2}$$

where s is the entropy per unit volume and θ is the temperature and again the

local heat source is not considered. The entropy is a crucial property of a body and represents a measure of the disorder of a system. Eq. (5.2) can be rewritten as:

$$D = \theta \dot{s} + q_{k,k} - \frac{q_k \theta_{,k}}{\theta} \geq 0 \tag{5.3}$$

where the total dissipation D is the sum of the thermal dissipation $-\frac{q_k \theta_{,k}}{\theta}$, which is always non-negative because the heat flux vector is opposite to the thermal gradient, and the mechanical dissipation d expressed as:

$$d = \theta \dot{s} + q_{k,k} \tag{5.4}$$

The second law states that the total dissipation in a closed system during any process must be always non-negative. For a purely elastic material the dissipation is zero and the process is fully reversible. Whether the process is sufficiently slow and the thermal dissipation is small in comparison with the other two terms, one can believe the two phenomena to be independent, thus requiring that $d \geq 0$ and $-\frac{q_k \theta_{,k}}{\theta} \geq 0$. This is a more stringent condition of eq. (5.3) but is widely accepted, thus in the following solely the mechanical dissipation will be considered. In addition, denoting with $\theta \dot{s}^r = -q_{k,k} + \frac{q_k \theta_{,k}}{\theta}$, where the apex r indicates the reversible contribute of the specific entropy, eq. (5.3) can be reformulated as:

$$D = \theta \dot{s}^i = \theta \left(\dot{s} - \dot{s}^r \right) \geq 0 \tag{5.5}$$

where $\dot{s}^i$ is the irreversible part of the rate of entropy. In the form of eq. (5.5), the second law is often referred to as Planck's inequality. In order to account for the irreversible character of the materials, the second law of thermodynamics has to be considered in the formulation, more conveniently in the form of eq. (5.3) or eq. (5.5).

The internal energy is a function of the current state of the body; in particular it depends on the strain tensor, on the entropy and on the tensor-type internal variable α_{ij}. Herein, because this variable can be conveniently identified with the plastic strain, a single tensor variable is considered, though the generalisation to more variables is straightforward. Depending on the independent variables employed to describe the state, one can adopt three additional forms for free energy: the Helmholtz free energy φ, the enthalpy h and the Gibbs free energy ψ. Note that they are specific energy because considered per unit volume. In detail, one can write:

$$\begin{aligned} u &= u\left(\varepsilon_{ij}, \alpha_{ij}, s\right) \\ \varphi &= \varphi\left(\varepsilon_{ij}, \alpha_{ij}, \theta\right) \\ h &= h\left(\sigma_{ij}, \alpha_{ij}, s\right) \\ \psi &= \psi\left(\sigma_{ij}, \alpha_{ij}, \theta\right) \end{aligned} \tag{5.6}$$

For isothermal processes it is more convenient to use the Helmholtz and the Gibbs energies because the temperature is an independent variable, whereas the internal energy and the enthalpy can be efficiently employed for adiabatic or isentropic processes. The four energies in eq. (5.6) are related to each other by a series of Legendre transforms. A generic function $X\left(x_i, \alpha_i\right)$, with $i = 1, ..., n$, can be replaced by the dual function $Y\left(y_i, \alpha_i\right)$, where x_i and y_i are the interchanged variables, such that $y_i = \frac{\partial X}{\partial x_i}$. In particular the Legendre transform reads:

$$Y = \pm\left(X - x_i y_i\right) \tag{5.7}$$

where the sign depends on the specific application. The independent variables α_i are not changed by the transformation, thus are called passive variables. From a geometrical perspective, $X\left(x_i\right)$ can be interpreted as a surface in the $(n+1)$-dimensional space $\left(x_i, X\right)$ and the function $Y\left(y_i\right)$ defines a family of tangent hyperplanes, thus a geometrical duality exists.

For instance, the Helmholtz free energy is a Legendre transform of the internal energy ($\varphi = u - \theta s$), in which the entropy and temperature are interchanged, with $\theta = \frac{\partial u}{\partial s}$, whereas the strain tensor and the internal variable α_{ij} are passive variables. The enthalpy and the Gibbs free energy are obtained by further Legendre transformations in which stresses and strains are interchanged. Once one function is specified, the other can be found through the Legendre transform, though in certain cases is not straightforward to find it analytically.

Enforcing in the first law of eq. (5.1) the mechanical dissipation, one obtains:

$$\dot{u} = \sigma_{ij}\dot{\varepsilon}_{ij} - q_{k,k} = \sigma_{ij}\dot{\varepsilon}_{ij} + \theta\dot{s} - d \tag{5.8}$$

which, under the hypothesis of isothermal process, by virtue of the Legendre transform can be rewritten as:

$$\dot{\varphi} + d = \sigma_{ij}\dot{\varepsilon}_{ij} \tag{5.9}$$

Eq. (5.9) is known as free energy balance equation. Furthermore, the rate of the internal free energy can also expressed as:

$$\dot{u} = \frac{\partial u}{\partial \varepsilon_{ij}}\dot{\varepsilon}_{ij} + \frac{\partial u}{\partial \alpha_{ij}}\dot{\alpha}_{ij} + \frac{\partial u}{\partial s}\dot{s} \tag{5.10}$$

Comparing eqs. (5.8) and (5.10) it results $\sigma_{ij} = \frac{\partial u}{\partial \varepsilon_{ij}}$ and $\theta = \frac{\partial u}{\partial s}$, in agreement with the Legendre transform. In addition, a new quantity called generalised stress $\bar{\chi}_{ij} = -\frac{\partial u}{\partial \alpha_{ij}}$ is defined, such that the dissipation function results:

$$d = \bar{\chi}_{ij}\dot{\alpha}_{ij} \geq 0 \tag{5.11}$$

From eq. (5.6), recalling that α_{ij} is a passive variable, the generalised stress is also:

$$\bar{\chi}_{ij} = -\frac{\partial \varphi}{\partial \alpha_{ij}} = -\frac{\partial \psi}{\partial \alpha_{ij}} = -\frac{\partial h}{\partial \alpha_{ij}} \tag{5.12}$$

Therefore, the dissipation function can be expressed in different forms according to which energy form is specified:

$$\begin{aligned} d &= d^u\left(\varepsilon_{ij}, \alpha_{ij}, s, \dot{\alpha}_{ij}\right) \\ d &= d^\varphi\left(\varepsilon_{ij}, \alpha_{ij}, \theta, \dot{\alpha}_{ij}\right) \\ d &= d^h\left(\sigma_{ij}, \alpha_{ij}, s, \dot{\alpha}_{ij}\right) \\ d &= d^\psi\left(\sigma_{ij}, \alpha_{ij}, \theta, \dot{\alpha}_{ij}\right) \end{aligned} \tag{5.13}$$

where the apex indicates the form of the specific energy.

5.2 Dissipative generalised stresses. Ziegler orthogonality principle

In addition to the generalised stress, a dissipative generalised stress is defined:

$$\chi_{ij} = \frac{\partial d}{\partial \dot{\alpha}_{ij}} \tag{5.14}$$

For a rate independent material the dissipation function is an omogeneous first order function in the rate of internal variable $\dot{\alpha}_{ij}$ because the magnitude of the dissipation is proportional to the magnitude of deformation. In such a way the material does not possess a characteristic time. This is a crucial hypothesis because the dissipation function can be consequently rewritten using the Euler's theorem, leading to:

$$d = \frac{\partial d}{\partial \dot{\alpha}_{ij}} \dot{\alpha}_{ij} = \chi_{ij} \dot{\alpha}_{ij} \geq 0 \tag{5.15}$$

Comparing eqs. (5.11) and (5.15) one can straightforwardly write:

$$\left(\bar{\chi}_{ij} - \chi_{ij}\right) \dot{\alpha}_{ij} = 0 \tag{5.16}$$

Because the generalised dissipative stresses may be function of $\dot{\alpha}_{ij}$, from eq. (5.16) one can solely conclude that the difference between the generalised stresses and the generalised dissipative stresses is orthogonal to the rate of the internal variable. A more restrictive hypothesis is that the difference $(\bar{\chi}_{ij} - \chi_{ij}) = 0$, commonly known as Ziegler's orthogonality principle (1983). The orthogonality principle is analogous to a maximum dissipation principle and despite it represents a stronger assumption as compared to eq. (5.16) it is widely accepted by the scientific community. In fact, the principle encompasses a very wide class of rate independent materials, even for instance frictional dissipative materials, characterised by non-associated flow rule. Along this line it is worth noting that the Ziegler's principle encompasses the Drucker's stability postulate. Whilst proof exists that the Drucker's postulate is not always true because admits only stable materials with associated flow rules, no proof exists that the Ziegler's principle is false. In addition, from the stability postulate it results that the yield surface must be convex in the stress space, whereas this does not hold necessarily true according to Ziegler, as will be discussed in detail in the following. The orhogonality principle provides realistic description of many materials, that Lemaitre & Chaboche (1999), Maugin (1992, 1999), Coussy (1995) called "standard" materials. From an analytical perspective, the fundamental consequence of the Ziegler's principle is that the generalised dissipative stresses and the generalised stresses coincide.

5.3 Dissipation and yield function

It is possible to establish a relationship between the dissipation function and the yield function, which represents a fundamental ingredient in classical elastoplasticity. The rate of the internal variable $\dot{\alpha}_{ij}$ and the dissipative generalised stresses χ_{ij} can be thought as interchanged variables of a Legendre transform with the form:

$$d\left(\varepsilon_{ij}, \alpha_{ij}, s, \dot{\alpha}_{ij}\right) + w\left(\varepsilon_{ij}, \alpha_{ij}, s, \chi_{ij}\right) = \chi_{ij} \dot{\alpha}_{ij} \tag{5.17}$$

where in the dissipation function and in the new function w the passive variables strain tensor and entropy can be substituted by the stress tensor and the temperat-

ure, depending on which form of energy is adopted. For a rate independent material, being the dissipation a first order omogeneous function in $\dot{\alpha}_{ij}$, the Legendre transform in eq. (5.17) is singular and usually denoted as a degenerate transform. The paramount consequence of this assumption is that the function w must be zero, as clearly evident when substituting eq. (5.15) in eq. (5.17). Since $w = 0$, the function w can always be decomposed in the product of a positive multiplier and a function f such that:

$$w = \langle L \rangle \; f = \chi_{ij}\dot{\alpha}_{ij} - d = 0 \tag{5.18}$$

The function f represents the yield function expressed in terms of the dissipative generalised stresses. It can be written, analogously to the dissipation function, in one of the following forms:

$$\begin{aligned} f &= f^u\left(\varepsilon_{ij}, \alpha_{ij}, s, \chi_{ij}\right) \\ f &= f^\varphi\left(\varepsilon_{ij}, \alpha_{ij}, \theta, \chi_{ij}\right) \\ f &= f^h\left(\sigma_{ij}, \alpha_{ij}, s, \chi_{ij}\right) \\ f &= f^\psi\left(\sigma_{ij}, \alpha_{ij}, \theta, \chi_{ij}\right) \end{aligned} \tag{5.19}$$

It is worth noting that if the hypothesis of rate independent material were not introduced, it would be impossible to obtain the yield function. In other words, within the framework of hyperplasticity, the rate independence of the material is a necessary condition for the yield function to exist. This fundamental result was already known in the literature, for instance by Moreau (1970) and Halphen & Nguyen (1975). Furthermore, in this framework the yield function is not an input equation, as commonly assumed in classical elastoplasticity, but directly stems from the dissipation function. Finally, the obtained yield function is expressed as a function of the dissipative generalised stresses and not in terms of the true stresses. In order to express the function in a more conventional way, the Ziegler orthogonality principle plays a crucial role, as will appear clear in the following.

The degenerate Legendre transform in eq. (5.17) provides other important information; in fact, although for the variable χ_{ij} the definition in eq. (5.14) is trivially recovered, for $\dot{\alpha}_{ij}$ it results:

$$\dot{\alpha}_{ij} = \langle L \rangle \frac{\partial f}{\partial \chi_{ij}} \tag{5.20}$$

Eq. (5.20) is nothing but a flow rule in the dissipative generalised stress space. If the internal variable α_{ij} is regarded as the plastic strain tensor, the scalar L takes the meaning of plastic multiplier, being positive or zero in case of absence

of plastic deformations. Note that in contrast with classical plasticity, the rate of plastic strain is related to the gradient of the yield function with respect to the dissipative generalised stresses and not to the differential of the plastic potential with respect to the stress σ_{ij}. The flow rule is by definition associated in the generalised stress space but it can be either associated or non-associated in the stress space. Eq. (5.20) represents a crucial result of the hyperplastic theory as, conversely to classical elastoplasticity, it does not require the definition of a plastic potential function to determine the plastic strain rate.

Furthermore, by virtue of eq. (5.20), the dissipation function in eq. (5.15) can be rewritten as:

$$d = \chi_{ij}\dot{\alpha}_{ij} = \chi_{ij} \langle L \rangle \frac{\partial f}{\partial \chi_{ij}} \geq 0 \tag{5.21}$$

The geometric interpretation of eq. (5.21) is that the yield function is convex in the dissipative generalised stress space. In fact, being L non-negative, the scalar product of the generalised stress and the gradient of f must be non-negative, thus indicating that the yield surface must be convex. As will be shown in the following, this does not necessarily imply that the yield surface is convex in the stress space, contrary to what occurs for a stable material according to the Drucker's postulate.

Furthermore, differentiating eq. (5.17) with respect to the passive variables one obtains:

$$\frac{\partial d}{\partial x_{(ij)}} = - \langle L \rangle \frac{\partial f}{\partial x_{(ij)}} \tag{5.22}$$

where $x_{(ij)} = \varepsilon_{ij}, \sigma_{ij}, \alpha_{ij}, s, \theta$, thus a close relationship between the dissipation and the yield function is established. Note that because of the presence of L, the yield function is not uniquely determined. The product $L\,f$ has the dimension of a stress times a strain rate, thus the yield surface can be a homogeneous first order function of stress if the multiplier has the dimension of a strain rate, or can be dimensionless if L is assumed to have the dimension of stress times strain rate. A priori, no particular requirement on the dimension of the yield function is necessary and can conveniently be selected depending on the specific application.

Within the framework of hyperplasticity, two potentials are necessary to define the constitutive behaviour; the first one is the free energy function expressed in one of the four possible forms in eq. (5.6) depending on the specific application while the second is the dissipation or the yield function, as related each other by a singular Legendre transform. However, the transformation from the dissipation function to the yield function and vice versa are not trivial from an analytical point

of view because they involve a singular transformation. Suppose first to know the dissipation function, which is expressed in terms of the internal variables α_{ij} and in the rate $\dot{\alpha}_{ij}$. The eq. (5.14) is homogeneous of degree zero in $\dot{\alpha}_{ij}$, thus dividing by the latter, supposed to be in the number of n variables (even though generally will be 6 because α_{ij} is a symmetric second order tensor), one obtains a system of n equations in n-1 variables. Therefore, if the determinant of the Hessian matrix is equal to zero $\left(\left|\frac{\partial^2 d}{\partial\dot{\boldsymbol{\alpha}}\otimes\partial\dot{\boldsymbol{\alpha}}}\right| = 0\right)$ one of the n equations is linearly dependent on the remaining n-1, it is possible to isolate one equation which does not contain the rate of the internal variables, representing exactly the yield function. Conversely, in case the yield function is known, one can divide the expression of the flow rule in eq. (5.20) by L in order to determine the dissipation function. The resulting system of n equations in the n variables $\frac{\dot{\alpha}_{ij}}{L}$ can be solved for χ_{ij} if the determinant of the Hessian matrix is not zero $\left(\left|\frac{\partial^2 f}{\partial\boldsymbol{\chi}\otimes\partial\boldsymbol{\chi}}\right| \neq 0\right)$. The multiplier can be determined substituting the solution for χ_{ij} in the yield function in order to express the dissipative generalised stresses in terms of $\dot{\alpha}_{ij}$. Finally, the dissipation function will be found recalling that $d = \chi_{ij}\dot{\alpha}_{ij}$. An example of this procedure is shown in appendix B with reference to the hyperplastic version of the Dafalias & Taiebat (2013) model.

Once the two scalar functions are defined, the entire constitutive model can be derived. Since in this work isothermal problems are considered, the Helmholtz and the Gibbs free energies will be taken into account. In particular, in the following a stress-based formulation will be adopted, thus the Gibbs free energy will be the starting point. For the sake of conciseness the bold face notation is employed, thus the Gibbs free energy reads:

$$\psi = \psi\left(\boldsymbol{\sigma}, \boldsymbol{\alpha}\right) \tag{5.23}$$

In principle, an energy function depending on both the stress and the internal variable $\boldsymbol{\alpha}$ would result in a model characterised by a form of coupling, for instance elastoplastic, as will be discussed in detail in chapter 6. Consider now a special form of eq. (5.23), in which the Gibbs free energy is a linear combination of three functions:

$$\psi = \psi_1\left(\boldsymbol{\sigma}\right) + \psi_2\left(\boldsymbol{\alpha}\right) + \psi_3\left(\boldsymbol{\sigma}\right)\boldsymbol{\alpha} \tag{5.24}$$

In particular, if ψ_3 is linear in the stress, no coupling is considered and eq. (5.24) further simplifies as:

$$\psi = \psi_1\left(\boldsymbol{\sigma}\right) + \psi_2\left(\boldsymbol{\alpha}\right) - \boldsymbol{\sigma} : \boldsymbol{\alpha} \tag{5.25}$$

Note that the negative sign in ψ_3 is introduced for consistency with the sign convention in eq. (5.12). Differentiating eq. (5.25) with respect to the stress one obtains the strain:

$$\boldsymbol{\varepsilon} = -\frac{\partial \psi_1}{\partial \boldsymbol{\sigma}} + \boldsymbol{\alpha} = \boldsymbol{\varepsilon}^e + \boldsymbol{\varepsilon}^p \tag{5.26}$$

where the derivative of the first component of the free energy with respect to the stress represents the elastic strain, depending solely on the stress, analogously to what happens for hyperelasticity, whereas $\boldsymbol{\alpha}$ plays exactly the role of plastic strain. Differentiating the free energy with respect to the tensor $\boldsymbol{\alpha}$, recalling the definition of the generalised stress (eq. (5.12)) one obtains:

$$\bar{\boldsymbol{\chi}} = \boldsymbol{\sigma} - \frac{\partial \psi_2}{\partial \boldsymbol{\alpha}} \tag{5.27}$$

Eq. (5.27) provides the relationship between the stress and the generalised stress, which is a function of the stress and the internal variable $\boldsymbol{\alpha}$. The term $\frac{\partial \psi_2}{\partial \boldsymbol{\alpha}}$ is called "back stress" and is the key feature to link any representations in the generalised stress space to the stress space. By virtue of the Ziegler's orthogonality principle ($\boldsymbol{\chi} = \bar{\boldsymbol{\chi}}$) and the eq. (5.27), the yield surface, originally formulated in the generalised space, can be also expressed in the stress space by eliminating the dependence on $\boldsymbol{\chi}$. In particular the surface in the stress space is "shifted" with respect to the same surface in the $\boldsymbol{\chi}$ space by the term $\frac{\partial \psi_2}{\partial \boldsymbol{\alpha}}$. Denoting with f the yield function in the generalised stress space and with $\hat{f}$ that in the stress space one can establish the equivalence:

$$f\left(\boldsymbol{\sigma},\, \boldsymbol{\alpha},\, \boldsymbol{\chi}\left(\boldsymbol{\sigma},\, \boldsymbol{\alpha}\right)\right) = \hat{f}\left(\boldsymbol{\sigma},\, \boldsymbol{\alpha}\right) \tag{5.28}$$

In general not only the shape of yield surfaces in the generalised stress and in the stress spaces does not coincide, but also the flow rules are different. To demonstrate this statement, from eq. (5.28) the rate of the yield function is evaluated:

$$\begin{aligned}
\dot{f} &= \frac{\partial f}{\partial \boldsymbol{\sigma}} : \dot{\boldsymbol{\sigma}} + \frac{\partial f}{\partial \boldsymbol{\alpha}} : \dot{\boldsymbol{\alpha}} + \frac{\partial f}{\partial \boldsymbol{\chi}} : \dot{\boldsymbol{\chi}} = \\
&= \frac{\partial f}{\partial \boldsymbol{\sigma}} : \dot{\boldsymbol{\sigma}} + \frac{\partial f}{\partial \boldsymbol{\alpha}} : \dot{\boldsymbol{\alpha}} + \frac{\partial f}{\partial \boldsymbol{\chi}} : \left(\frac{\partial \boldsymbol{\chi}}{\partial \boldsymbol{\sigma}}\dot{\boldsymbol{\sigma}} + \frac{\partial \boldsymbol{\chi}}{\partial \boldsymbol{\alpha}}\dot{\boldsymbol{\alpha}}\right) = \\
&= \frac{\partial f}{\partial \boldsymbol{\sigma}} : \dot{\boldsymbol{\sigma}} + \frac{\partial f}{\partial \boldsymbol{\alpha}} : \dot{\boldsymbol{\alpha}} + \frac{\partial f}{\partial \boldsymbol{\chi}} : \left(-\frac{\partial^2 \psi}{\partial \boldsymbol{\alpha} \otimes \partial \boldsymbol{\sigma}}\dot{\boldsymbol{\sigma}} - \frac{\partial^2 \psi}{\partial \boldsymbol{\alpha} \otimes \partial \boldsymbol{\alpha}}\dot{\boldsymbol{\alpha}}\right) = \\
&= \frac{\partial \hat{f}}{\partial \boldsymbol{\sigma}} : \dot{\boldsymbol{\sigma}} + \frac{\partial \hat{f}}{\partial \boldsymbol{\alpha}} : \dot{\boldsymbol{\alpha}} = \dot{\hat{f}}
\end{aligned} \tag{5.29}$$

Noting that for the Gibbs free energy of eq. (5.25) (uncoupled material) it results (see also appendix A):

$$\frac{\partial \boldsymbol{\chi}}{\partial \boldsymbol{\sigma}} = -\frac{\partial^2 \psi}{\partial \boldsymbol{\alpha} \otimes \partial \boldsymbol{\sigma}} = -\frac{\partial^2 \psi}{\partial \alpha_{ij} \partial \sigma_{kl}} = \delta_{ik}\delta_{jl} = \mathbf{I} \bar{\otimes} \mathbf{I} \tag{5.30}$$

equating the terms in $\dot{\boldsymbol{\sigma}}$ in eq. (5.29) one can write:

$$\frac{\partial f}{\partial \boldsymbol{\sigma}} + \frac{\partial f}{\partial \boldsymbol{\chi}} = \frac{\partial \hat{f}}{\partial \boldsymbol{\sigma}} \tag{5.31}$$

Recalling the flow rule in eq. (5.20), the term $\frac{\partial f}{\partial \boldsymbol{\chi}}$ denotes the direction of the plastic strain increments. The flow rule is by definition associated in the generalised stress space but, unless $\frac{\partial f}{\partial \boldsymbol{\sigma}} = 0$, the plastic strain increment vector is not normal to the yield surface in the stress space. Therefore, in the most general condition this leads to a non-associated flow rule in the conventional way. The flow rule is associated in the stress space only for the special case in which the yield surface in the generalised stress does not depend on the stresses. In order to clarify this point, multiplying all the terms in eq. (5.31) for the plastic multiplier L and recalling eqs. (5.20) and (5.22) one obtains:

$$-\frac{\partial d}{\partial \boldsymbol{\sigma}} + \dot{\boldsymbol{\alpha}} = \langle L \rangle \frac{\partial \hat{f}}{\partial \boldsymbol{\sigma}} \tag{5.32}$$

From eq. (5.32) it follows that for an uncoupled material, in order to guarantee the flow rule to be associated in the stress space, the dissipation function (or equivalently the yield surface in the generalised space) must be independent of $\boldsymbol{\sigma}$. Note that in general this condition is necessary but not sufficient to ensure the associativeness of the flow rule in the $\boldsymbol{\sigma}$ space. In fact, as will be widely explored in the following, in case of a form of coupling is considered, eq. (5.30) does not hold true and the flow rule becomes non-associated in the conventional way.

Once the formulation is derived, for nonlinear materials the incremental form of the constitutive relationship is required to perform numerical analyses. In particular the standard procedures of classical plasticity theory are still valid. A state lying within the yield surface is elastic and no dissipation occurs while if the state lies on the yield surface plastic deformation can occur and the plastic multiplier is positive. The incremental response is commonly obtained imposing the consistency condition:

$$\dot{f} = \frac{\partial f}{\partial \boldsymbol{\sigma}} : \dot{\boldsymbol{\sigma}} + \frac{\partial f}{\partial \boldsymbol{\alpha}} : \dot{\boldsymbol{\alpha}} + \frac{\partial f}{\partial \boldsymbol{\chi}} : \dot{\boldsymbol{\chi}} = 0 \tag{5.33}$$

Stemming from eq. (5.27), the rate of the generalised stress is:

$$\dot{\boldsymbol{\chi}} = \dot{\boldsymbol{\sigma}} - \frac{\partial^2 \psi_2}{\partial \boldsymbol{\alpha} \otimes \partial \boldsymbol{\alpha}} \dot{\boldsymbol{\alpha}} = \dot{\boldsymbol{\sigma}} - \frac{\partial^2 \psi_2}{\partial \boldsymbol{\alpha} \otimes \partial \boldsymbol{\alpha}} \langle L \rangle \frac{\partial f}{\partial \boldsymbol{\chi}} \tag{5.34}$$

Substituting eq. (5.34) in eq. (5.33) and recalling the definition of the flow rule in eq. (5.20) one obtains:

$$\frac{\partial f}{\partial \boldsymbol{\sigma}} : \dot{\boldsymbol{\sigma}} + \langle L \rangle \frac{\partial f}{\partial \boldsymbol{\alpha}} : \frac{\partial f}{\partial \boldsymbol{\chi}} + \frac{\partial f}{\partial \boldsymbol{\chi}} : \left(\dot{\boldsymbol{\sigma}} - \frac{\partial^2 \psi_2}{\partial \boldsymbol{\alpha} \otimes \partial \boldsymbol{\alpha}} \langle L \rangle \frac{\partial f}{\partial \boldsymbol{\chi}} \right) = 0 \tag{5.35}$$

from which the plastic multiplier can be determined:

$$L = \frac{\left(\frac{\partial f}{\partial \boldsymbol{\sigma}} + \frac{\partial f}{\partial \boldsymbol{\chi}} \right) : \dot{\boldsymbol{\sigma}}}{\frac{\partial f}{\partial \boldsymbol{\chi}} \frac{\partial^2 \psi}{\partial \boldsymbol{\alpha} \otimes \partial \boldsymbol{\alpha}} \frac{\partial f}{\partial \boldsymbol{\chi}} - \frac{\partial f}{\partial \boldsymbol{\alpha}} : \frac{\partial f}{\partial \boldsymbol{\chi}}} \tag{5.36}$$

To conclude, the entire constitutive response of an elastoplastic model can be derived within the framework of hyper-elastoplasticity from the specification of two scalar potential functions, the energy potential function and the dissipation function or, analogously, the free energy and the yield function in the dissipative generalised stresses. The described procedure, despite some relevant hypothesis adoted, such as rate independent materials, the Ziegler's orthogonality condition and isothermal processes is able to reproduce a wide class of materials, included those characterised by a non-associated flow rule, consistently with the first and the second laws of thermodynamics.

The following section is devoted to a wider discussion on the characteristics of the free energy and the dissipation functions.

5.4 Role of the free energy and the dissipation functions

In order to clarify the role of the dissipation function, an analogy with the plastic power input $\dot{W}^p = \boldsymbol{\sigma} : \dot{\boldsymbol{\varepsilon}}^p$ can be found. Recalling that $d = \boldsymbol{\chi} : \dot{\boldsymbol{\alpha}}$ and that the internal variable $\boldsymbol{\alpha}$ coincides with the plastic strain, one can straighforwardly write:

$$\dot{W}^p - d = (\boldsymbol{\sigma} - \boldsymbol{\chi}) : \dot{\boldsymbol{\alpha}} \tag{5.37}$$

from which it derives that the relationship between the plastic power input and the dissipation depends uniquely on the form of the energy function. In particular, in the special case of $\psi_2 = 0$, the plastic power and the dissipation coincide.

Furthermore, it is worth noting that the dissipation function must depend solely on the plastic strain because otherwise even an elastic material would dissipate

energy.

The free energy and the dissipation functions play an important role in hardening plasticity: this can be illustrated with reference to two one-dimensional examples for a decoupled material. In the first case in the Gibbs free energy function of eq. (5.25) the term ψ_2 is neglected, thus leading to:

$$\psi(\sigma, \alpha) = \psi_1(\sigma) - \sigma\alpha \tag{5.38}$$

where σ is a generic component of the stress tensor and the internal variable α represents the conjugate component of the plastic strain tensor. The dissipation function is chosen to be independent of the stress, so that the resulting multidimensional flow rule is associated even in the stress space and, according to the hypothesis of rate independent material, is a linear function of the rate of internal variables. Specifically, the simple function is adopted:

$$d(\alpha, \dot{\alpha}) = k(\alpha)\,|\dot{\alpha}| \tag{5.39}$$

where $k(\alpha)$ is a generic function of the plastic strains to be positive in order to guarantee the posiveness of the dissipation function. From eq. (5.39) the yield function in the dissipative generalised stress can be straightforwardly determined:

$$f = \chi^2 - [k(\alpha)]^2 = 0 \tag{5.40}$$

Furthermore, noting that the generalised stress is $\bar{\chi} = -\frac{\partial \psi}{\partial \alpha} = \sigma$ and recalling the Ziegler orthogonality condition, the yield function in terms of stress becomes:

$$\hat{f} = \sigma^2 - [k(\alpha)]^2 = 0 \tag{5.41}$$

The above formulation describes a one-dimensional elastoplastic model characterised by isotropic hardening. In fact, the yield function is symmetric with respect to the stress axis σ and the elastic locus can expand or shrink depending on the plastic strain α. Note that if the function $k(\alpha)$ is constant one obtains a perfect plasticity model.

Consider now the case in which the term ψ_2 in the Gibbs free energy is taken into account:

$$\psi(\sigma, \alpha) = \psi_1(\sigma) - \sigma\alpha + \psi_2(\alpha) \tag{5.42}$$

Contrary to the previous case, one considers that the dissipation function solely depends on the plastic strain increment:

$$d(\dot{\alpha}) = k|\dot{\alpha}| \tag{5.43}$$

where k is a positive constant. Similarly as above, the yield function in the dissipative generalised stress is:

$$f = \chi^2 - k^2 = 0 \tag{5.44}$$

Because of the term ψ_2 in the Gibbs free energy, the back stress ρ appears in the generalised stress $\bar{\chi} = -\frac{\partial \psi}{\partial \alpha} = \sigma - \rho(\alpha)$ and the yield function in terms of the stress σ takes the form:

$$\hat{f} = (\sigma - \rho(\alpha))^2 - k^2 = 0 \tag{5.45}$$

In this case no expansion of the yield locus occurs because k is constant but a translation along the stress axis is observed. In fact, because the back stress is in general a function of the plastic strain, this simple model is characterised by a kinematic hardening.

In order to synthetise the results described so far, a hierchical structure, based on the increasing complexity of these functions, can be identified. Recall that in the case of a uncoupled material the Gibbs free energy function can be expressed as the sum of a term ψ_1 depending on stress only, a term ψ_2 depending on the internal variables (plastic strains) and a mixed term due to the product of the stress and the internal variable tensors. The term ψ_2 determines a kinematic hardening because the resulting back stress controls the evolution of the centre of the yield surface without any change in its shape and size, whereas the function ψ_1 controls the elastic response. Even for uncoupled materials, the dissipation function controls the associativeness of the flow rule; whenever this function does depend on stress, as typically happens for frictional materials, the flow rule will be non-associated in the stress space. The dependence of the dissipation function on the internal variables leads to an isotropic hardening, thus characterised by expansion or contraction of the yield surface. Therefore, mixed hardening is obtained in hyperplastic formulation by employng the complete form of the Gibbs free energy and introducing a dependence of the dissipation function on the plastic strains. On the other side, if this latter dependence of d and the term ψ_2 are neclected, perfect plasticity is described.

However, it is worth noting that despite the general rules discussed above to develop an elastoplastic hardening model, in some cases different combinations of free energy and dissipation functions can lead to the same constitutive model. Consider first a hyperplastic model based on the following Gibbs free energy and dissipation

functions:

$$\begin{aligned} \psi &= \psi_1 (\boldsymbol{\sigma}, \boldsymbol{\alpha}) \\ d &= d_1 (\boldsymbol{\sigma}, \boldsymbol{\alpha}, \dot{\boldsymbol{\alpha}}) \geq 0 \end{aligned} \tag{5.46}$$

Employing the definitions of the generalised stress (eq. (5.12)) and the dissipative generalised stress (eq. (5.14)) one obtains:

$$\begin{aligned} \bar{\boldsymbol{\chi}} &= -\frac{\partial \psi_1}{\partial \boldsymbol{\alpha}} \\ \boldsymbol{\chi} &= \frac{\partial d_1}{\partial \dot{\boldsymbol{\alpha}}} \end{aligned} \tag{5.47}$$

from which, taking into account the Ziegler's principle, one can write the condition:

$$\frac{\partial \psi_1}{\partial \boldsymbol{\alpha}} + \frac{\partial d_1}{\partial \dot{\boldsymbol{\alpha}}} = 0 \tag{5.48}$$

Now, let's assume the following two functions instead of those in eq. (5.46):

$$\begin{aligned} \psi &= \psi_1 (\boldsymbol{\sigma}, \boldsymbol{\alpha}) + \psi_2 (\boldsymbol{\alpha}) \\ d &= d_1 (\boldsymbol{\sigma}, \boldsymbol{\alpha}, \dot{\boldsymbol{\alpha}}) - \frac{\partial \psi_2}{\partial \boldsymbol{\alpha}} \dot{\boldsymbol{\alpha}} \geq 0 \end{aligned} \tag{5.49}$$

Analogously as above, the generalised stress and the dissipative generalised stress become:

$$\begin{aligned} \bar{\boldsymbol{\chi}} &= -\frac{\partial \psi_1}{\partial \boldsymbol{\alpha}} - \frac{\partial \psi_2}{\partial \boldsymbol{\alpha}} \\ \boldsymbol{\chi} &= \frac{\partial d_1}{\partial \dot{\boldsymbol{\alpha}}} - \frac{\partial \psi_2}{\partial \boldsymbol{\alpha}} \end{aligned} \tag{5.50}$$

that lead to the same result of eq. (5.48). This result demonstrates that the same constitutive behaviour can be reproduced by two different pairs of Gibbs free energy and dissipation functions. In particular it is worth highlighting that the same response is obtained whether the term ψ_2, related to the kinematic hardening, is considered or not. This somehow surprising result was first achieved by Collins & Houlsby (1997) with reference to the modified Cam Clay model. In the following it is briefly discussed to further clarify this issue.

A first possibility is to employ a Gibbs free energy in the following triaxial form:

$$\psi = -\tilde{\kappa} p \left[\ln \left(\frac{p}{p_{in}} \right) - 1 \right] - \frac{q^2}{6G} - (p\alpha_p + q\alpha_q) + \left(\tilde{\lambda} - \tilde{\kappa} \right) \frac{p_{0,in}}{2} \exp \left(\frac{\alpha_p}{\tilde{\lambda} - \tilde{\kappa}} \right) \tag{5.51}$$

where p and q are the mean effective pressure and the deviatoric stress, α_p and α_q are the internal variables associated with the stress invariants, p_0 is the preconsolidation pressure, with the subscript in denoting its initial value, $\tilde{\lambda}$ and $\tilde{\kappa}$ are the slopes of the virgin and the swelling lines in the $(\ln p,\, \ln v)$ plane and G is the shear modulus. The first two terms of eq. (5.51) constitute the term ψ_1 and represent the elastic regime, the third term in parenthesis guarantees that the two internal variable coincide with the volumetric and deviatoric plastic strains, respectively and the last term is the ψ_2. In addition, the following dissipation function is provided:

$$d = \frac{p_{0,in}}{2} \exp\left(\frac{\alpha_p}{\tilde{\lambda} - \tilde{\kappa}}\right) \sqrt{\dot{\alpha}_p^2 + M^2 \dot{\alpha}_q^2} \tag{5.52}$$

that, according to a rate independent material, is a first order homogeneous function in the rates of plastic strains and is always positive if plastic deformations occur. As expected from the Cam Clay model, the preconsolidation pressure represents the isotropic hardening variable, depending on the volumetric plastic strains through the expression $p_0 = \frac{p_{0,in}}{2} \exp\left(\frac{\alpha_p}{\tilde{\lambda}-\tilde{\kappa}}\right)$. According to what established above, the isotropic hardening enters in the dissipation function, as reported in eq. (5.52). However, it is worth noting that a similar term also constitutes the ψ_2 in eq. (5.51). In fact, despite the Cam Clay model is not characterised by a proper kinematic hardening, the centre of the yield surface in the p-q plane translates along the p axis according to its expansion or contraction. The immediate consequence of this choice is that a back stress appears, equal to the p-coordinate of the centre of the yield surface $\frac{p_0}{2}$, as confirmed by the generalised stresses:

$$\begin{aligned} \bar{\chi}_p &= -\frac{\partial \psi}{\partial \alpha_p} = p - \frac{p_{0,in}}{2} \exp\left(\frac{\alpha_p}{\tilde{\lambda} - \tilde{\kappa}}\right) \\ \bar{\chi}_q &= -\frac{\partial \psi}{\partial \alpha_q} = q \end{aligned} \tag{5.53}$$

From the dissipation function in eq. (5.52) the yield surface in the dissipative generalised stress $(\chi_p,\, \chi_q)$ plane is:

$$f = \chi_p^2 + \frac{\chi_q^2}{M^2} - \frac{p_0^2}{4} = 0 \tag{5.54}$$

and, assuming the Ziegler's principle, the yield surface in the p-q plane becomes:

$$\hat{f} = p^2 + \frac{q^2}{M^2} - p p_0 = 0 \tag{5.55}$$

The yield surface in the generalised stress plane is an ellypse centered in the origin and able to expand or contract keeping fixed its shape whereas the yield

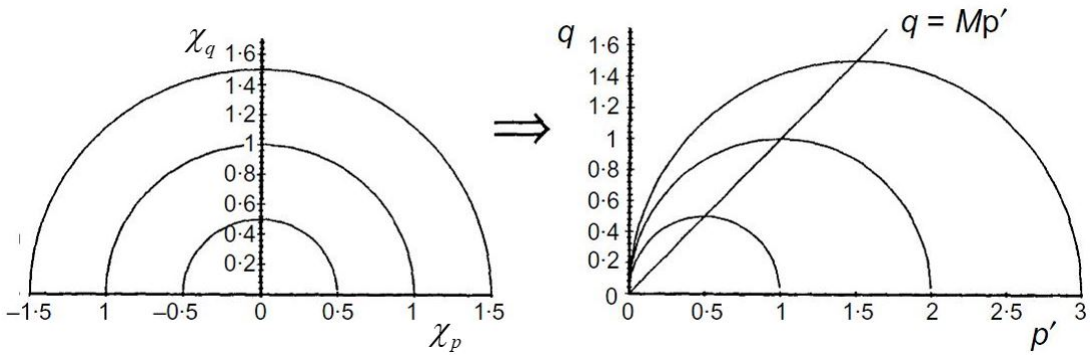

Figure 5.1: *Yield surface in generalised stress and stress plane for the modified Cam Clay (from Collins & Kelly (2002))*

surface in the stress plane intersects the origin and its centre moves along the p axis, as expected and reported in figure (5.1).

Alternatively, in the Gibbs free energy of eq. (5.51) the term ψ_2 can be neglected leading to:

$$\psi = -\tilde{\kappa} p \left[\ln\left(\frac{p}{p_{in}}\right) - 1 \right] - \frac{q^2}{6G} - (p\alpha_p + q\alpha_q) \tag{5.56}$$

In order to obtain the same constitutive response, the dissipation function is modified to the form:

$$d = \frac{p_{0,in}}{2} \exp\left(\frac{\alpha_p}{\tilde{\lambda} - \tilde{\kappa}}\right) \left(\dot{\alpha}_p + \sqrt{\dot{\alpha}_p^2 + M^2 \dot{\alpha}_q^2}\right) \tag{5.57}$$

In fact, an additional term equal to $\frac{\partial \psi_2}{\partial \alpha_p}\dot{\alpha}_p$, with ψ_2 of eq. (5.51) was introduced, according to the general rules discussed above. Furthermore, note that eq. (5.57) still respects the requirement to be non-negative with respect to the second law of thermodynamics. The generalised stresses can be straightforwardly calculated:

$$\begin{aligned} \bar{\chi}_p &= -\frac{\partial \psi}{\partial \alpha_p} = p \\ \bar{\chi}_q &= -\frac{\partial \psi}{\partial \alpha_q} = q \end{aligned} \tag{5.58}$$

Finally, following the same philosophy, the yield surface in the dissipative generalised space is determined:

$$f = \chi_p^2 + \frac{\chi_q^2}{M^2} - p_0 \chi_p = 0 \tag{5.59}$$

Note that because in this case the generalised stresses can be confused with the stress invariants p and q, the yield surfaces are the same in the generalised

stress plane and in the p-q plane and in particular eqs. (5.55) and (5.59) coincide, demonstrating that the two formulations lead to the same constitutive behaviour.

The interesting conclusion is that the same constitutive response can be obtained starting form different energy and dissipation functions, thus the energy functions are not objectively observable quantities as not uniquely determined by the constitutive behaviour.

5.5 Lagrangian multipliers. Constraints

In some cases the formulation of constitutive models can be enriched by introducing additional constraints. They are useful to take into account effects otherwise not included in the original constitutive behaviour; for instance in case of undrained conditions the constraint on the volumetric strains to be zero throughout the loading process is introduced. The constraints can be enforced in the formulation through the standard method of lagrangian multipliers. In case of a constraint on the strains, generally indicated with $c(\boldsymbol{\varepsilon}) = 0$, it results much more useful to employ the free energy in terms of strains (Helmholtz free energy). In particular the new free energy φ' can be defined as:

$$\varphi' = \varphi + \Lambda c \tag{5.60}$$

where Λ is an arbitrary constant. Note that being $c = 0$, φ' is numerically equal to φ but the resulting stress will be:

$$\boldsymbol{\sigma} = \frac{\partial \varphi'}{\partial \boldsymbol{\varepsilon}} = \frac{\partial \varphi}{\partial \boldsymbol{\varepsilon}} + \Lambda \frac{\partial c}{\partial \boldsymbol{\varepsilon}} \tag{5.61}$$

Then one obtains the Gibbs free energy performing a Legendre transformation on the new Helmholtz free energy.

In other cases it can be useful to introduce constraints on the rates of the internal variables; for instance Houlsby (1992) employed a constraint to take into account the effect of dilation into a plasticity model. In these cases the constraints are enforced in the dissipation function and, following the same philosophy of above and being $c(\dot{\boldsymbol{\alpha}}) = 0$, the modified dissipation function d' is defined as:

$$d' = d + \Lambda c \tag{5.62}$$

from which the yield surface can be determined through the degenerate Legendre transformation. Clearly, the constraint c must be a homogeneous first order equation in the rates of the internal variables for consistency with the dissipation function.

The resulting dissipative generalised stresses assume the form:

$$\boldsymbol{\chi} = \frac{\partial d'}{\partial \dot{\boldsymbol{\alpha}}} = \frac{\partial d}{\partial \dot{\boldsymbol{\alpha}}} + \Lambda \frac{\partial c}{\partial \dot{\boldsymbol{\alpha}}} \tag{5.63}$$

Remark As described in the previous section, the dissipation and the free energy functions control, within a hierchical structure, the isotropic and the kinematic hardening of the model. However, it is worth noting that the hardening rules are not directly encapsulated in the dissipation function. For instance, in the Cam Clay model the isotropic hardening variable enters through the current value of the preconsolidation pressure but its rate is not included in the dissipation function nor in the Gibbs free energy. One can conclude that no matter what is the choice of the evolution law for the hardening variable as long as the dissipation function is positive definite. In other words, the hardening laws represent external information, thus not necessarily subjected to the requirements of the laws of thermodynamics. Conversely, in a thermodynamically based constitutive framework, by definition the whole formulation should result as a direct application of the first and second laws and thus the hardening laws should be a priori thermodynamically consistent. In light of this, the hardening rules of the model should be more correctly incorporated in the dissipation function. A new procedure is proposed here. In particular, the technique of the Lagrangian multipliers allows to take directly into account the rates of the internal variables through additional kinematic constraints. In detail, defining with $\mathbf{q}$ the general tensor valued hardening variable such that $\dot{\mathbf{q}} = k\left(\boldsymbol{\sigma}, \mathbf{q}\right) \dot{\boldsymbol{\alpha}}$, with $k\left(\boldsymbol{\sigma}, \mathbf{q}\right)$ a generic hardening function, the dissipation function can be modified as follow:

$$d' = d + \boldsymbol{\Lambda} : \left(\dot{\mathbf{q}} - k\left(\boldsymbol{\sigma}, \mathbf{q}\right) \dot{\boldsymbol{\alpha}}\right) \tag{5.64}$$

where the second term in the brackets in the right side represents the kinematic constraint, analogous, though with a tensorial character, to the constraint c described above (eq. (5.62)). Note that this term is by definition $\dot{\mathbf{q}} - k\left(\boldsymbol{\sigma}, \mathbf{q}\right) \dot{\boldsymbol{\alpha}} = 0$ and, consistently with the dissipation function under the hypothesis of rate independent materials, the rate of hardening variable is a first order homogeneous function in the rate of the internal variables. From the new dissipation function of eq. (5.64) the following dissipative generalised stresses can be determined:

$$\boldsymbol{\chi} = \frac{\partial d'}{\partial \dot{\boldsymbol{\alpha}}} = \frac{\partial d}{\partial \dot{\boldsymbol{\alpha}}} - \boldsymbol{\Lambda} k\left(\boldsymbol{\sigma}, \mathbf{q}\right) \tag{5.65}$$

but an additional dissipative generalised stress has to be considered, as the derivative of the dissipation function with respect to the rate of the internal variable

$\dot{\mathbf{q}}$ is:

$$\boldsymbol{\chi}_{\mathbf{q}} = \frac{\partial d'}{\partial \dot{\mathbf{q}}} = \boldsymbol{\Lambda} \tag{5.66}$$

Obviously, it is still possible to evaluate the generalised stresses stemming from the Gibbs free energy. Consider first a more general case in which the material is coupled but, for simplicity, the ψ_2 term is neglected, leading to the free energy $\psi = \psi_1(\boldsymbol{\sigma}, \boldsymbol{\alpha}, \mathbf{q}) - \boldsymbol{\sigma} : \boldsymbol{\alpha}$. Differentiating the free energy with respect to the internal variables, the generalised stresses take the form:

$$\begin{aligned} \bar{\boldsymbol{\chi}} &= -\frac{\partial \psi}{\partial \boldsymbol{\alpha}} = -\frac{\partial \psi_1}{\partial \boldsymbol{\alpha}} + \boldsymbol{\sigma} \\ \bar{\boldsymbol{\chi}}_{\mathbf{q}} &= -\frac{\partial \psi}{\partial \mathbf{q}} \end{aligned} \tag{5.67}$$

Then, assuming the Ziegler's orthogonality principle, the lagrangian multipliers can be calculated as $\boldsymbol{\Lambda} = -\frac{\partial \psi}{\partial \mathbf{q}}$. This latter represents a new and fundamental result; in fact, as will be widely discussed in chapter 6, entirely devoted to the elastoplastic coupling, the kinematic constraint introduces an additional elastoplastic coupling via the new dissipative generalised stress $\boldsymbol{\chi}_{\mathbf{q}}$, leading to a stronger and richer form of coupling than that originally described by Collins & Houlsby (1997).

While in the case of a coupled material the introduction of the hardening rules in the dissipation function modifies the formulation, in the case of an uncoupled material the results are numerically identical to the case in which the kinematic constraints are not considered. In fact, in this case the Gibbs free energy results $\psi = \psi_1(\boldsymbol{\sigma}) - \boldsymbol{\sigma} : \boldsymbol{\alpha}$, with the elastic component ψ_1 solely function of the stress, thus the generalised stress $\bar{\boldsymbol{\chi}}_{\mathbf{q}} = \mathbf{0}$ and, by virtue of the Ziegler's principle, the lagrangian multipliers are zero. In other words it results:

$$\begin{aligned} \boldsymbol{\chi} &= \frac{\partial d'}{\partial \dot{\boldsymbol{\alpha}}} = \frac{\partial d}{\partial \dot{\boldsymbol{\alpha}}} \\ \bar{\boldsymbol{\chi}} &= -\frac{\partial \psi}{\partial \boldsymbol{\alpha}} = \boldsymbol{\sigma} \end{aligned} \tag{5.68}$$

as indicated by the hyperplasticity theory for uncoupled materials.

Nonetheless, including the hardening laws in the dissipation function as constraints using the method of lagrangian multipliers not only strongly affects the response of the model in case of elastoplastic coupling but represents a more rigorous approach to take into account the hardening rules in a consistent thermodynamic way.

5.6 A family of hyperplastic anisotropic models

Collins & Hilder (2002) proposed a family of single surface elastoplastic anisotropic models within the framework of hyperplasticity for uncoupled materials. These models can describe, in triaxial formulation, a wide range of yield conditions and flow rules in the stress space and reproduce the anisotropic behaviour of soils through a rotation of the yield surface, as usually done in classical elastoplasticity. First they introduced a dissipation function in which the term $\tan\theta_n$, representing the slope of the projection of the normal consolidation line (NCL) in the p-q plane in the current state of anisotropy, produces a coupling between the rate of plastic volumetric and deviatoric strain. For constant values of θ_n the normal consolidation lines in the e-ln$p$ plane are parallel straight lines.

$$d = \sqrt{A^2 \left(\dot{\alpha}_p + \tan\theta_n \dot{\alpha}_q\right)^2 + B^2 \dot{\alpha}_q^2} \tag{5.69}$$

A and B have the dimensions of stress and hence are homogeneous first order functions of the variables p, q and p_0. In particular, Collins & Hilder assume for simplicity that A and B are in fact linear functions of these three variables:

$$\begin{aligned} A &= a_1 p + a_2 q + a_3 p_0 \\ B &= b_1 p + b_2 q + b_3 p_0 \end{aligned} \tag{5.70}$$

Accordingly to what discussed above, the dependence of the dissipation function on the stress leads to a non-associated flow rule in the stress space; in detail the dependence on the deviatoric stress q is required to model different responses in compression and extension. Neglecting the dependence on q, they specialised the above functions in the form:

$$\begin{aligned} A &= (1-\gamma)\, p + \frac{\gamma p_0}{2} \\ B &= (1-\delta)\, p + \frac{\gamma \delta p_0}{2} \end{aligned} \tag{5.71}$$

where γ and δ are two additional parameters. For $\gamma = \delta = 1$ the case of associated flow rule in the stress space is recovered.

The model is first formulated in terms of dissipative generalised stresses, where the flow rule is by definition associated. From the dissipation function in eq. (5.69), they obtained a family of anisotropic yield surfaces in the dissipative generalised stress χ_p-χ_q plane:

$$\frac{\chi_p^2}{A^2} + \frac{\left(\chi_q - \tan\theta_n \chi_p\right)^2}{B^2} = 1 \tag{5.72}$$

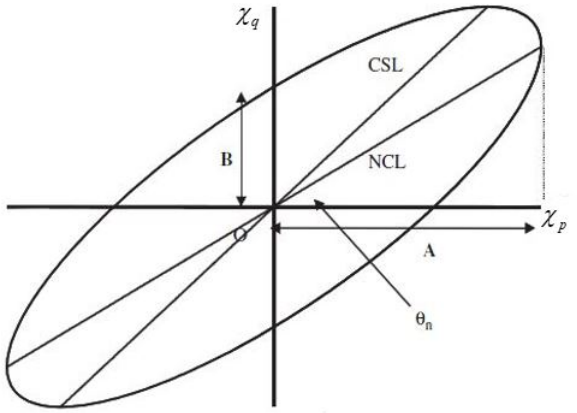

Figure 5.2: *Yield surface in dissipative stress space (Collins & Hilder (2002))*

that represents an inclined ellipse with the centre in the origin of the axes. The yield surface and the geometrical interpretation of the functions A and B are depicted in figure (5.2). In particular, A and B control, for fixed inclination $\tan\theta_n$, the shape and the size of the ellipse.

The yield locus in the p-q plane should intersect the origin and its centre should lie on the line with slope $\tan\theta_n$. Therefore, in order to transform the yield surface in the p-q plane, shift stresses have to be introduced along both p and q axes, so that the equation of the yield function takes the form:

$$\frac{\left(p-\frac{\gamma p_0}{2}\right)^2}{A^2}+\frac{\left(q-\tan\theta_n p\right)^2}{B^2}=1 \tag{5.73}$$

Note that because in general A and B depend on the stress, the yield function in the p-q plane is no longer an ellipse and, as expected, the flow rule becomes non-associated. Comparing eqs. (5.72) and (5.73) the relationships between the stresses and the generalised stresses can be easily identified; in particular, recalling the definition of the generalised stresses for an uncoupled material (eq. (5.27)) and assuming the orthogonality principle, one can write:

$$\begin{aligned}\bar{\chi}_p &= -\frac{\partial\psi}{\partial\alpha_p}=p-\frac{\partial\psi_2}{\partial\alpha_p}=p-\frac{\gamma p_0}{2}\\ \bar{\chi}_q &= -\frac{\partial\psi}{\partial\alpha_q}=q-\frac{\partial\psi_2}{\partial\alpha_q}=q-\tan\theta_n\frac{\gamma p_0}{2}\end{aligned} \tag{5.74}$$

from which it follows that the term ψ_2 of the Gibbs free energy is:

$$\psi_2=\left(\tilde{\lambda}-\tilde{k}\right)\frac{\gamma p_0}{2}=\left(\tilde{\lambda}-\tilde{k}\right)\frac{\gamma p_{0,in}}{2}\exp\left(\frac{\alpha_p+\tan\theta_n\alpha_q}{\tilde{\lambda}-\tilde{k}}\right) \tag{5.75}$$

where $\tilde{\lambda}$ and $\tilde{\kappa}$ are the slopes of the virgin and the swelling lines in the $(\ln p, \ln v)$ plane. Note that in order to obtain the desired shift stresses, the term ψ_2, and consequently the preconsolidation pressure p_0, must be functions of both the volumetric and the deviatoric plastic strains. Therefore, the model is characterised by an isotropic hardening that is not only volumetric but also deviatoric, according to eq. (5.76). In fact, Collins & Hilder assert that in order to keep the thermomechanical models internally consistent, the introduction of shear hardening implies that the yield surfaces must necessarily rotate in stress space, leading to an anisotropic response.

$$\dot{p}_0 = \frac{p_0}{\tilde{\lambda} - \tilde{k}} \left(\dot{\alpha}_p + \tan\theta_n \dot{\alpha}_q \right) \tag{5.76}$$

As will be demonstrated in the following section, this condition is not always true. Conversely, it is possible to formulate, within the framework of hyperplasticity, anisotropic models in which the yield surface can rotate in order to reproduce the anisotropic behaviour of soils without necessarily introducing an isotropic shear hardening.

5.7 Thermodynamic reformulation of the Dafalias & Taiebat (2013) model

In this section the elastoplastic model originally proposed by Dafalias & Taiebat (2013) and illustrated in chapter 4 is reformulated within the framework of hyperelastoplasticity. The reasons for this operation are manifold. First of all, a thermodynamically consistent version of this single surface rotational hardening model will be obtained for both the elastic and plastic regime. Secondly, the implications of a non-associative flow rule will be investigated in comparison with the non-associated version of the original elastoplastic model. Finally, as will be discussed in detail in the following chapter, the hyperplasticity permits to take into account stronger forms of elastoplastic coupling than that described in chapter 4.

The model is derived in the triaxial formulation, by defining of the Gibbs free energy and the dissipation function. In the free energy the term ψ_2 is neglected and for the elastic part the nonlinear isotropic hyperelastic formulation by Houlsby *et al.* (2005) is adopted. In particular, specialising the free energy of eq. (2.21) to the triaxial form (see appendix A), the Gibbs free energy function reads:

$$\psi = -\frac{1}{p_r^{1-n} k\,(1-n)\,(2-n)} \left[p^2 + \frac{k\,(1-n)}{3g} q^2 \right]^{\frac{2-n}{2}} - (p\alpha_p + q\alpha_q) \tag{5.77}$$

Differentiating the latter equation with respect to the stress one can calculate the volumetric and deviatoric strains, with the internal variables representing the plastic components:

$$\begin{aligned} \varepsilon_v &= -\frac{\partial \psi}{\partial p} = \varepsilon_v^e + \varepsilon_v^p = \frac{1}{p_r^{1-n} k\,(1-n)} \left[p^2 + \frac{k\,(1-n)}{3g} q^2 \right]^{-\frac{n}{2}} p + \alpha_p \\ \varepsilon_s &= -\frac{\partial \psi}{\partial q} = \varepsilon_s^e + \varepsilon_s^p = \frac{1}{p_r^{1-n}} \left[p^2 + \frac{k\,(1-n)}{3g} q^2 \right]^{-\frac{n}{2}} \frac{q}{3g} + \alpha_q \end{aligned} \tag{5.78}$$

Because the term ψ_2 is not considered, the generalised stresses $\bar{\chi}_p$ and $\bar{\chi}_q$ coincide with the mean pressure p and the deviatoric stress q, respectively:

$$\begin{aligned} \bar{\chi}_p &= -\frac{\partial \psi}{\partial \alpha_p} = p \\ \bar{\chi}_q &= -\frac{\partial \psi}{\partial \alpha_q} = q \end{aligned} \tag{5.79}$$

5.7.1 Associated flow rule

For the associated version of the Dafalias & Taiebat (2013) model the yield function is:

$$\hat{f}\,(p, q, \beta, p_0) = (q - \beta p)^2 - \left(M^2 - \beta^2\right) p\,(p_0 - p) = 0 \tag{5.80}$$

where, as usual, β represents the rotational hardening internal variable and p_0 the preconsolidation pressure. The yield function in the stress space represents the starting point in order to maintain, if possible, exactly the same properties of the model in the hyperplastic formulation. Recalling that the Ziegler's orthogonality principle holds and considering eq. (5.79) the yield surface in the dissipative generalised stresses becomes:

$$f\,(\chi_p, \chi_q, \beta, p_0) = (\chi_q - \beta \chi_p)^2 - \left(M^2 - \beta^2\right) \chi_p\,(p_0 - \chi_p) = 0 \tag{5.81}$$

At this point few considerations on the hyperplastic formulation of the Dafalias & Taiebat (2013) model in comparison to the results obtained by Collins & Hilder (2002) for a general class of anisotropic models are necessary. Apart from the slighty

different form of the equations of the yield surface, the crucial difference between the two approaches is whether employ or not the term ψ_2 in the Gibbs free energy function. In the present section, the model is formulated neglecting the former term; in this way the stresses and the generalised stresses coincide and even the yield function in the χ_p-χ_q plane is represented by a distorted ellipse intersecting the origin of the axes and with the centre lying on the straight line with slope β. Conversely, according to Collins & Hilder (2002), the yield surface in the generalised stress plane is an ellipse centred in the origin, thus the term ψ_2 must be non-zero in order to properly shift the yield surface in the p-q plane. In particular, because even a shift component along the q axis has to be introduced, ψ_2 is a function of both volumetric and deviatoric plastic strains. The direct consequence of this choice is that the preconsolidation pressure, representing the isotropic hardening variable, is a function of both volumetric and deviatoric plastic strains. In other words, whilst in the work by Collins & Hilder (2002) the evolution law for p_0 follows necessarily eq. (5.76) in order to guarantee the correct form of the yield locus in the p-q plane, in the model proposed herein the desired yield function in the stress plane is obtained regardless of the adopted isotropic hardening rule. In this sense the present formulation is less restrictive and permits to employ any isotropic hardening law, including those that solely depend on the volumetric plastic strains, as often assumed when modelling clayey soils. As discussed before, in some special circumstances, as for the modified Cam Clay model, equivalent formulations can be developed accounting or not for the function ψ_2, but for the sake of clarity it is preferred here to consider this latter term of the Gibbs free energy only when kinematic hardening has to be taken into account. Therefore in this case the choice of $\psi_2 = 0$ seems more appropriate, with the isotropic and rotational hardening rules incorporated in the dissipation function.

From the yield surface in eq. (5.81) expressed in terms of generalised stresses, it is possible to obtain the dissipation function. The analytical procedure to obtain the dual function is not straightforward as such, for the sake of brevity, it is reported in detail in appendix B. The same appendix also reports the reverse procedure to reobtain the yield function from the dissipation one, to verify that the whole calculation is correct. Hence, the dissipation function is:

$$d\left(\dot{\alpha}_p, \dot{\alpha}_q, \beta, p_0\right) = \frac{p_0}{2}\left[\sqrt{\left(\dot{\alpha}_p + \beta\dot{\alpha}_q\right)^2 + \left(M^2 - \beta^2\right)\dot{\alpha}_q^2} + \dot{\alpha}_p + \beta\dot{\alpha}_q\right] \tag{5.82}$$

According to what discussed above, the dissipation function should also include two additional kinematic constraints due to the isotropic hardening via the precon-

solidation pressure p_0 (eq. (4.6)) and the rotational hardening via the rotational internal variable β (eq. (4.20)). The modified dissipation function becomes:

$$\begin{aligned} d'\left(\dot{\alpha}_p, \dot{\alpha}_q, \beta, \dot{\beta}, p_0, \dot{p}_0\right) &= d\left(\dot{\alpha}_p, \dot{\alpha}_q, \beta, p_0\right) + \Lambda_1 c_1 + \Lambda_2 c_2 = \\ &= \frac{p_0}{2}\left[\sqrt{\left(\dot{\alpha}_p + \beta\dot{\alpha}_q\right)^2 + \left(M^2 - \beta^2\right)\dot{\alpha}_q^2} + \dot{\alpha}_p + \beta\dot{\alpha}_q\right] + \\ &+ \Lambda_1\left[\dot{\beta} - \left(\beta_b - \beta\right) cp \left\langle L\right\rangle\right] + \Lambda_2\left(\dot{p}_0 - p_0\frac{1+e_{in}}{\lambda-\kappa}\dot{\alpha}_p\right) \end{aligned} \tag{5.83}$$

However, because the function ψ_1 does not depend on p_0 nor on β, the generalised stresses $\bar{\chi}_{p_0} = \bar{\chi}_\beta = 0$ and, by virtue of the Ziegler's orthogonality principle, $\Lambda_1 = \Lambda_2 = 0$. Therefore, the introduction of the two kinematic constraints in eq. (5.83) does not affect the results, while correctly accounting for the hardening processes in the dissipation function.

As expected for a rate independent material, the dissipation function is a homogeneous first order function of the rates of the internal variables and, according to the hypothesis of associated flow rule, is independent on the stress. The dependence on the internal variables α_p and α_q or, analogously, the volumeric and deviatoric plastic strains, is encapsulated in the hardening variables β and p_0. Note that the dissipation function in eq. (5.82) is always non-negative if $|\beta| < M$; this is the same requirement necessary in the original Dafalias & Taiebat (2013) model to guarantee a real solution of the yield function. However, in this case the same condition stems from a thermodynamic requirement. Furthermore, the only way for which eq. (5.82) is zero, besides the obvious case in which the behaviour is purely elastic, is for $\dot{\alpha}_q = 0$ and $\dot{\alpha}_p$ negative, which is phisically unrealistic because it would imply $p = 0$.

Stemming from the above results, one can assert that the original Dafalias & Taiebat (2013) model with associated flow rule, apart from the elastic regime that is hypoelastic, is consistent with the laws of thermodynamics.

As for classical elastoplasticity, the consistency condition can be imposed to obtain the plastic multiplier and express the constitutive relationship in the incremental form. For the specific case one can write:

$$\begin{aligned} \dot{f} &= \frac{\partial f}{\partial \chi_p}\dot{\chi}_p + \frac{\partial f}{\partial \chi_q}\dot{\chi}_q + \frac{\partial f}{\partial \beta}\dot{\beta} + \frac{\partial f}{\partial p_0}\dot{p}_0 = \\ &= \frac{\partial f}{\partial \chi_p}\dot{\chi}_p + \frac{\partial f}{\partial \chi_q}\dot{\chi}_q + \frac{\partial f}{\partial \beta}\left\langle L\right\rangle cp\left(\beta_b - \beta\right) + \frac{\partial f}{\partial p_0}\frac{\partial p_0}{\partial \alpha_p}\left\langle L\right\rangle\frac{\partial f}{\partial \chi_p} = 0 \end{aligned} \tag{5.84}$$

where the rate of the internal variables β and p_0 are consistent with the rotational

and isotropic hardening rules of the Dafalias & Taiebat (2013) model, reported in eqs. (4.20) and (4.6), respectively. From eq. (5.84) the plastic multiplier can be specified:

$$L = -\frac{\frac{\partial f}{\partial \chi_p}\dot{\chi}_p + \frac{\partial f}{\partial \chi_q}\dot{\chi}_q}{\frac{\partial f}{\partial \beta} cp\left(\beta_b - \beta\right) + \frac{\partial f}{\partial p_0}\frac{\partial p_0}{\partial \alpha_p}\frac{\partial f}{\partial \chi_p}} \tag{5.85}$$

The derivatives appearing in eq. (5.85) are reported below.

$$\frac{\partial f}{\partial \chi_p} = -2\beta\chi_q - M^2 p_0 + 2M^2\chi_p + \beta^2 p_0 \tag{5.86}$$

$$\frac{\partial f}{\partial \chi_q} = 2\chi_q - 2\beta\chi_p \tag{5.87}$$

$$\frac{\partial f}{\partial \beta} = -2\chi_p\chi_q + 2\beta p_0\chi_p \tag{5.88}$$

$$\frac{\partial f}{\partial p_0} = -M^2\chi_p + \beta^2\chi_p \tag{5.89}$$

$$\frac{\partial p_0}{\partial \alpha_p} = \frac{1 + e_{in}}{\lambda - \kappa} p_0 \tag{5.90}$$

5.7.2 Non-associated flow rule

As emerges from eq. (5.32), the only way to develop a constitutive model with a non-associated flow rule for an uncoupled material within the framework of hyperplasticity is to introduce a direct dependency of the dissipation function on the stress or, that is the same, of the yield function in the generalised stress space. In principle there are several ways in which the current stress can be enforced in the dissipation function. In this work the approach proposed by Collins & Hilder (2002) is followed. In particular, the dissipation function is assumed as:

$$d\left(\dot{\alpha}_p, \dot{\alpha}_q, \beta, p_0, p\right) = \sqrt{A^2\left(\dot{\alpha}_p + \beta\dot{\alpha}_q\right)^2 + B^2\left(M^2 - \beta^2\right)\dot{\alpha}_q^2} + \frac{\gamma p_0}{2}\left(\dot{\alpha}_p + \beta\dot{\alpha}_q\right) \tag{5.91}$$

where the quantities A and B, stemming from the work by Collins & Hilder (2002), are defined as:

$$\begin{aligned} A &= \left(1 - \gamma\right) p + \frac{\gamma p_0}{2} \\ B &= \left(1 - \delta\right) p + \frac{\gamma\delta p_0}{2} \end{aligned} \tag{5.92}$$

Two additional parameters, γ and δ, varying from zero to one, are introduced in the formulation. The first one, as will be more clear in the following, controls the ratio $\frac{p}{p_0}$ at critical state and the second one controls the slope of the tangent to the yield surface at the critical state condition. For $\gamma = \delta = 1$ the associated version of the model is recovered. Because A and B do not depend on the deviatoric stress q, the shape of the yield surface is symmetric in compression and extension.

In addition, analogously to the case of associated flow rule, the two kinematic constraints should be added in eq. (5.91), despite they do not modify the constitutive behaviour. From eq. (5.91), as illustrated in detail in appendix B, one obtains the yield function in the dissipative generalised stresses χ_p and χ_q:

$$\begin{aligned} &f\left(\chi_p, \chi_q, \beta, p_0, p\right) = A^2\left(\chi_q - \beta\chi_p\right)^2 + B^2\left(M^2 - \beta^2\right)\left(\chi_p - \frac{\gamma}{2}p_0\right)^2 + \\ &- A^2B^2\left(M^2 - \beta^2\right) = 0 \end{aligned} \tag{5.93}$$

and recalling the orthogonality condition and the form of the generalised stresses in eq. (5.79), one can write the new yield function in the p-q plane:

$$\hat{f}\left(p, q, \beta, p_0\right) = A^2\left(q - \beta p\right)^2 + B^2\left(M^2 - \beta^2\right)\left(p - \frac{\gamma}{2}p_0\right)^2 - A^2B^2\left(M^2 - \beta^2\right) = 0 \tag{5.94}$$

It is worth mentioning at this point that it is not possible to reproduce the original non-associated flow rule proposed by Dafalias & Taiebat (2013), in which both the yield and the plastic potential surfaces are ellipses in the stress space characterised by different shape, as a function of the parameters N and M, respectively. First of all, within the framework of hyperplasticity, the modification of the dissipation function by the introduction of a dependence on the mean effective pressure leads to a yield surface in the stress space that is no longer an ellipse. Similarly, if the flow rule is non-associated, the yield and the plastic potential surfaces in the stress space can not be characterised by the same shape. Although not necessary in the hyperplastic procedure, the plastic potential function could be determined analytically as the derivatives of this function with respect to p and q are known and represent the direction of plastic flow. In other words, the problem reduces to the determination of the family of two variables primitive functions stemming from the knowledge of their derivatives. Clearly, if the yield surface were an ellipse and the direction of the plastic flow did not coincide with the normal to the yield surface, in general the plastic potential would be not an ellipse. Therefore, it is not possible to reproduce the original non-associated version of the Dafalias & Taiebat (2013)

model employing the present thermodynamic approach.

In order to express the constitutive relationship in the incremental form, the consistency condition can be imposed to obtain the plastic multiplier. Note that for the specific case of non-associated flow rule, the additional derivative of yield function with respect to the mean effective pressure must be considered:

$$\begin{aligned}\dot{f} &= \frac{\partial f}{\partial \chi_p}\dot{\chi}_p + \frac{\partial f}{\partial \chi_q}\dot{\chi}_q + \frac{\partial f}{\partial p}\dot{p} + \frac{\partial f}{\partial \beta}\dot{\beta} + \frac{\partial f}{\partial p_0}\dot{p}_0 = \\ &= \frac{\partial f}{\partial \chi_p}\dot{\chi}_p + \frac{\partial f}{\partial \chi_q}\dot{\chi}_q + \frac{\partial f}{\partial p}\dot{p} + \frac{\partial f}{\partial \beta}\langle L\rangle\, cp\,(\beta_b - \beta) + \frac{\partial f}{\partial p_0}\frac{\partial p_0}{\partial \alpha_p}\langle L\rangle\frac{\partial f}{\partial \chi_p} = 0\end{aligned} \tag{5.95}$$

where, as above, the hardening rules are those reported in eqs. (4.20) and (4.6). From eq. (5.95) the plastic multiplier can be specified as:

$$L = -\frac{\frac{\partial f}{\partial \chi_p}\dot{\chi}_p + \frac{\partial f}{\partial \chi_q}\dot{\chi}_q + \frac{\partial f}{\partial p}\dot{p}}{\frac{\partial f}{\partial \beta}cp\,(\beta_b - \beta) + \frac{\partial f}{\partial p_0}\frac{\partial p_0}{\partial \alpha_p}\frac{\partial f}{\partial \chi_p}} \tag{5.96}$$

To guarantee that all the derivatives useful to calculate the plastic multiplier are dimensionally consistent, the yield function in eq. (5.93) is divided by the term A^2. The directions of plastic flow are:

$$\frac{\partial f}{\partial \chi_p} = -2\beta\,(\chi_q - \beta\chi_p) + 2\left(M^2 - \beta^2\right)\frac{B^2}{A^2}\left(\chi_p - \frac{\gamma p_0}{2}\right) \tag{5.97}$$

$$\frac{\partial f}{\partial \chi_q} = 2\chi_q - 2\beta\chi_p \tag{5.98}$$

It is worth noting that in this case the direction of plastic strain rates depends on the parameters γ and δ and on the mean effective pressure via the quantities A and B. The other useful derivatives are:

$$\frac{\partial f}{\partial \beta} = -2\chi_p\,(\chi_q - \beta\chi_p) - 2\beta\frac{B^2}{A^2}\left(\chi_p - \frac{\gamma p_0}{2}\right)^2 + 2\beta B^2 \tag{5.99}$$

$$\begin{aligned}\frac{\partial f}{\partial p_0} = &-\left(M^2 - \beta^2\right)\frac{B^2}{A^2}\gamma\left(\chi_p - \frac{\gamma p_0}{2}\right) - 2B\left(M^2 - \beta^2\right)\frac{\partial B}{\partial p_0} + \\ &+\left(M^2 - \beta^2\right)\left(\chi_p - \frac{\gamma p_0}{2}\right)^2\frac{2BA^2\frac{\partial B}{\partial p_0} - 2AB^2\frac{\partial A}{\partial p_0}}{A^4}\end{aligned} \tag{5.100}$$

with

$$\begin{aligned} \frac{\partial A}{\partial p_0} &= \frac{\gamma}{2} \\ \frac{\partial B}{\partial p_0} &= \frac{\gamma\delta}{2} \end{aligned} \tag{5.101}$$

$$\begin{aligned} \frac{\partial f}{\partial p} = \left(M^2 - \beta^2\right) \left(\chi_p - \frac{\gamma p_0}{2}\right)^2 \frac{2BA^2\frac{\partial B}{\partial p} - 2AB^2\frac{\partial A}{\partial p}}{A^4} - \\ + 2B\left(M^2 - \beta^2\right)\frac{\partial B}{\partial p} \end{aligned} \tag{5.102}$$

with

$$\begin{aligned} \frac{\partial A}{\partial p} &= 1 - \gamma \\ \frac{\partial B}{\partial p} &= 1 - \delta \end{aligned} \tag{5.103}$$

$$\frac{\partial p_0}{\partial \alpha_p} = \frac{1 + e_{in}}{\lambda - \kappa} p_0 \tag{5.104}$$

5.8 Response of the model

In this section the response of the Dafalias & Taiebat (2013) model reformulated within the framework of hyper-elastoplasticity is illustrated. First of all some considerations about the influence of the parameters γ and δ on the shape of the yield surface in the stress space and on the flow rule are presented and subsequently the results of simulations of stress-controlled drained triaxial test for both associated and non-associated flow rule are shown. In this latter case particular care is devoted to the identification of critical state conditions and compared with the results predicted by Collins & Hilder (2002) and Coomb (2017).

The yield surface in the generalised stress space is the distorted ellipse proposed by Dafalias & Taiebat (2013) whereas, unless $\gamma = 1$ and $\delta = 1$, the shape of the yield surface is different in the stress space. In order to highlight the role of the parameters γ and δ entering in the terms A and B (eq. (5.92)) on the shape of the yield surface it is convenient to specialise the formulation to the modified Cam clay model ($\beta = 0$). The first parameter controls the ratio $\frac{p_{cs}}{p_0}$, namely the intersection of the surface with the line of slope M, with respect to the preconsolidation pressure by the relationship $p_{cs} = \frac{\gamma p_0}{2}$. For instance, as depicted in figure (5.3), for $\gamma = 1$ the yield surface intersects the critical state line (CSL) in correspondence of $p_{cs} = \frac{p_0}{2}$ and for $\gamma = 0.5$ at $p_{cs} = \frac{p_0}{4}$. The parameter δ controls the slope of the yield surface in correspondence of the critical state: for $\delta = 1$ the tangent to the curve at (p_{cs}, Mp_{cs})

is horizontal whereas for the limit case $\delta = 0$ its slope is M. Clearly, when $\gamma = 1$ and $\delta = 1$ the classical Cam Clay ellipse is recovered.

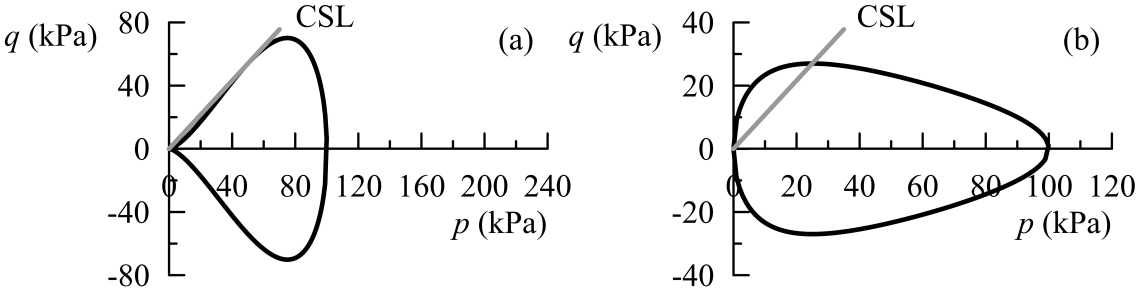

Figure 5.3: *Modified Cam clay yield surface in the stress space for* (a) $\delta = 0$, $\gamma = 1$ *and* (b) $\delta = 1$, $\gamma = 0.5$

A similar role of the parameters γ and δ can be identified for the rotational hardening model. In figure (5.4) the yield surfaces are reported for four couples of these parameters for the case $\beta = 0.3$.

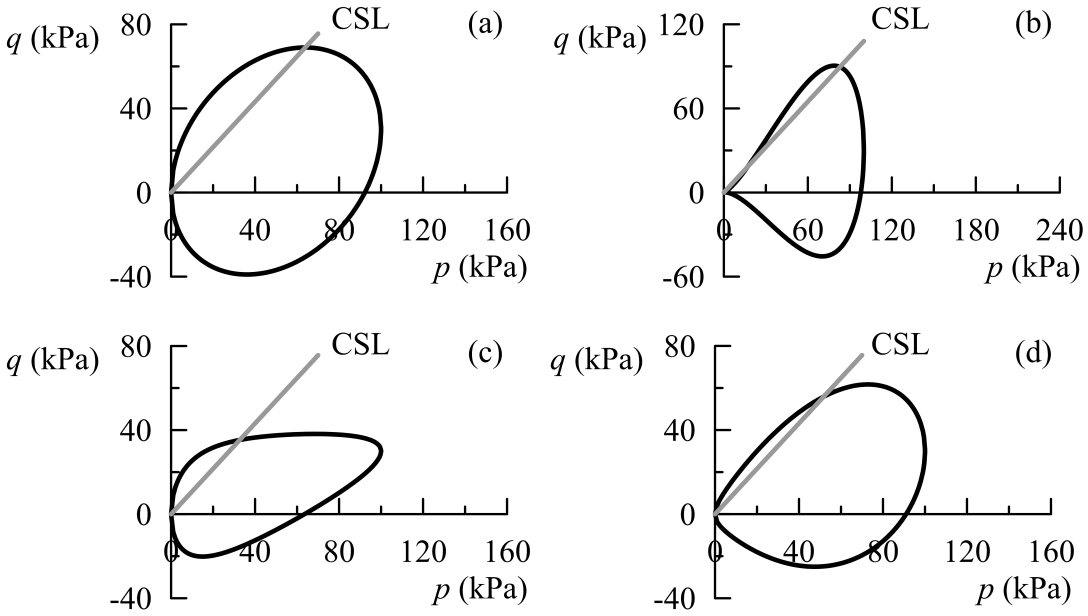

Figure 5.4: *Yield surface in the stress space for* (a) $\delta = 1$, $\gamma = 1$, (b) $\delta = 0$, $\gamma = 1$, (c) $\delta = 1$, $\gamma = 0.5$ *and* (d) $\delta = 0.4$, $\gamma = 0.6$

Different shapes of the yield surface in the stress space can be generated depending on the values of the parameters and, as expected, only for $\gamma = 1$ and $\delta = 1$ the original distorted ellipse is retrieved. In particular, the case (a) in figure (5.3) and (b) in figure (5.4) show that for $\delta = 0$ (but in general for small values of δ) the yield locus has concave segments. This striking result is thermodinamically consistent as the hyperplastic theory requires the yield surface to be convex in the generalised

space but in principle there are no limits in the shape of the yield locus in the stress space. In classical elastoplasticity is common practice to adopt convex yield surfaces, as prescribed by the Drucker's postulate. However, as discussed in section (5.2), the Ziegler's orthogonality principle describes a wider class of material, including the frictional ones, characterised by non-associated flow rule.

The parameters γ and δ also control the non-associativeness of the flow rule in the stress space as they introduce a stress dependence in the dissipation function. Therefore, a change of shape of the yield surface in the stress space is directly related to a non-associated flow rule in the same space. The only case in which the flow rule is associated in the p-q plane is when $\gamma = 1$ and $\delta = 1$ whereas the flow rule is by definition associated in the generalised stress space. Figure (5.5) shows the yield surface in the p-q plane and, under the hypothesis of coaxiality between the stress and strain principal directions, the plastic strain rate vectors. Note that when the flow rule is not associated, as will be clear in the following, the slope M does not identify the critical state condition any more.

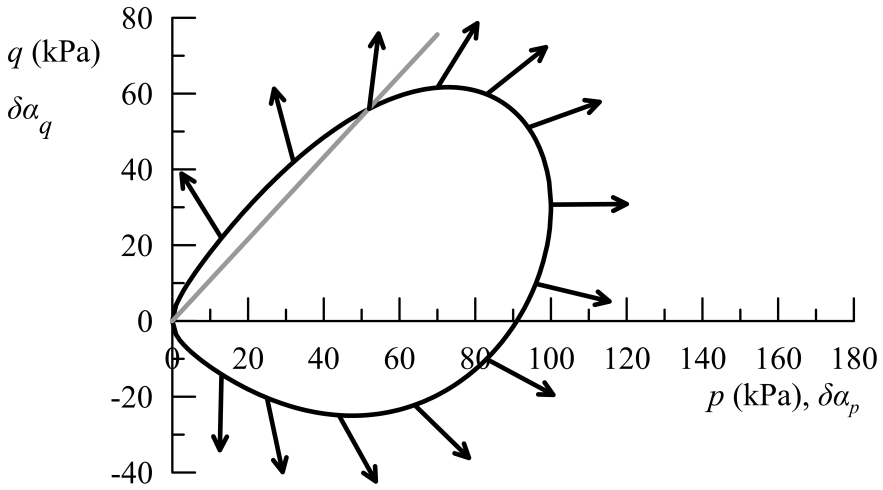

Figure 5.5: *Direction of plastic strain rates for* $\delta = 0.4$, $\gamma = 0.6$

The direction of the plastic strain rate is defined as the normal to the yield surface in the generalised stress space and, by virtue of eq. (5.79), is known for any couple of (p, q). This represents an advantage from a numerical perspective as the definition of a plastic potential surface is not required. In fact, in classical elastoplasticity, to evaluate the plastic strain rate vector in the current stress state a computational effort is needed to determine the intersection between the yield and the plastic potential surfaces. Conversely, in the present case the direction of the flow for the current stress state is directly provided by the derivatives of the yield function in the generalised stresses. An alternative way to prove this statement is to

represent the dissipative yield surface in the stress space, fixing A and B for a given p and using eq. (5.79), as suggested by Collins (2005). In correspondence of the same p the flow rule vector is normal to the dissipative distorted ellipse, as depicted in figure (5.6).

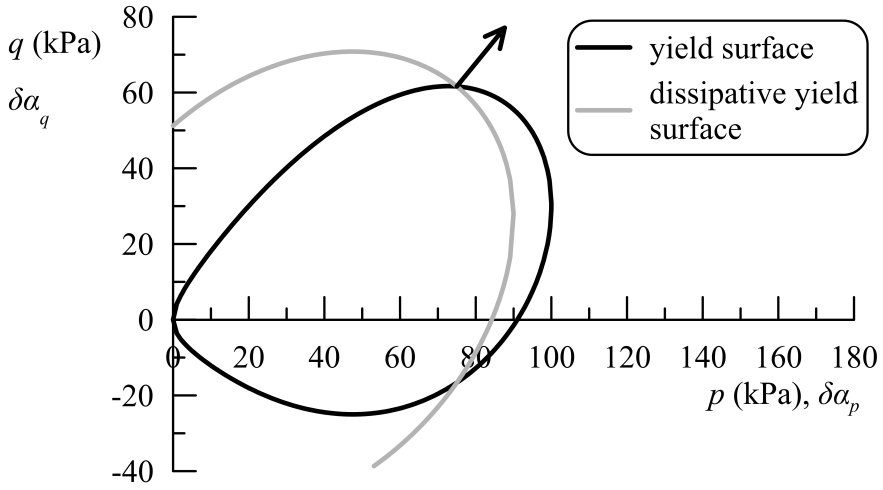

Figure 5.6: *Direction of plastic strain rate* ($\delta = 0.4$, $\gamma = 0.6$)

In the following the results of simulations of stress-controlled drained triaxial tests are illustrated. The hyper-elastoplastic Dafalias & Taiebat (2013) model has been implemented in the incremental form derived in section (5.7) to reproduce the response of the model for drained conditions along prescribed stress paths. The results of three drained triaxial tests in which the material is characterised by different flow rules and shapes of the yield surface via the parameters γ and δ are shown. The model constants are reported in table (5.1) and refer to the reconstituted Lucera clay. In addition, the parameter controlling the pace of the rotation of the yield surface is $c = 50$ and for the asymptotic value of the rotational variable β_b the linear law in eq. (4.8) is adopted, with $x = 2$.

The simulations start from an isotropic stress state of $p_{in} = 70\,\text{kPa}$ and are characterised by an initial preconsolidation pressure of $p_{0,in} = 100\,\text{kPa}$ and an initial rotation of the yield surface of $\beta_{in} = 0.3$. Figure (5.7) shows the response of the model for the case of associated flow rule. The yield surface in the initial configuration is plotted in black line and, as depicted in grey lines, it expands and rotates during the triaxial test by virtue of the isotropic and rotational hardening laws. The material is characterised by a contractive and ductile response and, as expected, for $\eta \to M$ the critical state condition is approached, as clearly indicated by the direction of the plastic strain rate vector.

Parameter	Value
p_r	100
n	0.78
k	888.3
g	533
M	1.08
λ	0.143
κ	0.025
e_{in}	0.8

Table 5.1: *Model parameters for Lucera clay*

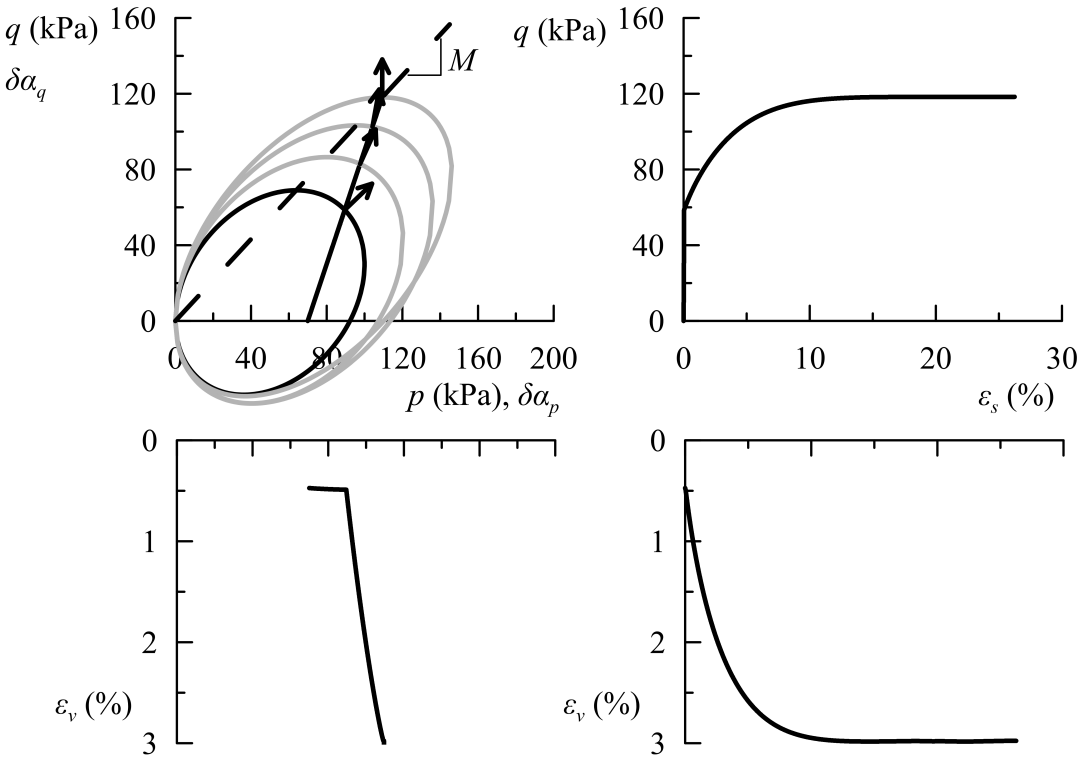

Figure 5.7: *Drained triaxial test for associated flow rule* ($\delta = 1$, $\gamma = 1$)

Figure (5.8) shows the results of the same simulation for $\gamma = 0.6$ and $\delta = 0.4$. The introduction of a non-associated flow rule does not modify the general trend of the response in comparison with the associated case (figure (5.7)) but the results are different from a numerical perspective not only for the plastic strain rate but also for the change of the first yielding stress state due to the different shape of the yield surface. Furthermore, it is worth noting that the critical state condition is no

longer attained for the stress ratio M; in fact the condition $\dot{\varepsilon}_v^p = 0$ is approached for a higher value of the stress ratio.

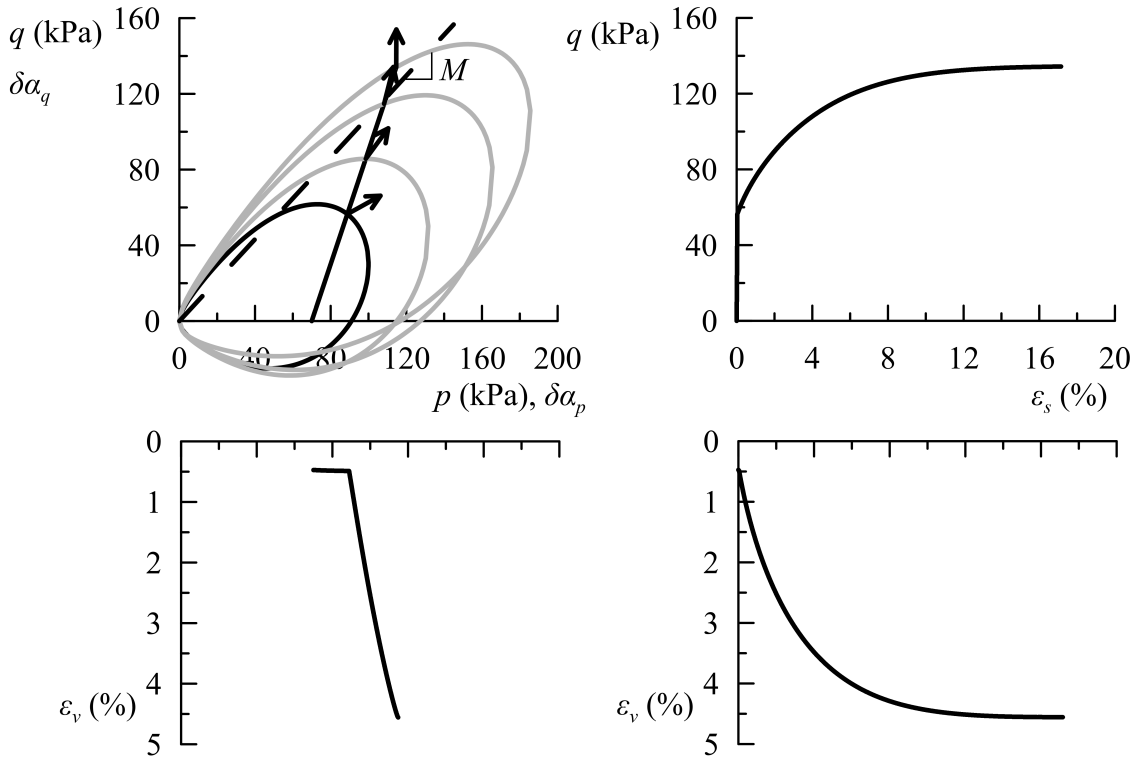

Figure 5.8: *Drained triaxial test for non-associated flow rule* ($\delta = 0.4$, $\gamma = 0.6$)

Finally, in figure (5.9) the response of the same drained triaxial test for $\gamma = 0.5$ and $\delta = 0.7$ is plotted. The relevant result is that not only the critical state is approached for a stress ratio $\eta \neq M$ but its value is different from that observed in the previous case. In particular the critical state condition is attained for a stress ratio lower than M.

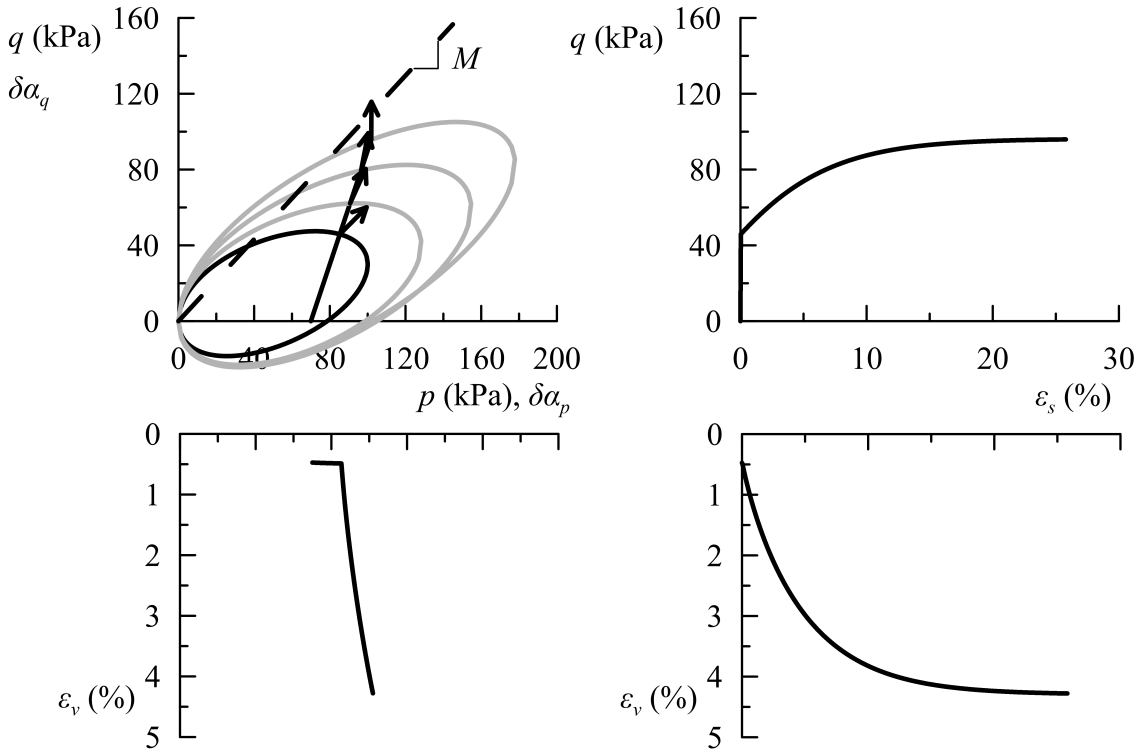

Figure 5.9: *Drained triaxial test for non-associated flow rule* ($\delta = 0.7$, $\gamma = 0.5$)

The above results suggest that the critical state condition depends on the parameters γ and δ and on the current value of β. This represents a drawback of this class of hyperplastic anisotropic models, even though already known in the literature. Collins & Hilder (2002) illustrated, as shown in figure (5.10), the yield loci for associated and non-associated flow rules for a generic instant together with the current positions of the normal consolidation line (NCL), critical state line (CSL) and drained failure line (DFL). One can recognise that in the stress space the critical state line rotates but the other two lines are fixed.

More recently, Coombs (2017) made an effort to guarantee the uniqueness of critical state for this class of rotational hardening models in the framework of hyperplasticity. He modified the original formulation by Collins & Hilder (2002) by introducing a dependence of the parameters γ and δ on the rotational variable β. In such a way when the yield surface rotates the parameters adapt their values such that the critical state condition keeps being constant. Although through this modification Coombs (2017) ensures a constant critical state, the analytical complexity of the model increases and, as in general γ and δ evolve with the stress path as a function of β, even the shape of the yield surface and the flow rule change. Furthermore, the dependence of γ and δ on the rotational variable is introduced as an external condition, thus in principle it might not result in a thermodynamically

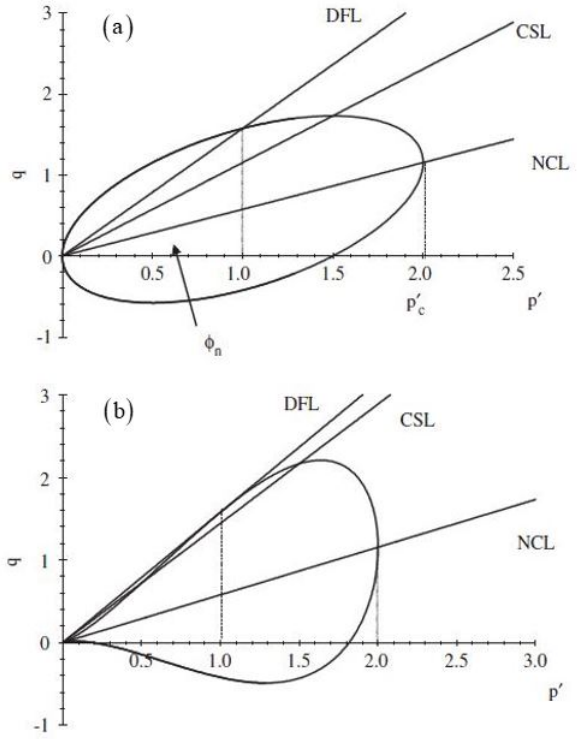

Figure 5.10: *Yield surface in the stress space for* (a) $\delta = 1$, $\gamma = 1$ *and* (b) $\delta = 0$, $\gamma = 1$ *(from Collins & Hilder (2002))*

consistent assumption.

In summary, in this chapter the hyperplastic theory has been illustrated based on the fundamental works by Collins, Houlsby and Puzrin. According to this theory, under the hypothesis of rate independent material and adopting the Ziegler's orthogonality principle, any constitutive relationship can be formulated in a thermodynamically consistent way from the definition of two scalar function: the free energy potential and the dissipation or the yield function. In this chapter a more general form of dissipation function has been proposed to take into account the hardening rules of the model through the technique of the lagrangian multipliers. Subsequently the Dafalias & Taiebat (2013) model has been reformulated within this framework for triaxial conditions and under the hypothesis of uncoupled material. By introducing a dependence of the dissipation function on the mean effective pressure a non-associated version of the model is obtained, different from that originally proposed by Dafalias & Taiebat (2013). In comparison with the works achieved by Collins & Hilder (2002) and Coombs (2017), the formulation developed here is characterised by a volumetric isotropic hardening, which is consistent with the original assumption of Dafalias & Taiebat (2013) for clays. In the stress space the

non-associated flow rule entails different shapes of the yield locus whereas in the generalised space the yield surface is always a distorted ellipse with associated flow rule. The numerical simulations of drained triaxial tests show that the uniqueness of critical state is not guaranteed for the non-associated case as this asymptotic condition depends on the current value of β. Further studies should be devoted to this issue to improve the predictive capability of this class of anisotropic models for clays.

Chapter 6

Thermodynamic based elastoplastic coupling

In this chapter two thermodynamically consistent forms of elastoplastic coupling are developed. As discussed in chapter 1, the small strain behaviour of soils, pertaining to the elastic regime, is affected by the plastic response. In fact, experimental results show that, at least in clays, the elastic stiffness depends on the plastic strains through the preconsolidation pressure and the small strain stiffness anisotropy evolves during the loading process by virtue of the modification of the internal structure driven by the occurrence of plastic strains. In chapter 4 the evolution of the small strain stiffness anisotropy of clays has been modelled by linking the fabric tensor introduced in the elastic formulation to the hardening internal variable controlling the rotation of the yield and plastic potential surfaces of the Dafalias & Taiebat (2013) model within the framework of classical elastoplasticity. After a general discussion on the implications of a coupled material on the overall response of a thermodynamically consistent model, the elastoplastic coupling via the preconsolidation pressure and anisotropy will be formulated within the framework of hyperplasticity in the triaxial case. In such a way both elastic and plastic responses will be modified by the coupling, thus leading to stronger forms of coupling as compared to those derived in classical elastoplasticity. In detail, the associated version of the hyperelastoplastic Dafalias & Taiebat (2013) model illustrated chapter 5 will be adopted, with the Gibbs free energy appropriately modified to take into account separately the two forms of coupling. In particular, for each case, two formulations are proposed, differing for the presence or not of the kinematic constraints in the dissipation function through the technique of lagrangian multipliers. In fact, as will be clear in the following, the adoption of the kinematic constraints represents an alternative strategy leading to different results than those obtained for instance by Houlsby

(1981), Collins and Houlsby (1997) and Houlsby & Puzrin (2006).

6.1 Generality

As discussed in chapter 5, the Gibbs free energy for isothermal processes is a function of the stress tensor $\boldsymbol{\sigma}$ and the internal variable tensor $\boldsymbol{\alpha}$ that, for uncoupled elastoplastic models corresponds to the plastic strain tensor. If one now assumes that elasticity depends on the plastic strains, considering the free energy in eq. (5.25) and neglecting for the sake of clarity the term ψ_2, in order to introduce a dependency of the elasticity on the plastic strains the elastic term ψ_1 of the free energy can be modified into:

$$\psi = \psi_1 \left(\boldsymbol{\sigma}, \boldsymbol{\alpha} \right) - \boldsymbol{\sigma} : \boldsymbol{\alpha} \tag{6.1}$$

In such a way, being the term ψ_1 function of both the stress and the plastic strains, the elastic strain will be consequently a function of both $\boldsymbol{\sigma}$ and $\boldsymbol{\alpha}$:

$$\boldsymbol{\varepsilon} = -\frac{\partial \psi}{\partial \boldsymbol{\sigma}} = -\frac{\partial \psi_1 \left(\boldsymbol{\sigma}, \boldsymbol{\alpha} \right)}{\partial \boldsymbol{\sigma}} + \boldsymbol{\alpha} = \boldsymbol{\varepsilon}^e + \boldsymbol{\varepsilon}^p \tag{6.2}$$

Note that the definition of plastic strains is consistent with that used for uncoupled materials and is independent of the current stress. When from eq. (6.2) the total strain rate is calculated, great care is required to make distinction between the plastic and the irreversible components of strain. Hueckel (1976), Hueckel & Maier (1977) and Maier & Hueckel (1979), in the context of classical elastoplasticity, highlighted that additional terms arise as a consequence of the elastoplastic coupling:

$$\dot{\boldsymbol{\varepsilon}} = -\frac{\partial^2 \psi_1}{\partial \boldsymbol{\sigma} \otimes \partial \boldsymbol{\sigma}} \dot{\boldsymbol{\sigma}} - \frac{\partial^2 \psi_1}{\partial \boldsymbol{\sigma} \otimes \partial \boldsymbol{\alpha}} \dot{\boldsymbol{\alpha}} + \dot{\boldsymbol{\alpha}} = \dot{\boldsymbol{\varepsilon}}^r + \dot{\boldsymbol{\varepsilon}}^c + \dot{\boldsymbol{\varepsilon}}^p = \dot{\boldsymbol{\varepsilon}}^r + \dot{\boldsymbol{\varepsilon}}^i = \dot{\boldsymbol{\varepsilon}}^e + \dot{\boldsymbol{\varepsilon}}^p \tag{6.3}$$

where $\dot{\boldsymbol{\varepsilon}}^r$ is the reversible component of the strain increment, $\dot{\boldsymbol{\varepsilon}}^c$ is the coupling strain rate such that the elastic strain rate is $\dot{\boldsymbol{\varepsilon}}^e = \dot{\boldsymbol{\varepsilon}}^r + \dot{\boldsymbol{\varepsilon}}^c$ and $\dot{\boldsymbol{\varepsilon}}^i$ is the irreversible one, sum of the coupled and the plastic strain rates. $\dot{\boldsymbol{\varepsilon}}^r$ represents the elastic response at fixed plastic strain whereas $\dot{\boldsymbol{\varepsilon}}^c$ accounts for the change of elastic behaviour as the plastic strains occur. In particular, Hueckel and Maier realised that whenever an associated flow rule in the conventional sense, namely with respect to the plastic strain rate, is considered, the irreversible strain increment will not be normal to the yield surface in the stress space. However, they did not fully explore the consequences of the elastoplastic coupling on the plastic response. In fact, within the

total strain	ε_{ij}		
elastic + plastic	ε_{ij}^{e}		ε_{ij}^{p}
recoverabe + coupled + plastic	ε_{ij}^{r}	ε_{ij}^{c}	ε_{ij}^{p}
recoverabe + irrecoverable	ε_{ij}^{r}	ε_{ij}^{i}	

Table 6.1: *Decomposition of strains for coupled materials (from Collins & Houlsby (1997))*

framework of classical elastoplasticity the coupling solely affects the elastic response and is impossible to explore its effects on the plastic regime. Therefore, this latter form of coupling is commonly referred to as "weak" or "one way" coupling. A first attempt to model the elastoplastic coupling in a thermodynamically consistent way was achieved by Houlsby (1981), considering the case of an isotropic material in which the elastic shear modulus depends on plastic strains. Later, Collins & Houlsby (1997) discussed the elastoplastic coupling within the hyperplastic framework and analysed its consequences on the overall behaviour of soils. Obviously, the decomposition of the elastic strain rate originally shown by Hueckel and Maier in their pioneering works is still valid and can be synthetised in table (6.1).

The hyperplastic formulation allows to highlight important implications of the coupling on the plastic response. Recalling the definition of the generalised stresses in eq. (5.12) one can write:

$$\bar{\boldsymbol{\chi}} = -\frac{\partial \psi}{\partial \boldsymbol{\alpha}} = -\frac{\partial \psi_1 \left(\boldsymbol{\sigma}, \boldsymbol{\alpha}\right)}{\partial \boldsymbol{\alpha}} + \boldsymbol{\sigma} \tag{6.4}$$

where, conversely to an uncoupled material, the additional derivative of the term ψ_1 appears. Note that this term acts as a shift between $\bar{\boldsymbol{\chi}}$ and $\boldsymbol{\sigma}$ but must not be confused with the effect due to the ψ_2 term as ψ_1 not only depends on the plastic strain but also on the current stress. This represents a key result leading to two relevant consequences. Suppose that, stemming from the dissipation function, the yield function in terms of dissipative generalised stresses is known and the Ziegler's orthogonality principle is true. The first direct outcome is that the shape of yield function in the stress space changes whether the coupling is considered or not. Secondly, the flow rule in the stress space results as non-associated with respect to the plastic strain rate. To demonstrate this statement, differentiating the generalised

stress in eq. (6.4) with respect to the stress one obtains (with $\boldsymbol{\chi} = \bar{\boldsymbol{\chi}}$):

$$\frac{\partial \boldsymbol{\chi}}{\partial \boldsymbol{\sigma}} = -\frac{\partial^2 \psi}{\partial \boldsymbol{\alpha} \otimes \partial \boldsymbol{\sigma}} = -\frac{\partial^2 \psi_1}{\partial \boldsymbol{\alpha} \otimes \partial \boldsymbol{\sigma}} + \mathbf{I} \bar{\otimes} \mathbf{I} \tag{6.5}$$

Then, analogously to what done in chapter 5, equating the terms in $\dot{\boldsymbol{\sigma}}$ in the consistency condition in eq. (5.29) one can write:

$$\frac{\partial f}{\partial \boldsymbol{\sigma}} + \frac{\partial f}{\partial \boldsymbol{\chi}} \left(-\frac{\partial^2 \psi_1}{\partial \boldsymbol{\alpha} \otimes \partial \boldsymbol{\sigma}} + \mathbf{I} \bar{\otimes} \mathbf{I} \right) = \frac{\partial \hat{f}}{\partial \boldsymbol{\sigma}} \tag{6.6}$$

with f denoting the yield function in the dissipative generalised stress space and with $\hat{f}$ that in the stress space. The flow rule is by definition associated in the dissipative generalised stress space (eq. (5.20)), thus the term $\frac{\partial f}{\partial \boldsymbol{\chi}}$ denotes the direction of the plastic strain rates. Multiplying all the terms in eq. (6.6) for the plastic multiplier L and recalling eqs. (5.20) and (5.22) one obtains:

$$-\frac{\partial d}{\partial \boldsymbol{\sigma}} + \dot{\boldsymbol{\alpha}} \left(-\frac{\partial^2 \psi_1}{\partial \boldsymbol{\alpha} \otimes \partial \boldsymbol{\sigma}} + \mathbf{I} \bar{\otimes} \mathbf{I} \right) = \langle L \rangle \frac{\partial \hat{f}}{\partial \boldsymbol{\sigma}} \tag{6.7}$$

From eqs. (6.5) and (6.6) follow that for a coupled material the flow rule is non-associated even in the case in which the dissipation function (or the yield function in the dissipative generalised stresses) does not depend directly on the stress. In other words, in general the direction of the plastic strain rate is not normal to the yield surface in the stress space, unless the dissipation function does not depend on $\boldsymbol{\sigma}$ and no elastoplastic coupling is considered. Therefore, the two sources of non-associativeness of the flow rule are the elastoplastic coupling and the dissipation function. If this latter contribution is neglected, namely the dissipation is not a function of the stress, the normal to the yield surface in the stress space coincide with the direction of the irreversible strain rate. In fact, by virtue of eq. (6.3), eq. (6.7) can be specialised as:

$$\dot{\boldsymbol{\varepsilon}}^i = \dot{\boldsymbol{\varepsilon}}^c + \dot{\boldsymbol{\varepsilon}}^p = \langle L \rangle \frac{\partial \hat{f}}{\partial \boldsymbol{\sigma}} \tag{6.8}$$

Therefore, from the considerations of above, the hyperplastic approach permits to reproduce a "stronger" form of coupling, in which plasticity is affected by the elastic behaviour and vice versa, thus commonly referred to as "two ways coupling". If the effect on the plastic regime is ignored, like in classical elastoplasticity, the laws of thermodynamics will be violated. In other words, even when the strain rates are evaluated correctly using eq. (6.3), employing associated plasticity to derive the plastic strains will lead to thermodynamically inconsistent results. In addition, the derivation of a thermodynamic-based elastoplastic model for coupled materials

modifies the shape of the yield surface in the stress space and inevitably leads to a non-associated flow rule with respect to the plastic strain rates in the same space.

6.2 Isotropic elastoplastic coupling via the preconsolidation pressure

In this section a thermodynamically consistent isotropic elastoplastic coupling via the preconsolidation pressure is proposed. The elastic stiffness of clays can be expressed, according to the empirical relationships reported in chapter 1, as a power function of the preconsolidation pressure as well as the mean effective pressure. In order to reproduce the dependence of the elastic stiffness on the preconsolidation pressure, the elastic part of the Gibbs free energy in triaxial formulation in eq. (5.77) was modified by Houlsby *et al.* (2005) leading to the following function, which is adopted here:

$$\psi = -\left(\frac{p_r}{p_0}\right)^r \frac{1}{p_r^{1-n} k\,(1-n)\,(2-n)} \left[p^2 + \frac{k\,(1-n)}{3g} q^2\right]^{\frac{2-n}{2}} - (p\alpha_p + q\alpha_q) \tag{6.9}$$

where p_0 is the preconsolidation pressure and r is an additional parameter to be considered like the exponent k^* in the empirical relationships by Viggiani (1992) and Rampello *et al.* (1997) reported in eqs. (1.2) and (1.4), respectively. This parameter depends on the plasticity index and according to Viggiani & Atkinson (1995) generally varies from 0.2 to 0.3 for plasticity index between 0 and 60. Clearly, for $r = 0$ the uncoupled material is recovered.

Differentiating the above equation with respect to the stress one can calculate the volumetric and deviatoric strains, with the internal variables representing the plastic ones:

$$\begin{aligned} \varepsilon_v &= -\frac{\partial \psi}{\partial p} = \varepsilon_v^e + \varepsilon_v^p = \left(\frac{p_r}{p_0}\right)^r \frac{1}{p_r^{1-n} k\,(1-n)} \left[p^2 + \frac{k\,(1-n)}{3g} q^2\right]^{-\frac{n}{2}} p + \alpha_p \\ \varepsilon_s &= -\frac{\partial \psi}{\partial q} = \varepsilon_s^e + \varepsilon_s^p = \left(\frac{p_r}{p_0}\right)^r \frac{1}{p_r^{1-n}} \left[p^2 + \frac{k\,(1-n)}{3g} q^2\right]^{-\frac{n}{2}} \frac{q}{3g} + \alpha_q \end{aligned} \tag{6.10}$$

where the preconsolidation pressure, according to the classical Cam Clay hardening law also adopted by Dafalias & Taiebat (2013) in eq. (4.6), depends on the volumetric plastic strains by the form:

$$p_0 = p_{0,in} \exp\left(\frac{1+e_{in}}{\lambda-\kappa}\alpha_p\right) \tag{6.11}$$

From the Gibbs free energy (6.9) the generalised stresses can be calculated as follow:

$$\begin{aligned}
\bar{\chi}_p &= -\frac{\partial\psi}{\partial\alpha_p} = -\frac{\partial\psi_1}{\partial p_0}\frac{\partial p_0}{\partial\alpha_p} + p = \\
&= -r\left(\frac{p_r}{p_0}\right)^r \frac{1}{p_r^{1-n}k\,(1-n)\,(2-n)}\left[p^2 + \frac{k\,(1-n)}{3g}q^2\right]^{\frac{2-n}{2}} \frac{1+e_{in}}{\lambda-\kappa} + p \\
\bar{\chi}_q &= -\frac{\partial\psi}{\partial\alpha_q} = -\frac{\partial\psi_1}{\partial p_0}\frac{\partial p_0}{\partial\alpha_q} + q = q \\
\bar{\chi}_{p_0} &= -\frac{\partial\psi}{\partial p_0} = -r\left(\frac{p_r}{p_0}\right)^r \frac{1}{p_0}\frac{1}{p_r^{1-n}k\,(1-n)\,(2-n)}\left[p^2 + \frac{k\,(1-n)}{3g}q^2\right]^{\frac{2-n}{2}}
\end{aligned} \tag{6.12}$$

It is worth noting that, contrary to the case of uncoupled material (eq. (5.79)), the generalised stress $\bar{\chi}_p$ does not coincide with the stress invariant p and, due to the dependence of the free energy on p_0, the additional component $\bar{\chi}_{p_0}$ appears.

At this point two alternative formulations are proposed, depending on the choice of the dissipation function, both based on the associated version of the hyper-elastoplastic Dafalias & Taiebat (2013) model developed in chapter 5: the first one follows the traditional approach illustrated in the works by Collins, Houlsby and Puzrin, in which no additional constraints appear in the dissipation functions, whereas in the second case the hardening laws of the model are included as kinematic constraints in the dissipation function through the technique of lagrangian multipliers. As will be shown, these approaches lead to different results, even in terms of flow rule and shape of the yield surface in the stress space. For the sake of conciseness these two forms of thermodynamic (strong) elastoplastic coupling are denoted hereinafter with the acronyms SEPC1 and SEPC2, respectively.

6.2.1 Traditional hyperplastic approach (SEPC1)

Here the employed dissipation function is that discussed in chapter 5 for the development of the hyper-elastoplastic version of the Dafalias & Taiebat (2013) model:

$$d\left(\dot{\alpha}_p, \dot{\alpha}_q, \beta, p_0\right) = \frac{p_0}{2}\left[\sqrt{\left(\dot{\alpha}_p + \beta\dot{\alpha}_q\right)^2 + \left(M^2 - \beta^2\right)\dot{\alpha}_q^2} + \dot{\alpha}_p + \beta\dot{\alpha}_q\right] \tag{6.13}$$

The corresponding yield surface in the dissipative generalised stress χ_p-χ_q plane

is:

$$f\left(\chi_p, \chi_q, \beta, p_0\right) = \left(\chi_q - \beta\chi_p\right)^2 - \left(M^2 - \beta^2\right)\chi_p\left(p_0 - \chi_p\right) = 0 \tag{6.14}$$

Recalling the definition in eq. (5.14), the dissipative generalised stresses result:

$$\begin{aligned} \chi_p &= \frac{\partial d}{\partial \dot{\alpha}_p} \\ \chi_q &= \frac{\partial d}{\partial \dot{\alpha}_q} \\ \chi_{p_0} &= \frac{\partial d}{\partial \dot{p}_0} = 0 \end{aligned} \tag{6.15}$$

Assuming the Ziegler's orthogonality principle, the dissipative generalised and the generalised stresses coincide and since the dissipation function does not depend explicitly on $\dot{p}_0$, only the components χ_p and χ_q are retained. By simple substitution of the generalised stresses of eq. (6.12) in eq. (6.14), the yield function $\hat{f}$ in the p-q plane is obtained, albeit not reported herein due to the inelegant and complex expression. As expected, for an uncoupled material the flow rule is no longer associated. To clarify this issue the following procedure is followed. Specialising eq. (6.6) to the present formulation one can write:

$$\begin{aligned} \frac{\partial \hat{f}}{\partial p} &= \frac{\partial f}{\partial \chi_p}\frac{\partial \chi_p}{\partial p} + \frac{\partial f}{\partial \chi_q}\frac{\partial \chi_q}{\partial p} = \frac{\partial f}{\partial \chi_p}\left(-\frac{\partial^2 \psi_1}{\partial \alpha_p \partial p} + 1\right) \\ \frac{\partial \hat{f}}{\partial q} &= \frac{\partial f}{\partial \chi_p}\frac{\partial \chi_p}{\partial q} + \frac{\partial f}{\partial \chi_q}\frac{\partial \chi_q}{\partial q} = \frac{\partial f}{\partial \chi_p}\left(-\frac{\partial^2 \psi_1}{\partial \alpha_p \partial q}\right) + \frac{\partial f}{\partial \chi_q} \end{aligned} \tag{6.16}$$

where $\frac{\partial \chi_q}{\partial p} = 0$, $\frac{\partial \chi_q}{\partial q} = 1$ and the remaining derivatives assume the form:

$$\frac{\partial \chi_p}{\partial p} = 1 - \frac{\partial^2 \psi_1}{\partial \alpha_p \partial p} = 1 - r\left(\frac{p_r}{p_0}\right)^r \frac{1}{p_r^{1-n} k\left(1-n\right)}\left[p^2 + \frac{k\left(1-n\right)}{3g}q^2\right]^{-\frac{n}{2}} \frac{1+e_{in}}{\lambda-\kappa}p \tag{6.17}$$

$$\frac{\partial \chi_p}{\partial q} = -\frac{\partial^2 \psi_1}{\partial \alpha_p \partial q} = -r\left(\frac{p_r}{p_0}\right)^r \frac{1}{p_r^{1-n}}\left[p^2 + \frac{k\left(1-n\right)}{3g}q^2\right]^{-\frac{n}{2}} \frac{1+e_{in}}{\lambda-\kappa}\frac{q}{3g} \tag{6.18}$$

$$\frac{\partial f}{\partial \chi_p} = -2\beta\chi_q - M^2 p_0 + 2M^2\chi_p + \beta^2 p_0 \tag{6.19}$$

$$\frac{\partial f}{\partial \chi_q} = 2\chi_q - 2\beta\chi_p \tag{6.20}$$

The total volumetric and deviatoric strain rates can be calculated as:

$$\begin{aligned}\dot{\varepsilon}_v &= \left(-\frac{\partial^2\psi_1}{\partial p^2}\dot{p} - \frac{\partial^2\psi_1}{\partial p\partial q}\dot{q}\right) - \frac{\partial^2\psi_1}{\partial p\partial\alpha_p}\dot{\alpha}_p + \dot{\alpha}_p = \dot{\boldsymbol{\varepsilon}}_v^r + \dot{\boldsymbol{\varepsilon}}_v^c + \dot{\boldsymbol{\varepsilon}}_v^p \\ \dot{\varepsilon}_s &= \left(-\frac{\partial^2\psi_1}{\partial q\partial p}\dot{p} - \frac{\partial^2\psi_1}{\partial q^2}\dot{q}\right) - \frac{\partial^2\psi_1}{\partial q\partial\alpha_p}\dot{\alpha}_p + \dot{\alpha}_q = \dot{\boldsymbol{\varepsilon}}_s^r + \dot{\boldsymbol{\varepsilon}}_s^c + \dot{\boldsymbol{\varepsilon}}_s^p\end{aligned} \tag{6.21}$$

where the terms in the brackets are the reversible components. Then, multiplying for $\langle L\rangle$ all the members of eq. (6.16) and recalling that by virtue of eq. (5.20) is $\dot{\alpha}_p = \langle L\rangle \frac{\partial f}{\partial \chi_p}$ and $\dot{\alpha}_q = \langle L\rangle \frac{\partial f}{\partial \chi_q}$, one can write:

$$\begin{aligned}\langle L\rangle \frac{\partial \hat{f}}{\partial p} &= -\frac{\partial^2\psi_1}{\partial\alpha_p\partial p}\dot{\alpha}_p + \dot{\alpha}_p = \dot{\boldsymbol{\varepsilon}}_v^c + \dot{\boldsymbol{\varepsilon}}_v^p = \dot{\boldsymbol{\varepsilon}}_v^i \\ \langle L\rangle \frac{\partial \hat{f}}{\partial q} &= -\frac{\partial^2\psi_1}{\partial\alpha_p\partial q}\dot{\alpha}_p + \dot{\alpha}_q = \dot{\boldsymbol{\varepsilon}}_s^c + \dot{\boldsymbol{\varepsilon}}_s^p = \dot{\boldsymbol{\varepsilon}}_s^i\end{aligned} \tag{6.22}$$

Therefore, as expected, the flow rule is non-associated in the p-q plane but, in the same representation, the irreversible strain rate is directed along the normal to the yield surface, as pointed out by Collins & Houlsby (1997). In other words, in the stress space the flow rule can be thought as associated with respect to the irreversible strain rates.

In order to express the constitutive relationship in the incremental form the consistency condition can be imposed to obtain the plastic multiplier, analogously to what done in classical elastoplasticity. For the specific case one has:

$$\begin{aligned}\dot{f} &= \frac{\partial f}{\partial\chi_p}\dot{\chi}_p + \frac{\partial f}{\partial\chi_q}\dot{\chi}_q + \frac{\partial f}{\partial\beta}\dot{\beta} + \frac{\partial f}{\partial p_0}\dot{p}_0 = \\ &= \frac{\partial f}{\partial\chi_p}\left(\frac{\partial\chi_p}{\partial p}\dot{p} + \frac{\partial\chi_p}{\partial q}\dot{q} + \frac{\partial\chi_p}{\partial p_0}\dot{p}_0\right) + \frac{\partial f}{\partial\chi_q}\dot{q} + \frac{\partial f}{\partial\beta}\dot{\beta} + \frac{\partial f}{\partial p_0}\dot{p}_0 = \\ &= \frac{\partial f}{\partial\chi_p}\frac{\partial\chi_p}{\partial p}\dot{p} + \left(\frac{\partial f}{\partial\chi_p}\frac{\partial\chi_p}{\partial q} + \frac{\partial f}{\partial\chi_q}\right)\dot{q} + \frac{\partial f}{\partial\beta}\dot{\beta} + \left(\frac{\partial f}{\partial\chi_p}\frac{\partial\chi_p}{\partial p_0} + \frac{\partial f}{\partial p_0}\right)\dot{p}_0 = \\ &= \frac{\partial f}{\partial\chi_p}\frac{\partial\chi_p}{\partial p}\dot{p} + \left(\frac{\partial f}{\partial\chi_p}\frac{\partial\chi_p}{\partial q} + \frac{\partial f}{\partial\chi_q}\right)\dot{q} + \frac{\partial f}{\partial\beta}\langle L\rangle\, cp\,(\beta_b - \beta) + \\ &+ \left(\frac{\partial f}{\partial\chi_p}\frac{\partial\chi_p}{\partial p_0} + \frac{\partial f}{\partial p_0}\right)\frac{\partial p_0}{\partial\alpha_p}\langle L\rangle\frac{\partial f}{\partial\chi_p} = 0\end{aligned} \tag{6.23}$$

where the rate of the hardening variables β and p_0 are those reported in eqs. (4.20) and (4.6), respectively. The plastic multiplier can be specified from eq. (6.23) as follow:

$$L = -\frac{\frac{\partial f}{\partial \chi_p}\frac{\partial \chi_p}{\partial p}\dot{p} + \left(\frac{\partial f}{\partial \chi_p}\frac{\partial \chi_p}{\partial q} + \frac{\partial f}{\partial \chi_q}\right)\dot{q}}{\frac{\partial f}{\partial \beta} cp\left(\beta_b - \beta\right) + \left(\frac{\partial f}{\partial \chi_p}\frac{\partial \chi_p}{\partial p_0} + \frac{\partial f}{\partial p_0}\right)\frac{\partial p_0}{\partial \alpha_p}\frac{\partial f}{\partial \chi_p}} \tag{6.24}$$

where the derivative of χ_p with respect to p_0 is:

$$\frac{\partial \chi_p}{\partial p_0} = r^2\left(\frac{p_r}{p_0}\right)^r \frac{1}{p_0}\frac{1}{p_r^{1-n}k\left(1-n\right)\left(2-n\right)}\left[p^2 + \frac{k\left(1-n\right)}{3g}q^2\right]^{\frac{2-n}{2}}\frac{1+e_{in}}{\lambda-\kappa} \tag{6.25}$$

and the derivatives of the yield function with respect to the hardening variables and the derivative of p_0 with respect to the plastic strain are the same as those calculated in section (5.7.1) and reported herein for completeness:

$$\frac{\partial f}{\partial \beta} = -2\chi_p\chi_q + 2\beta p_0\chi_p \tag{6.26}$$

$$\frac{\partial f}{\partial p_0} = -M^2\chi_p + \beta^2\chi_p \tag{6.27}$$

$$\frac{\partial p_0}{\partial \alpha_p} = \frac{1+e_{in}}{\lambda-\kappa}p_0 \tag{6.28}$$

6.2.2 Use of kinematic constraints (SEPC2)

In this section the model is developed following the original alternative procedure based on the inclusion of the kinematic constraints in the dissipation function. The technique of lagrangian multipliers permits to modify this function adding two constraints due to the isotropic and the rotational hardening via the preconsolidation pressure p_0 and the rotational internal variable β, respectively:

$$\begin{aligned} &d'\left(\dot{\alpha}_p, \dot{\alpha}_q, \beta, \dot{\beta}, p_0, \dot{p}_0\right) = d\left(\dot{\alpha}_p, \dot{\alpha}_q, \beta, p_0\right) + \Lambda_1 c_1 + \Lambda_2 c_2 = \\ &= \frac{p_0}{2}\left[\sqrt{\left(\dot{\alpha}_p + \beta\dot{\alpha}_q\right)^2 + \left(M^2 - \beta^2\right)\dot{\alpha}_q^2} + \dot{\alpha}_p + \beta\dot{\alpha}_q\right] + \\ &+ \Lambda_1\left[\dot{\beta} - \left(\beta_b - \beta\right)cp\left\langle L\right\rangle\right] + \Lambda_2\left(\dot{p}_0 - p_0\frac{1+e_{in}}{\lambda-\kappa}\dot{\alpha}_p\right) \end{aligned} \tag{6.29}$$

with d denoting the dissipation function of eq. (6.13). From eq. (6.29) the dissipative generalised stresses can be calculated as:

$$\begin{aligned}
\chi_p &= \frac{\partial d'}{\partial \dot{\alpha}_p} = \frac{\partial d}{\partial \dot{\alpha}_p} - \Lambda_2 \frac{1+e_{in}}{\lambda-\kappa} p_0 \\
\chi_q &= \frac{\partial d'}{\partial \dot{\alpha}_q} = \frac{\partial d}{\partial \dot{\alpha}_q} \\
\chi_{p_0} &= \frac{\partial d'}{\partial \dot{p}_0} = \Lambda_2 \\
\chi_\beta &= \frac{\partial d'}{\partial \dot{\beta}} = \Lambda_1
\end{aligned} \tag{6.30}$$

Note that the Ziegler's orthogonality principle entails that the lagrangian multiplier Λ_1 is equal to zero because the term ψ_1 of the Gibbs free energy does not depend on the rotational variable β ($\bar{\chi}_\beta = 0$). However, the elastoplastic coupling on the preconsolidation pressure implies that $\bar{\chi}_{p_0} = \chi_{p_0} = \Lambda_2 \neq 0$. Therefore, unlike in the case SEPC1, an additional component of the generalised stresses has to be considered and, even more relevant, the expression of the yield function in the generalised stresses modifies, becoming a surface in the tridimensional space $(\chi_p, \chi_q, \chi_{p_0})$. In fact, the function in eq. (6.14) derives from the dissipation function d, thus a different expression will be obtained stemming from the new dissipation function d'. To avoid complex and unnecessary analytical calculations, employing the first definition in eq. (6.30) and recalling the definition of $\bar{\chi}_p$ and $\bar{\chi}_{p_0}$ in eq. (6.12) and the derivative in eq. (6.28), one can define the generalised stress $\hat{\chi}_p$ such that

$$\begin{aligned}
\hat{\chi}_p &= \frac{\partial d}{\partial \dot{\alpha}_p} = \chi_p + \chi_{p_0} \frac{1+e_{in}}{\lambda-\kappa} p_0 = \chi_p + \chi_{p_0} \frac{\partial p_0}{\partial \alpha_p} = -2 \frac{\partial \psi_1}{\partial p_0} \frac{\partial p_0}{\partial \alpha_p} + p = \\
&= -2r \left(\frac{p_r}{p_0}\right)^r \frac{1}{p_r^{1-n} k (1-n)(2-n)} \left[p^2 + \frac{k(1-n)}{3g} q^2\right]^{\frac{2-n}{2}} \frac{1+e_{in}}{\lambda-\kappa} + p
\end{aligned} \tag{6.31}$$

This position allows for the derivation of the same expression of the yield surface employed till now, where the term $\hat{\chi}_p$ substitutes for χ_p in eq. (6.14):

$$f(\hat{\chi}_p, \chi_q, \beta, p_0) = (\chi_q - \beta \hat{\chi}_p)^2 - \left(M^2 - \beta^2\right) \hat{\chi}_p (p_0 - \hat{\chi}_p) = 0 \tag{6.32}$$

Subsequently, by substitution of eq. (6.31) in eq. (6.32), one obtains the equation of the yield surface in the generalised space $(\chi_p, \chi_q, \chi_{p_0})$ as follow:

$$\begin{aligned}
f(\chi_p, \chi_q, \chi_{p_0}, \beta, p_0) &= \left[\chi_q - \beta \left(\chi_p + \chi_{p_0} \frac{1+e_{in}}{\lambda-\kappa} p_0\right)\right]^2 + \\
&- \left(M^2 - \beta^2\right) \left(\chi_p + \chi_{p_0} \frac{1+e_{in}}{\lambda-\kappa} p_0\right) \left(p_0 - \chi_p - \chi_{p_0} \frac{1+e_{in}}{\lambda-\kappa} p_0\right) = 0
\end{aligned} \tag{6.33}$$

The yield function in terms of generalised stresses is no longer the original distorted ellipse proposed by Dafalias & Taiebat (2013) and a more complicated 3D surface in the generalised space $(\chi_p, \chi_q, \chi_{p_0})$ arises. Consequently, even the resulting yield function in the p-q plane modifies with respect to the SEPC1 case. In fact, it is sufficient to substitute eq. (6.31) and the second of eq. (6.12) in eq. (6.32) to express the yield function in terms of stresses.

According to eq. (5.20), the rates of the internal variables can be written as:

$$\begin{aligned} \dot{\alpha}_p &= \langle L \rangle \frac{\partial f}{\partial \chi_p} \\ \dot{\alpha}_q &= \langle L \rangle \frac{\partial f}{\partial \chi_q} \\ \dot{p}_0 &= \langle L \rangle \frac{\partial f}{\partial \chi_{p_0}} \end{aligned} \tag{6.34}$$

and consequently, as expected, the flow rule will be associated in the generalised stress space. It is worth analysing more carefully the third expression in eq. (6.34), which specifically stems from the adoption of the lagrangian multipliers in the dissipation function. Consider first the derivative of the yield surface with respect to the generalised stress χ_p:

$$\begin{aligned} \frac{\partial f}{\partial \chi_p} &= -2\beta\chi_q + 2M^2\chi_p + 2M^2\chi_{p_0}\frac{1+e_{in}}{\lambda-\kappa}p_0 - M^2 p_0 + \beta^2 p_0 = \\ &= -2\beta\chi_q + 2M^2\hat{\chi}_p - M^2 p_0 + \beta^2 p_0 = \frac{\partial f}{\partial \hat{\chi}_p} \end{aligned} \tag{6.35}$$

Then, employing this latter equation one can express the rate of the internal variable p_0 as follow:

$$\begin{aligned} \dot{p}_0 = \langle L \rangle \frac{\partial f}{\partial \chi_{p_0}} &= \langle L \rangle \frac{1+e_{in}}{\lambda-\kappa}p_0 \left(-2\beta\chi_q + 2M^2\chi_p + \right. \\ &\left. + 2M^2\chi_{p_0}\frac{1+e_{in}}{\lambda-\kappa}p_0 - M^2 p_0 + \beta^2 p_0\right) = \\ &= \langle L \rangle \frac{1+e_{in}}{\lambda-\kappa}p_0\frac{\partial f}{\partial \chi_p} = \frac{1+e_{in}}{\lambda-\kappa}p_0\dot{\alpha}_p \end{aligned} \tag{6.36}$$

which is exactly the isotropic hardening rule adopted by Dafalias & Taiebat (2013) and reported in eq. (4.6). This result is what expected but it is worth remarking that here the hardening rule is an outcome of the formulation and is no longer an external ingredient as commonly assumed in the hyperplastic approach. This is due to the fact that the hardening rule is directly encapsulated in the dis-

sipation function. Another interesting result stemming from eq. (6.35) is that the derivatives of the yield surface f with respect to $\hat{\chi}_p$ and χ_p coincide (alternatively, for chain rule one can write $\frac{\partial f}{\partial \chi_p} = \frac{\partial f}{\partial \hat{\chi}_p}\frac{\partial \hat{\chi}_p}{\partial \chi_p}$ where $\frac{\partial \hat{\chi}_p}{\partial \chi_p} = 1$), thus the normal to the yield surface in the plane $(\hat{\chi}_p, \chi_q)$ represents the direction of the plastic strain rate.

The yield surface in the stress space modifies from the original distorted ellipse, thus the flow rule is no longer associated. Furthermore, following the same procedure described for the case SEPC1, it is possible to link the direction of the normal to the yield surface $\hat{f}$ in the p-q plane to the strain rates. In particular, specialising eq. (6.6) to the current case, the components of the normal vector to the yield surface $\hat{f}$ can be evaluated as:

$$\begin{aligned}\frac{\partial \hat{f}}{\partial p} &= \frac{\partial f}{\partial \chi_p}\frac{\partial \chi_p}{\partial p} + \frac{\partial f}{\partial \chi_q}\frac{\partial \chi_q}{\partial p} + \frac{\partial f}{\partial \chi_{p_0}}\frac{\partial \chi_{p_0}}{\partial p} \\ \frac{\partial \hat{f}}{\partial q} &= \frac{\partial f}{\partial \chi_p}\frac{\partial \chi_p}{\partial q} + \frac{\partial f}{\partial \chi_q}\frac{\partial \chi_q}{\partial q} + \frac{\partial f}{\partial \chi_{p_0}}\frac{\partial \chi_{p_0}}{\partial q}\end{aligned} \tag{6.37}$$

Now multiply the first of eq. (6.37) by the plastic multiplier $\langle L \rangle$, recalling eq. (6.17) and the flow rule in eq. (6.34). Then, noting that $\frac{\partial \chi_q}{\partial p} = 0$ and that from eq. (6.12) is $\chi_p = \chi_{p_0}\frac{\partial p_0}{\partial \alpha_p} + p$, one can write:

$$\begin{aligned}\langle L \rangle \frac{\partial \hat{f}}{\partial p} &= \frac{\partial \chi_p}{\partial p}\dot{\alpha}_p + \dot{p}_0\frac{\partial \chi_{p_0}}{\partial p} = \frac{\partial \chi_p}{\partial p}\dot{\alpha}_p + \frac{\partial p_0}{\partial \alpha_p}\dot{\alpha}_p\frac{\partial}{\partial p}\left[\left(\frac{\partial p_0}{\partial \alpha_p}\right)^{-1}(\chi_p - p)\right] = \\ &= \frac{\partial \chi_p}{\partial p}\dot{\alpha}_p + \dot{\alpha}_p\left(\frac{\partial \chi_p}{\partial p} - 1\right) = \left(1 - 2\frac{\partial^2 \psi_1}{\partial \alpha_p \partial p}\right)\dot{\alpha}_p = \dot{\varepsilon}_v^p + 2\dot{\varepsilon}_v^c\end{aligned} \tag{6.38}$$

Analogously, multiplying the second of eq. (6.37) for the plastic multiplier $\langle L \rangle$, recalling eq. (6.18) and noting that $\frac{\partial \chi_q}{\partial q} = 1$ the equation becomes:

$$\begin{aligned}\langle L \rangle \frac{\partial \hat{f}}{\partial q} &= \frac{\partial \chi_p}{\partial q}\dot{\alpha}_p + \dot{\alpha}_q + \dot{p}_0\frac{\partial \chi_{p_0}}{\partial q} = \frac{\partial \chi_p}{\partial q}\dot{\alpha}_p + \dot{\alpha}_q + \frac{\partial p_0}{\partial \alpha_p}\dot{\alpha}_p\frac{\partial}{\partial q}\left[\left(\frac{\partial p_0}{\partial \alpha_p}\right)^{-1}(\chi_p - p)\right] = \\ &= \frac{\partial \chi_p}{\partial q}\dot{\alpha}_p + \dot{\alpha}_q + \dot{\alpha}_p\frac{\partial \chi_p}{\partial q} = \dot{\alpha}_q - 2\frac{\partial^2 \psi_1}{\partial \alpha_p \partial q}\dot{\alpha}_p = \dot{\varepsilon}_s^p + 2\dot{\varepsilon}_s^c\end{aligned} \tag{6.39}$$

From the above emerges that the technique of lagrangian multipliers modifies significantly the flow rule in the stress space; in fact, not only this latter becomes even more non-associated in comparison with the well-established procedure adopted in section (6.2.1) (SEPC1) but in addition eqs. (6.38) and (6.39) suggest that the flow rule is not associated with respect to the irreversible strain rates. Therefore,

the fundamental result pointed out by Collins & Houlsby (1997) holds true solely for the SEPC1 approach, in which the hardening rules of the model are not directly enforced in the formulation.

Finally, for numerical purposes, the formulation can be expressed in the incremental form. The consistency condition is conveniently imposed on the yield function in eq. (6.32) leading to:

$$\begin{aligned}
\dot{f} &= \frac{\partial f}{\partial \hat{\chi}_p}\dot{\hat{\chi}}_p + \frac{\partial f}{\partial \chi_q}\dot{\chi}_q + \frac{\partial f}{\partial \beta}\dot{\beta} + \frac{\partial f}{\partial p_0}\dot{p}_0 = \\
&= \frac{\partial f}{\partial \hat{\chi}_p}\left(\frac{\partial \hat{\chi}_p}{\partial p}\dot{p} + \frac{\partial \hat{\chi}_p}{\partial q}\dot{q} + \frac{\partial \hat{\chi}_p}{\partial p_0}\dot{p}_0\right) + \frac{\partial f}{\partial \chi_q}\dot{q} + \frac{\partial f}{\partial \beta}\dot{\beta} + \frac{\partial f}{\partial p_0}\dot{p}_0 = \\
&= \frac{\partial f}{\partial \hat{\chi}_p}\frac{\partial \hat{\chi}_p}{\partial p}\dot{p} + \left(\frac{\partial f}{\partial \hat{\chi}_p}\frac{\partial \hat{\chi}_p}{\partial q} + \frac{\partial f}{\partial \chi_q}\right)\dot{q} + \frac{\partial f}{\partial \beta}\dot{\beta} + \left(\frac{\partial f}{\partial \hat{\chi}_p}\frac{\partial \hat{\chi}_p}{\partial p_0} + \frac{\partial f}{\partial p_0}\right)\dot{p}_0 = \\
&= \frac{\partial f}{\partial \hat{\chi}_p}\frac{\partial \hat{\chi}_p}{\partial p}\dot{p} + \left(\frac{\partial f}{\partial \hat{\chi}_p}\frac{\partial \hat{\chi}_p}{\partial q} + \frac{\partial f}{\partial \chi_q}\right)\dot{q} + \frac{\partial f}{\partial \beta}\langle L\rangle\, cp\,(\beta_b - \beta) + \\
&+ \left(\frac{\partial f}{\partial \hat{\chi}_p}\frac{\partial \hat{\chi}_p}{\partial p_0} + \frac{\partial f}{\partial p_0}\right)\frac{\partial p_0}{\partial \alpha_p}\langle L\rangle\frac{\partial f}{\partial \chi_p} = 0
\end{aligned} \tag{6.40}$$

from which the plastic multiplier can be evaluated as:

$$L = -\frac{\frac{\partial f}{\partial \hat{\chi}_p}\frac{\partial \hat{\chi}_p}{\partial p}\dot{p} + \left(\frac{\partial f}{\partial \hat{\chi}_p}\frac{\partial \hat{\chi}_p}{\partial q} + \frac{\partial f}{\partial \chi_q}\right)\dot{q}}{\frac{\partial f}{\partial \beta}cp\,(\beta_b - \beta) + \left(\frac{\partial f}{\partial \hat{\chi}_p}\frac{\partial \hat{\chi}_p}{\partial p_0} + \frac{\partial f}{\partial p_0}\right)\frac{\partial p_0}{\partial \alpha_p}\frac{\partial f}{\partial \chi_p}} \tag{6.41}$$

with the derivatives assuming the expressions:

$$\frac{\partial \hat{\chi}_p}{\partial p} = 1 - 2r\left(\frac{p_r}{p_0}\right)^r \frac{1}{p_r^{1-n}k\,(1-n)}\left[p^2 + \frac{k\,(1-n)}{3g}q^2\right]^{-\frac{n}{2}}\frac{1+e_{in}}{\lambda-\kappa}p \tag{6.42}$$

$$\frac{\partial \hat{\chi}_p}{\partial q} = -2r\left(\frac{p_r}{p_0}\right)^r \frac{1}{p_r^{1-n}}\left[p^2 + \frac{k\,(1-n)}{3g}q^2\right]^{-\frac{n}{2}}\frac{1+e_{in}}{\lambda-\kappa}\frac{q}{3g} \tag{6.43}$$

$$\frac{\partial \hat{\chi}_p}{\partial p_0} = 2r^2\left(\frac{p_r}{p_0}\right)^r \frac{1}{p_0}\frac{1}{p_r^{1-n}k\,(1-n)\,(2-n)}\left[p^2 + \frac{k\,(1-n)}{3g}q^2\right]^{\frac{2-n}{2}}\frac{1+e_{in}}{\lambda-\kappa} \tag{6.44}$$

$$\frac{\partial f}{\partial \chi_q} = 2\chi_q - 2\beta\hat{\chi}_p \tag{6.45}$$

$$\frac{\partial f}{\partial \beta} = -2\hat{\chi}_p\chi_q + 2\beta p_0\hat{\chi}_p \tag{6.46}$$

$$\frac{\partial f}{\partial p_0} = -M^2 \hat{\chi}_p + \beta^2 \hat{\chi}_p \tag{6.47}$$

6.3 Anisotropic elastoplastic coupling via the fabric tensor

In chapter 4 an empirical based relationship linking the fabric tensor $\mathbf{B}$ of the proposed nonlinear anisotropic hyperelastic model with the tensor value rotational variable $\boldsymbol{\beta}$ was illustrated and the evolution of the elastic stiffness anisotropy with the plastic strains was reproduced. In this section the same relationship is employed to develop a thermodynamically consistent form of elastoplastic coupling via the anisotropy character of soils. Analogously to what done in the previous section for the preconsolidation pressure, to introduce the dependence of the elastic striffness on the rotational internal variable of the Dafalias & Taiebat (2013) model, the elastic part of Gibbs free energy, namely the term ψ_1, has to be properly modified. Specialising eq. (A.30) to the triaxial formulation and, for simplicity, in the case of linear elasticity, under the hypothesis of transverse isotropy, enforcing the correlation between $\mathbf{B}$ and $\boldsymbol{\beta}$ in eq. (4.32) with $\omega = 1$, the free energy can be expressed in terms of stress invariants p and q and of the scalar-valued rotational variable β in the following form:

$$\psi = -\frac{1}{2kp_r}\left[\left(\frac{1}{9}-\frac{k}{6g}\right)\frac{\left(3p-\beta^2 p+\frac{2}{3}\beta^2 q\right)^2}{\left(1-\frac{1}{3}\beta^2-\frac{2}{9}\beta^4\right)^2}+\frac{k}{2g}\frac{\left(p+\frac{2}{3}q\right)^2}{\left(1-\frac{2}{3}\beta^2\right)^2}+\frac{k}{g}\frac{\left(p-\frac{1}{3}q\right)^2}{\left(1+\frac{1}{3}\beta^2\right)^2}\right]+ \\ -\left(p\alpha_p+q\alpha_q\right) \tag{6.48}$$

where k and g are the parameters of the hyperelastic model and p_r is the reference pressure and, as usual, α_p and α_q denote the volumetric and deviatoric plastic strains, respectively.

Differentiating the Gibbs free energy with respect to the stress one can calculate the total volumetric and deviatoric strains as follow:

$$
\begin{aligned}
\varepsilon_v &= -\frac{\partial \psi}{\partial p} = \varepsilon_v^e + \varepsilon_v^p = \frac{1}{2kp_r}\left[\left(\frac{1}{9}-\frac{k}{6g}\right)\frac{2\left(3p-\beta^2 p+\frac{2}{3}\beta^2 q\right)\left(3-\beta^2\right)}{\left(1-\frac{1}{3}\beta^2-\frac{2}{9}\beta^4\right)^2}+\right. \\
&\left.+\frac{k}{g}\frac{\left(p+\frac{2}{3}q\right)}{\left(1-\frac{2}{3}\beta^2\right)^2}+\frac{k}{g}\frac{2\left(p-\frac{1}{3}q\right)}{\left(1+\frac{1}{3}\beta^2\right)^2}\right]+\alpha_p \\
\varepsilon_s &= -\frac{\partial \psi}{\partial q} = \varepsilon_s^e + \varepsilon_s^p = \frac{1}{2kp_r}\left[\left(\frac{1}{9}-\frac{k}{6g}\right)\frac{2\left(3p-\beta^2 p+\frac{2}{3}\beta^2 q\right)\frac{2}{3}\beta^2}{\left(1-\frac{1}{3}\beta^2-\frac{2}{9}\beta^4\right)^2}+\right. \\
&\left.+\frac{2}{3}\frac{k}{g}\frac{\left(p+\frac{2}{3}q\right)}{\left(1-\frac{2}{3}\beta^2\right)^2}-\frac{2}{3}\frac{k}{g}\frac{\left(p-\frac{1}{3}q\right)}{\left(1+\frac{1}{3}\beta^2\right)^2}\right]+\alpha_q
\end{aligned}
\tag{6.49}
$$

It is worth noting at this point that the rotational hardening law in the form of eq. (4.20) is not adequate to determine the generalised stresses because cannot be integrated in a closed form unless for constant stress ratio loading paths. In other words, the rotational variable β should be directly expressed in terms of plastic strain to determine the derivatives $\frac{\partial \beta}{\partial \alpha_p}$ and $\frac{\partial \beta}{\partial \alpha_q}$. Therefore, a modified rotational hardening rule is proposed herein. From a physical perspective a reasonable assumption is that the rotation and the consequent distorsion of the yield surface is manly governed by the shear strains rather than the volumetric one. Hence, according to the works by Collins & Hilder (2002) and Coombs (2017), a rate of the rotational variable function of the deviatoric plastic strain rate is adopted. In detail, in lieu of eq. (4.20) the following form is considered:

$$
\dot{\beta} = c\left(\beta_b - \beta\right)\dot{\alpha}_q \tag{6.50}
$$

where c is still a dimensionless parameter controlling the pace of the evolution. Integrating eq. (6.50) by separation of the variables from an initial value β_{in} corresponding to $\alpha_q = 0$, the rotational internal variable reads:

$$
\beta = \beta_b - \left(\beta_b - \beta_{in}\right)\exp\left(-c\alpha_q\right) \tag{6.51}
$$

Taking into account the Gibbs free energy in eq. (6.48) and noting that from eq. (6.50) it follows $\frac{\partial \beta}{\partial \alpha_q} = c\left(\beta_b - \beta\right)$, the generalised stresses can be calculated as:

$$
\begin{aligned}
\bar{\chi}_p &= -\frac{\partial \psi}{\partial \alpha_p} = -\frac{\partial \psi_1}{\partial \beta}\frac{\partial \beta}{\partial \alpha_p} + p = p \\
\bar{\chi}_q &= -\frac{\partial \psi}{\partial \alpha_q} = -\frac{\partial \psi_1}{\partial \beta}\frac{\partial \beta}{\partial \alpha_q} + q = \frac{1}{2kp_r}\left[\left(\frac{1}{9}-\frac{k}{6g}\right)\frac{2\left(3p-\beta^2 p+\frac{2}{3}\beta^2 q\right)}{\left(1-\frac{1}{3}\beta^2-\frac{2}{9}\beta^4\right)^2}\right. \\
&\left(-2\beta p+\frac{4}{3}\beta q\right)+\left(\frac{1}{9}-\frac{k}{6g}\right)\frac{2\left(3p-\beta^2 p+\frac{2}{3}\beta^2 q\right)^2\left(\frac{2}{3}\beta+\frac{8}{9}\beta^3\right)}{\left(1-\frac{1}{3}\beta^2-\frac{2}{9}\beta^4\right)^3}+ \\
&\left.+\frac{4}{3}\frac{k}{g}\frac{\beta\left(p+\frac{2}{3}q\right)^2}{\left(1-\frac{2}{3}\beta^2\right)^3}-\frac{4}{3}\frac{k}{g}\frac{\beta\left(p-\frac{1}{3}q\right)^2}{\left(1+\frac{1}{3}\beta^2\right)^3}\right]c\left(\beta_b-\beta\right)+q \\
\bar{\chi}_\beta &= -\frac{\partial \psi}{\partial \beta} = \frac{1}{2kp_r}\left[\left(\frac{1}{9}-\frac{k}{6g}\right)\frac{2\left(3p-\beta^2 p+\frac{2}{3}\beta^2 q\right)\left(-2\beta p+\frac{4}{3}\beta q\right)}{\left(1-\frac{1}{3}\beta^2-\frac{2}{9}\beta^4\right)^2}+\right. \\
&+\left(\frac{1}{9}-\frac{k}{6g}\right)\frac{2\left(3p-\beta^2 p+\frac{2}{3}\beta^2 q\right)^2\left(\frac{2}{3}\beta+\frac{8}{9}\beta^3\right)}{\left(1-\frac{1}{3}\beta^2-\frac{2}{9}\beta^4\right)^3}+\frac{4}{3}\frac{k}{g}\frac{\beta\left(p+\frac{2}{3}q\right)^2}{\left(1-\frac{2}{3}\beta^2\right)^3}+ \\
&\left.-\frac{4}{3}\frac{k}{g}\frac{\beta\left(p-\frac{1}{3}q\right)^2}{\left(1+\frac{1}{3}\beta^2\right)^3}\right]
\end{aligned}
\tag{6.52}
$$

Even for the above anisotropic elastoplastic coupling, the generalised stresses do not coincide with the stress invariants. Specifically, an additional term arises in $\bar{\chi}_q$ and as the free energy depends directly on β, the new component $\bar{\chi}_\beta$ appears.

In the following, similarly to what done for the isotropic coupling via the pre-consolidation pressure, two possible formulations are proposed; in the first one the hyper-elastoplastic Dafalias & Taiebat (2013) model developed in chapter 5 is adopted with the traditional form of the dissipation functions (SEPC1), whereas in the second one the dissipation function takes into account the isotropic and rotational hardening rules through two kinematic constraints (SEPC2).

6.3.1 Traditional hyperplastic approach (SEPC1)

Following the approach SEPC1 the dissipation and the yield functions are those reported in eqs. (6.13) and (6.14). Recalling the definition in eq. (5.14), the dissipative generalised stresses result:

$$
\begin{aligned}
\chi_p &= \frac{\partial d}{\partial \dot{\alpha}_p} \\
\chi_q &= \frac{\partial d}{\partial \dot{\alpha}_q} \\
\chi_\beta &= \frac{\partial d}{\partial \dot{\beta}} = 0
\end{aligned}
\tag{6.53}
$$

As the dissipation function does not depend explicitly on $\dot{\beta}$, only the components χ_p and χ_q are retained, coinciding with the generalised stresses in eq. (6.52) for the orthogonality principle. By substitution of the generalised stresses in eq. (6.14) one determines the yield function $\hat{f}$ in the p-q plane that, as expected, it is no longer an ellipse and is characterised by a non-associated flow rule. In fact, specialising eq. (6.6) to the present case it follows:

$$\begin{aligned}\frac{\partial \hat{f}}{\partial p} &= \frac{\partial f}{\partial \chi_p}\frac{\partial \chi_p}{\partial p} + \frac{\partial f}{\partial \chi_q}\frac{\partial \chi_q}{\partial p} = \frac{\partial f}{\partial \chi_p} + \frac{\partial f}{\partial \chi_q}\left(-\frac{\partial^2 \psi_1}{\partial \alpha_q \partial p}\right) \\ \frac{\partial \hat{f}}{\partial q} &= \frac{\partial f}{\partial \chi_p}\frac{\partial \chi_p}{\partial q} + \frac{\partial f}{\partial \chi_q}\frac{\partial \chi_q}{\partial q} = \frac{\partial f}{\partial \chi_q}\left(1 - \frac{\partial^2 \psi_1}{\partial \alpha_q \partial q}\right)\end{aligned} \tag{6.54}$$

where $\frac{\partial \chi_p}{\partial p} = 1$, $\frac{\partial \chi_p}{\partial q} = 0$, $\frac{\partial f}{\partial \chi_p}$ and $\frac{\partial f}{\partial \chi_q}$ are reported in eqs. (6.19) and (6.20), respectively and the remaining derivatives take the form:

$$\begin{aligned}\frac{\partial \chi_q}{\partial p} = -\frac{\partial^2 \psi_1}{\partial \alpha_q \partial p} = \frac{1}{2kp_r}\Bigg[&\left(\frac{1}{9} - \frac{k}{6g}\right)\frac{2\left(3-\beta^2\right)\left(-2\beta p + \frac{4}{3}\beta q\right)}{\left(1 - \frac{1}{3}\beta^2 - \frac{2}{9}\beta^4\right)^2} + \\ &- \left(\frac{1}{9} - \frac{k}{6g}\right)\frac{4\beta\left(3p - \beta^2 p + \frac{2}{3}\beta^2 q\right)}{\left(1 - \frac{1}{3}\beta^2 - \frac{2}{9}\beta^4\right)^2} + \left(\frac{1}{9} - \frac{k}{6g}\right)\frac{4\left(3p - \beta^2 p + \frac{2}{3}\beta^2 q\right)}{\left(1 - \frac{1}{3}\beta^2 - \frac{2}{9}\beta^4\right)^3} \\ &\left(3-\beta^2\right)\left(\frac{2}{3}\beta + \frac{8}{9}\beta^3\right) + \frac{8}{3}\frac{k}{g}\frac{\beta\left(p + \frac{2}{3}q\right)}{\left(1 - \frac{2}{3}\beta^2\right)^3} - \frac{8}{3}\frac{k}{g}\frac{\beta\left(p - \frac{1}{3}q\right)}{\left(1 + \frac{1}{3}\beta^2\right)^3}\Bigg] c\left(\beta_b - \beta\right)\end{aligned} \tag{6.55}$$

$$\begin{aligned}\frac{\partial \chi_q}{\partial q} = 1 - \frac{\partial^2 \psi_1}{\partial \alpha_q \partial q} = 1 + \frac{1}{2kp_r}\Bigg[&\left(\frac{1}{9} - \frac{k}{6g}\right)\frac{\frac{4}{3}\beta^2\left(-2\beta p + \frac{4}{3}\beta q\right)}{\left(1 - \frac{1}{3}\beta^2 - \frac{2}{9}\beta^4\right)^2} + \\ &+ \left(\frac{1}{9} - \frac{k}{6g}\right)\frac{\frac{8}{3}\beta\left(3p - \beta^2 p + \frac{2}{3}\beta^2 q\right)}{\left(1 - \frac{1}{3}\beta^2 - \frac{2}{9}\beta^4\right)^2} + \left(\frac{1}{9} - \frac{k}{6g}\right)\frac{\frac{8}{3}\beta^2\left(3p - \beta^2 p + \frac{2}{3}\beta^2 q\right)}{\left(1 - \frac{1}{3}\beta^2 - \frac{2}{9}\beta^4\right)^3} \\ &\left(\frac{2}{3}\beta + \frac{8}{9}\beta^3\right) + \frac{16}{9}\frac{k}{g}\frac{\beta\left(p + \frac{2}{3}q\right)}{\left(1 - \frac{2}{3}\beta^2\right)^3} + \frac{8}{9}\frac{k}{g}\frac{\beta\left(p - \frac{1}{3}q\right)}{\left(1 + \frac{1}{3}\beta^2\right)^3}\Bigg] c\left(\beta_b - \beta\right)\end{aligned} \tag{6.56}$$

Analogously to what shown for the coupling with respect to the preconsolidation pressure, one can demonstrate that the irreversible strain rate is directed along the normal to the yield surface in the p-q plane. The total strain rate are by definition:

$$\begin{aligned}\dot{\varepsilon}_v &= \left(-\frac{\partial^2 \psi_1}{\partial p^2}\dot{p} - \frac{\partial^2 \psi_1}{\partial p \partial q}\dot{q}\right) - \frac{\partial^2 \psi_1}{\partial p \partial \alpha_q}\dot{\alpha}_q + \dot{\alpha}_p = \dot{\varepsilon}_v^r + \dot{\varepsilon}_v^c + \dot{\varepsilon}_v^p \\ \dot{\varepsilon}_s &= \left(-\frac{\partial^2 \psi_1}{\partial q \partial p}\dot{p} - \frac{\partial^2 \psi_1}{\partial q^2}\dot{q}\right) - \frac{\partial^2 \psi_1}{\partial q \partial \alpha_q}\dot{\alpha}_q + \dot{\alpha}_q = \dot{\varepsilon}_s^r + \dot{\varepsilon}_s^c + \dot{\varepsilon}_s^p\end{aligned} \tag{6.57}$$

Then, multiplying for $\langle L \rangle$ all the members of eq. (6.54) and recalling that, by virtue of eq. (5.20), is $\dot{\alpha}_p = \langle L \rangle \frac{\partial f}{\partial \chi_p}$ and $\dot{\alpha}_q = \langle L \rangle \frac{\partial f}{\partial \chi_q}$, one can write:

$$\begin{aligned} \langle L \rangle \frac{\partial \hat{f}}{\partial p} &= -\frac{\partial^2 \psi_1}{\partial \alpha_q \partial p} \dot{\alpha}_q + \dot{\alpha}_p = \dot{\varepsilon}_v^c + \dot{\varepsilon}_v^p = \dot{\varepsilon}_v^i \\ \langle L \rangle \frac{\partial \hat{f}}{\partial q} &= -\frac{\partial^2 \psi_1}{\partial \alpha_q \partial q} \dot{\alpha}_q + \dot{\alpha}_q = \dot{\varepsilon}_s^c + \dot{\varepsilon}_s^p = \dot{\varepsilon}_s^i \end{aligned} \tag{6.58}$$

Hence, the flow rule is non-associated with respect to the plastic strain rates but can be considered associated with reference to the irreversible strain rates.

The consistency condition allows to express the consitituve relationship in the incremental form and to obtain the plastic multiplier. In detail it is:

$$\begin{aligned} \dot{f} &= \frac{\partial f}{\partial \chi_p} \dot{\chi}_p + \frac{\partial f}{\partial \chi_q} \dot{\chi}_q + \frac{\partial f}{\partial \beta} \dot{\beta} + \frac{\partial f}{\partial p_0} \dot{p}_0 = \\ &= \frac{\partial f}{\partial \chi_p} \dot{p} + \frac{\partial f}{\partial \chi_q} \left(\frac{\partial \chi_q}{\partial p} \dot{p} + \frac{\partial \chi_q}{\partial q} \dot{q} + \frac{\partial \chi_q}{\partial \beta} \dot{\beta} \right) + \frac{\partial f}{\partial \beta} \dot{\beta} + \frac{\partial f}{\partial p_0} \dot{p}_0 = \\ &= \left(\frac{\partial f}{\partial \chi_p} + \frac{\partial f}{\partial \chi_q} \frac{\partial \chi_q}{\partial p} \right) \dot{p} + \frac{\partial f}{\partial \chi_q} \frac{\partial \chi_q}{\partial q} \dot{q} + \left(\frac{\partial f}{\partial \chi_q} \frac{\partial \chi_q}{\partial \beta} + \frac{\partial f}{\partial \beta} \right) \dot{\beta} + \frac{\partial f}{\partial p_0} \dot{p}_0 = \\ &= \left(\frac{\partial f}{\partial \chi_p} + \frac{\partial f}{\partial \chi_q} \frac{\partial \chi_q}{\partial p} \right) \dot{p} + \frac{\partial f}{\partial \chi_q} \frac{\partial \chi_q}{\partial q} \dot{q} + \left(\frac{\partial f}{\partial \chi_q} \frac{\partial \chi_q}{\partial \beta} + \frac{\partial f}{\partial \beta} \right) \langle L \rangle \, c \, (\beta_b - \beta) \frac{\partial f}{\partial \chi_q} + \\ &+ \frac{\partial f}{\partial p_0} \frac{\partial p_0}{\partial \alpha_p} \langle L \rangle \frac{\partial f}{\partial \chi_p} = 0 \end{aligned} \tag{6.59}$$

where the rate of the hardening variables β and p_0 are those reported in eqs. (6.50) and (4.6), respectively. The plastic multiplier follows as:

$$L = -\frac{\left(\frac{\partial f}{\partial \chi_p} + \frac{\partial f}{\partial \chi_q} \frac{\partial \chi_q}{\partial p} \right) \dot{p} + \frac{\partial f}{\partial \chi_q} \frac{\partial \chi_q}{\partial q} \dot{q}}{\left(\frac{\partial f}{\partial \chi_q} \frac{\partial \chi_q}{\partial \beta} + \frac{\partial f}{\partial \beta} \right) c \, (\beta_b - \beta) \frac{\partial f}{\partial \chi_q} + \frac{\partial f}{\partial p_0} \frac{\partial p_0}{\partial \alpha_p} \frac{\partial f}{\partial \chi_p}} \tag{6.60}$$

where the derivative of χ_q with respect to β is:

$$\begin{aligned}
\frac{\partial \chi_q}{\partial \beta} &= \frac{1}{2kp_r}\left[\left(\frac{1}{9}-\frac{k}{6g}\right)\frac{2\left(-2\beta p+\frac{4}{3}\beta q\right)^2+2\left(3p-\beta^2 p+\frac{2}{3}\beta^2 q\right)\left(-2p+\frac{4}{3}q\right)}{\left(1-\frac{1}{3}\beta^2-\frac{2}{9}\beta^4\right)^2}+\right.\\
&= +\left(\frac{1}{9}-\frac{k}{6g}\right)\frac{8\left(3p-\beta^2 p+\frac{2}{3}\beta^2 q\right)\left(-2\beta p+\frac{4}{3}\beta q\right)\left(\frac{2}{3}\beta+\frac{8}{9}\beta^3\right)}{\left(1-\frac{1}{3}\beta^2-\frac{2}{9}\beta^4\right)^3}+\\
&= +\left(\frac{1}{9}-\frac{k}{6g}\right)\frac{2\left(3p-\beta^2 p+\frac{2}{3}\beta^2 q\right)^2\left(\frac{2}{3}+\frac{8}{9}\beta^2\right)}{\left(1-\frac{1}{3}\beta^2-\frac{2}{9}\beta^4\right)^3}+\\
&= +\left(\frac{1}{9}-\frac{k}{6g}\right)\frac{6\left(3p-\beta^2 p+\frac{2}{3}\beta^2 q\right)^2\left(\frac{2}{3}\beta+\frac{8}{9}\beta^3\right)^2}{\left(1-\frac{1}{3}\beta^2-\frac{2}{9}\beta^4\right)^4}+\frac{4}{3}\frac{k}{g}\frac{\left(p+\frac{2}{3}q\right)^2}{\left(1-\frac{2}{3}\beta^2\right)^3}+\\
&= \left.+\frac{16}{3}\frac{k}{g}\frac{\beta^2\left(p+\frac{2}{3}q\right)^2}{\left(1-\frac{2}{3}\beta^2\right)^4}-\frac{4}{3}\frac{k}{g}\frac{\left(p-\frac{1}{3}q\right)^2}{\left(1+\frac{1}{3}\beta^2\right)^3}+\frac{8}{3}\frac{k}{g}\frac{\beta^2\left(p-\frac{1}{3}q\right)^2}{\left(1+\frac{1}{3}\beta^2\right)^4}\right]c\left(\beta_b-\beta\right)+\frac{q-\chi_q}{\beta_b-\beta}
\end{aligned} \tag{6.61}$$

and the other derivatives $\frac{\partial f}{\partial \beta}$, $\frac{\partial f}{\partial p_0}$ and $\frac{\partial p_0}{\partial \alpha_p}$ are the same reported in eqs. (6.26), (6.27) and (6.28), respectively.

6.3.2 Use of kinematic constraints (SEPC2)

In this section the isotropic and the rotational hardening laws are included in the dissipation function as kinematic constraints in the form:

$$\begin{aligned}
&d'\left(\dot{\alpha}_p,\dot{\alpha}_q,\beta,\dot{\beta},p_0,\dot{p}_0\right)=d\left(\dot{\alpha}_p,\dot{\alpha}_q,\beta,p_0\right)+\Lambda_1 c_1+\Lambda_2 c_2=\\
&=\frac{p_0}{2}\left[\sqrt{\left(\dot{\alpha}_p+\beta\dot{\alpha}_q\right)^2+\left(M^2-\beta^2\right)\dot{\alpha}_q^2}+\dot{\alpha}_p+\beta\dot{\alpha}_q\right]+\\
&+\Lambda_1\left[\dot{\beta}-c\left(\beta_b-\beta\right)\dot{\alpha}_q\right]+\Lambda_2\left(\dot{p}_0-p_0\frac{1+e_{in}}{\lambda-\kappa}\dot{\alpha}_p\right)
\end{aligned} \tag{6.62}$$

with d denoting the dissipation function of eq. (6.13) and Λ_1 and Λ_2 being the lagrangian multipliers. From eq. (6.62) the dissipative generalised stresses can be calculated as:

$$\begin{aligned}
\chi_p &= \frac{\partial d'}{\partial \dot{\alpha}_p}=\frac{\partial d}{\partial \dot{\alpha}_p}-\Lambda_2\frac{1+e_{in}}{\lambda-\kappa}p_0\\
\chi_q &= \frac{\partial d'}{\partial \dot{\alpha}_q}=\frac{\partial d}{\partial \dot{\alpha}_q}-\Lambda_1 c\left(\beta_b-\beta\right)\\
\chi_{p_0} &= \frac{\partial d'}{\partial \dot{p}_0}=\Lambda_2\\
\chi_\beta &= \frac{\partial d'}{\partial \dot{\beta}}=\Lambda_1
\end{aligned} \tag{6.63}$$

The Ziegler's orthogonality principle and the dependence of the term ψ_1 of the

Gibbs free energy on the rotational variable β imply $\bar{\chi}_{p_0} = \chi_{p_0} = \Lambda_2 = 0$ and $\bar{\chi}_\beta = \chi_\beta = \Lambda_1 \neq 0$. The introduction of the kinematic constraints in the dissipation function produces the additional component of the generalised stresses χ_β and modifies the expression of the yield function in the generalised stresses, this latter becoming a surface in the tridimensional space $(\chi_p, \chi_q, \chi_\beta)$. Similarly to what done in the case of isotropic coupling, taking into account eq. (6.63) and recalling the definition of $\bar{\chi}_q$ and $\bar{\chi}_\beta$ in eq. (6.52) and the derivative of β with respect to the deviatoric plastic strain, it is convenient to define the generalised stress $\hat{\chi}_q$ such that

$$\begin{aligned} \hat{\chi}_q = \frac{\partial d}{\partial \dot{\alpha}_q} = \chi_q + \chi_\beta c\left(\beta_b - \beta\right) = \chi_q + \chi_\beta \frac{\partial \beta}{\partial \alpha_q} = \\ = -2\frac{\partial \psi_1}{\partial \beta}\frac{\partial \beta}{\partial \alpha_q} + q = 2\chi_q - q \end{aligned} \tag{6.64}$$

This position allows for the derivation of the same elliptical yield surface employed till now, where the term $\hat{\chi}_q$ substitutes for χ_q in eq. (6.14). In the $\chi_p - \hat{\chi}_q$ plane the yield surface reads:

$$f\left(\chi_p, \hat{\chi}_q, \beta, p_0\right) = \left(\hat{\chi}_q - \beta\chi_p\right)^2 - \left(M^2 - \beta^2\right)\chi_p\left(p_0 - \chi_p\right) = 0 \tag{6.65}$$

Subsequently, by substitution of eq. (6.64) in eq. (6.65), one obtains the equation of the yield surface in the generalised space $(\chi_p, \chi_q, \chi_\beta)$ as follow:

$$\begin{aligned} f\left(\chi_p, \chi_q, \chi_\beta, \beta, p_0\right) = \left[\chi_q + \chi_\beta c\left(\beta_b - \beta\right) - \beta\chi_p\right]^2 + \\ - \left(M^2 - \beta^2\right)\chi_p\left(p_0 - \chi_p\right) = 0 \end{aligned} \tag{6.66}$$

Analogously to the case of isotropic coupling, the yield function in terms of generalised stresses is no longer the original distorted ellipse proposed by Dafalias & Taiebat (2013) but becomes a more complicated 3D surface in the generalised space $(\chi_p, \chi_q, \chi_\beta)$. As a consequence, even the resulting yield function in the p-q plane modifies in comparison with the previous case SEPC1. The yield function in terms of stresses is derived by substitution of eq. (6.64) and the second of eq. (6.52) in eq. (6.65), though not reported here for the sake of conciseness.

Once the yield function in the dissipative generalised stresses is defined, according to eq. (5.20), its normal vector components times $\langle L \rangle$ define the direction of the rates of the internal variables, leading to an associated flow rule in the generalised space $(\chi_p, \chi_q, \chi_\beta)$:

$$\begin{aligned}\dot{\alpha}_p &= \langle L \rangle \frac{\partial f}{\partial \chi_p} \\ \dot{\alpha}_q &= \langle L \rangle \frac{\partial f}{\partial \chi_q} \\ \dot{\beta} &= \langle L \rangle \frac{\partial f}{\partial \chi_\beta}\end{aligned} \tag{6.67}$$

Once again, the third equation emerging from the flow rule in eq. (6.67) demonstrates that the rotational hardening rule is a direct result of the formulation when the technique of the lagrangian multipliers is adopted in the dissipation function. In fact, consider first the derivative of the yield surface with respect to the generalised stress χ_q:

$$\frac{\partial f}{\partial \chi_q} = 2\left[\chi_q + \chi_\beta c\left(\beta_b - \beta\right) - \beta\chi_p\right] = 2\left(\hat{\chi}_q - \beta\chi_p\right) = \frac{\partial f}{\partial \hat{\chi}_q} \tag{6.68}$$

Then, employing eq. (6.68) one can explicit the rate of the internal variable β as follow:

$$\begin{aligned}\dot{\beta} = \langle L \rangle \frac{\partial f}{\partial \chi_\beta} &= 2\langle L \rangle c\left(\beta_b - \beta\right)\left[\chi_q + \chi_\beta c\left(\beta_b - \beta\right) - \beta\chi_p\right] = \\ &= \langle L \rangle c\left(\beta_b - \beta\right)\frac{\partial f}{\partial \chi_q} = c\left(\beta_b - \beta\right)\dot{\alpha}_p\end{aligned} \tag{6.69}$$

that is exactly the rotational hardening rule of eq. (6.50). As expected, the flow rule in the stress space is neither associated with respect to the plastic strain rates, nor with respect to the irreversible ones. In fact, as already shown for the isotropic coupling, when the hardening rules are encapsulated in the dissipation function, the relationship between the normal direction to the yield surface in the p-q plane and the irreversible strain rates pointed out by Collins & Houlsby (1997) is no longer true. In order to assess this statement, specialising eq. (6.6) to the present case one can write:

$$\begin{aligned}\frac{\partial \hat{f}}{\partial p} &= \frac{\partial f}{\partial \chi_p}\frac{\partial \chi_p}{\partial p} + \frac{\partial f}{\partial \chi_q}\frac{\partial \chi_q}{\partial p} + \frac{\partial f}{\partial \chi_\beta}\frac{\partial \chi_\beta}{\partial p} \\ \frac{\partial \hat{f}}{\partial q} &= \frac{\partial f}{\partial \chi_p}\frac{\partial \chi_p}{\partial q} + \frac{\partial f}{\partial \chi_q}\frac{\partial \chi_q}{\partial q} + \frac{\partial f}{\partial \chi_\beta}\frac{\partial \chi_\beta}{\partial q}\end{aligned} \tag{6.70}$$

Multiplying the first of eq. (6.70) for the plastic multiplier $\langle L \rangle$ and recalling eq. (6.55), the flow rule in eq. (6.67) and noting that $\frac{\partial \chi_p}{\partial p} = 1$ and that from eq. (6.52) it results $\chi_q = \chi_\beta \frac{\partial \beta}{\partial \alpha_q} + q$ one can write:

$$\langle L\rangle \frac{\partial \hat{f}}{\partial p} = \dot{\alpha}_p + \frac{\partial \chi_q}{\partial p}\dot{\alpha}_q + \dot{\beta}\frac{\partial \chi_\beta}{\partial p} = \dot{\alpha}_p + \frac{\partial \chi_q}{\partial p}\dot{\alpha}_q + \frac{\partial \beta}{\partial \alpha_q}\dot{\alpha}_q \frac{\partial}{\partial p}\left[\left(\frac{\partial \beta}{\partial \alpha_q}\right)^{-1}(\chi_q - q)\right] =$$
$$= \dot{\alpha}_p + \frac{\partial \chi_q}{\partial p}\dot{\alpha}_q + \dot{\alpha}_q\frac{\partial \chi_q}{\partial p} = \dot{\alpha}_p - 2\frac{\partial^2 \psi_1}{\partial \alpha_q \partial p}\dot{\alpha}_q = \dot{\varepsilon}_v^p + 2\dot{\varepsilon}_v^c \tag{6.71}$$

Analogously, multiplying the second of eq. (6.70) for the plastic multiplier $\langle L\rangle$, recalling eq. (6.56) and noting that $\frac{\partial \chi_p}{\partial q} = 0$ the equation becomes:

$$\langle L\rangle \frac{\partial \hat{f}}{\partial q} = \frac{\partial \chi_q}{\partial q}\dot{\alpha}_q + \dot{\beta}\frac{\partial \chi_\beta}{\partial q} = \frac{\partial \chi_q}{\partial q}\dot{\alpha}_q + \frac{\partial \beta}{\partial \alpha_q}\dot{\alpha}_q \frac{\partial}{\partial q}\left[\left(\frac{\partial \beta}{\partial \alpha_q}\right)^{-1}(\chi_q - q)\right] =$$
$$= \frac{\partial \chi_q}{\partial q}\dot{\alpha}_q + \dot{\alpha}_q\left(\frac{\partial \chi_p}{\partial q} - 1\right) = \dot{\alpha}_q\left(1 - 2\frac{\partial^2 \psi_1}{\partial \alpha_q \partial q}\right) = \dot{\varepsilon}_s^p + 2\dot{\varepsilon}_s^c \tag{6.72}$$

Therefore, the normal direction to the yield surface in the stress space does not coincide neither with the direction of the plastic strain rates nor with the direction of the irreversible ones.

Finally, imposing the consistency on the yield surface in eq. (6.65) one obtains:

$$\begin{aligned}
\dot{f} &= \frac{\partial f}{\partial \chi_p}\dot{\chi}_p + \frac{\partial f}{\partial \hat{\chi}_q}\dot{\hat{\chi}}_q + \frac{\partial f}{\partial \beta}\dot{\beta} + \frac{\partial f}{\partial p_0}\dot{p}_0 = \\
&= \frac{\partial f}{\partial \chi_p}\dot{p} + \frac{\partial f}{\partial \hat{\chi}_q}\left(\frac{\partial \hat{\chi}_q}{\partial p}\dot{p} + \frac{\partial \hat{\chi}_q}{\partial q}\dot{q} + \frac{\partial \hat{\chi}_q}{\partial \beta}\dot{\beta}\right) + \frac{\partial f}{\partial \beta}\dot{\beta} + \frac{\partial f}{\partial p_0}\dot{p}_0 = \\
&= \left(\frac{\partial f}{\partial \chi_p} + \frac{\partial f}{\partial \hat{\chi}_q}\frac{\partial \hat{\chi}_q}{\partial p}\right)\dot{p} + \frac{\partial f}{\partial \hat{\chi}_q}\frac{\partial \hat{\chi}_q}{\partial q}\dot{q} + \left(\frac{\partial f}{\partial \hat{\chi}_q}\frac{\partial \hat{\chi}_q}{\partial \beta} + \frac{\partial f}{\partial \beta}\right)\dot{\beta} + \frac{\partial f}{\partial p_0}\dot{p}_0 = \\
&= \left(\frac{\partial f}{\partial \chi_p} + \frac{\partial f}{\partial \hat{\chi}_q}\frac{\partial \hat{\chi}_q}{\partial p}\right)\dot{p} + \frac{\partial f}{\partial \hat{\chi}_q}\frac{\partial \hat{\chi}_q}{\partial q}\dot{q} + \left(\frac{\partial f}{\partial \hat{\chi}_q}\frac{\partial \hat{\chi}_q}{\partial \beta} + \frac{\partial f}{\partial \beta}\right)\langle L\rangle\, c\,(\beta_b - \beta)\frac{\partial f}{\partial \chi_q} + \\
&+ \frac{\partial f}{\partial p_0}\frac{\partial p_0}{\partial \alpha_p}\langle L\rangle \frac{\partial f}{\partial \chi_p} = 0
\end{aligned} \tag{6.73}$$

where, again, the rate of the hardening variables β and p_0 are reported in eqs. (6.50) and (4.6), respectively. The plastic multiplier can be specified from eq. (6.73) as follow:

$$L = -\frac{\left(\frac{\partial f}{\partial \chi_p} + \frac{\partial f}{\partial \hat{\chi}_q}\frac{\partial \hat{\chi}_q}{\partial p}\right)\dot{p} + \frac{\partial f}{\partial \hat{\chi}_q}\frac{\partial \hat{\chi}_q}{\partial q}\dot{q}}{\left(\frac{\partial f}{\partial \hat{\chi}_q}\frac{\partial \hat{\chi}_q}{\partial \beta} + \frac{\partial f}{\partial \beta}\right)c\,(\beta_b - \beta)\frac{\partial f}{\partial \chi_q} + \frac{\partial f}{\partial p_0}\frac{\partial p_0}{\partial \alpha_p}\frac{\partial f}{\partial \chi_p}} \tag{6.74}$$

with the derivatives assuming the expressions:

$$\begin{aligned}\frac{\partial \hat{\chi}_q}{\partial p} &= 2\frac{\partial \chi_q}{\partial p} \\ \frac{\partial \hat{\chi}_q}{\partial q} &= 2\frac{\partial \chi_q}{\partial q} - 1 \\ \frac{\partial \hat{\chi}_q}{\partial \beta} &= 2\frac{\partial \chi_q}{\partial \beta}\end{aligned} \tag{6.75}$$

$$\frac{\partial f}{\partial \chi_p} = -2\beta\hat{\chi}_q - M^2 p_0 + 2M^2\chi_p + \beta^2 p_0 \tag{6.76}$$

$$\frac{\partial f}{\partial \hat{\chi}_q} = \frac{\partial f}{\partial \chi_q} = 2\hat{\chi}_q - 2\beta\chi_p \tag{6.77}$$

$$\frac{\partial f}{\partial \beta} = -2\chi_p\hat{\chi}_q + 2\beta p_0\chi_p \tag{6.78}$$

$$\frac{\partial f}{\partial p_0} = -M^2\chi_p + \beta^2\chi_p \tag{6.79}$$

6.4 Response of the model

In this section the effects of the elastoplastic coupling within the hyper-elastoplastic formulation of the Dafalias & Taiebat (2013) model are illustrated by a series of numerical simulations. First, the response of the model with the isotropic coupling via the preconsolidation pressure is presented followed by the anisotropic coupling via the rotational variable β. For both forms of coupling the response of the model is shown with reference to the case in which the dissipation function does not include the kinematic constraints (SEPC1) and the case in which the new proposed dissipation function *d'* is considered (SEPC2). In addition, aiming at comparing the results to those that would be obtained for the elastoplastic coupling within the framework of classical elastoplasticity, the terms $\frac{\partial \psi_1}{\partial \alpha_p}$ and $\frac{\partial \psi_1}{\partial \alpha_q}$, naturally arising in hyperplasticity, and the generalised stresses χ_{p_0} and χ_β are neglected, thus leading to a form of coupling in which this latter solely affects the elastic response of the model. The consequent formulation corresponds to what originally proposed by Hueckel and Maier in their works. It represents a weak form of coupling that is not thermodynamically consistent, thus indicated in the following as "weak elastoplastic coupling" (WEPC). In the case of the anisotropic elastoplastic coupling, the weak form coincides, except for the rotational hardening rule, to the model developed in chapter 4.

In order to highlight the consequences of the elastoplastic coupling on the flow

rule and on the shape of the yield surface, the yield loci in the generalised stress space and in the stress space and the plastic strain rate vectors are plotted. Furthermore, the effect of the parameters and the internal variables on the response of the model are investigated. In addition, simulations of drained triaxial tests are performed to identify the effect of coupling on the plastic regime and finally the evolution of the elastic stiffness and the stiffness anisotropy due to the development of plastic strains are explored.

6.4.1 Isotropic elastoplastic coupling via the preconsolidation pressure

The dependence of the Gibbs free energy on the preconsolidation pressure is introduced by the term $\left(\frac{p_r}{p_0}\right)^r$ as reported in eq. (6.9). This term clearly shows that the effect of coupling depends both on the parameter r and on the current value of the preconsolidation pressure. The influence of the exponent r is limited since, according to Viggiani & Atkinson (1995), generally varies from 0.2 to 0.3 for plasticity index between 0 and 60 and for $r = 0$ the elastoplastic coupling vanishes. The parameters of the model are shown in table (6.2).

Parameter	Value
p_r	100
n	0.78
k	296.1
g	177.7
M	1.08
λ	0.143
κ	0.025
e_{in}	0.8
r	0.3

Table 6.2: *Model parameters*

In the case of weak coupling it is only the elastic regime to be modified by the plastic bahaviour, thus the flow rule is associated in the stress space and the yield surface is the original distorted ellipse of the Dafalias & Taiebat (2013) model. When a thermodynamically based elastoplastic coupling is introduced, the flow rule is no longer associated in the stress space as the shape of the yield surface modifies by

virtue of the additional term $\frac{\partial \psi_1}{\partial \alpha_p}$ in the generalised stress χ_p in eq. (6.12). Figure (6.1) shows the yield surface in the generalised space and in the stress space for $p_0 = 80\,\text{kPa}$ and, under the hypothesis of coaxiality of the principal strain and stress directions, the plastic strain rates vectors for the formulation developed in section 6.2.1 (SEPC1). As the component χ_p does not coicide with the mean pressure p while $\chi_q = q$, in the stress space the yield surface is stretched along the p-axis.

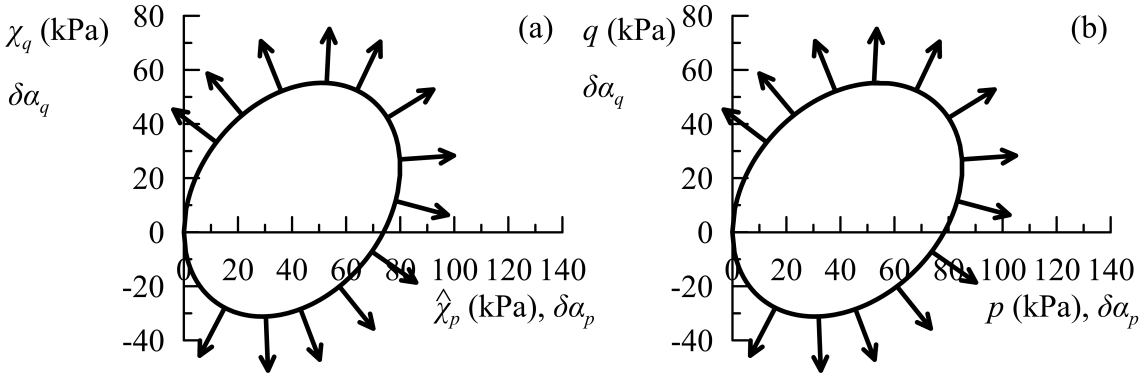

Figure 6.1: *Yield surfaces for the case SEPC1* ($p_0 = 80\,\text{kPa}$, $\beta = 0.3$)

The difference in shape between the yield surfaces in the generalised stress space and in the stress space increases if the kinematic constraints are accounted for in the dissipation function (SEPC2), as the additional generalised stresses χ_{p_0} appears. For the same preconsolidation pressure $p_0 = 80\,\text{kPa}$ the yield loci are depicted in figure (6.2). Note that the yield surface is the original distorted ellipse of the Dafalias & Taiebat (2013) model in the generalised stress plane $(\hat{\chi}_p, \chi_q)$ and in the same plane the flow rule is by definition associated, while it is non-associated in the p-q plane.

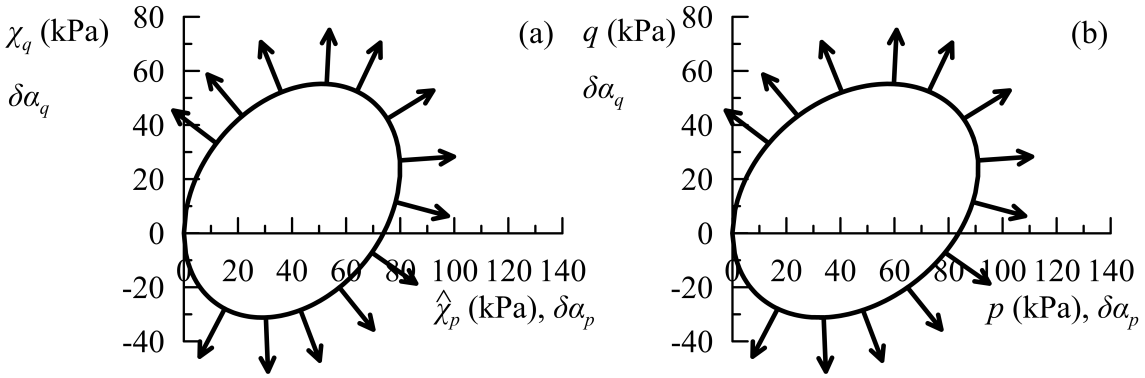

Figure 6.2: *Yield surfaces for the case SEPC2* ($p_0 = 80\,\text{kPa}$, $\beta = 0.3$)

Furthermore, eq. (6.12) suggests that χ_p and χ_{p_0} depend on the hyperelastic parameters k, g and n. In detail, for increasing values of k and g, χ_p tends towards

the value of p and χ_{p_0} tends to zero. In other words, for the same test conditions, the effects of elastoplastic coupling becomes more evident when the elastic stiffness decreases. To demonstrate this statement, figure (6.3) depicts the yield surfaces in the $\hat{\chi}_p - \chi_q$ plane and in the p-q plane for the case of SEPC2, $p_0 = 50\,\text{kPa}$ and for $k = 100$ and $g = 70$. A remarkable difference is evident when the graphs (a) and (b) of figure (6.3) are compared, highlighting that the smaller the values of the elastic parameters the larger is the modification of the shape of the yield surface. Therefore, the elastoplastic coupling involves a non-associated flow rule and a change in shape of the yield surface in the stress space, even though the direction of plastic strain rates is not dramatically different from the direction of the normal vector to the surface.

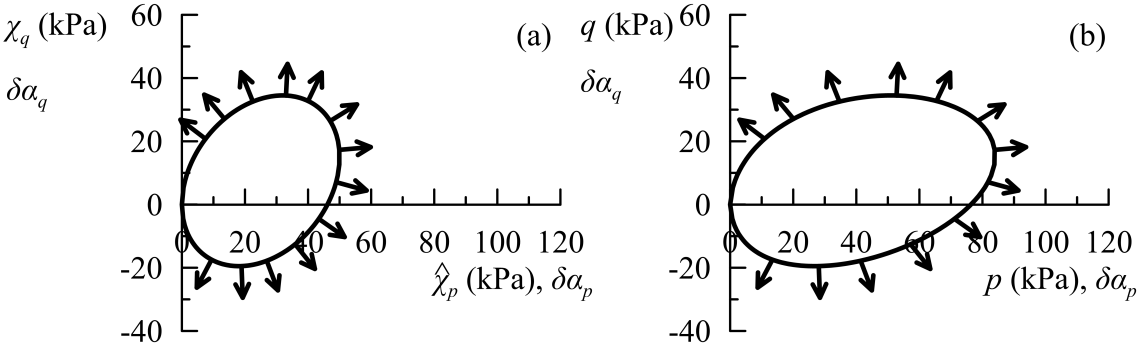

Figure 6.3: *Yield surfaces for the case SEPC2* ($p_0 = 50\,\text{kPa}$, $\beta = 0.3$, $k = 100$, $g = 70$)

In the case of weak coupling the plastic response corresponds to that of the uncoupled version of the model as the elastoplastic coupling affects solely the elastic behaviour. Conversely, the strong coupling modifies the plastic regime, as depicted in figure (6.4) for the simulation of a stress controlled drained triaxial test. The model parameters are reported in table (6.2), with the asymptotic value of the rotational variable β calculated using the linear law in eq. (4.8), with $c = 50$ and $x = 2$. From the numerical analysis clearly emerges that by taking into account the hardening rules in the dissipation function through the technique of lagrangian multipliers (SEPC2) results in a stronger form of coupling. Again, the thermodynamically based coupling is characterised by a different shape of the yield surface, as shown in figure (6.4), and a non-associated flow rule in the stress space. These two aspects are the main responsible for the different stress-strain responses observed in the numerical tests.

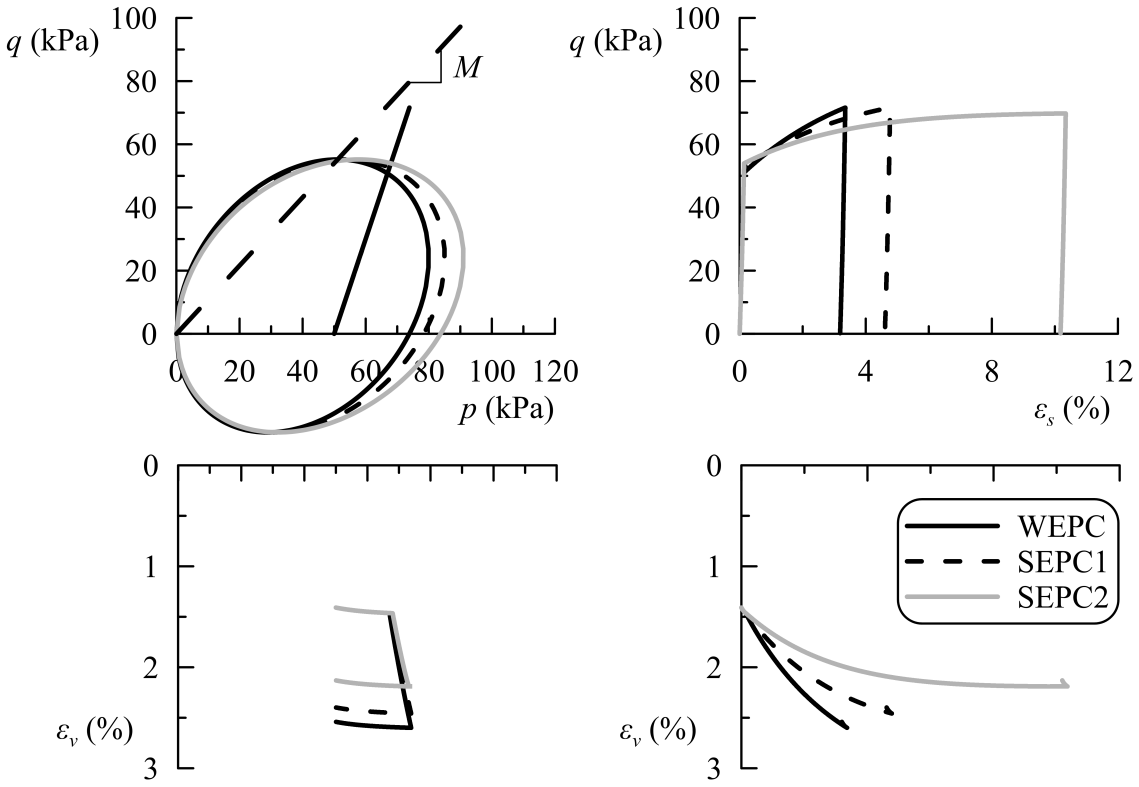

Figure 6.4: *Drained triaxial test* ($p_{in} = 50\,\text{kPa}$, $p_{0,in} = 80\,\text{kPa}$, $\beta_{in} = 0.3$)

Finally, the effect of elastoplastic coupling on the elastic response is investigated. The presence of the preconsolidation pressure in the term ψ_1 of the Gibbs free energy modifies the values of the elastic stiffnesses and introduces a dependence of these latter on the volumetric plastic strain by virtue of the isotropic hardening rule of eq. (4.6). An isotropic stress path has been performed till reaching values of the mean effective pressure significantly high such that volumetric plastic strains are developed. During the simulation the elastic shear and bulk moduli G and K are calculated and the evolution of the current moduli normalised with respect to the initial values at the beginning of the test is plotted with p in figure (6.5). To isolate the effect of the preconsolidation pressure on the elastic stiffness, the hyperelastic formulation is specialised to the linear case ($n = 0$); in such a way the effect of the nonlinear dependence of the stiffness with the stress state is not considered and the variation of the moduli is uniquely due to the elastoplastic coupling. The parameters are those summarised in table (6.2), eccept for $k = 100$, $g = 70$ and $n = 0$.

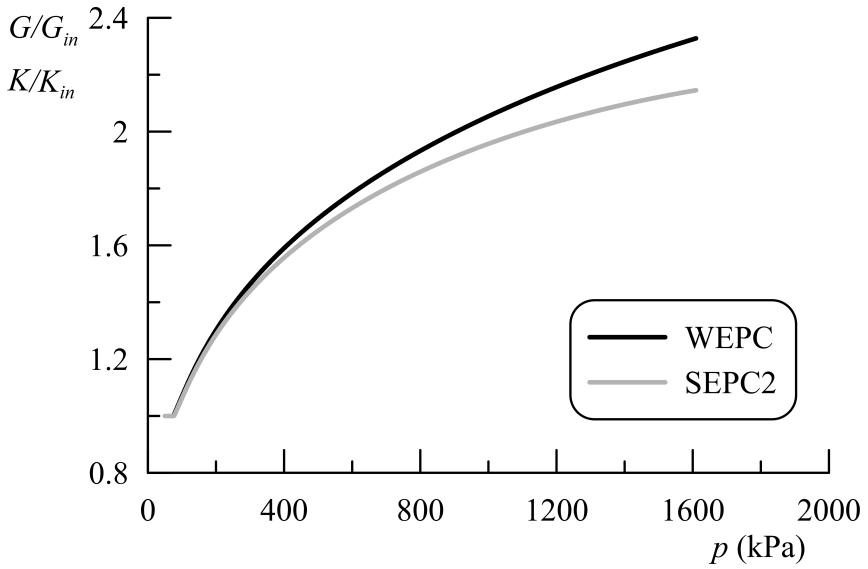

Figure 6.5: *Evolution of elastic stiffness along isotropic stress path* ($p_{in} = 50\,\text{kPa}$, $p_{0,in} = 80\,\text{kPa}$, $\beta_{in} = 0.3$)

It is worth noting that as the term $\left(\frac{p_r}{p_0}\right)^r$ multiplies the whole elastic Gibbs free energy, the effect of the preconsolidation pressure acts in the same way on each component of the elastic stiffness tensor, thus the curves for $\frac{K}{K_{in}}$ and $\frac{G}{G_{in}}$ coincide. As expected with reference to the typical experimental results shown in chapter 1 for clays, the elastic stiffness increases as the preconsolidation pressure increases. Furthermore, when the preconsolidation pressure significantly increases the elastic stiffnesses tend to stabilise as the term $\left(\frac{p_r}{p_0}\right)^r$ reaches an asymptotic value. From figure (6.5) also emerges a different elastic response whether a weak or a strong form of coupling is considered. In fact, within the framework of hyper-elastoplasticity the coupling alters the response in the plastic regime, which in turn modifies the elastic behaviour. This effect of coupling is more evident if the approach based on the kinematic constraints is adopted within the dissipation function.

Finally, to show how the proposed formulation is able to take into account the dependence of the elastic stiffness of clays on the preconsolidation pressure, a comparison is made between the predictions of the model for the case of SEPC2 and the observed behaviour of the reconstituted Vallericca clay (Rampello *et al.* (1997)). As described in chapter 1, the samples were loaded and unloaded along radial stress paths and during the compression stages bender element measurements were performed. In particular, figure (1.4) depicts the elastic shear modulus for the radial stress path characterised by $\eta = 0.3$ starting from an initial mean effective pressure $p_{in} = 50\,\text{kPa}$. The simulations are conducted considering the Cam Clay ellipse with a preconsolidation pressure $p_0 = 100\,\text{kPa}$, neglecting the rotational hardening of

the model ($\beta = 0$, $\dot{\beta} = 0$) . The material is characterised by an initial void ratio $e_{in} = 1.05$ and by the set of parameters reported in table (6.3).

Parameter	Value
p_r	100
n	0.56
k	700
g	430
M	0.8
λ	0.148
κ	0.03
r	0.35

Table 6.3: *Model parameters for the reconstituted Vallericca clay*

The values of the constants λ and κ are those reported by Rampello *et al.* (1997). The graph (a) of figure (6.6) depicts the sequence of the compression states followed in the numerical simulations and the graph (b) the evolution of the elastic shear modulus together with the experimental data. This latter shows that the model is able to satisfactorily mimic the dependence of the elastic stiffness on the previous stress history experienced by the material.

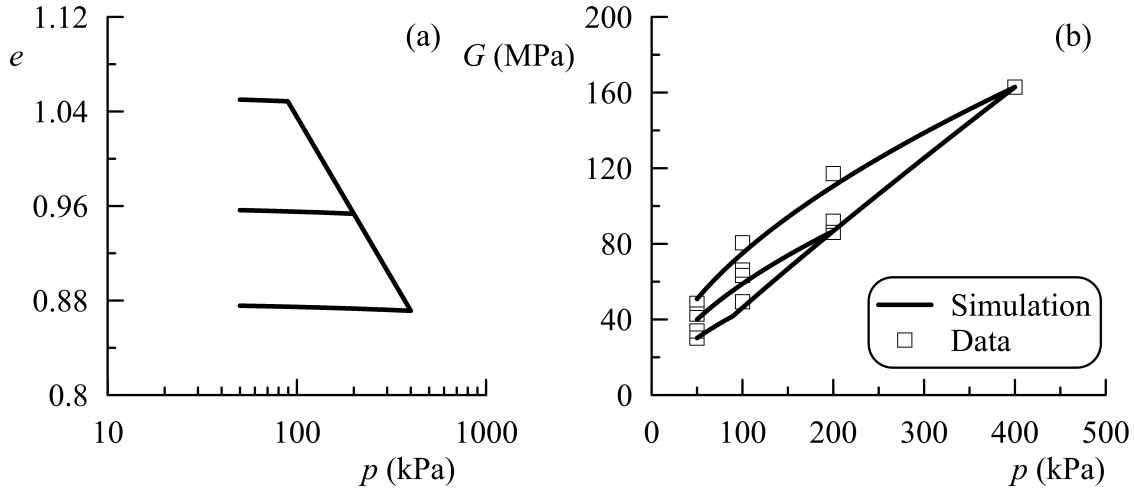

Figure 6.6: *Sequence of compression states* (a) *and elastic shear modulus* (b) *for radial stress path* $\eta = 0.3$ *for the reconstituted Vallericca clay*

6.4.2 Anisotropic elastoplastic coupling via the fabric tensor

The elastoplastic coupling on the directional properties of clays is introduced by a dependence of the term ψ_1 of the Gibbs free energy on the rotational hardening variable β for a transverse isotropic material. From eq. (6.52) follows that, similarly to the case of the preconsolidation pressure, the elastoplastic coupling depends on the elastic stiffness. In fact, as k and g increase, χ_q tends to the value of q and χ_β decreases. Furthermore, it clearly emerges that the effect of coupling on the plastic response depends on the current value of the rotational variable β and on the difference between its bounding value β_b and β. The higher are these entities the more intense is the coupling, while for $\beta = 0$ or whenever $\beta_b - \beta = 0$ the generalised stress $\chi_q = q$ and the weak form of coupling is recovered. In order to clarify these results, the effects of these internal variables on the shape of the yield surface in the stress space are illustrated. The parameters of the model are listed in table (6.4).

Parameter	Value
p_r	100
k	296.1
g	177.7
M	1.08
λ	0.143
κ	0.025
e_{in}	0.8

Table 6.4: *Model parameters*

In figure (6.7) the yield loci in the generalised stress $\chi_p - \hat{\chi}_q$ plane and in the p-q plane for the three possible forms of coupling are plotted for $\beta = 0.4$, $\beta_b = 0.2$, $c = 100$ and $p_0 = 80\,\text{kPa}$. As expected, the weak form does not modify neither the shape of the surface with respect to the distorted ellipse by Dafalias & Taiebat (2013), nor the flow rule in the stress space. Conversely, the coupling within the framework of hyperplasticity produces a change of shape of the yield surface in the stress space, as the generalised stress χ_q (and even more $\hat{\chi}_q$) does no longer coincide with the deviatoric stress q. Therefore, the yield locus in the stress space is distorted along the q-axis and consequently the flow rule will be non-associated with respect to the plastic strain rates, while will be associated in the generalised stress space. These effects are more evident whenever the dissipation function is modified by adding of the hardening rules via the lagrangian multipliers (SEPC2).

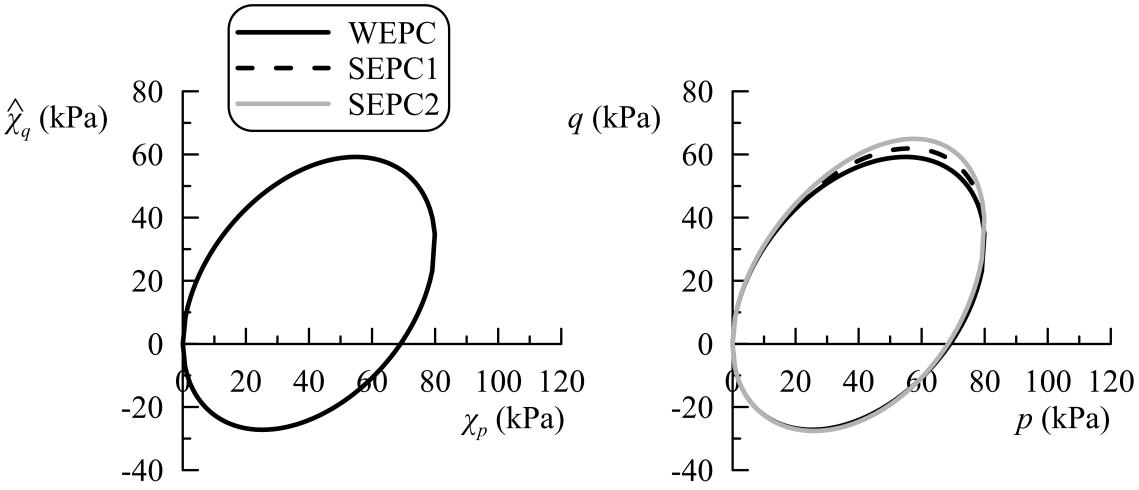

Figure 6.7: *Yield surfaces in the generalised stress and stress spaces for* $\beta = 0.4$ *and* $\beta_b = 0.2$

To highlight the effect of the current rotation of the yield surface on the coupling, the yield loci are represented in figure (6.8) for $\beta = 0.6$ and $\beta_b = 0.4$, for the same parameters and preconsolidation pressure of above. Note that both β and β_b are increased, such that the difference $\beta_b - \beta = 0.2$ is identical to the case of figure (6.7). Nevertheless, the shape of the yield surfaces in the stress space shows bigger modifications as compared to that of the previous case, as the yield surface in the generalised stress space is characterised by a higher rotation.

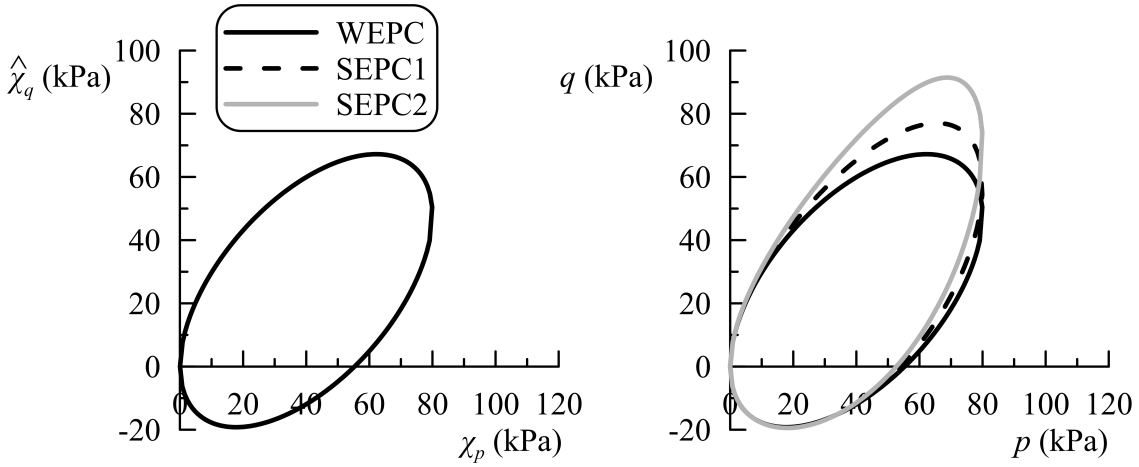

Figure 6.8: *Yield surfaces in the generalised stress and stress spaces for* $\beta = 0.6$ *and* $\beta_b = 0.4$

Subsequently the bounding value is set to $\beta_b = 0.3$ with the same $\beta = 0.6$, such that the difference $\beta_b - \beta = 0.3$. Figure (6.9) shows that this produces a further change of the yield surface in the p-q plane as compared to figure (6.8).

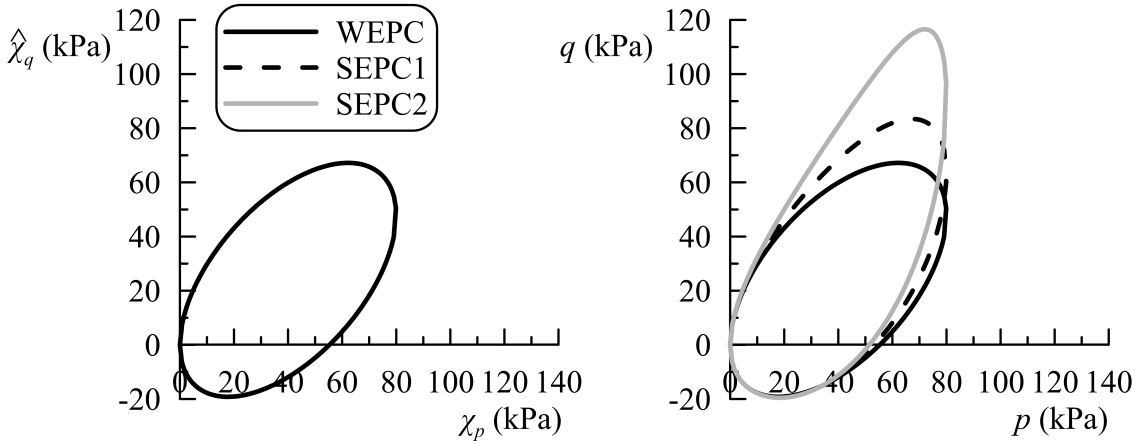

Figure 6.9: *Yield surfaces in the generalised stress and stress spaces for* $\beta = 0.6$ *and* $\beta_b = 0.3$

Limiting the attention to the case of strong coupling with the dissipation function enriched by the kinematic constraints (SEPC2), figure (6.10) depicts the plastic strain rate vectors under the hypothesis of coaxiality on the yield surfaces in the generalised space and in the stress space. It clearly emerges that the flow rule is no longer associated in the p-q plane but is, by definition, associated in the $\chi_p - \hat{\chi}_q$ one.

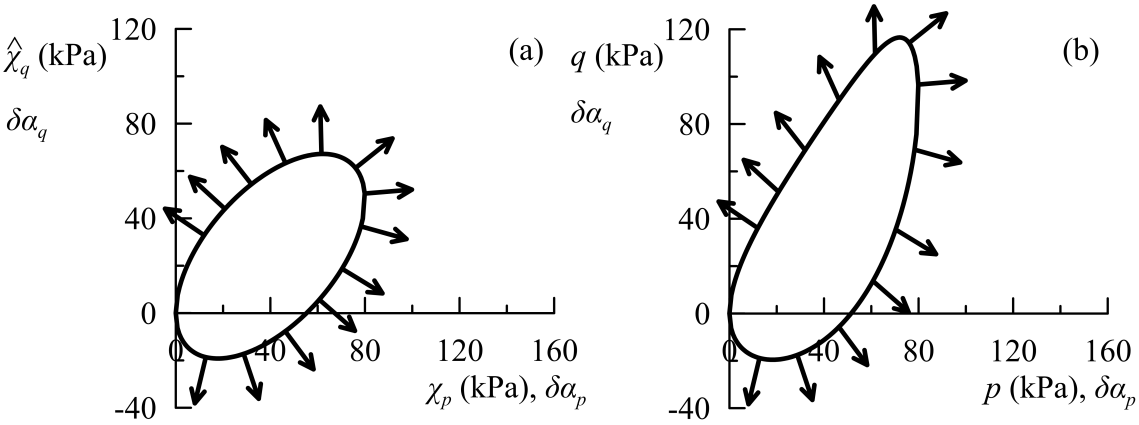

Figure 6.10: *Yield surfaces in the generalised stress and stress spaces for* $\beta = 0.6$ *and* $\beta_b = 0.3$ *for SEPC2*

To illustrate the effect of elastoplastic coupling on the plastic response of the model, a radial stress path characterised by $\eta = 0.8$ and an initial mean effective pressure $p_{in} = 20\,\text{kPa}$ is performed. The weak coupling does not modify the behaviour in the plastic regime while the response changes if the thermodynamically consistent forms of coupling are considered. The results of the simulations are shown in figure (6.11) for the three forms of coupling, while the initial yield surfaces are

depicted in the p-q plane. The model parameters are listed in table (6.4) and the bounding value β_b is determined using the linear law in eq. (4.8) with $c = 100$ and $x = 2$.

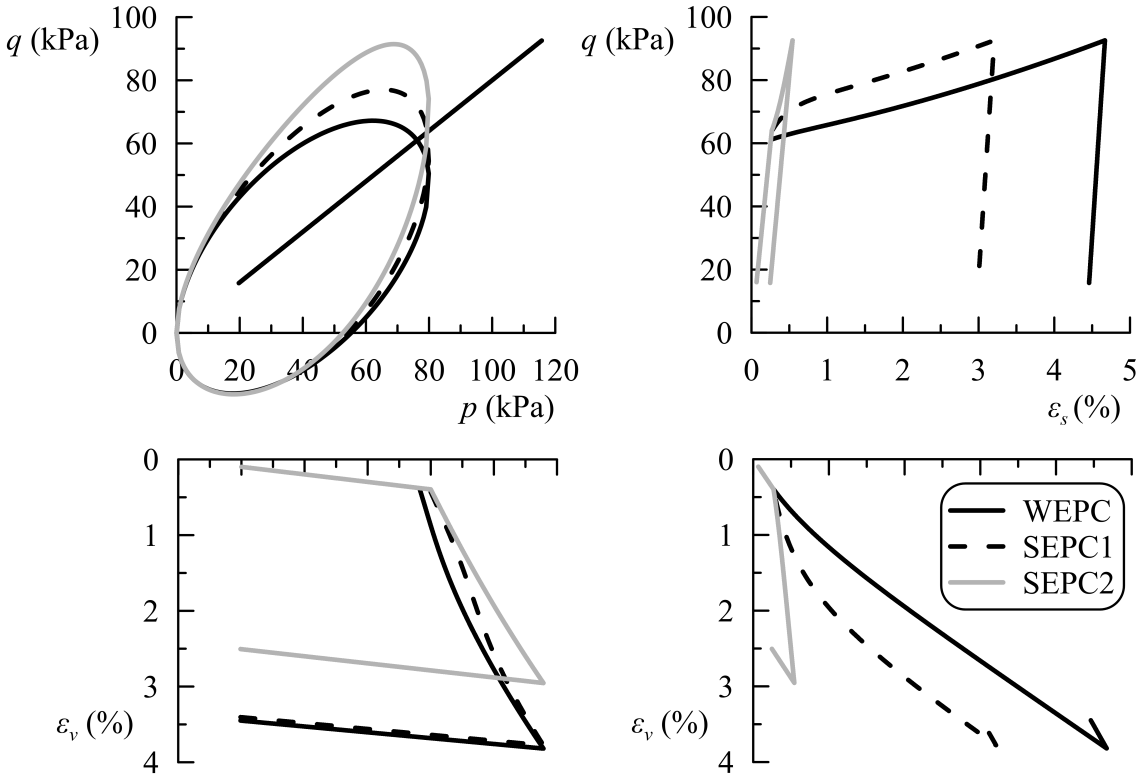

Figure 6.11: *Simulation for radial stress path* ($\eta = 0.8$, $p_{in} = 20\,\text{kPa}$, $p_{0,in} = 80\,\text{kPa}$, $\beta_{in} = 0.6$)

The effect of the elastoplastic coupling on the elastic response is now discussed. Unlike the case of preconsolidation pressure, this coupling involves a tensorial entity controlling not only the intensity of the elastic stiffness but also its directional properties. In order to illustrate the evolution of the elastic stiffness anisotropy once plastic strains occur, a numerical simulation has been performed following the stress path shown in figure (6.12) with $c = 100$ and $x = 1.35$. First a radial path characterised by $\eta = 0.8$ starting from $p_{in} = 50\,\text{kPa}$ is followed until β attains the asymptotic value β_b; this is followed by a p constant path until reaching $\eta = 0$ and at that point an isotropic stress path is prescribed. In such a way β increases from the initial value of 0.3 during the first phase and subsequently decreases till reaching zero. The same figure depicts the evolution of the yield surface during the test for the cases of WEPC and SEPC2.

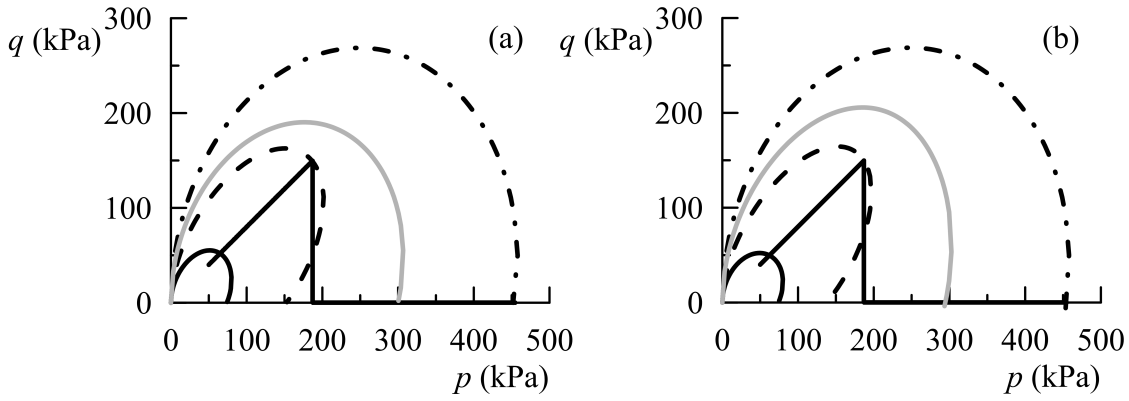

Figure 6.12: *Stress path and evolution of the yield surface for* (a) *WEPC and* (b) *SEPC2*

Since the elastic anisotropy depends on the rotational internal variable via eq. (4.32), a change in β determines a modification of the stiffness anisotropy. Specialising eq. (A.32) for $n = 0$ and for a transverse isotropic material, with 1 denoting the vertical direction and the other two defining the horizontal plane of isotropy and using eq. (4.33), the Young's moduli along the vertical and horizontal direction E_v and E_h and the shear moduli G_{hh} and G_{vh} can be determined. In figure (6.13) the evolution of the ratios G_{hh}/G_{vh} and E_h/E_v with the mean effective pressure is illustrated for both cases of weak (WEPC) and strong coupling (SEPC2). The material is initially anisotropic, then the anisotropy ratio evolves according to the rotational hardening law as plastic deviatoric strains occur and at the end of the test, when $\beta \simeq 0$, the soil becomes approximately isotropic. Furthermore, as expected, a slightly different response is obtained if the weaker or the stronger form of coupling are adopted. In particular, it is worth noting that when the anisotropy ratio becomes approximately constant, i.e. β attains its bounding value β_b, the two forms of coupling lead to the same results.

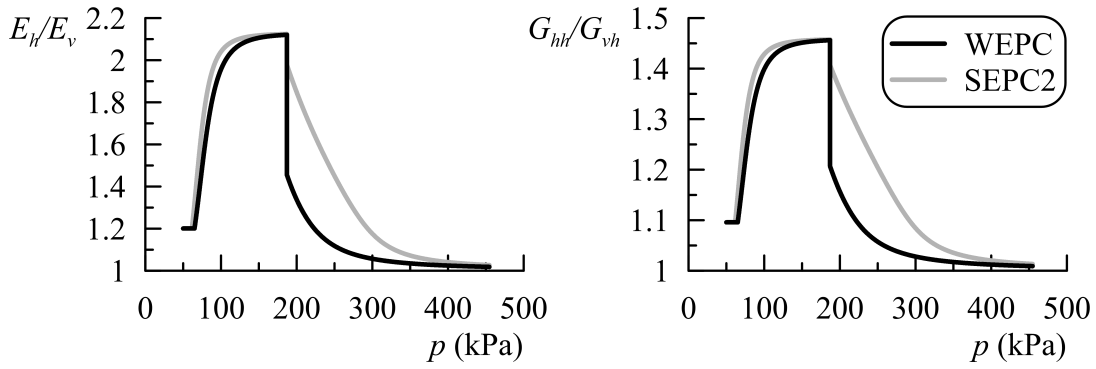

Figure 6.13: *Evolution of elastic stiffness anisotropy*

Finally, the hyper-elastoplastic model characterised by the SEPC2 form is em-

ployed in a back analysis of the experimental data carried out by Mitaritonna *et al.* (2014) on the Lucera clay. In particular, the evolution of the anisotropy ratio G_{hh}/G_{vh} observed along different radial stress paths (figure (1.20)) can be reproduced with the present formulation, as depicted in figure (6.14). The model parameters are those reported in table (6.4), except for the elastic constants $k = 888.3$ and $g = 533$, while for the rotational hardening rule the values $c = 250$ and $x = 1.86$ are assumed. It is worth noting that the parameter c controlling the pace of the rotation of the surface is significantly higher than the value employed for the calibration of the same experimental data in chapter 4; this is due to the fact that the rotational hardening law employed here (eq. (6.51)) is different from that of eq. (4.20). Nonetheless, even the present model is capable to satisfactorily predict the evolution of the elastic stiffness anisotropy.

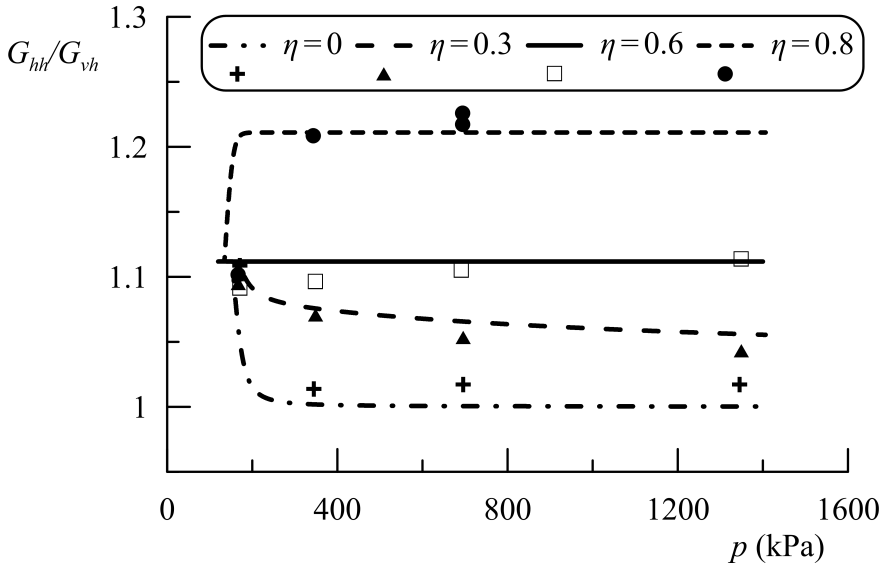

Figure 6.14: *Evolution of elastic stiffness anisotropy for Lucera clay*

In this chapter two forms of elastoplastic coupling have been proposed to reproduce, within a thermodynamically consistent framework, the evolution of the elastic stiffness and the small strain anisotropy with the plastic strains typically observed in clays . The first one has been achieved by a dependence of the elastic formulation on the preconsolidation pressure and the second one by a dependence on the rotational internal variable. The use of hyperplasticity theory allows to take into account a stronger form of coupling in which this latter not only affect the elastic response but also the plastic regime. In particular the elastoplastic coupling produces a change of shape of the yield surface in the stress space as compared to an uncoupled material and as a consequence the flow rule is no longer associated. These features are

impossible to be reproduced within the framework of classical elastoplasticity. The two couplings of above have been explored for both cases in which the dissipation function is enriched or not by the hardening rules of the hyper-elastoplastic version of the Dafalias & Taiebat (2013) model using the technique of lagrangian multipliers. If the kinematic constraints are included in the dissipation a stronger form of coupling is obtained, different from that examined by Collins, Houlsby and Puzrin in their works. Finally the derived formulations have been explored by numerical simulations to highlight the effects of elastoplastic coupling on both the elastic and plastic responses.

Conclusions

The thesis deals with the constitutive modelling of geomaterials from a thermodynamic perspective. As discussed in chapter 1, the mechanical behaviour of soils is characterised, even for small strain levels, by a remarkable nonlinearity and anisotropy due to the current strain/stress state and to the microstructural properties of the material. Furthermore, at least for clays, the small strain behaviour, usually modelled as elastic, depends on the past stress history experienced by the material, thus on its plastic response. These features are commonly referred to as elastoplastic coupling. Some experimental data from the literature show that the small strain stiffness depends on the plastic strains through the preconsolidation pressure and the elastic stiffness anisotropy evolves as plastic strains occur in the material. New formulations have been developed in this study to reproduce the above mentioned mechanical features of soils.

Firstly, a nonlinear hyperelastic anisotropic model has been formulated. The anisotropic character of soils is introduced by a symmetric second order fabric tensor that condenses all scalar and directional information pertaining to the anisotropy of the material. According to the representation theorems for isotropic scalar functions, the definition of a free energy potential as function of a series of mixed invariants of the stress/strain and fabric tensors permits to model the permanent anisotropic characteristics of soils in a thermodynamically consistent way. The proposed formulation can reproduce the nonlinear dependence of the elastic stiffness on the current stress, including both the inherent and stress/strain induced anisotropy. The second order fabric tensor restricts the material symmetry to orthotropy and depending on its eingenvalues the formulation can be specialised to a transverse isotropic or isotropic material. Also, by a proper choice of the parameters, the linear case can be recovered. Therefore, the model encompasses most of the existing elastic formulations and since both the stress and strain energy are defined it allows to derive the constitutive equations in both stiffness and compliance forms. The model is able to nicely reproduce the small strain response as observed in laboratory tests for both sandy and clayey soils.

Subsequently, the above hyperelastic formulation has been introduced in the single surface elastoplastic model for clays proposed by Dafalias & Taiebat (2013), characterised by isotropic and rotational hardening rules. In order to reproduce the evolution of the elastic stiffness anisotropy with plastic strains observed in clays, a relationship between the rotational internal variable, governing the anisotropy within the plastic regime and the fabric tensor defined with reference to the elastic response has been identified. In such a way the fabric tensor is no longer constant but evolves by virtue of the rotational hardening law of the model. This leads to a form of elastoplastic coupling in which the plastic regime affects the elastic response of the model. The consequent formulation is able to mimic, with solely one extra parameter to be calibrated, the evolution of the elastic stiffness anisotropy along radial stress paths observed in laboratory tests for the reconstituted Lucera clay. Clearly, a possible drawback of the proposed formulation is that the above relationship was empirically determined on the base of a specific set of experimental data. Nonetheless, this part of the thesis results in an original weak form of elastoplastic coupling for clays.

The main limitation in developing elastoplastic coupling within the framework of classical elastoplasticity is that, besides not guaranteeing the respect of the laws of thermodynamics, solely the elastic response of the model is influenced by the coupling, therefore leading to a "one way" form of coupling. In the last two chapters of the thesis a thermodynamically based constitutive framework has been adopted to model the mechanical behaviour of clays. According to the hyperplastic theory for rate independent materials, mainly based on the works by Collins, Houlsby and Puzrin, for isothermal processes and under the fundamental assumption of orthogonality condition, any constitutive model can be formulated by the definition of two scalar functions: the free energy potential and the dissipation function or alternatively the yield one. Within this theoretical framework the Dafalias & Taiebat (2013) model has first been reformulated for triaxial conditions for an uncoupled material, for both associated and non-associated flow rule. For the first case, apart from the elastic regime, the original formulation proposed by Dafalias & Taiebat (2013) is recovered. The non-associated flow rule is introduced by imposing a dependence of the dissipation function on the stress, similarly to what done by Collins & Hilder (2002) and Coombs (2017) for a wider class of single surface anisotropic models. This leads to a modification of the shape of the yield surface in the stress space with respect to the distorted ellipse of the original elastoplastic model. The main difference between the proposed formulation and the existing ones is that the isotropic hardening law adopted here is characterised by the dependence of the pre-

consolidation pressure on the volumetric plastic strains only, consistently with the assumption made by Dafalias & Taiebat (2013). Furthermore, a more general form of dissipation function has been proposed to take into account the hardening rules of the model through the technique of the lagrangian multipliers. The performance of the model has been investigated through a series of numerical simulations of stress controlled drained triaxial test and the effect of the parameters and of the non-associated flow rule on the response has been highlighted.

In the last part of the research the hyper-elastoplastic formulation of the Dafalias & Taiebat (2013) model has been enriched to reproduce the evolution of the elastic stiffness with the plastic strains via the preconsolidation pressure and the evolution of the small strain stiffness anisotropy through the relationship introduced above between the rotational internal variable and the fabric tensor. The hyperplasticity theory allows to take into account a new stronger (two ways) form of coupling in which this latter not only affects the elastic response but also the plastic regime. The derived formulation allows to take into account the dependence of the elastic stiffness on the previous stress history experienced by the soil and to back-predict the evolution of the anisotropy ratio observed on the samples of Lucera clay. Furthermore, the thermodynamically consistent elastoplastic coupling determines a change of shape of the yield surface in the stress space with respect to the distorted ellipse and consequently a non-associated flow rule arises. Finally, the approach based on the kinematic constraints has been employed to develop an alternative form of coupling never pursued before, in which the dissipation function takes directly into account the hardening rules of the model. This technique leads to significantly different results than those obtained following the more traditional hyperplastic approach. Numerical simulations have been performed to clarify the effects of elastoplastic coupling on the overall response of the model.

After being implemented in FEM codes, the proposed formulations could be employed to analyse geotechnical boundary value problems, such as those related to tunnelling and deep excavations, in which the anisotropy of soils plays a relevant role. As an alternative, the model could be used to examine strain localisation related problems, for which the non-associativeness of the flow rule represents a crucial factor. At this scope, the hyper-elastoplastic formulation presented in this thesis should be extended to the generalised stress/strain space taking into account the tensorial character of the anisotropy and the rotational hardening variable.

Appendix A

In common with most works in continuum mechanics, in this thesis extensive use of tensors is made. The bold face (component-free) notation is preferred because more compact but in this section also the index notation is employed in order to clarify the tensor operations and in particular the derivatives. The notations set out by Chaves (2013), Holzapfel (2000) and Bigoni (2012) are principally followed.

In order to express the free energy in terms of the two strain invariants ε_v, ε_s or in terms of the stress invariants p and q starting from the multiaxial formulation and vice versa, the following identities are useful. Particulalry, in terms of strains, denoting with $\mathbf{e}$ the deviatoric part of the strain tensor, one can write:

$$\begin{aligned} &\mathrm{tr}\left(\boldsymbol{\varepsilon}\right) = \varepsilon_v \\ &\mathrm{tr}\left(\boldsymbol{\varepsilon}^2\right) = \mathrm{tr}\left(\mathbf{e}^2\right) + \frac{1}{3}\left(\mathrm{tr}\boldsymbol{\varepsilon}\right)^2 = \frac{3}{2}\varepsilon_s^2 + \frac{1}{3}\varepsilon_v^2 \end{aligned} \tag{A.1}$$

Analogously, for the stress tensor, denoting with $\mathbf{s}$ its deviatoric part, one obtains:

$$\begin{aligned} &\mathrm{tr}\left(\boldsymbol{\sigma}\right) = 3p \\ &\mathrm{tr}\left(\boldsymbol{\sigma}^2\right) = \mathrm{tr}\left(\mathbf{s}^2\right) + \frac{1}{3}\left(\mathrm{tr}\boldsymbol{\sigma}\right)^2 = \frac{3}{2}q^2 + 3p^2 \end{aligned} \tag{A.2}$$

The details of the derivatives of a second order tensor are shown with reference to the strain tensor $\boldsymbol{\varepsilon}$, but the procedure is obviously valid for any second order tensor. The derivative of the strain tensor with respect to itself is:

$$\frac{\partial \boldsymbol{\varepsilon}}{\partial \boldsymbol{\varepsilon}} = \frac{\partial \varepsilon_{ij}}{\partial \varepsilon_{kl}} = \delta_{ik}\delta_{jl} = \mathbf{I} \bar{\otimes} \mathbf{I} \tag{A.3}$$

The derivatives of two recursive invariants of the strain tensor are:

$$\frac{\partial \mathrm{tr}\left(\boldsymbol{\varepsilon}\right)}{\partial \boldsymbol{\varepsilon}} = \frac{\partial \varepsilon_{kk}}{\partial \varepsilon_{ij}} = \delta_{ij} = \mathbf{I} \tag{A.4}$$

and

$$\frac{\partial \mathrm{tr}\left(\boldsymbol{\varepsilon}^2\right)}{\partial \boldsymbol{\varepsilon}} = \frac{\partial \varepsilon_{kl}\varepsilon_{lk}}{\partial \varepsilon_{ij}} = 2\varepsilon_{ij} = 2\boldsymbol{\varepsilon} \tag{A.5}$$

Denoting with $\boldsymbol{\varepsilon}^T = \varepsilon_{ji}$ the transpose of $\boldsymbol{\varepsilon} = \varepsilon_{ij}$, the following derivative reads:

$$\frac{\partial \boldsymbol{\varepsilon}^T}{\partial \boldsymbol{\varepsilon}} = \frac{\partial \varepsilon_{ji}}{\partial \varepsilon_{kl}} = \delta_{jk}\delta_{il} = \mathbf{I} \underline{\otimes} \mathbf{I} \tag{A.6}$$

The symmetric part of the strain tensor is:

$$\boldsymbol{\varepsilon}^{sym} = \frac{1}{2}\left(\boldsymbol{\varepsilon} + \boldsymbol{\varepsilon}^T\right) = \frac{1}{2}\left(\varepsilon_{ij} + \varepsilon_{ji}\right) \tag{A.7}$$

As will be clear below, a relevant operation is the derivative of the symmetric part of the strain tensor with respect to $\boldsymbol{\varepsilon}$:

$$\frac{\partial \boldsymbol{\varepsilon}^{sym}}{\partial \boldsymbol{\varepsilon}} = \frac{\partial \varepsilon_{ij}^{sym}}{\partial \varepsilon_{kl}} = \frac{1}{2}\left(\delta_{ik}\delta_{jl} + \delta_{jk}\delta_{il}\right) = \mathbf{I} \underline{\otimes} \mathbf{I} \tag{A.8}$$

Then, considering the deviatoric part of the strain tensor, the derivative with respect to $\boldsymbol{\varepsilon}$ assumes the form:

$$\begin{aligned} \frac{\partial \mathbf{e}}{\partial \boldsymbol{\varepsilon}} &= \frac{\partial\left(\boldsymbol{\varepsilon} - \frac{1}{3}\mathrm{tr}\left(\boldsymbol{\varepsilon}\right)\mathbf{I}\right)}{\partial \boldsymbol{\varepsilon}} = \frac{\partial\left(\varepsilon_{ij} - \frac{1}{3}\varepsilon_{mm}\delta_{ij}\right)}{\partial \varepsilon_{kl}} = \\ &= \delta_{ik}\delta_{jl} - \frac{1}{3}\delta_{ij}\delta_{kl} = \mathbf{I} \underline{\otimes} \mathbf{I} - \frac{1}{3}\mathbf{I} \otimes \mathbf{I} \end{aligned} \tag{A.9}$$

For the anisotropic formulation, the following derivatives of the mixed invariants with respect to the strain are useful:

$$\frac{\partial \mathrm{tr}\left(\mathbf{a}\boldsymbol{\varepsilon}\mathbf{a}\right)}{\partial \boldsymbol{\varepsilon}} = \frac{\partial\left(a_{kl}\varepsilon_{lm}a_{mk}\right)}{\partial \varepsilon_{ij}} = \frac{1}{2}\left(a_{ki}a_{jk} + a_{kj}a_{ik}\right) = \frac{1}{2}\left[\mathbf{a}^2 + \left(\mathbf{a}^2\right)^T\right] \tag{A.10}$$

with $\mathbf{a}$ denoting the second order symmetric fabric tensor.

$$\begin{aligned} &\frac{\partial \mathrm{tr}\left[\left(\mathbf{a}\boldsymbol{\varepsilon}\mathbf{a}\right)^2\right]}{\partial \boldsymbol{\varepsilon}} = \frac{\partial\left(a_{kl}\varepsilon_{lm}a_{mn}a_{np}\varepsilon_{pq}a_{qk}\right)}{\partial \varepsilon_{ij}} = \\ &= \frac{1}{2}\left(a_{ki}a_{jn}a_{np}\varepsilon_{pq}a_{qk} + a_{kj}a_{in}a_{np}\varepsilon_{pq}a_{qk} + a_{kl}\varepsilon_{lm}a_{mn}a_{ni}a_{jk} + a_{kl}\varepsilon_{lm}a_{mn}a_{nj}a_{ik}\right) = \\ &= \frac{1}{2}\left(a_{ik}a_{kq}\varepsilon_{qp}a_{pn}a_{nj} + a_{in}a_{np}\varepsilon_{pq}a_{qk}a_{kj} + a_{in}a_{nm}\varepsilon_{ml}a_{lk}a_{kj} + a_{ik}a_{kl}\varepsilon_{lm}a_{mn}a_{nj}\right) = \\ &= 2a_{ik}a_{kl}\varepsilon_{lm}a_{mn}a_{nj} = 2\mathbf{aa}\boldsymbol{\varepsilon}\mathbf{aa} = 2\mathbf{a}^2\boldsymbol{\varepsilon}\mathbf{a}^2 \end{aligned} \tag{A.11}$$

The strain and stress tensors are symmetric, namely $\varepsilon_{ij} = \varepsilon_{ji}$ and $\sigma_{ij} = \sigma_{ji}$, thus each of them has just 6 independent components. The stiffness (or compliance) matrix associated to the fourth order tensor has 81 components but, because of above symmetries, the stress-strain incremental relationship can be written in the

form of a 6x6 matrix with just 36 components. Therefore, there is an ambiguity in the way the stiffness matrix can be expressed: multiple choices of the form of $\mathbb{D}$ (D_{ijkl}) can result in the same incremental stress-strain response. This ambiguity is almost universally resolved by requiring that the stiffness (or compliance) tensor possesses the "minor symmetries", such that $D_{ijkl} = D_{ijlk}$ and $D_{ijkl} = D_{jikl}$ and as well as the "major symmetry" $D_{ijkl} = D_{klij}$ which arises from the existence of a strain energy potential. When all the symmetries are applied the number of independent components reduces to 21.

The symmetries of the stiffness tensor are discussed herein with reference to the linear isotropic case. Let start with the following well-known strain energy function, where no information about the symmetry of the strain tensor is introduced:

$$\varphi(\boldsymbol{\varepsilon}) = \frac{\lambda}{2}\left[\mathrm{tr}(\boldsymbol{\varepsilon})\right]^2 + \mu \mathrm{tr}\left(\boldsymbol{\varepsilon}^2\right) \tag{A.12}$$

When differentiated with respect to the strain following the rules reported above, the stress tensor reads:

$$\sigma_{ij} = \frac{\partial \varphi}{\partial \varepsilon_{ij}} = \lambda \varepsilon_{mm}\delta_{ij} + 2\mu\varepsilon_{ji} \tag{A.13}$$

and the stiffness tensor:

$$D_{ijkl} = \frac{\partial \sigma_{ij}}{\partial \varepsilon_{kl}} = \lambda \delta_{ij}\delta_{kl} + 2\mu\delta_{il}\delta_{jk} \tag{A.14}$$

In the incremental form the constitutive law can be rewritten as:

$$\begin{Bmatrix} \dot{\sigma}_{11} \\ \dot{\sigma}_{22} \\ \dot{\sigma}_{33} \\ \dot{\sigma}_{12} \\ \dot{\sigma}_{13} \\ \dot{\sigma}_{23} \\ \dot{\sigma}_{21} \\ \dot{\sigma}_{31} \\ \dot{\sigma}_{32} \end{Bmatrix} = \begin{bmatrix} \lambda+2\mu & \lambda & \lambda & 0 & 0 & 0 & 0 & 0 & 0 \\ \lambda & \lambda+2\mu & \lambda & 0 & 0 & 0 & 0 & 0 & 0 \\ \lambda & \lambda & \lambda+2\mu & 0 & 0 & 0 & 0 & 0 & 0 \\ 0 & 0 & 0 & 0 & 0 & 0 & 2\mu & 0 & 0 \\ 0 & 0 & 0 & 0 & 0 & 0 & 0 & 2\mu & 0 \\ 0 & 0 & 0 & 0 & 0 & 0 & 0 & 0 & 2\mu \\ 0 & 0 & 0 & 2\mu & 0 & 0 & 0 & 0 & 0 \\ 0 & 0 & 0 & 0 & 2\mu & 0 & 0 & 0 & 0 \\ 0 & 0 & 0 & 0 & 0 & 2\mu & 0 & 0 & 0 \end{bmatrix} \begin{Bmatrix} \dot{\varepsilon}_{11} \\ \dot{\varepsilon}_{22} \\ \dot{\varepsilon}_{33} \\ \dot{\varepsilon}_{12} \\ \dot{\varepsilon}_{13} \\ \dot{\varepsilon}_{23} \\ \dot{\varepsilon}_{21} \\ \dot{\varepsilon}_{31} \\ \dot{\varepsilon}_{32} \end{Bmatrix} \tag{A.15}$$

It is worth noting that the stiffness tensor in eq. (A.14) violates the minor symmetries. In fact, in general $D_{ijkl} - D_{ijlk} \neq 0$. Note for instance that the terms corresponding to D_{1212} and D_{1221} do not coincide in eq. (A.15). The deficiency of

the previous procedure consists in not taking into account explicitly the symmetry of the strain and stress tensors. This is the reason why the minor symmetries of the stiffness tensor are not automatically satisfied. Therefore, it is necessary to take care in differentiating the stress tensor with respect to the strain in order to guarantee the minor symmetries. Here the approach proposed by Malvern (1969) within a hyperelastic framework is adopted, to maintain the differentiation rules described above while taking into account the symmetries of the strain and stress tensors. In detail, the free energy function in eq. (A.12) can therefore rewritten as:

$$\varphi\left(\boldsymbol{\varepsilon}\right) = \frac{\lambda}{2}\left[\mathrm{tr}\left(\boldsymbol{\varepsilon}^{sym}\right)\right]^2 + \mu \mathrm{tr}\left[\left(\boldsymbol{\varepsilon}^{sym}\right)^2\right] \tag{A.16}$$

The above rewriting may seem to be unnecessary pedantry as the symmetry of the strain tensor means that it rewriting does not change the numerical value of the strain energy. However, when twice differentiated with respect to strain, the alternative form results in different entries in the stiffness matrix. The strain energy in eq. (A.16) is rewritten in this form for purely formal purposes so that when twice differentiated it gives the required canonical form of the stiffness matrix, respecting the minor symmetries. Particularly, the stress tensor assumes the form:

$$\sigma_{ij} = \frac{\partial \varphi}{\partial \varepsilon_{ij}} = \lambda \varepsilon_{mm} \delta_{ij} + \mu\left(\varepsilon_{ji} + \varepsilon_{ij}\right) \tag{A.17}$$

and by further differentiation, the stiffness tensor is obtained:

$$D_{ijkl} = \frac{\partial \sigma_{ij}}{\partial \varepsilon_{kl}} = \lambda \delta_{ij}\delta_{kl} + 2\mu\left(\delta_{il}\delta_{jk} + \delta_{ik}\delta_{jl}\right) \tag{A.18}$$

Similarly as above, the incremental form now is:

$$\begin{Bmatrix} \dot{\sigma}_{11} \\ \dot{\sigma}_{22} \\ \dot{\sigma}_{33} \\ \dot{\sigma}_{12} \\ \dot{\sigma}_{13} \\ \dot{\sigma}_{23} \\ \dot{\sigma}_{21} \\ \dot{\sigma}_{31} \\ \dot{\sigma}_{32} \end{Bmatrix} = \begin{bmatrix} \lambda+2\mu & \lambda & \lambda & 0 & 0 & 0 & 0 & 0 & 0 \\ \lambda & \lambda+2\mu & \lambda & 0 & 0 & 0 & 0 & 0 & 0 \\ \lambda & \lambda & \lambda+2\mu & 0 & 0 & 0 & 0 & 0 & 0 \\ 0 & 0 & 0 & \mu & 0 & 0 & \mu & 0 & 0 \\ 0 & 0 & 0 & 0 & \mu & 0 & 0 & \mu & 0 \\ 0 & 0 & 0 & 0 & 0 & \mu & 0 & 0 & \mu \\ 0 & 0 & 0 & \mu & 0 & 0 & \mu & 0 & 0 \\ 0 & 0 & 0 & 0 & \mu & 0 & 0 & \mu & 0 \\ 0 & 0 & 0 & 0 & 0 & \mu & 0 & 0 & \mu \end{bmatrix} \begin{Bmatrix} \dot{\varepsilon}_{11} \\ \dot{\varepsilon}_{22} \\ \dot{\varepsilon}_{33} \\ \dot{\varepsilon}_{12} \\ \dot{\varepsilon}_{13} \\ \dot{\varepsilon}_{23} \\ \dot{\varepsilon}_{21} \\ \dot{\varepsilon}_{31} \\ \dot{\varepsilon}_{32} \end{Bmatrix} \tag{A.19}$$

In this case the minor symmetries are automatically respected.

In other words, in order to guarantee the respect of the minor symmetries of

the stiffness and compliance tensors, the symmetries of the stress and strain tensors must be explicitly considered in the diffentiation procedure. It is worth noting that, for the anisotropic models, the symmetry of the fabric tensor could be enforced just at the end of the differentiation. However, this is possible solely whenever the fabric tensor is constant, i.e. no evolution or dependence with the stresses or strains is considered. Conversely, even the symmetry of the fabric tensor must be analytically taken into account.

Spectral decomposition of the fabric tensor

A generic second order tensor can be always expressed using the spectral decomposition. In particular, for the fabric tensor $\mathbf{a}$ denoting with $\boldsymbol{a}_i$ its orthonormal eigenvectors defining the direction of orthotropy and with a_i its eigenvalues, to be positive because of the positive definiteness of the fabric tensor, one can write:

$$\mathbf{a} = \sum_{i=1}^{3} a_i \boldsymbol{a}_i \otimes \boldsymbol{a}_i = \sum_{i=1}^{3} a_i \mathbf{M}_i \tag{A.20}$$

where the $\mathbf{M}_i = \boldsymbol{a}_i \otimes \boldsymbol{a}_i$ represents the dyadic product of the eigenvectors $\boldsymbol{a}_i$ and are called eigenprojections of $\mathbf{a}$. The tensors $\mathbf{M}_i$ are characterised by the relevant properties $\mathbf{M}_i^k = \mathbf{M}_i$, with k positive integer and $\mathbf{M}_1 + \mathbf{M}_2 + \mathbf{M}_3 = \mathbf{I}$. Particularly, recalling that $\mathbf{B} = \mathbf{a}^2$, the spectral decomposition of the fabric tensor $\mathbf{B}$ is:

$$\mathbf{B} = \sum_{i=1}^{3} b_i \boldsymbol{b}_i \otimes \boldsymbol{b}_i = \sum_{i=1}^{3} b_i \mathbf{M}_i \tag{A.21}$$

where b_i are the eigenvalues of $\mathbf{B}$, such that $b_i = a_i^2$. Therefore, $\mathbf{a}$ and $\mathbf{B}$ have the same eigenvectors (i.e. the same principal directions), the eigenvalues of $\mathbf{B}$ being the square of those of $\mathbf{a}$.

Another important property of the generic eigenprojection $\mathbf{M}$ is that $\mathbf{M} \otimes \mathbf{M} = \mathbf{M} \bar{\otimes} \mathbf{M}$. In fact, recalling that the generic eigenvector $\boldsymbol{b}$ is a unit vector, such that only two of its three components are independent ($b_1^2 = 1 - b_2^2 - b_3^2$), the matrix associated to the second order tensor $\mathbf{M}$ results:

$$\mathbf{M} = \begin{bmatrix} 1 - b_2^2 - b_3^2 & b_2\sqrt{1 - b_2^2 - b_3^2} & b_3\sqrt{1 - b_2^2 - b_3^2} \\ b_2\sqrt{1 - b_2^2 - b_3^2} & b_2^2 & b_2 b_3 \\ b_3\sqrt{1 - b_2^2 - b_3^2} & b_2 b_3 & b_3^2 \end{bmatrix} \tag{A.22}$$

From eq. (A.22) descends that $M_{ij}M_{kl} = \frac{1}{2}\left(M_{ik}M_{jl} + M_{il}M_{jk}\right)$, thus proving the previous property.

As pointed out by Bigoni & Loret (1999), adopting the spectral decomposition in eq. (A.21), the free energy in eq. (2.38) valid for the linear anisotropic case can be rewritten in terms of a series of mixed invariants of the strain and the $\mathbf{M}_i$ tensors. At this point it is worth mentioning that the very special property $\left[\mathrm{tr}\left(\mathbf{M}_i\boldsymbol{\varepsilon}\right)\right]^2 = \mathrm{tr}\left[\left(\mathbf{M}_i\boldsymbol{\varepsilon}\right)^2\right]$ holds. In order to demonstrate this feature the procedure proposed by Itskov (2007) is followed. In detail:

$$\mathrm{tr}\left(\mathbf{M}_i\boldsymbol{\varepsilon}\right) = \mathbf{M}_i : \boldsymbol{\varepsilon} = \left(\boldsymbol{b}_i \otimes \boldsymbol{b}_i\right) : \boldsymbol{\varepsilon} = \boldsymbol{b}_i\boldsymbol{\varepsilon}\boldsymbol{b}_i \tag{A.23}$$

Furthermore, by virtue of eq. (A.23), it results:

$$\mathrm{tr}\left[\left(\mathbf{M}_i\boldsymbol{\varepsilon}\right)^2\right] = \mathrm{tr}\left(\boldsymbol{\varepsilon}\boldsymbol{b}_i \otimes \boldsymbol{b}_i\boldsymbol{\varepsilon}\boldsymbol{b}_i \otimes \boldsymbol{b}_i\right) = \mathrm{tr}\left(\mathbf{M}_i\boldsymbol{\varepsilon}\right)\mathrm{tr}\left(\boldsymbol{\varepsilon}\boldsymbol{b}_i \otimes \boldsymbol{b}_i\right) = \left[\mathrm{tr}\left(\mathbf{M}_i\boldsymbol{\varepsilon}\right)\right]^2 \tag{A.24}$$

Taking into account the previous properties, free energy for the linear anisotropic model for an orthotropic material takes the form:

$$\begin{aligned}\varphi\left(\boldsymbol{\varepsilon}, \mathbf{M}_i\right) = \frac{c_1}{2}\left[\mathrm{tr}\left(\mathbf{M}_1\boldsymbol{\varepsilon}\right)\right]^2 + \frac{c_2}{2}\left[\mathrm{tr}\left(\mathbf{M}_2\boldsymbol{\varepsilon}\right)\right]^2 + \frac{c_3}{2}\left[\mathrm{tr}\left(\mathbf{M}_3\boldsymbol{\varepsilon}\right)\right]^2 + \\ + c_4\mathrm{tr}\left(\mathbf{M}_1\boldsymbol{\varepsilon}\right)\mathrm{tr}\left(\mathbf{M}_2\boldsymbol{\varepsilon}\right) + c_5\mathrm{tr}\left(\mathbf{M}_1\boldsymbol{\varepsilon}\right)\mathrm{tr}\left(\mathbf{M}_3\boldsymbol{\varepsilon}\right) + \\ + c_6\mathrm{tr}\left(\mathbf{M}_2\boldsymbol{\varepsilon}\right)\mathrm{tr}\left(\mathbf{M}_3\boldsymbol{\varepsilon}\right) + + c_7\mathrm{tr}\left(\mathbf{M}_1\boldsymbol{\varepsilon}^2\right) \\ + c_8\mathrm{tr}\left(\mathbf{M}_2\boldsymbol{\varepsilon}^2\right) + c_9\mathrm{tr}\left(\mathbf{M}_3\boldsymbol{\varepsilon}^2\right)\end{aligned} \tag{A.25}$$

Specialising eq. (A.25) to the case of transverse isotropy, with $b_1 \neq b_2 = b_3$ and recalling that $\mathbf{M}_1 + \mathbf{M}_2 + \mathbf{M}_3 = \mathbf{I}$, one can retain only one of the three eigenprojections $\mathbf{M}_i$, simply denoted with $\mathbf{M}$, thus leading to

$$\begin{aligned}\varphi\left(\boldsymbol{\varepsilon}, \mathbf{M}\right) = \frac{c_1}{2}\left[\mathrm{tr}\left(\boldsymbol{\varepsilon}\right)\right]^2 + \frac{c_2}{2}\mathrm{tr}\left(\boldsymbol{\varepsilon}^2\right) + c_3\mathrm{tr}\left(\boldsymbol{\varepsilon}\right)\mathrm{tr}\left(\mathbf{M}\boldsymbol{\varepsilon}\right) + \\ + \frac{c_4}{2}\left[\mathrm{tr}\left(\mathbf{M}\boldsymbol{\varepsilon}\right)\right]^2 + c_5\mathrm{tr}\left(\mathbf{M}\boldsymbol{\varepsilon}^2\right)\end{aligned} \tag{A.26}$$

Alternative representation of the fabric tensor

Recalling that $\mathbf{B} = \mathbf{a}^2$, employing the two mixed invariants $\mathrm{tr}\left(\mathbf{B}\boldsymbol{\varepsilon}\right)$ and $\mathrm{tr}\left[\left(\mathbf{B}\boldsymbol{\varepsilon}\right)^2\right]$, one can equivalently rewrite the strain energy of eq. (3.1) as follows:

$$\begin{aligned}\varphi\left(\boldsymbol{\varepsilon}, \mathbf{B}\right) = \frac{p_r}{k\left(2-n\right)}k^{\frac{2-n}{2-2n}}\left(1-n\right)^{\frac{2-n}{2-2n}} \\ \left\{\left[k\left(1-n\right) - \frac{2}{3}g\right]\left[\mathrm{tr}\left(\mathbf{B}\boldsymbol{\varepsilon}\right)\right]^2 + 2g\mathrm{tr}\left[\left(\mathbf{B}\boldsymbol{\varepsilon}\right)^2\right]\right\}^{\frac{2-n}{2-2n}}\end{aligned} \tag{A.27}$$

The stress tensor is thus obtained differentiating the strain energy function with respect to the strain:

$$\boldsymbol{\sigma} = p_r r_0^{\frac{n}{1-n}} \left\{ \left[k\left(1-n\right) - \frac{2}{3}g \right] \mathrm{tr}\left(\mathbf{B}\boldsymbol{\varepsilon}\right) \mathbf{B} + 2g\mathbf{B}\boldsymbol{\varepsilon}\mathbf{B} \right\} \tag{A.28}$$

and, with further differentiation, the stiffness tensor results:

$$\begin{aligned} \mathbb{D} = {} & p_r \left[k\left(1-n\right) - \frac{2}{3}g \right] \left\{ k r_0^{\frac{3n-2}{1-n}} n \left[k\left(1-n\right) - \frac{2}{3}g \right] \left[\mathrm{tr}\left(\mathbf{B}\boldsymbol{\varepsilon}\right)\right]^2 + r_0^{\frac{n}{1-n}} \right\} \mathbf{B} \otimes \mathbf{B} + \\ & + 2p_r k r_0^{\frac{3n-2}{1-n}} n g \left[k\left(1-n\right) - \frac{2}{3}g \right] \mathrm{tr}\left(\mathbf{B}\boldsymbol{\varepsilon}\right) \left(\mathbf{B}\boldsymbol{\varepsilon}\mathbf{B} \otimes \mathbf{B} + \mathbf{B} \otimes \mathbf{B}\boldsymbol{\varepsilon}\mathbf{B}\right) + \\ & + 4p_r k r_0^{\frac{3n-2}{1-n}} n g^2 \left(\mathbf{B}\boldsymbol{\varepsilon}\mathbf{B} \otimes \mathbf{B}\boldsymbol{\varepsilon}\mathbf{B}\right) + 2p_r r_0^{\frac{n}{1-n}} g \left(\mathbf{B} \underset{-}{\otimes} \mathbf{B} \right) \end{aligned} \tag{A.29}$$

Analogously, the complementary energy expressed via the tensor $\mathbf{B}$ is:

$$\begin{aligned} \psi\left(\boldsymbol{\sigma}, \mathbf{B}\right) = {} & \frac{1}{p_r^{1-n} k\left(1-n\right)\left(2-n\right)} p_0^{2-n} = \frac{1}{p_r^{1-n} k\left(1-n\right)\left(2-n\right)} \\ & \left\{ \left(\frac{1}{9} - \frac{k\left(1-n\right)}{6g} \right) \left[\mathrm{tr}\left(\mathbf{B}^{-1}\boldsymbol{\sigma}\right)\right]^2 + \frac{k\left(1-n\right)}{2g} \mathrm{tr}\left[\left(\mathbf{B}^{-1}\boldsymbol{\sigma}\right)^2 \right] \right\}^{\frac{2-n}{2}} \end{aligned} \tag{A.30}$$

The strain tensor is obtained differentiating the complementary energy with respect to the stress:

$$\boldsymbol{\varepsilon} = \frac{1}{2p_r^{1-n} k\left(1-n\right)} p_0^n \left[2\left(\frac{1}{9} - \frac{k\left(1-n\right)}{6g} \right) \mathrm{tr}\left(\mathbf{B}^{-1}\boldsymbol{\sigma}\right) \mathbf{B}^{-1} + \frac{k\left(1-n\right)}{g} \mathbf{B}^{-1}\boldsymbol{\sigma}\mathbf{B}^{-1} \right] \tag{A.31}$$

and, with further differentiation, the compliance tensor results:

$$\begin{aligned} \mathbb{C} = {} & \frac{1}{p_r^{1-n} k\left(1-n\right)} \left\{ \left(-\frac{n}{2}\right) p_0^{-(n+2)} 2 \left(\frac{1}{9} - \frac{k\left(1-n\right)}{6g} \right) \left[\mathrm{tr}\left(\mathbf{B}^{-1}\boldsymbol{\sigma}\right)\right]^2 + \right. \\ & \left. + p_0^{-n} \left(\frac{1}{9} - \frac{k\left(1-n\right)}{6g} \right) \right\} \mathbf{B}^{-1} \otimes \mathbf{B}^{-1} + \frac{1}{2p_r^{1-n} g} p_0^{-n} \left(\mathbf{B}^{-1} \underset{-}{\otimes} \mathbf{B}^{-1} \right) \\ & - \frac{n}{4p_r^{1-n}} p_0^{-(n+2)} \frac{k\left(1-n\right)}{g^2} \left(\mathbf{B}^{-1}\boldsymbol{\sigma}\mathbf{B}^{-1} \otimes \mathbf{B}^{-1}\boldsymbol{\sigma}\mathbf{B}^{-1} \right) + \\ & - \frac{n}{2p_r^{1-n} g} p_0^{-(n+2)} \left(\frac{1}{9} - \frac{k\left(1-n\right)}{6g} \right) \mathrm{tr}\left(\mathbf{B}^{-1}\boldsymbol{\sigma}\right) \\ & \left(\mathbf{B}^{-1}\boldsymbol{\sigma}\mathbf{B}^{-1} \otimes \mathbf{B}^{-1} + \mathbf{B}^{-1} \otimes \mathbf{B}^{-1}\boldsymbol{\sigma}\mathbf{B}^{-1} \right) \end{aligned} \tag{A.32}$$

The strain energy function of the proposed nonlinear anisotropic hyperelastic model expressed in terms of the isotropic and deviatoric parts of $\mathbf{B}$ assumes the form:

$$\varphi(\boldsymbol{\varepsilon}, f, \mathbf{F}) = \frac{p_r}{k(2-n)} k^{\frac{2-n}{2-2n}} (1-n)^{\frac{2-n}{2-2n}} \left\{ \left[k(1-n) - \frac{2}{3}g \right] \left[\operatorname{tr}(\boldsymbol{\varepsilon}) f + \operatorname{tr}(\mathbf{F}\boldsymbol{\varepsilon}) \right]^2 + 2g \operatorname{tr}\left[(f\boldsymbol{\varepsilon} + \mathbf{F}\boldsymbol{\varepsilon})^2 \right] \right\}^{\frac{2-n}{2-2n}} \tag{A.33}$$

Differentiating eq. (A.33) with respect to the strains, one obtains the stress tensor:

$$\begin{aligned} \boldsymbol{\sigma} = p_r r_0^{\frac{n}{1-n}} \Bigg\{ & \left[k(1-n) - \frac{2}{3}g \right] \operatorname{tr}(f\boldsymbol{\varepsilon} + \mathbf{F}\boldsymbol{\varepsilon}) (f\mathbf{I} + \mathbf{F}) + \\ & + 2g \left(f^2\boldsymbol{\varepsilon} + f\boldsymbol{\varepsilon}\mathbf{F} + f\mathbf{F}\boldsymbol{\varepsilon} + \mathbf{F}\boldsymbol{\varepsilon}\mathbf{F} \right) \Bigg\} \end{aligned} \tag{A.34}$$

and, with a further differentiation, the stiffness tensor:

$$\begin{aligned} \mathbb{D} = {} & p_r \left[k(1-n) - \frac{2}{3}g \right] \left\{ k r_0^{\frac{3n-2}{1-n}} n \left[k(1-n) - \frac{2}{3}g \right] \left[\operatorname{tr}(f\boldsymbol{\varepsilon} + \mathbf{F}\boldsymbol{\varepsilon}) \right]^2 + r_0^{\frac{n}{1-n}} \right\} \\ & \left[f^2 \mathbf{I}\otimes\mathbf{I} + f(\mathbf{I}\otimes\mathbf{F} + \mathbf{F}\otimes\mathbf{I}) + \mathbf{F}\otimes\mathbf{F} \right] + \\ & + 2p_r k r_0^{\frac{3n-2}{1-n}} n g \left[k(1-n) - \frac{2}{3}g \right] \operatorname{tr}(f\boldsymbol{\varepsilon} + \mathbf{F}\boldsymbol{\varepsilon}) \left(f^3 \mathbf{I}\otimes\boldsymbol{\varepsilon} + f^2 \mathbf{I}\otimes\boldsymbol{\varepsilon}\mathbf{F} + \right. \\ & + f\mathbf{I}\otimes\mathbf{F}\boldsymbol{\varepsilon}\mathbf{F} + f^2\mathbf{I}\otimes\mathbf{F}\boldsymbol{\varepsilon} + f^2\mathbf{F}\otimes\boldsymbol{\varepsilon} + f\mathbf{F}\otimes\boldsymbol{\varepsilon}\mathbf{F} + \mathbf{F}\otimes\mathbf{F}\boldsymbol{\varepsilon}\mathbf{F} + \\ & + f\mathbf{F}\otimes\mathbf{F}\boldsymbol{\varepsilon} + f^3\boldsymbol{\varepsilon}\otimes\mathbf{I} + f^2\boldsymbol{\varepsilon}\mathbf{F}\otimes\mathbf{I} + f\mathbf{F}\boldsymbol{\varepsilon}\mathbf{F}\otimes\mathbf{I} + f^2\mathbf{F}\boldsymbol{\varepsilon}\otimes\mathbf{I} + \\ & \left. + f^2\boldsymbol{\varepsilon}\otimes\mathbf{F} + f\boldsymbol{\varepsilon}\mathbf{F}\otimes\mathbf{F} + \mathbf{F}\boldsymbol{\varepsilon}\mathbf{F}\otimes\mathbf{F}\boldsymbol{\varepsilon}\mathbf{F} + f\mathbf{F}\boldsymbol{\varepsilon}\otimes\mathbf{F} \right) + \\ & + 4p_r k r_0^{\frac{3n-2}{1-n}} n g^2 \left(f^4\boldsymbol{\varepsilon}\otimes\boldsymbol{\varepsilon} + f^3\boldsymbol{\varepsilon}\otimes\boldsymbol{\varepsilon}\mathbf{F} + f^2\boldsymbol{\varepsilon}\otimes\mathbf{F}\boldsymbol{\varepsilon}\mathbf{F} + \right. \\ & + f^3\boldsymbol{\varepsilon}\otimes\mathbf{F}\boldsymbol{\varepsilon} + f^3\boldsymbol{\varepsilon}\mathbf{F}\otimes\boldsymbol{\varepsilon} + f^2\boldsymbol{\varepsilon}\mathbf{F}\otimes\boldsymbol{\varepsilon}\mathbf{F} + f\boldsymbol{\varepsilon}\mathbf{F}\otimes\mathbf{F}\boldsymbol{\varepsilon}\mathbf{F} + \\ & + f^2\boldsymbol{\varepsilon}\mathbf{F}\otimes\mathbf{F}\boldsymbol{\varepsilon} + f^2\mathbf{F}\boldsymbol{\varepsilon}\mathbf{F}\otimes\boldsymbol{\varepsilon} + f\mathbf{F}\boldsymbol{\varepsilon}\mathbf{F}\otimes\boldsymbol{\varepsilon}\mathbf{F} + \mathbf{F}\boldsymbol{\varepsilon}\mathbf{F}\otimes\mathbf{F}\boldsymbol{\varepsilon}\mathbf{F} + \\ & + f\mathbf{F}\boldsymbol{\varepsilon}\mathbf{F}\otimes\mathbf{F}\boldsymbol{\varepsilon} + f^3\mathbf{F}\boldsymbol{\varepsilon}\otimes\boldsymbol{\varepsilon} + f^2\mathbf{F}\boldsymbol{\varepsilon}\otimes\boldsymbol{\varepsilon}\mathbf{F} + f\mathbf{F}\boldsymbol{\varepsilon}\otimes\mathbf{F}\boldsymbol{\varepsilon}\mathbf{F} + \\ & \left. + f^2\mathbf{F}\boldsymbol{\varepsilon}\otimes\mathbf{F}\boldsymbol{\varepsilon} \right) + \\ & + 2p_r r_0^{\frac{n}{1-n}} g \left(f^2 \mathbf{I} \underset{-}{\otimes} \mathbf{I} + f\mathbf{F} \underset{-}{\otimes} \mathbf{I} + f\mathbf{I} \underset{-}{\otimes} \mathbf{F} + \mathbf{F} \underset{-}{\otimes} \mathbf{F} \right) \end{aligned} \tag{A.35}$$

Finally, employing the spectral decomposition technique, the free energy of the proposed nonlinear anisotropic model can be analogously expressed, under the hypothesis of transverse isotropy, as:

$$\varphi(\boldsymbol{\varepsilon},\mathbf{M}) = \frac{p_r}{k(2-n)} k^{\frac{2-n}{2-2n}} (1-n)^{\frac{2-n}{2-2n}} \left\{ c_1 \left[\mathrm{tr}(\boldsymbol{\varepsilon})\right]^2 + c_2 \mathrm{tr}\left(\boldsymbol{\varepsilon}^2\right) + \right. \\ \left. + c_3 \mathrm{tr}(\boldsymbol{\varepsilon}) \mathrm{tr}(\mathbf{M}\boldsymbol{\varepsilon}) + c_4 \left[\mathrm{tr}(\mathbf{M}\boldsymbol{\varepsilon})\right]^2 + c_5 \mathrm{tr}\left(\mathbf{M}\boldsymbol{\varepsilon}^2\right) \right\}^{\frac{2-n}{2-2n}} \tag{A.36}$$

with the five coefficients c_i function of material constants k, g and n and the eigenvalues a_1 and a_2 of the tensor $\mathbf{a}$.

$$c_1 = \left(k - \frac{2}{3}\frac{g}{1-n}\right) a_2^4,\ c_2 = \frac{2g}{1-n} a_2^4,\ c_3 = 2\left(k - \frac{2}{3}\frac{g}{1-n}\right) a_2^2 \left(a_1^2 - a_2^2\right) \\ c_4 = \left(k + \frac{4}{3}\frac{g}{1-n}\right) \left(a_1^2 - a_2^2\right)^2,\ c_5 = \frac{4g}{1-n} a_2^2 \left(a_1^2 - a_2^2\right) \tag{A.37}$$

In a dual way, the complementary free energy reads:

$$\psi(\boldsymbol{\sigma},\mathbf{N}) = \frac{1}{p_r^{1-n} k(1-n)(2-n)} \left[c_1 (\mathrm{tr}\boldsymbol{\sigma})^2 + c_2 \mathrm{tr}\left(\boldsymbol{\sigma}^2\right) + c_3 \mathrm{tr}\boldsymbol{\sigma} \mathrm{tr}(\mathbf{N}\boldsymbol{\sigma}) + \right. \\ \left. + c_4 \left[\mathrm{tr}(\mathbf{N}\boldsymbol{\sigma})\right]^2 + c_5 \mathrm{tr}\left(\mathbf{N}\boldsymbol{\sigma}^2\right) \right]^{\frac{2-n}{2}} \tag{A.38}$$

with again the five coefficients c_i function of material constants k, g and n and the eigenvalues a_1^{-1} and a_2^{-1} of the tensor $\mathbf{a}^{-1}$.

$$c_1 = \left(\frac{1}{9} - \frac{k(1-n)}{6g}\right) a_2^{-4},\ c_2 = \frac{k(1-n)}{2g} a_2^{-4} \\ c_3 = 2\left(\frac{1}{9} - \frac{k(1-n)}{6g}\right) a_2^{-2} \left(a_1^{-2} - a_2^{-2}\right) \\ c_4 = \left(\frac{1}{9} + \frac{k(1-n)}{3g}\right) \left(a_1^{-2} - a_2^{-2}\right)^2,\ c_5 = \frac{k(1-n)}{g} a_2^{-2} \left(a_1^{-2} - a_2^{-2}\right) \tag{A.39}$$

Appendix B

In this appendix the analytical details of the hyperplastic formulation of the Dafalias & Taiebat (2013) model are reported. In particular, the procedure to determine the dissipation function stemming from the original yield function of the model is illustrated and subsequently, in order to verify the result is correct, the inverse procedure is carried out. The results are illustrated in the triaxial formulation, first in the case of associative flow rule and then for the non-associated version of the model.

As described in chapter 5, being the generalised stresses χ_p and χ_q equal to the stress invariants p and q, respectively, the yield surface in terms of generalised stresses under the hypothesis of associative flow rule can be written as:

$$f\left(\chi_p, \chi_q, \beta, p_0\right) = \left(\chi_q - \beta\chi_p\right)^2 - \left(M^2 - \beta^2\right)\chi_p\left(p_0 - \chi_p\right) = 0 \tag{B.1}$$

The dissipation function has to be expressed as a function of the rate of internal variables. Therefore, recalling the definition in eq. (5.20), one can determine these latter as:

$$\begin{aligned} \frac{\dot{\alpha}_p}{L} &= \frac{\partial f}{\partial \chi_p} = -2\beta\chi_q - M^2 p_0 + 2M^2\chi_p + \beta^2 p_0 \\ \frac{\dot{\alpha}_q}{L} &= \frac{\partial f}{\partial \chi_q} = 2\chi_q - 2\beta\chi_p \end{aligned} \tag{B.2}$$

First, the plastic multiplier has to be determined. To do that, from the two eqs. (B.2) one expresses the dissipative generalised stresses as a function of L:

$$\begin{aligned} \chi_p &= \frac{\dot{\alpha}_p + \beta\dot{\alpha}_q}{2L\left(M^2 - \beta^2\right)} + \frac{p_0}{2} \\ \chi_q &= \frac{\dot{\alpha}_q}{2L} + \beta\frac{\dot{\alpha}_p + \beta\dot{\alpha}_q}{2L\left(M^2 - \beta^2\right)} + \beta\frac{p_0}{2} \end{aligned} \tag{B.3}$$

Then the dissipative generalised stress just calculated can be substituted in the yield function in eq. (B.1) in order to obtain the plastic multiplier. In particular one has:

$$\begin{aligned}
&\frac{\dot{\alpha}_q^2}{4L^2}+\beta^2\frac{\left(\dot{\alpha}_p+\beta\dot{\alpha}_q\right)^2}{4L^2\left(M^2-\beta^2\right)^2}+\beta^2\frac{p_0^2}{4}+\frac{\beta\dot{\alpha}_q\left(\dot{\alpha}_p+\beta\dot{\alpha}_q\right)}{2L^2\left(M^2-\beta^2\right)}+\frac{\beta p_0\dot{\alpha}_q}{2L}+\\
&+\frac{\beta^2 p_0\left(\dot{\alpha}_p+\beta\dot{\alpha}_q\right)}{2L\left(M^2-\beta^2\right)}-\frac{\beta\dot{\alpha}_q\left(\dot{\alpha}_p+\beta\dot{\alpha}_q\right)}{2L^2\left(M^2-\beta^2\right)}-\beta^2\frac{\left(\dot{\alpha}_p+\beta\dot{\alpha}_q\right)^2}{2L^2\left(M^2-\beta^2\right)^2}+\\
&-\frac{\beta^2 p_0\left(\dot{\alpha}_p+\beta\dot{\alpha}_q\right)}{2L\left(M^2-\beta^2\right)}-\frac{\beta p_0\dot{\alpha}_q}{2L}-\frac{\beta^2 p_0\left(\dot{\alpha}_p+\beta\dot{\alpha}_q\right)}{2L\left(M^2-\beta^2\right)}-\beta^2\frac{p_0^2}{2}+\\
&-\frac{M^2 p_0\left(\dot{\alpha}_p+\beta\dot{\alpha}_q\right)}{2L\left(M^2-\beta^2\right)}-\frac{M^2 p_0^2}{2}+M^2\frac{\left(\dot{\alpha}_p+\beta\dot{\alpha}_q\right)^2}{4L^2\left(M^2-\beta^2\right)^2}+\frac{M^2 p_0\left(\dot{\alpha}_p+\beta\dot{\alpha}_q\right)}{2L\left(M^2-\beta^2\right)}+\\
&+\frac{M^2 p_0^2}{4}+\frac{\beta^2 p_0\left(\dot{\alpha}_p+\beta\dot{\alpha}_q\right)}{2L\left(M^2-\beta^2\right)}+\beta^2\frac{p_0^2}{2}=0
\end{aligned}\tag{B.4}$$

that, after some simplifications and multiplying for L^2 reads:

$$\dot{\alpha}_q^2-\beta^2\frac{\left(\dot{\alpha}_p+\beta\dot{\alpha}_q\right)^2}{\left(M^2-\beta^2\right)^2}+M^2\frac{\left(\dot{\alpha}_p+\beta\dot{\alpha}_q\right)^2}{\left(M^2-\beta^2\right)^2}-\left(M^2-\beta^2\right)p_0^2L^2=0 \tag{B.5}$$

from which the plastic multiplier reads:

$$L=\frac{1}{p_0\left(M^2-\beta^2\right)}\sqrt{\left(\dot{\alpha}_p+\beta\dot{\alpha}_q\right)^2+\left(M^2-\beta^2\right)\dot{\alpha}_q^2} \tag{B.6}$$

Once the plastic multiplier is known, eq. (B.6) can be resubstituted in eq. (B.3) in order to express the dissipative generalised stresses as uniquely function of the rate of the internal variables, leading, after few manipulations, to:

$$\begin{aligned}
\chi_p&=\frac{p_0}{2}\left[\frac{\dot{\alpha}_p+\beta\dot{\alpha}_q}{\sqrt{\left(\dot{\alpha}_p+\beta\dot{\alpha}_q\right)^2+\left(M^2-\beta^2\right)\dot{\alpha}_q^2}}+1\right]\\
\chi_q&=\frac{p_0}{2}\left[\frac{\left(M^2-\beta^2\right)\dot{\alpha}_q+\beta\left(\dot{\alpha}_p+\beta\dot{\alpha}_q\right)}{\sqrt{\left(\dot{\alpha}_p+\beta\dot{\alpha}_q\right)^2+\left(M^2-\beta^2\right)\dot{\alpha}_q^2}}+\beta\right]
\end{aligned}\tag{B.7}$$

Finally, employing the definition of the dissipation of eq. (5.15) one can write:

$$
\begin{aligned}
d &= \chi_p \dot{\alpha}_p + \chi_q \dot{\alpha}_q = \\
&= \frac{p_0}{2}\left[\frac{\left(\dot{\alpha}_p + \beta\dot{\alpha}_q\right)\dot{\alpha}_p + \left(M^2-\beta^2\right)\dot{\alpha}_q^2 + \beta\left(\dot{\alpha}_p + \beta\dot{\alpha}_q\right)\dot{\alpha}_q}{\sqrt{\left(\dot{\alpha}_p + \beta\dot{\alpha}_q\right)^2 + \left(M^2-\beta^2\right)\dot{\alpha}_q^2}} + \dot{\alpha}_p + \beta\dot{\alpha}_q\right] = \\
&= \frac{p_0}{2}\left[\frac{\left(\dot{\alpha}_p + \beta\dot{\alpha}_q\right)^2 + \left(M^2-\beta^2\right)\dot{\alpha}_q^2}{\sqrt{\left(\dot{\alpha}_p + \beta\dot{\alpha}_q\right)^2 + \left(M^2-\beta^2\right)\dot{\alpha}_q^2}} + \dot{\alpha}_p + \beta\dot{\alpha}_q\right] = \\
&= \frac{p_0}{2}\left[\sqrt{\left(\dot{\alpha}_p + \beta\dot{\alpha}_q\right)^2 + \left(M^2-\beta^2\right)\dot{\alpha}_q^2} + \dot{\alpha}_p + \beta\dot{\alpha}_q\right]
\end{aligned}
\tag{B.8}
$$

To prove the dissipation function in eq. (B.8) is correct, the yield function is now deduced from this latter. For this scope, the dissipative generalised stresses are calculated stemming from eq. (5.14):

$$
\begin{aligned}
\chi_p &= \frac{\partial d}{\partial \dot{\alpha}_p} = \frac{p_0}{2}\left[\frac{\dot{\alpha}_p + \beta\dot{\alpha}_q}{\sqrt{\left(\dot{\alpha}_p + \beta\dot{\alpha}_q\right)^2 + \left(M^2-\beta^2\right)\dot{\alpha}_q^2}} + 1\right] \\
\chi_q &= \frac{\partial d}{\partial \dot{\alpha}_q} = \frac{p_0}{2}\left[\frac{\left(M^2-\beta^2\right)\dot{\alpha}_q + \beta\left(\dot{\alpha}_p + \beta\dot{\alpha}_q\right)}{\sqrt{\left(\dot{\alpha}_p + \beta\dot{\alpha}_q\right)^2 + \left(M^2-\beta^2\right)\dot{\alpha}_q^2}} + \beta\right]
\end{aligned}
\tag{B.9}
$$

The next step consists in eliminating the dependence on the rate of internal variables, thus $\dot{\alpha}_p$ and $\dot{\alpha}_q$ can be recalculated from eq. (B.9). Particulalry, for the sake of conciseness the position $\bar{d} = \sqrt{\left(\dot{\alpha}_p + \beta\dot{\alpha}_q\right)^2 + \left(M^2-\beta^2\right)\dot{\alpha}_q^2}$ is adopted, leading to:

$$
\begin{aligned}
\frac{2\chi_p}{p_0} - 1 &= \frac{\dot{\alpha}_p + \beta\dot{\alpha}_q}{\bar{d}} \\
\frac{2\chi_q}{p_0} - \beta &= \frac{\beta\dot{\alpha}_p + M^2\dot{\alpha}_q}{\bar{d}}
\end{aligned}
\tag{B.10}
$$

from which, after few calculations, the rate of the internal variables can be expressed as functions of the dissipative generalised stresses as follow:

$$
\begin{aligned}
\dot{\alpha}_p &= \left(\frac{2\chi_p}{p_0} - 1\right)\bar{d} - \frac{\beta}{M^2-\beta^2}\left[\frac{2\chi_q}{p_0} - \beta - \left(\frac{2\chi_p}{p_0} - 1\right)\beta\right]\bar{d} \\
\dot{\alpha}_q &= \frac{1}{M^2-\beta^2}\left[\frac{2\chi_q}{p_0} - \beta - \left(\frac{2\chi_p}{p_0} - 1\right)\beta\right]\bar{d}
\end{aligned}
\tag{B.11}
$$

Finally, an equation expressed in terms of the dissipative generalised stresses only has to be found. This can be achieved substituting the rate of the internal variables in eq. (B.11) in the expression of $\bar{d}$ and raising to the square:

$$\begin{aligned}\bar{d}^2 &= \left(\dot{\alpha}_p + \beta\dot{\alpha}_q\right)^2 + \left(M^2 - \beta^2\right)\dot{\alpha}_q^2 = \\ &= \left(\frac{2\chi_p}{p_0} - 1\right)^2 \bar{d}^2 + \frac{1}{M^2 - \beta^2}\left[\frac{2\chi_q}{p_0} - \frac{2\chi_p}{p_0}\beta\right]^2 \bar{d}^2\end{aligned} \tag{B.12}$$

Therefore $\bar{d}^2$ can be eliminated from eq. (B.12) and consequently it results:

$$1 = \frac{4\chi_p^2}{p_0^2} + 1 - \frac{4\chi_p}{p_0} + \frac{1}{M^2 - \beta^2}\frac{4}{p_0^2}\left(\chi_q - \beta\chi_p\right)^2 \tag{B.13}$$

that can be nicely rewritten leading exactly to the starting yield function in eq. (B.1).

In the case of non-associated flow rule, the dissipation function depends on the mean effective pressure p and takes the form:

$$d = \sqrt{A^2\left(\dot{\alpha}_p + \beta\dot{\alpha}_q\right)^2 + B^2\left(M^2 - \beta^2\right)\dot{\alpha}_q^2} + \frac{\gamma p_0}{2}\left(\dot{\alpha}_p + \beta\dot{\alpha}_q\right) \tag{B.14}$$

with the quantities A and B defined as:

$$\begin{aligned}A &= \left(1 - \gamma\right)p + \frac{\gamma p_0}{2} \\ B &= \left(1 - \delta\right)p + \frac{\gamma\delta p_0}{2}\end{aligned} \tag{B.15}$$

being γ and δ positive constants. In order to obtain the corresponding yield surface the dissipative generalised stresses are calculated stemming from their definition in eq. (5.14):

$$\begin{aligned}\chi_p &= \frac{\partial d}{\partial\dot{\alpha}_p} = \frac{A^2\left(\dot{\alpha}_p + \beta\dot{\alpha}_q\right)}{\sqrt{A^2\left(\dot{\alpha}_p + \beta\dot{\alpha}_q\right)^2 + B^2\left(M^2 - \beta^2\right)\dot{\alpha}_q^2}} + \frac{\gamma p_0}{2} \\ \chi_q &= \frac{\partial d}{\partial\dot{\alpha}_q} = \frac{B^2\left(M^2 - \beta^2\right)\dot{\alpha}_q + A^2\beta\left(\dot{\alpha}_p + \beta\dot{\alpha}_q\right)}{\sqrt{A^2\left(\dot{\alpha}_p + \beta\dot{\alpha}_q\right)^2 + B^2\left(M^2 - \beta^2\right)\dot{\alpha}_q^2}} + \beta\frac{\gamma p_0}{2}\end{aligned} \tag{B.16}$$

Then the rates of internal variables $\dot{\alpha}_p$ and $\dot{\alpha}_q$ are deduced from eq. (B.16). Similarly as above, the position $\bar{d} = \sqrt{A^2\left(\dot{\alpha}_p + \beta\dot{\alpha}_q\right)^2 + B^2\left(M^2 - \beta^2\right)\dot{\alpha}_q^2}$ is made, leading to:

$$\begin{aligned}\chi_p - \frac{\gamma p_0}{2} &= \frac{A^2\left(\dot{\alpha}_p + \beta\dot{\alpha}_q\right)}{\bar{d}} \\ \chi_q - \beta\frac{\gamma p_0}{2} &= \frac{B^2\left(M^2 - \beta^2\right)\dot{\alpha}_q + A^2\beta\left(\dot{\alpha}_p + \beta\dot{\alpha}_q\right)}{\bar{d}}\end{aligned} \tag{B.17}$$

from which the rate of the internal variables can be expressed as functions of the dissipative generalised stresses as follow:

$$\begin{aligned}\dot{\alpha}_p &= \left(\chi_p - \frac{\gamma p_0}{2}\right)\frac{\bar{d}}{A^2} - \frac{\beta}{B^2\left(M^2-\beta^2\right)}\left(\chi_q - \beta\chi_p\right)\bar{d} \\ \dot{\alpha}_q &= \frac{\chi_q - \beta\chi_p}{B^2\left(M^2-\beta^2\right)}\bar{d}\end{aligned} \tag{B.18}$$

Subsequently, substituting the rate of the internal variables of eq. (B.18) in the expression of $\bar{d}$ and raising to the square one can write:

$$\begin{aligned}\bar{d}^2 &= A^2\left(\dot{\alpha}_p + \beta\dot{\alpha}_q\right)^2 + B^2\left(M^2-\beta^2\right)\dot{\alpha}_q^2 = \\ &= \left(\chi_p - \frac{\gamma p_0}{2}\right)^2\frac{\bar{d}^2}{A^2} + \frac{\left(\chi_q - \beta\chi_p\right)^2}{B^2\left(M^2-\beta^2\right)}\bar{d}^2\end{aligned} \tag{B.19}$$

Therefore $\bar{d}^2$ can be eliminated from eq. (B.19) and multiplying all the members for $A^2B^2\left(M^2-\beta^2\right)$one obtains:

$$A^2\left(\chi_q - \beta\chi_p\right)^2 + B^2\left(M^2-\beta^2\right)\left(\chi_p - \frac{\gamma}{2}p_0\right)^2 - A^2B^2\left(M^2-\beta^2\right) = 0 \tag{B.20}$$

representing the equation of the yield function in the dissipative generalised stress plane.

In order to verify that eq. (B.20) is correct, the dissipation function is derived from the yield function. As usual, recalling the definition in eq. (5.20), one can determine the rate of internal variables necessary to determine the dissipation function as follow:

$$\begin{aligned}\frac{\dot{\alpha}_p}{L} &= \frac{\partial f}{\partial \chi_p} = -2\beta A^2\chi_q + 2\beta^2A^2\chi_p + B^2\left(M^2-\beta^2\right)\left(2\chi_p - \gamma p_0\right) \\ \frac{\dot{\alpha}_q}{L} &= \frac{\partial f}{\partial \chi_q} = 2A^2\chi_q - 2A^2\beta\chi_p\end{aligned} \tag{B.21}$$

The plastic multiplier L can be determined once the dissipative generalised stresses χ_p and χ_q are expressed as functions of the rate of internal variables and L:

$$\begin{aligned}\chi_p &= \frac{\dot{\alpha}_p + \beta\dot{\alpha}_q}{2B^2L\left(M^2-\beta^2\right)} + \frac{\gamma p_0}{2} \\ \chi_q &= \frac{\dot{\alpha}_q}{2A^2L} + \beta\frac{\dot{\alpha}_p + \beta\dot{\alpha}_q}{2B^2L\left(M^2-\beta^2\right)} + \beta\frac{\gamma p_0}{2}\end{aligned} \tag{B.22}$$

Then one substitutes the dissipative generalised stresses of eq. (B.22) in the yield function in eq. (B.20) and obtains the plastic multiplier. In particular one has:

$$A^2\left(\frac{\dot{\alpha}_q}{2A^2L}+\beta\frac{\dot{\alpha}_p+\beta\dot{\alpha}_q}{2B^2L\left(M^2-\beta^2\right)}+\beta\frac{\gamma p_0}{2}-\beta\frac{\dot{\alpha}_p+\beta\dot{\alpha}_q}{2B^2L\left(M^2-\beta^2\right)}-\beta\frac{\gamma p_0}{2}\right)^2+$$
$$+B^2\left(M^2-\beta^2\right)\left(\frac{\dot{\alpha}_p+\beta\dot{\alpha}_q}{2B^2L\left(M^2-\beta^2\right)}+\frac{\gamma p_0}{2}-\frac{\gamma p_0}{2}\right)^2-A^2B^2\left(M^2-\beta^2\right)=0 \tag{B.23}$$

that, after few manipulations becomes:

$$\frac{\dot{\alpha}_q^2}{4L^2A^2}+\frac{B^2\left(\dot{\alpha}_p+\beta\dot{\alpha}_q\right)^2}{4B^4L^2\left(M^2-\beta^2\right)}-A^2B^2\left(M^2-\beta^2\right)=0 \tag{B.24}$$

Solving this latter for L one obtains:

$$L=\frac{\sqrt{A^2\left(\dot{\alpha}_p+\beta\dot{\alpha}_q\right)^2+\left(M^2-\beta^2\right)B^2\dot{\alpha}_q^2}}{2A^2B^2\left(M^2-\beta^2\right)} \tag{B.25}$$

Now the plastic multiplier can be resubstituted in eq. (B.22) such that the dissipative generalised stresses after few manipulations read:

$$\begin{aligned}\chi_p&=\frac{A^2\left(\dot{\alpha}_p+\beta\dot{\alpha}_q\right)}{\sqrt{A^2\left(\dot{\alpha}_p+\beta\dot{\alpha}_q\right)^2+B^2\left(M^2-\beta^2\right)\dot{\alpha}_q^2}}+\frac{\gamma p_0}{2}\\ \chi_q&=\frac{B^2\left(M^2-\beta^2\right)\dot{\alpha}_q+A^2\beta\left(\dot{\alpha}_p+\beta\dot{\alpha}_q\right)}{\sqrt{A^2\left(\dot{\alpha}_p+\beta\dot{\alpha}_q\right)^2+B^2\left(M^2-\beta^2\right)\dot{\alpha}_q^2}}+\beta\frac{\gamma p_0}{2}\end{aligned} \tag{B.26}$$

Finally, recalling the definition in eq. (5.15), the dissipation function assumes the form:

$$\begin{aligned}d&=\chi_p\dot{\alpha}_p+\chi_q\dot{\alpha}_q=\\ &=\frac{A^2\left(\dot{\alpha}_p+\beta\dot{\alpha}_q\right)\dot{\alpha}_p+B^2\left(M^2-\beta^2\right)\dot{\alpha}_q^2+A^2\beta\left(\dot{\alpha}_p+\beta\dot{\alpha}_q\right)\dot{\alpha}_q}{\sqrt{A^2\left(\dot{\alpha}_p+\beta\dot{\alpha}_q\right)^2+B^2\left(M^2-\beta^2\right)\dot{\alpha}_q^2}}+\frac{\gamma p_0}{2}\left(\dot{\alpha}_p+\beta\dot{\alpha}_q\right)=\\ &=\frac{A^2\left(\dot{\alpha}_p+\beta\dot{\alpha}_q\right)^2+B^2\left(M^2-\beta^2\right)\dot{\alpha}_q^2}{\sqrt{A^2\left(\dot{\alpha}_p+\beta\dot{\alpha}_q\right)^2+B^2\left(M^2-\beta^2\right)\dot{\alpha}_q^2}}+\frac{\gamma p_0}{2}\left(\dot{\alpha}_p+\beta\dot{\alpha}_q\right)=\\ &=\sqrt{A^2\left(\dot{\alpha}_p+\beta\dot{\alpha}_q\right)^2+B^2\left(M^2-\beta^2\right)\dot{\alpha}_q^2}+\frac{\gamma p_0}{2}\left(\dot{\alpha}_p+\beta\dot{\alpha}_q\right)\end{aligned} \tag{B.27}$$

Bibliography

Amorosi, A., Boldini, D., Germano, V. (2008). A generalised backward euler scheme for the integration of a mixed isotropic-kinematic hardening model for clays. *International Journal of Numerical and Analytical Methods in Geomechanics,* 32, 1173-1203.

Bellotti, R., Jamiolkowski, M., Lo Presti, D. & O'Neill, D. A. (1996). Anisotropy of small strain stiffness in Ticino sand. *Géotechnique,* 46(1), 115-131.

Bieniawski, Z. T. (1969). Deformational behaviour of fractured rock under multiaxial compression, *Structure, Solid Mechanics and Engineering Desian, Proc.*, Southampton, Part 1 (Edited by Te'eni), pp. 589-597.

Bigoni, D. (2012). Nonlinear solid mechanics: bifurcation theory and material instability. Cambridge University Press.

Bigoni, D., and Loret. B. (1999) Effects of elastic anisotropy on strain localization andflutter instability in plastic solids. *Journal of the Mechanics and Physics of Solids,* 47.7, 1409-1436.

Boehler, J. P. (1987). Applications of tensor functions in solid mechanics. Ed. Jean-Paul Boehler. Vol. 292. New York, Springer.

Borja, R.I., Tamagnini, C., Amorosi, A. (1997). Coupling plasticity and energy-conserving elasticity models for clays. *ASCE, Journal of the Geotechnical and Geoenviromental Engineering Division*, 123(10), 948-957.

Callisto, L., & Rampello, S. (2002). Shear strength and small-strain stiffness of a natural clay under general stress conditions. *Géotechnique*, 52(8), 547-560.

Casagrande, A., & Carrillo, N. (1944). Discussion on Study of Failure Envelope Soils. *Journal of the Soil Mechanics and Foudations Division*, ASCE, 89, 243.

Chang, C. S., Misra, A., & Sundaram, S. S. (1991). Properties of granular packings under low amplitude cyclic loading. *Soil Dynamics and Earthquake Engineering*, 10(4), 201-211.

Chang, C. S., Sundaram, S. S., and Misra, A. (1989). Initial moduli of particulated mass with frictional contacts. *Int. J. Numer. Anal. Methods Geomech.*, 13(6), 629-644.

Chaudary, S. K., Kuwano, J. & Hayano, Y. H. (2004). Measurement of quasi-elastic stiffness parameters of dense Toyoura sand in hollow cylinder apparatus and triaxial apparatus with bender elements. *Geotech. Test. J.* 27, No. 1, 1-13.

Chaves, E. W. (2013). Notes on continuum mechanics. Springer Science & Business Media.

Cho, W., & Finno, R. J. (2009). Stress-strain responses of block samples of compressible Chicago glacial clays. *Journal of geotechnical and geoenvironmental engineering*, 136(1), 178-188.

Clayton, C. R. I. (2011). Stiffness at small strain: research and practice. *Géotechnique*, 61(1), 5-37.

Coleman, B. D. (1964). Thermodynamics of materials with memory. *Archive for Rational Mechanics and Analysis*, 17(1), 1-46.

Coleman, B. D., & Gurtin, M. E. (1967). Thermodynamics with internal state variables. *The Journal of Chemical Physics*, 47(2), 597-613.

Collins, I. F. (2005). Elastic/plastic models for soils and sands. *International Journal of Mechanical Sciences*, 47(4-5), 493-508.

Collins, I. F., & Hilder, T. (2002). A theoretical framework for constructing elastic/plastic constitutive models of triaxial tests. *International Journal for Numerical and Analytical Methods in Geomechanics*, 26(13), 1313-1347.

Collins, I. F., & Houlsby, G. T. (1997). Application of thermomechanical principles to the modelling of geotechnical materials. *Proc. of the Royal Society of London A: Mathematical, physical and engineering sciences* (Vol. 453, No. 1964, pp. 1975-2001).

Collins, I. F., & Kelly, P. A. (2002). A thermomechanical analysis of a family of soil models. *Géotechnique*, 52(7), 507-518.

Coombs, W. M. (2017). Continuously unique anisotropic critical state hyperplasticity. *International journal for numerical and analytical methods in geomechanics*, 41 (4), 578-601.

Coussy, O. (1995) Mechanics of porous continua, Wiley, New York

Cowin, S. C. (1985). The relationship between the elasticity tensor and the fabric tensor. *Mechanics of Materials*, 4(2), 137-147.

Cudny, M., & Partyka, E. (2017) Influence of anisotropic stiffness in numerical analyses of tunneling and excavation problems in stiff soils. In Lee, Woojin, Lee, Jong-Sub, Kim, Hyun-Ki, & Kim, Dong-Soo (Eds.) *Proceedings of the 19th International Conference on Soil Mechanics and Geotechnical Engineering*, Seoul 2017, International Society for Soil Mechanics and Geotechnical Engineering, Seoul, Korea, pp. 719-722.

Dafalias, Y. F. (1986). Bounding surface plasticity. I: Mathematical foundation and hypoplasticity. *J. Eng. Mech.*, 112(9), 966-987.

Dafalias, Y. F., & Manzari, M. T. (2004). Simple plasticity sand model accounting for fabric change effects. *Journal of Engineering mechanics*, 130(6), 622-634.

Dafalias, Y. F., & Taiebat, M. (2013). Anatomy of rotational hardening in clay plasticity. *Géotechnique*, 63(16), 1406-1418.

Dafalias, Y. F., & Taiebat, M. (2014). Rotational hardening with and without anisotropic fabric at critical state. *Géotechnique*, 64(6), 507-511.

De Silva, L. I. N. (2004). Locally Measured Quasi-Elastic Deformation Properties of Geo-materials under Torsional Shear and Triaxial loadings. Master's degree Dissertation, The University of Tokyo.

Diaz-Rodriguez, J.A., Leroueil, S., Aleman, J.D. (1992). Yielding of Mexico City clay and other natural clays. *J. Geotech. Eng.*, 118(7), 981-995.

Einav, I., Houlsby, G. T., & Nguyen, G. D. (2007). Coupled damage and plasticity models derived from energy and dissipation potentials. *International Journal of Solids and Structures*, 44(7-8), 2487-2508.

Ezaoui, A., & Benedetto, H. D. (2009). Experimental measurements of the global anisotropic elastic behaviour of dry Hostun sand during triaxial tests, and effect of sample preparation. *Géotechnique*, 59(7), 621-635.

Franzius, J. N., Potts, D. M., & Burland, J. B. (2005). The influence of soil anisotropy and K0 on ground surface movements resulting from tunnel excavation. *Géotechnique*, 55(3), 189-199.

Fung, Y. C. (1965). Foundation of Solid Mechanics. Prentice Hall, Englewood Cliffs, NJ.

Gajo, A., and Bigoni. D. (2008) A model for stress and plastic strain induced nonlinear, hyperelastic anisotropy in soils. *International Journal for Numerical and Analytical Methods in Geomechanics,* 32(7), 833-861.

Gao, Y., Wang, Y. H., & Su, J. C. (2012). Mechanisms of aging-induced modulus changes in sand under isotropic and anisotropic loading. *Journal of Geotechnical and Geoenvironmental Engineering*, 139(3), 470-482.

Gasparre, A. (2005). Advanced laboratory characterisation of London Clay. PhD thesis, Imperial College, London.

Gasparre, A., Nishimura, S., Minh, N. A., Coop, M. R., & Jardine, R. J. (2007). The stiffness of natural London Clay. *Géotechnique*, 57(1), 33-47.

Goddard, J. D. (1990). Nonlinear elasticity and pressure-dependent wave speeds in granular media. *Proc. R. Soc. Lond.* A 430, No. 1878, 105-131.

Graham, J., & Houlsby, G. T. (1983). Anisotropic elasticity of a natural clay. *Géotechnique*, 33(2), 165-180.

Green, A. E., & Naghdi, P. M. (1965). A general theory of an elastic-plastic continuum. *Archive for rational mechanics and analysis*, 18(4), 251-281.

Gu, X., Yang, J., & Huang, M. (2013). Laboratory measurements of small strain properties of dry sands by bender element. *Soils and Foundations*, 53(5), 735-745.

Halphen, B., & Nguyen, Q. S. (1975). Sur les matériaux standard généralisés. *Journal de mécanique*, 14, 39-63.

Hardin, B. O. (1978, June). The nature of stress-strain behavior for soils. In From Volume I of Earthquake Engineering and Soil Dynamics--*Proceedings of the ASCE Geotechnical Engineering Division Specialty Conference*, June 19-21, 1978, Pasadena, California.

Hardin, B. O., & Black, W. (1969). Closure on vibration modulus of normally consolidated clay. *Journal of Soil Mechanics & Foundations Div.*, 95, SM6, 1531-1537.

Hardin, B. O. & Blandford, G. E. (1989). Elasticity of particulate materials. *J. Geotech. Engng Div., Am. Soc. Civ. Engrs* 115(6), 788-805.

Hardin, B. O., & Kalinski, M. E. (2005). Estimating the shear modulus of gravelly soils. *Journal of geotechnical and geoenvironmental engineering*, 131(7), 867-875.

Hardin, B. O., & Richart Jr, F. E. (1963). Elastic wave velocities in granular soils. *Journal of Soil Mechanics & Foundations Div*, 89, 33-65 (Proc. Paper 3407).

Hashiguchi, K. (1977). An expression of anisotropy in a plastic constitutive equation of soils. S. Murayama and A. N. Schoþeld (eds), *Constitutive Equations of Soils, Proc. 9th Int. Conf. Soil Mech. Found. Eng., Spec. Session 9*, JSSMFE, Tokyo, pp. 302-305.

Hight, D. W., Bennell, J. D., Chana, B., Davis, P. D., Jardine, R. J. & Porovic, E. (1997). Wave velocity and stiffness measurements of the Crag and Lower London Tertiaries at Sizewell. *Géotechnique,* 47(3), 451-474, doi: 10.1680/geot.1997.47.3.451.

Hight, D. W., Gasparre, A., Nishimura, S., Minh, N. A., Jardine, R. J., & Coop, M. R. (2007). Characteristics of the London Clay from the Terminal 5 site at Heathrow Airport. *Géotechnique*, 57(1), 3-18.

Hight, D. W., McMillan, F., Powell, J. J. M., Jardine, R. J. & Allenou, C. P. (2003). Some characteristics of London clay. *Proc. of the Int. workshop on characterization and engineering properties of natural soils*, Singapore, Vol. 2, pp. 851-907.

Holzapfel, A. G. (2000). Nonlinear Solid Mechanics II. John Wiley & Sons, LTD.

HongNam, N., & Koseki, J. (2005). Quasi-elastic deformation properties of Toyoura sand in cyclic triaxial and torsional loadings. *Soils and foundations*, 45(5), 19-37.

Hoque, E. & Tatsuoka, F. (1998). Anisotropy in the elastic deformation of granular materials. *Soils Found.* 38, No. 1, 163-179.

Houlsby, G. T. (1981). Study of plasticity theories and their applicability to soils (Doctoral dissertation, University of Cambridge).

Houlsby, G.T. (1992) Interpretation of dilation as a kinematic constraint, *Proc. Workshop on Modern Approaches to Plasticity*, Horton, Greece, June 12-16, 19-38.

Houlsby, G.T., Amorosi, A., Rojas, E. (2005). Elastic moduli of soils dependent on pressure: a hyperelastic formulation. *Géotechnique,* 55 (5), 383-392.

Houlsby, G. T., Amorosi, A., & Rollo, F. (2019). Non-linear anisotropic hyperelasticity for granular materials. Submitted for publication.

Houlsby, G. T., & Puzrin, A. M. (2000). A thermomechanical framework for constitutive models for rate-independent dissipative materials. *International Journal of Plasticity*, 16(9), 1017-1047.

Houlsby, G. T., & Puzrin, A. M. (2006). Principles of hyperplasticity: an approach to plasticity theory based on thermodynamics principles. Springer

Houlsby, G. T., & Wroth, C. P. (1991). The variation of shear modulus of a clay with pressure and overconsolidation ratio. *Soils and Foundations*, 31(3), 138-143.

Hueckel, T. (1976). Coupling of elastic and plastic deformations of bulk solids. *Meccanica*, 11(4), 227-235.

Hueckel, T., & Maier, G. (1977). Incremental boundary value problems in the presence of coupling of elastic and plastic deformations: a rock mechanics oriented theory. *International Journal of Solids and Structures*, 13(1), 1-15.

Hueckel, T., & Tutumluer, E. (1994). Modeling of elastic anisotropy due to one-dimensional plastic consolidation of clays. *Computers and Geotechnics*, 16(4), 311-349.

Ibraim, E., Christiaens, P., & Pope, M. (2011). Development of a hollow cylinder torsional apparatus for pre-failure deformation and large strains behaviour of sand. *Geotechnical Engineering Journal of the South-east Asian Geotechnical Society (SEAGS) & Association of Geotechnical Societies in South-East Asia (AGSSEA), Special Issue on Soil Behaviour*, 42, 58-68.

Ibrahim, A. A. & Kagawa, T. (1991). Microscopic measurement of sand fabric from cyclic tests causing liquefaction. *Geotech. Test. J.* 14, No. 4, 371-382.

Ishihara, K. (1982). Evaluation of soil properties for use in earthquake response analysis. In *Proc. Int. Symp. on Nyumerical Models in Geomechanics*, pp. 237-259.

Itskov, M. (2007). Tensor algebra and tensor analysis for engineers. Springer-Verlag Berlin Heidelberg.

Iwasaki, T., & Tatsuoka, F. (1977). Effects of grain size and grading on dynamic shear moduli of sands. *Soils and foundations*, 17(3), 19-35.

Jamiolkowski, M., Lancellotta, R., & Lo Presti, D. C. F. (1994). Remarks on the stiffness at small strains of six Italian clays. In *Pre-failure deformation of geomaterials. Proceedings of the International Symposium, 12-14 September 1994,* Sapporo, Japan, 2 Vols.

Jovičić, V. (1995). Small strain shear modulus of soils and soft rocks. Geotechnical Engineering Research Centre, City University, London, Report GE/5/95.

Jovičić, V., Coop, M. R. & Simic, M. (1996). Objective criteria for determining Gmax from bender element tests. *Géotechnique* 46(2), 357-362.

Jovičić, V. & Coop, M. R. (1998). The measurement of stiffness anisotropy in clays with bender element tests in the triaxial apparatus. *ASTM Geotech. Test. J.* 21, No. 1, 3-10.

Kim, T., & Finno, R. J. (2014). Elastic shear modulus of compressible Chicago clay. *KSCE Journal of Civil Engineering*, 18(7), 1996-2006.

Kumar, J., & Madhusudhan, B. N. (2010). Effect of relative density and confining pressure on Poisson ratio from bender and extender elements tests. *Géotechnique*, 60(7), 561-567.

Kuwano, R., & Jardine, R. J. (2002). On the applicability of cross-anisotropic elasticity to granular materials at very small strains. *Géotechnique*, 52(10), 727-749.

Lashkari, A. (2010) A SANISAND model with anisotropic elasticity. *Soil Dynamics and Earthquake Engineering,* 30(12), 1462-1477.

Lee, K. M., & Rowe, R. K. (1989). Deformations caused by surface loading and tunnelling: the role of elastic anisotropy. *Géotechnique*, 39(1), 125-140.

Lemaitre, J., Chaboche, J.L., 1990. Mechanics of Solid Materials. Cambridge University Press, Cambridge.

Lings, M. L., Pennington, D. S. & Nash, D. F. T. (2000). Anisotropic stiffness parameters and their measurement in a stiff natural clay. *Géotechnique* 50 (2), 109-125, doi: 10.1680/ geot.2000.50.2.109.

Lodge, A. S. (1955). The transformation to isotropic form of the equilibrium equations for a class of anisotropic elastic solids. *Quarterly Journal of Mechanics and Applied Mathematics*, 8(2), 211-225.

Lo Presti, D. C. F., & O'Neill, D. A. (1991). Laboratory investigation of small strain modulus anisotropy in sands. *Proc. ISOCCTI*, Clarkson University, Potsdam, 213-224.

Lubliner, J. (1972). On the thermodynamic foundations of non-linear solid mechanics. *International Journal of Non-Linear Mechanics*, 7(3), 237-254.

Maier, G., & Hueckel, T. (1979, April). Nonassociated and coupled flow rules of elastoplasticity for rock-like materials. *International Journal of Rock Mechanics and Mining Sciences & Geomechanics Abstracts*. 16(2), 77-92. Pergamon.

Malvern, L. E. (1969). Introduction to the Mechanics of a Continuous Medium, Prentice-Hall Inc., Englewood Cliffs, N J.

Mašín, D., and Rott. J. (2014) Small strain stiffness anisotropy of natural sedimentary clays: review and a model. *Acta Geotechnica,* 9(2), 299-312.

Maugin, G.A. (1992) The thermomechanics of plasticity and fracture, Cambridge University Press.

Maugin, G.A. (1999) The thermodynamics of nonlinear irreversible processes, World Scientific, Singapore.

Mitaritonna, G., Amorosi, A., & Cotecchia, F. (2014). Experimental investigation of the evolution of elastic stiffness anisotropy in a clayey soil. *Géotechnique*, 64(6), 463-475.

Moreau, J. J. (1970). Sur les lois de frottement, de viscosité et de plasticité. *CR Acad. Sci.*, Paris, 271, 608-611.

Mulilis, J. P., Seed, H. B., Chan, C. K., Mitchell, J. K. & Arulnadan, K. (1977). Effects of sample preparation on sand liquefaction. *J. Geotech. Engng.,* 103(2), 91-108.

Ng, C. W., Leung, E. H., & Lau, C. K. (2004). Inherent anisotropic stiffness of weathered geomaterial and its influence on ground deformations around deep excavations. *Canadian Geotechnical Journal*, 41(1), 12-24.

Ng, C. W. W., & Yung, S. Y. (2008). Determination of the anisotropic shear stiffness of an unsaturated decomposed soil. *Géotechnique*, 58(1), 23-35.

Ni, S. H. (1987). Dynamic properties of sand under true triaxial stress states from resonant column and torsion shear tests. The University of Texas, Austin, PhD thesis.

Oda, M., Nemat-Nasser, S., and Konishi, J. (1985). Stress-induced anisotropy in granular masses. *Soils Found.*, 25(3), 85-97.

Pennington, D. S., Nash, D. F. T. & Lings, M. L. (1997). Anisotropy of G0 shear stiffness in Gault Clay. *Géotechnique* 47(3), 391-398, doi: 10.1680/geot.1997.47.3.391.

Puzrin, A. M., Burland, J. B., & Standing, J. R. (2012). Simple approach to predicting ground displacements caused by tunnelling in undrained anisotropic elastic soil. *Géotechnique*, 62(4), 341.

Rampello, S., Silvestri, F. & Viggiani G. (1994a). The dependence of small strain stiffness on stress state and history for fine grained soils: the example of Vallericca clay. *Proc. 1st Int. Conf. Pre-failure Deform. Character. Geomater.*, Sapporo 1, 273-278.

Rampello, S., Viggiani, G. M. B., & Amorosi, A. (1997). Small-strain stiffness of reconstituted clay compressed along constant triaxial effective stress ratio paths. *Géotechnique*, 47(3), 475-489.

Roesler, S. K. (1979). Anisotropic shear modulus due to stress anisotropy. *J. Geotech. Engng Div.* ASCE 105(7), 871-879.

Rothenburg, L., and Bathurst, R. J. (1989). Analytical study of induced anisotropy in idealized granular materials. *Géotechnique*, 39(4), 601-614.

Rothenburg, L., and Bathurst, R. J. (1992). Micromechanical features of granular assemblies with planar elliptical particles. *Géotechnique*, 42(1), 79-95.

Sekiguchi, H., and Ohta, H. (1977). Induced anisotropy and time dependency in clays, in S. Murayama and A. N. Schofield (eds), *Constitutive Equations of Soils, Proc. 9th Int. Conf. Soil Mech. Found. Eng., Spec. Session 9*, JSSMFE, Tokyo, pp. 229-238.

Simpson, B., Atkinson, J. H. & Jovicˇicˇ, V. (1996). The influence of anisotropy on calculations of ground settlement above tunnels. In *Geotechnical aspects of underground construction in soft ground* (eds R. J. Mair and R. N. Taylor), pp. 591-594. Rotterdam: Balkema.

Stokoe, K. H. II, Hwang, S. K., Lee, N. K. J. & Andrus, R. D. (1995). Effect of various parameters on the stiffness and damping of soils at small to medium strains. Keynote Lecture. *Proc. 1st Int. Symp. on Pre-failure Deformation of Geomaterials*, Hokkaido 2, 785-816.

Stokoe, K. I., Lee, J. N. K. and Lee, S. H. H. (1991). Characterization of soil in calibration chambers with seismic waves. *Calibration Chamber Testing*. Elsevier Science Publishing, 363-376.

Suwal, L. P., & Kuwano, R. (2013). Statically and dynamically measured poisson's ratio of granular soils on triaxial laboratory specimens. *Geotechnical Testing Journal*, 36(4), 493-505.

Tamagnini, C., Castellanza, R., Nova, R. (2002). A generalized backward Euler algorithm for the numerical integration of an isotropic hardening elastoplastic model for mechanical and chemical degradation of bonded geomaterials. *International Journal of Analytical and Numerical Methods in Geomechanics*, 26, 963-1004.

Teachavorasinskun, S., & Lukkanaprasit, P. (2008). Stress induced and inherent anisotropy on elastic stiffness of soft clays. *Soils and Foundations*, 48(1), 127-132.

Truesdell, C. A., & Noll, W. (1965). Handbuch der physik. Springer.

Vermeer, P. A. (1982). A five-constant model unifying well-established concepts. Gudehus, Darve and Vardoulakis (eds). *Results of the International Workshop on Constitutive Relations for Soils*, Grenoble, Balkema, 175-197.

Viggiani, G. (1992). Small strain stiffness of fine grained soils (Doctoral dissertation, City University London).

Viggiani, G. & Atkinson, J. H. (1995). Stiffness of fine grained soil at very small strains. *Géotechnique,* 45(2), 249-265.

Wang, C. C. (1970). A new representation theorem for isotropic functions: An answer to Professor GF Smith's criticism of my papers on representations for isotropic functions. *Archive for Rational Mechanics and Analysis*, 36(3), 166-197.

Wang, Y. H., and Mok, C.M.B. (2008). Mechanisms of small-strain shearmodulus anisotropy in soils. *J. Geotech. Geoenviron. Eng.*, 134(10), 1516-1530.

Weiler, W. A. (1988). Small strain shear modulus of clay. *Proceedings of a special conference on earthquake engineering and soil dynamics*, pp. 331-345. Park City: American Society of Civil Engineers.

Wheeler, S. J., Na¨a¨ta¨nen, A., Karstunen, M. & Lojander, M. (2003). An anisotropic elastoplastic model for soft clays. *Can. Geotech. J.*, 40(2), 403-418.

Wu, W., & Kolymbas, D. (1990). Numerical testing of the stability criterion for hypoplastic constitutive equations. *Mechanics of Materials*, 9(3), 245-253.

Yamashita, S. & Suzuki, T. (1999). Young's and shear moduli under different principal stress directions of sand. *Proc. 2nd Int. Symp. on Pre-failure Deformation Characteristics of Geomaterials*, Torino 1, 149-158.

Yimsiri, S., and Soga, K. (2000). Micromechanics-based stress-strain behaviour of soils at small strains. *Géotechnique*, 50(5), 559-571.

Yimsiri, S., and Soga, K. (2002). Application of micromechanics model to study anisotropy of soils at small strains. *Soils Found.*, 42(5), 15-26.

Yimsiri, S., & Soga, K. (2011). Cross-anisotropic elastic parameters of two natural stiff clays. *Géotechnique*, 61(9), 809-814.

Yu, P., & Richart Jr, F. E. (1984). Stress ratio effects on shear modulus of dry sands. *Journal of Geotechnical Engineering*, 110(3), 331-345.

Zdravković, L., Potts, D. M., & Hight, D. W. (2002). The effect of strength anisotropy on the behaviour of embankments on soft ground. *Géotechnique*, 52(6), 447-457.

Zeng, X., & Ni, B. (1999). Stress-induced anisotropic G max of sands and its measurement. *Journal of geotechnical and geoenvironmental engineering*, 125(9), 741-749.

Zhao, J., & Gao, Z. (2015). Unified anisotropic elastoplastic model for sand. *Journal of Engineering Mechanics*, 142(1), 04015056-1-12.

Ziegler, H. (1977, 1983) An introduction to thermomechanics, North Holland, Amsterdam (2nd ed. 1983).

Zysset, P. K., and A. Curnier. (1995). An alternative model for anisotropic elasticity based on fabric tensors. *Mechanics of Materials,* 21(4), 243-250.